January 2010

Studies Toward The Synthesis Of Lomaiviticins A and B and Englerin A

Srinivas Achanta
Washington University in St. Louis

WASHINGTON UNIVERSITY IN ST. LOUIS

Department of Chemistry

Dissertation Examination Committee:
Prof. Vladimir B Birman, Chair
Prof. Kevin D Moeller
Prof. John S Taylor
Prof. John R. Bleeke
Prof. Garland R Marshall
Prof. Donald L Elbert

STUDIES TOWARD THE SYNTHESIS OF

LOMAIVITICINS A AND B AND ENGLERIN A

by

SRINIVAS ACHANTA

A dissertation presented to the
Graduate School of Arts and Sciences
of Washington University in
partial fulfillment of the
requirements for the degree
of Doctor of Philosophy

December 2009

Saint Louis, Missouri

Acknowledgements

I would like to thank my advisor Professor Vladimir B. Birman for his unwavering support, enthusiasm and general concern for my development as an organic chemist.

I would also like to thank my thesis committee, Professor Kevin D. Moeller and Professor John-Stephen A. Taylor for their guidance throughout my PhD. I would especially like to thank Professor Kevin D. Moeller for helpful discussions and advice over the years and also for allowing me to attend their group meetings and treating me as a part of their group. Thanks also go to my other committee members Professor Garland R. Marshall, Professor John R. Bleeke and Professor Donald L. Elbert for serving on my thesis committee. I appreciate their input and the effort that they made to evaluate all of my graduate work.

Special thanks go to Dr. Andre' d'Avignon and Dr. Jeff Kao for solving my NMR related problems. Thanks to Dr. Ed Hiss who has always been there to solve non chemistry problems throughout my graduate work. Jessica Owens and Norma Taylor are also thanked for their help over the years.

I would also like to thank all the current and former members of Birman and Moeller group for their friendship and support. I would like to thank Dr. Clifford A. Schlecht, Dr. Jagadish Boppisetti, Prashanth Padakanti, Valentina Bumbu and Dr. Feili Tang for their friendship and support over the years. I was fortunate to work with a very talented

undergraduate Curtis Seizert, who has always been a constant source of inspiration. I'll never forget the fun time we had in lab. Thanks also go to Xing Yang and Haichao Xu with whom I had thoughtful discussions during the last couple of years.

Endless thanks to my friends Mahesh Madhusudanan, Vamshi Krishna Bommena, Pramod Muppala and Dr. Meher Kumar Perambuduru for their unwavering support and advice throughout my life. I would especially like to thank my friend Dr. Tirumala Hanuma Satya Krishna Jujjuri for his unselfish friendship. He has been my friend, philosopher and guide and truly deserves much more credit than whatever platitudes I could offer on this meager page.

To my family, (Mom, Dad and Anjani) who have shown me all the love and support a son or brother could ever ask for, I certainly cannot put into words how much I owe you and how much you all mean to me but can only hope to show you over time. I am forever grateful to my grandparents for their affection and support throughout my life.

Finally, I wish to thank my wife Sravanti Pasumarti, who has been a constant source of enthusiasm. More importantly, I would like to thank you for believing in me and for putting up with me and cannot imagine what these last two years would have been like without you in my life. My only regret is that I didn't meet you sooner.

Table of contents

List of Schemes

ABSTRACT OF THE DISSERTATION

Studies toward the Total Synthesis of

Lomaiviticins A and B and Englerin A

by

Srinivas Achanta

Doctor of Philosophy in Chemistry

Washington University in St. Louis, 2009

Professor Vladimir B. Birman, Chairperson

Part I: Studies toward the central core of lomaiviticins A and B

Lomaiviticins A and B are novel C_2-symmetric dimeric molecules with profound cytotoxic activity. The most challenging feature of these molecules is the densely functionalized central core. Despite the effort by several research groups, the total synthesis of lomaiviticins has not been reported so far. We envisioned the synthesis of the lomaiviticin core by an unprecedented Diels-Alder dimerization of *ortho*-quinols and masked *ortho*-benzoquinones, followed by the fragmentation of the extra carbon-carbon bond. This chapter describes the stereoselective elaboration of the *ortho*-quinol and masked *ortho*-benzoquinone dimers to the fragmentation precursors and the unsuccessful attempts to effect the scission of the extra bond.

Part II: Studies toward the total synthesis of englerin A

Englerin A is a new guaiane sesquiterpene isolated recently in 2008. It has been shown to be a selective renal cancer inhibitor. We envisioned the synthesis of englerin A via a novel strategy featuring Wagner-Meerwein rearrangement followed by intramolecular cation trapping. This chapter describes the stereoselective synthesis of the key cis-decalin intermediate from (-)-carvone and the unsuccessful attempts to realize the skeletal rearrangement.

Chapter 1: Studies toward the synthesis of lomaiviticins A and B

1.1 Background

1.1.1 Isolation and biological activity

In 2001, He and co-workers reported the isolation and characterization of two new dimeric compounds Lomaivitcins A and B from a strain of actinomycetes, *Micromonospora lomaivitiensis*, which was isolated from the inner core of a host ascidian.[1] These two novel compounds bear structural similarities to the much simpler monomeric diazobenzofluorene antibiotics kinamycins, with the former incorporating a higher level of complexity by dimerization of the common tetracyclic ring system.[2] Although the absolute stereochemistry was not rigorously established, extensive NMR, IR and MS analysis has led to the formulation of the structures shown in Scheme 1-1.

Scheme 1-1. Lomaiviticins A and B and Kinamycins A-D

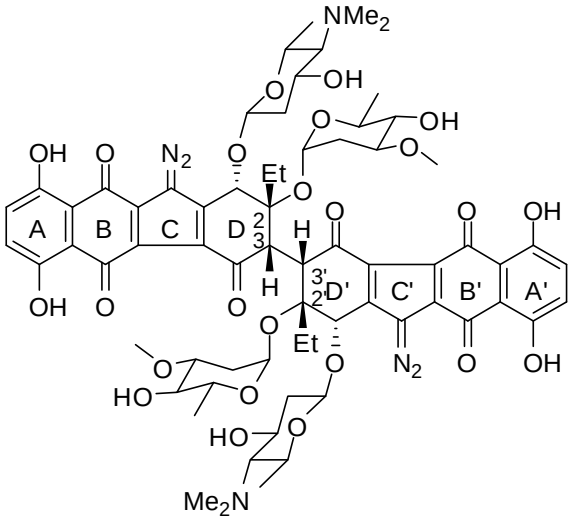

1.1 Lomaiviticin A

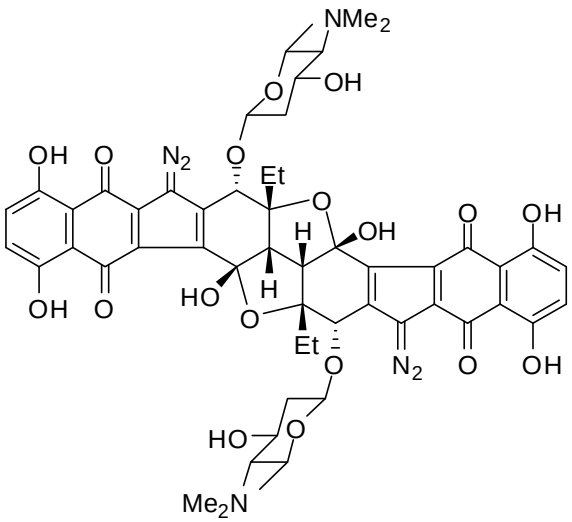

1.2 Lomaiviticin B

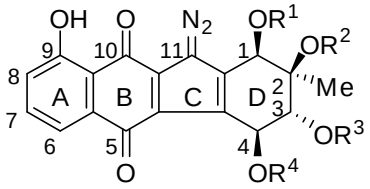

1.3 - 1.6: Kinamycins A-D

kinamycin	R^1	R^2	R^3	R^4
A **(1.3)**	Ac	Ac	Ac	H
B **(1.4)**	H	Ac	H	H
C **(1.5)**	Ac	H	Ac	Ac
D **(1.6)**	Ac	H	Ac	H

In addition to the structural complexity, lomaiviticins A and B were shown to be highly active DNA-damaging agents by Biochemical Induction Assay (BIA), both with a minimum induction concentration ≤ 0.1 ng/spot.[1] Specifically, lomaiviticin A displayed extremely potent cytotoxicity against a broad range of cancer cell lines in vitro, with IC_{50} values ranging from 98 to 0.01 ng/mL^{-1}.[1] In contrast to the known DNA-damaging anticancer drugs, adriamycin and mitomicin C, these two new compounds exhibited a unique cytotoxicity profile in the 24-cancer cell line panel suggesting a different mechanism of interaction with DNA molecules.[3] Furthermore, lomaiviticins A and B displayed powerful antibiotic activity against the pathogenic Gram-positive bacteria, S*taphylococcus aureus and Enterococcus faecium* (MIC's, 6-25 ng/spot) in a plate assay.[1] The bioactivity of both lomaiviticins and kinamycins is presumably due to the diazobenzofluorene moiety. However, lomaiviticins are several orders of magnitude more potent.

1.1.2 Biosynthesis of kinamycins and lomaiviticins

Based on their common structural characteristics, lomaiviticins and kinamycins are likely to share a biosynthetic ancestry. The kinamycin antibiotics were first isolated

from *Streptomyces murayamaensis*.[5] Originally characterized by Omura and coworkers, kinamycins were initially misassigned as N-cyanobenzo[b]carbazoles. Using spectroscopic techniques these structures were later revised by Gould to be 5-diazo benzo[b]fluorenes.[6] A putative biosynthetic pathway to kinamycins proposed by Gould is depicted in Scheme 1-2.[2]

Scheme 1-2. Biosynthesis of kinamycins

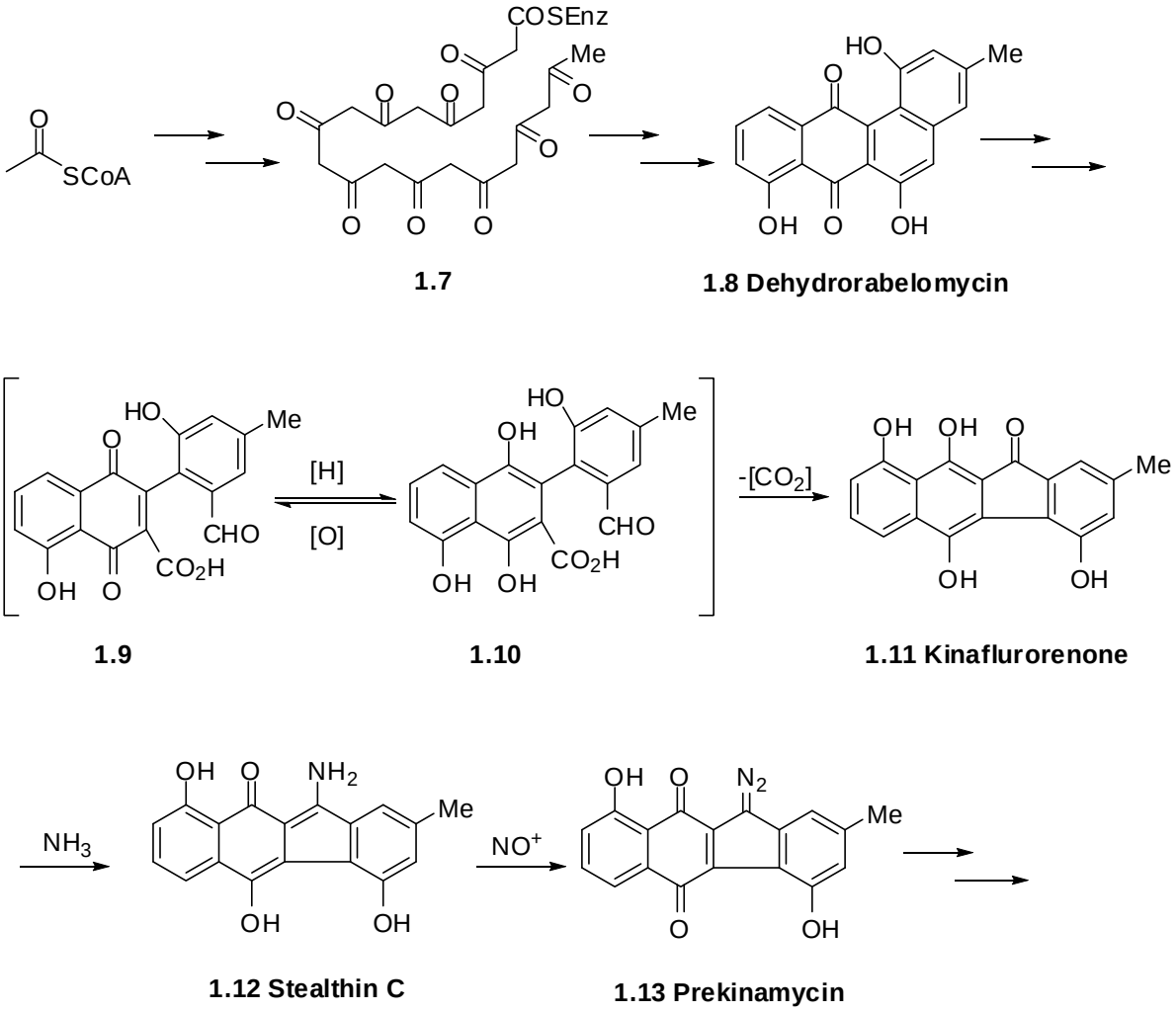

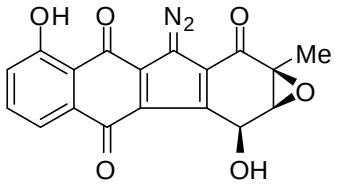

1.14 Ketoanhydrokinamycin

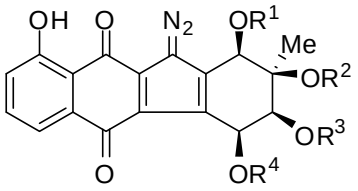

1.3-1.6 Kinamycins
R^1, R^2, R^3, R^4 = Ac or H

Given the structural similarity of the lomaiviticins A and B to kinamycins, the biosynthesis of these dimeric diazobenzofluorene glycosides lomaiviticins A and B can be envisioned to arise from an oxidative dearomatization of the diazobenzo[b]fluorene precursor **1.15** to give the epoxide **1.16** as shown in Scheme 1-3. Reductive epoxide opening followed the oxidative coupling of the resulting enolate **1.18** produces lomaiviticinone **1.19**. Glycosylation of the lomaiviticinone **1.19** affords lomaiviticins A and B.

Scheme 1-3. Proposed biosynthesis of lomaiviticins A and B

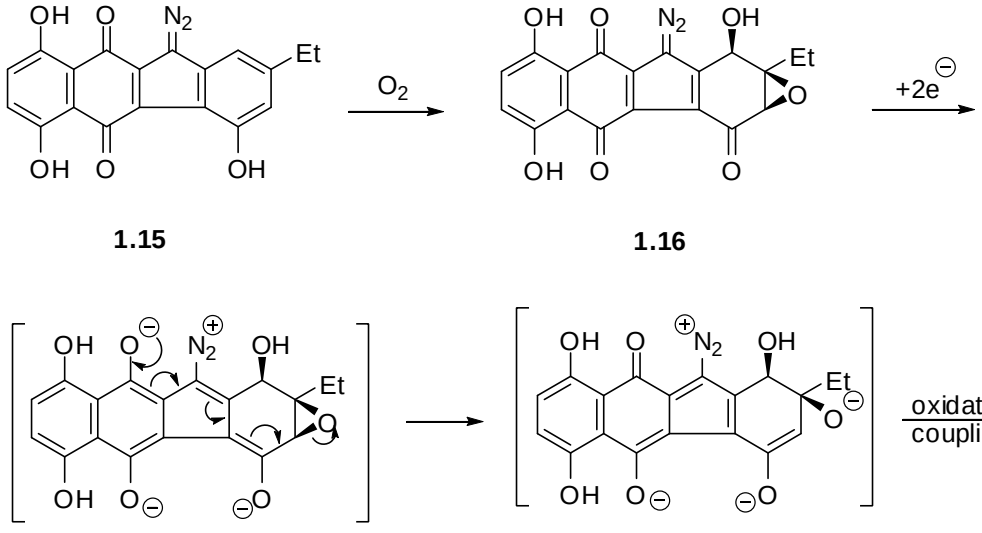

1.15 **1.16**

1.17 **1.18**

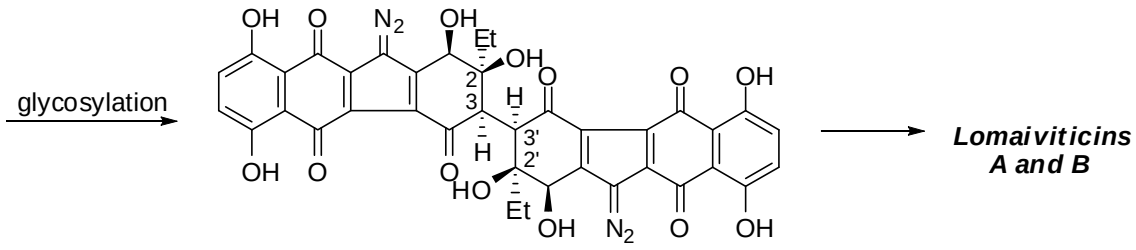

1.19 Lomaiviticinone

1.1.3 Mode of action of benzo[b]fluorene antibiotics

Although much is known about the biosynthesis of the kinamycins, given the rarity of the diazo function in naturally occurring compounds, it is not surprising that little information exists concerning the chemical basis for their biological activity. The unique biological activity of kinamycins and lomaiviticins has rekindled interest and several hypotheses have been proposed regarding their mechanism of action.[7,8] To date, three hypotheses have been proposed to explain the mode of action of these compounds. Arya and Jebaratnam were the first to submit a defined proposal working with model compound diazofluroene **1.20**.[8a] They observed that **1.20** nicks plasmid DNA upon exposure to the oxidant $Cu(OAc)_2$ and suggested that upon exposure to endogenous oxidants, kinamycins may lead to a reactive radical intermediate **1.21** (Scheme 1-4) that could damage DNA via known oxygen-mediated pathways.[9]

Scheme 1-4. Hypothesis by Arya and Jebaratnam

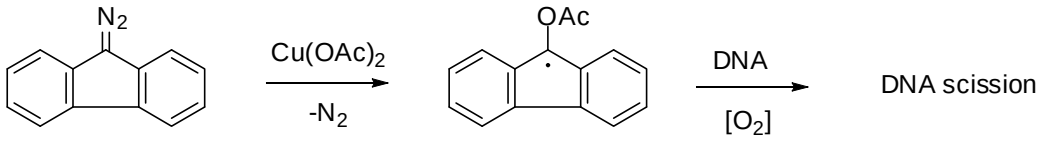

1.20 **1.21**

On the other hand, Dmitrienko and co-workers argued for the nucleophilic attack on the terminal nitrogen of the diazonium group **1.22** as an obligatory step for the radical formation via loss of N_2 to produce a DNA-damaging radical **1.24**, and that the mode of action may not involve the use of an oxidizing agent under physiological conditions.[8b] Dmitrienko's hypothesis is depicted in Scheme 1-5.

Scheme 1-5. Hypothesis by Dmitrienko

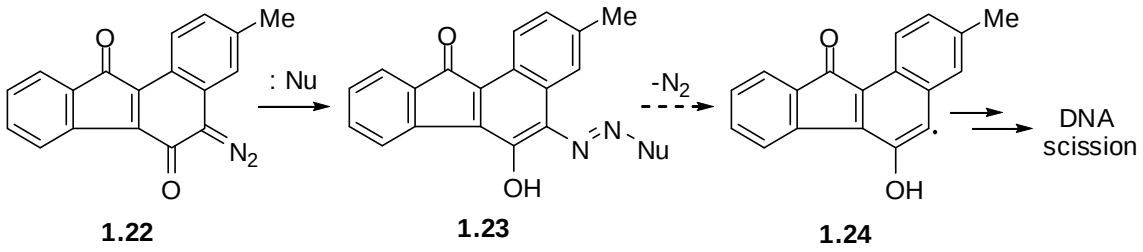

An important finding by He et. al. on the structure and biological activity of lomaiviticin A attributed its profound cytotoxicity to double stranded DNA cleavage under reducing conditions.[1] Although the two proposals discussed above were based on the activation of diazo group, neither study included the diazoparaquinone moiety commonly present in kinamycins and lomaiviticins to explain these observations under reductive conditions. Hence, alternative mechanism of action incorporating the reductive activation on the diazoparaquinone needed to be considered. A proposal by Feldman[8c,d] taking these observations in to account is shown in Scheme 1-6. One electron reduction of the generic diazoparaquinone **1.25** following protonation produces the reactive semiquinone **1.26**, also represented by the resonance form **1.27**. This radical then by the loss of N_2 generates the vinyl radical **1.28** which abstracts a hydrogen from DNA leading to the strand cleavage.[10]

Scheme 1-6. Hypothesis by Feldman

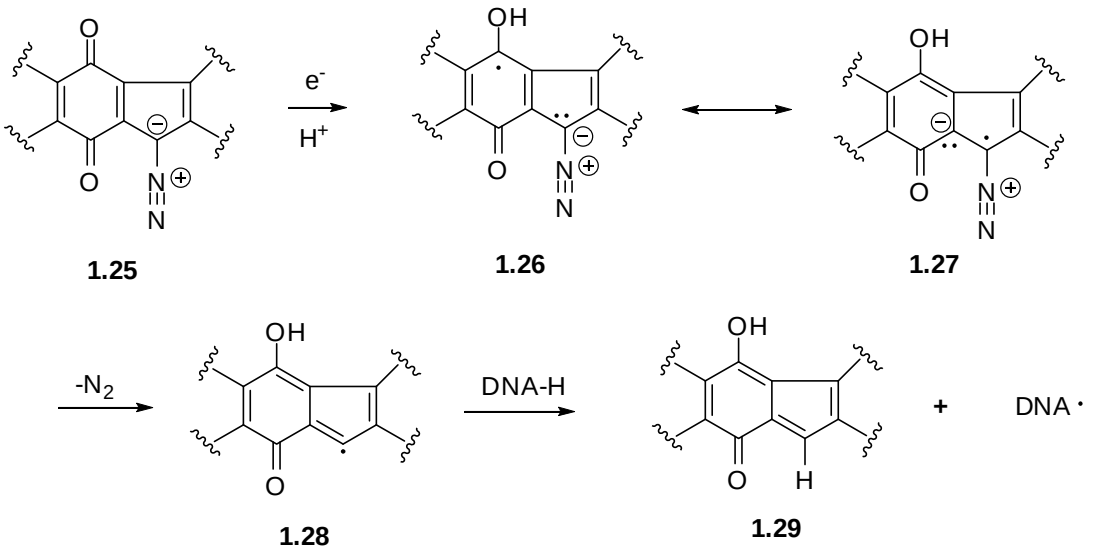

1.1.4 Previous synthetic approaches to lomaiviticins

The unique C_2-symmetrical architecture coupled with remarkable biological activity makes lomaiviticins an attractive target for chemical synthesis. During the last few years, several groups have initiated programs toward the total synthesis of these molecules. Despite this significant synthetic interest, total synthesis of lomaiviticins has not been achieved so far. From a strategic standpoint, the total synthesis of lomaiviticinone (lomaiviticin aglycon) requires two major issues to be addressed: the assembly of the tetracyclic diazobenzofluorene ring system and the more challenging stereocontrolled construction of the hindered central carbon-carbon bond. The synthesis of the tetracyclic ring system was accomplished by several research groups including ours.[11] Stereoselective construction of the central core of the lomaiviticins (Scheme 1-7), pertinent to the discussion in this section has been achieved by Nicolaou,[12] Shair[13] and

Sulikowski.[14] Apart from these studies, the synthesis of the fully glycosylated monomeric cyclohexenone core of lomaiviticin A has been accomplished by Herzon's group.[15]

Scheme 1-7. Central core of lomaiviticins A and B

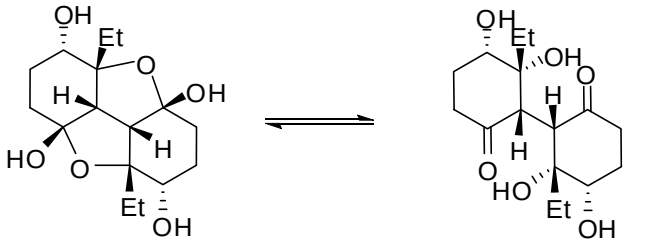

1.30 **1.31**

Lomaiviticin B **Lomaiviticin A**

1.1.4.1 Nicolaou's approach to the central core of lomaiviticins

The Nicolaou group was the first to report their synthetic efforts to the construction of the central core of lomaiviticin. Their retrosynthetic analysis is depicted in Scheme 1-8. The stereochemistry on the hindered central carbon-carbon bond was envisioned to arise from a double Michael addition on **1.36**, to give a C_2-symmetric compound **1.35**. This conformationally locked tricyclic compound then forms a scaffold to introduce the remaining two stereocenters by a stereoselective double nucleophilic addition on the bis-ketone. Finally, the tethering group was then elaborated into the sensitive 1,4 dicarbonyl moiety.

Scheme 1-8. Nicolaou's retrosynthetic analysis

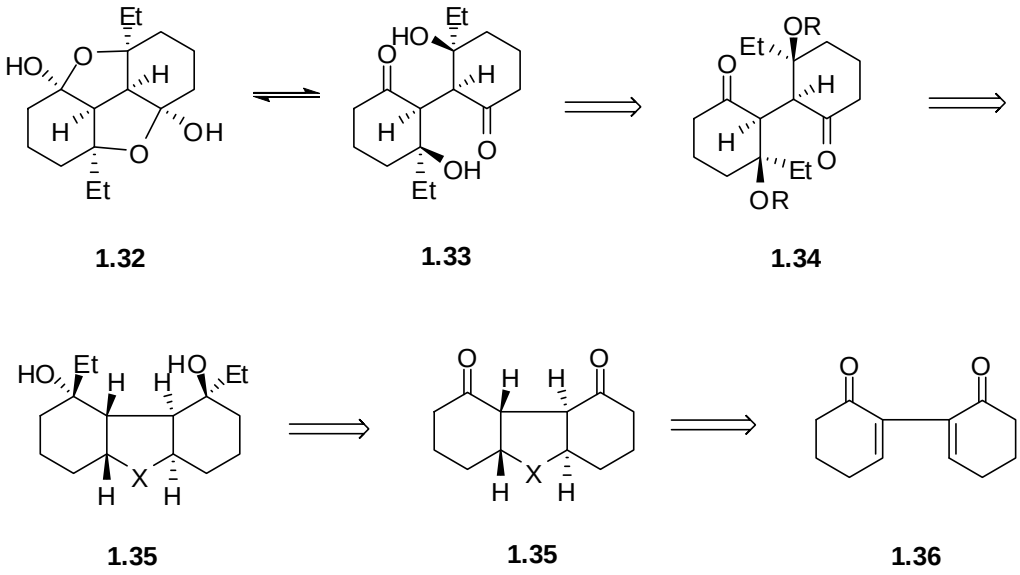

The use of sulfide as the tethering group illustrated in Scheme 1-9 was investigated first. This was introduced *via* a double Michael addition on to the dimeric ketone **1.36**. A single C_2-symmetric compound was obtained as expected. Stereoselective addition of the ethyl groups was achieved with ethyl cerium reagent. Protection of the tertiary alcohols as bis-TBS ethers and oxidation with H_2O_2 gave sulfoxide **1.37**. Unfortunately, attempted iterative Pummerer rearrangement on the sulfoxide **1.37** with trifluoroacetic anhydride and pyridine did not produce **1.38.** Instead, vinylogous sulfide **1.39** was obtained in 54% yield presumably via the vinyl sulfide **1.40**.

Scheme 1-9. Nicolaou's first generation approach

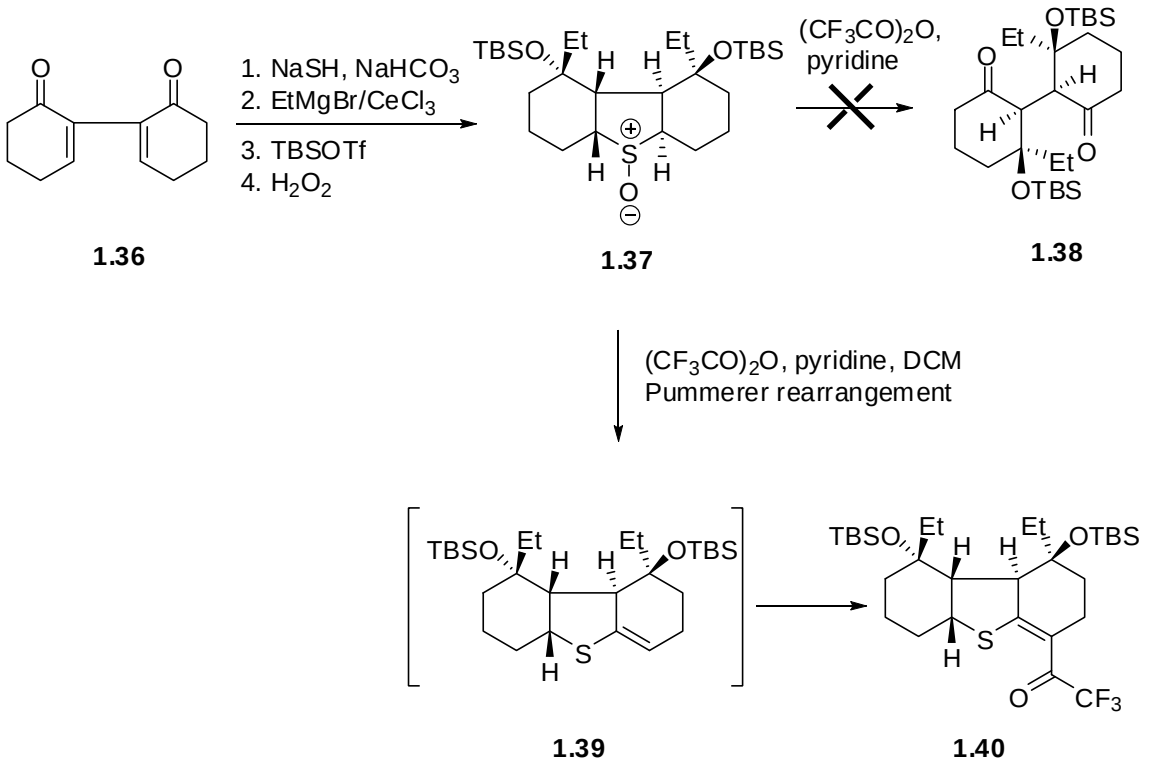

Faced with this roadblock, dimethyl malonate anion as the tethering group was investigated next, as shown in Scheme 1-10. It should be noted that this double Michael addition did not produce a C_2-symmetric adduct. Compound **1.41** was obtained with the correct relative stereochemistry α to the ketone groups. Unfortunately, due to the unsymmetrical nature of the Michael adduct, addition of excess ethyl cerium reagent gave a mixture of diastereomers with the required diastereomer **1.42**, in 57% yield. After a series of steps, the diol **1.42** was eventually converted in to the triol **1.44**.

Scheme 1-10. Nicolaou's second generation approach

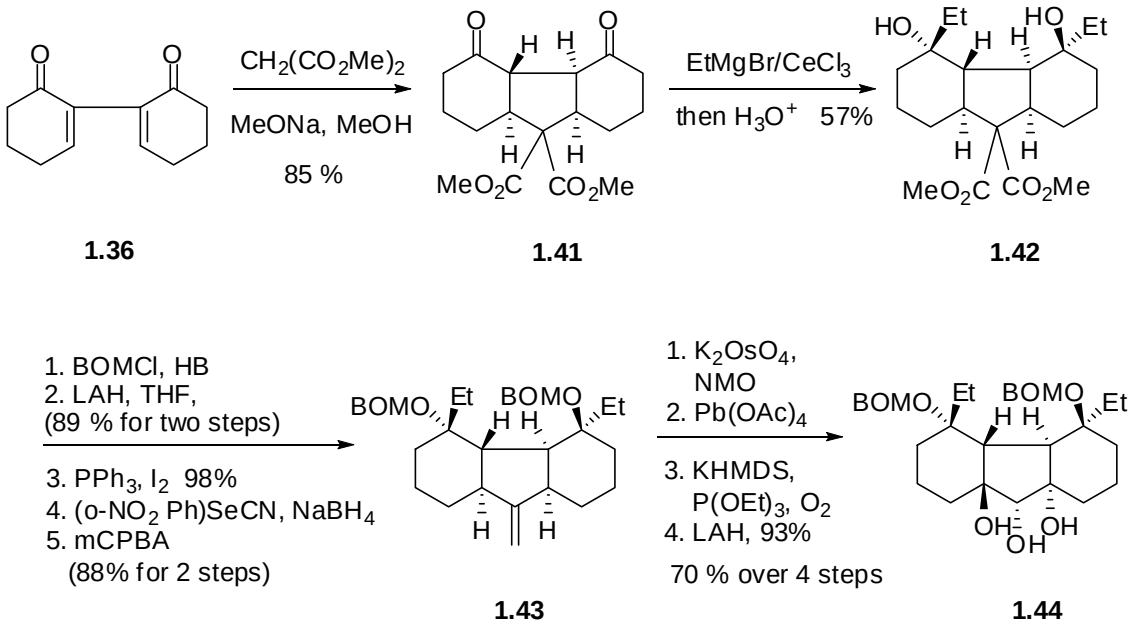

1.36 **1.41** **1.42** **1.43** **1.44**

At this point, routes to lomaiviticins A and B diverged. Complete cleavage of the triol **1.44** to furnish central core of lomaiviticin A **1.46** could not be achieved by treatment with excess $Pb(OAc)_4$ or $NaIO_4$ in one step. This transformation was eventually achieved in four steps as shown in Scheme 1-11.

Scheme 1-11. Nicolaou's synthesis of the central core of lomaiviticin A

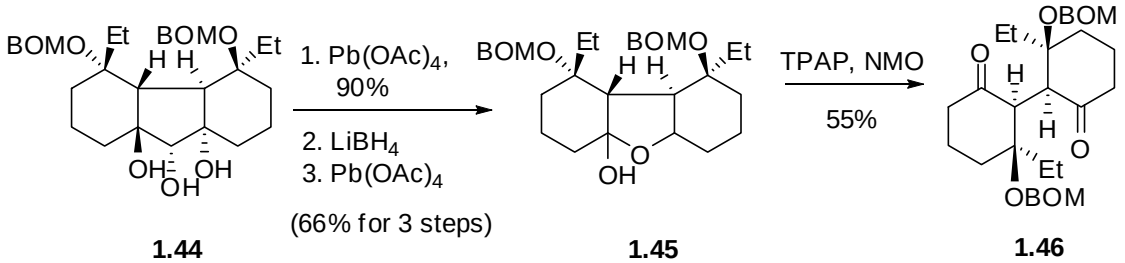

1.44 **1.45** **1.46**

On the other hand, hydrogenation of **1.44** gave **1.45**. Treatment with $Pb(OAc)_4$ followed by the hydrolysis of the intermediate formate ester using methanolic ammonia as shown in Scheme 1-12, produced the dimeric hydroxyl model compound **1.32** present in the central core of lomaiviticin B.

Scheme 1-12. Nicolaou's synthesis of the core structure of lomaiviticin B

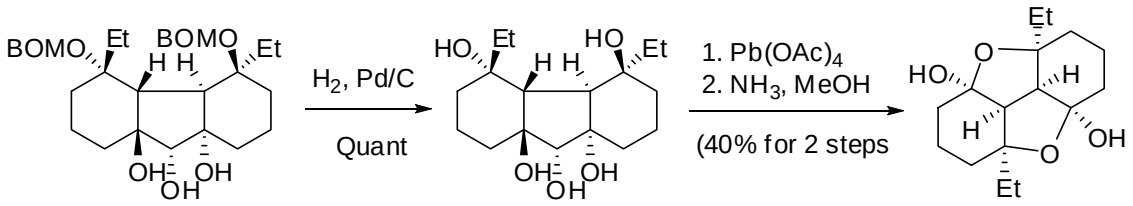

1.44 **1.45** **1.32**

1.1.4.2 Shair's approach to the central core of lomaiviticins

In contrast to the linear approach by Nicolaou, Shair proposed a convergent approach to these C_2-symmetric molecules. Inspired by the biosynthesis of lomaiviticins, a late stage stereoselective oxidative enolate coupling was envisioned to construct the hindered central carbon-carbon bond. This stereoselective oxidative dimerization was achieved by tethering the C3 tertiary alcohol to C6 to give 7-oxanorbornanone **1.48** (Scheme 1-13). This also prevented the β-elimination of the C3 hydroxyl, due to the orthogonal orientation of the enolate π system and the antibonding σ* orbital of the bridging C-O bond. Shair's retrosynthetic analysis is shown in Scheme 1-13.

Scheme 1-13. Shair's retrosynthetic analysis

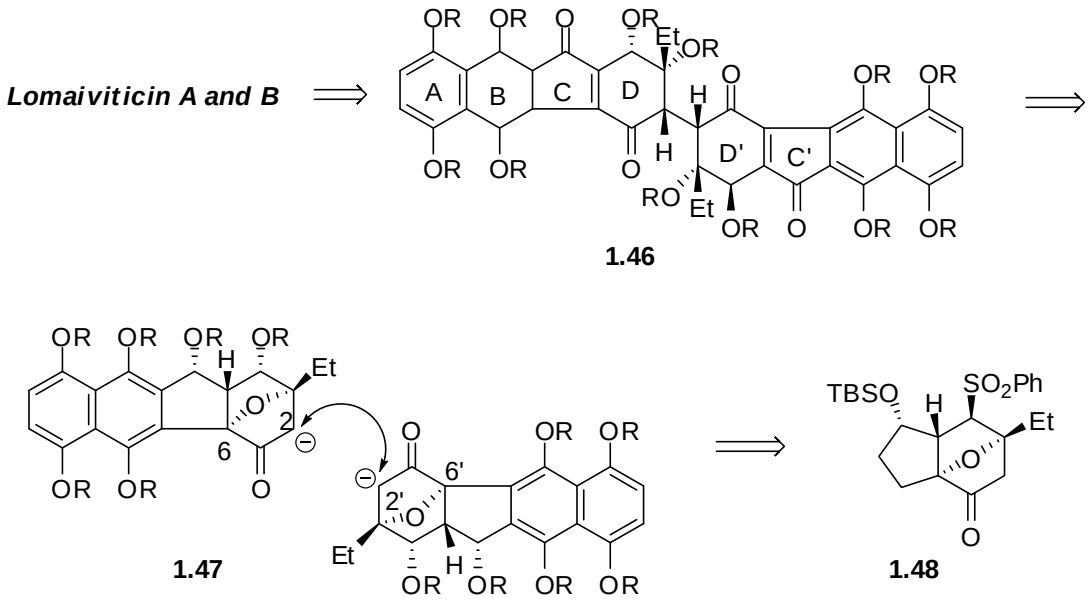

The synthesis began with the Michael addition of the lithium enolate of furanone **1.50** to the oxazolidinone acrylate **1.49** in 88% yield to furnish **1.51** as a 1:1 mixture of diastereomers. Mg^{II}-catalyzed anti-selective aldol reaction following the protocol by Evans with β-thiophenylacrolein and protected acetoxyfuran gave **1.52** in 77% yield. Scheme 1-14 shows Shair's synthesis of lomaiviticin A core structure. In a sequence of steps consisting of TBS protection, acetoxyfuran hydrolysis followed by oxidation with mCPBA, sulfone **1.53** was obtained. Intramolecular Diels-Alder cycloaddition smoothly led to the *endo* product as a 3:1 mixture of separable diastereomers. After a series of steps consisting of deprotection, hydrolysis and decarboxylation bicyclic compound **1.48**, was obtained in 45% yield. The pivotal oxidative dimerization was achieved stereoselectively using $[Cp_2Fe]PF_6$ at -20 °C, where a C_2-symmetric compound **1.55** was obtained as a single diastereomer. Desilylation followed by oxidation with Dess-Martin periodinane gave the cyclic hydrate **1.56**. Conversion of this cyclic hydrate to the lomaiviticin A core

system **1.57** was achieved by treatment with excess K_2CO_3/MeOH. However, all attempts to generate lomaiviticin B core system **1.58**, by the acid catalyzed dehydration only led to decomposition.

Scheme 1-14. Shair's synthesis of central core of lomaiviticin A

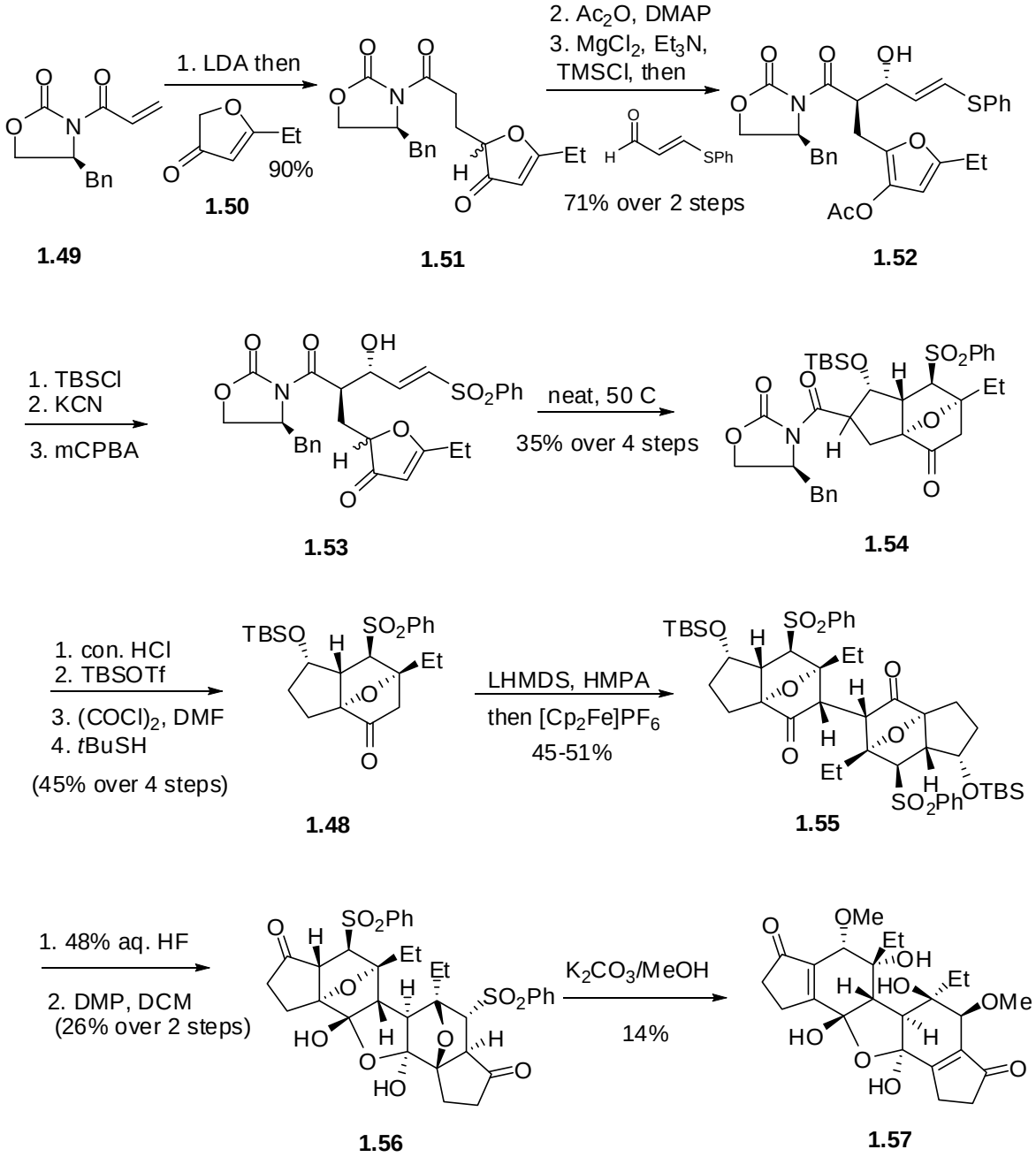

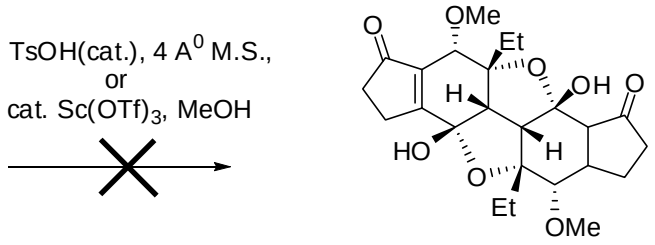

1.58

1.1.4.3 Sulikowski's approach to dideoxy core of lomaiviticin A/B

Recently, Sulikowski reported the synthesis of dideoxy core of lomaiviticins A and B **1.59**. The retrosynthetic analysis is shown in Scheme 1-15. Stereoselective construction of the four contiguous stereocenters in **1.59** were envisioned to arise via a tandem reaction consisting of double Michael addition on **1.61**, from the convex face of the molecule, followed by the stereoselective protonation of the enolates.

Scheme 1-15. Sulikowski's retrosynthetic analysis

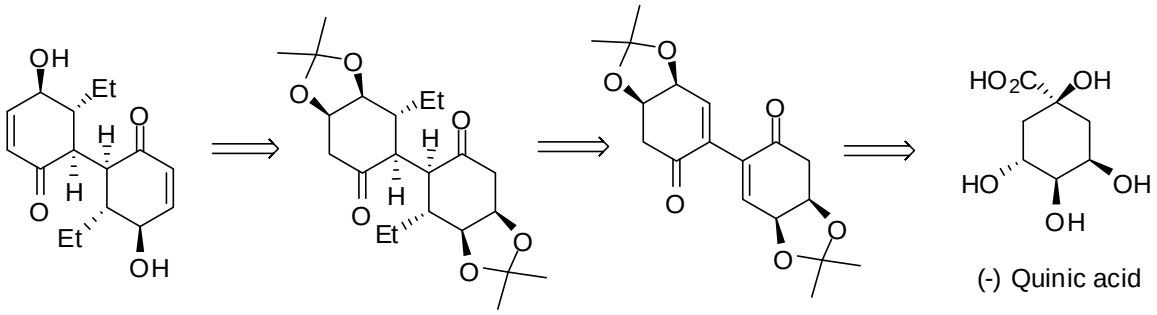

1.59 **1.60** **1.61**

The synthesis began from cyclohexenone **1.62**, which was prepared from (-)-quinic acid following a known procedure. Scheme 1-16 depicts the forward synthesis. α-iodination followed by Ni(0)-catalyzed homocoupling provided bisenone **1.61** in 64% yield. An allyl group was envisaged as a latent source of ethyl group, which was

introduced by the stereoselective conjugate addition of allyltributylstannane promoted by TBSOTf. The conjugate addition proceeded as expected from the convex face of the molecule away from the acetonide moiety. The bis-silylenol ether adduct **1.63**, was obtained in 97% yield. Transformation of the allyl group into an ethyl moiety was achieved in six steps. Stereoselective protonation and α,β-unsaturation was achieved in a single step by using TBAF, in 55% yield over 2 steps, thus furnishing the dideoxy core of lomaiviticin **1.59**.

Scheme 1-16. Sulikowski's synthesis of central core of dideoxy lomaiviticin

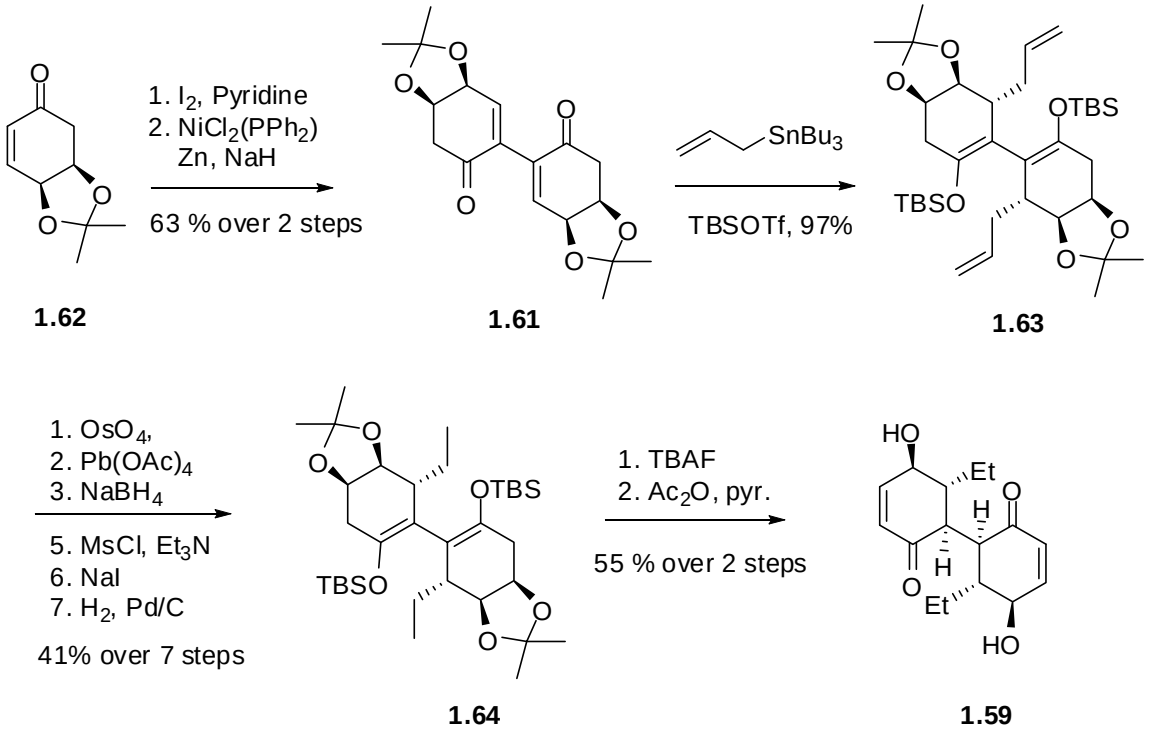

1.62 **1.61** **1.63**

1.64 **1.59**

In comparing the three strategies, Nicolaou's approach involved the use of a tether which served two purposes. Not only does it function as a latent source for the installation of the sensitive 1,4 dicarbonyls, but also formed a rigid tricyclic system to

stereoselectively introduce four of the six stereocenters present in the central core. Starting from the known bisenone **1.36**, the synthesis of lomaiviticin A and B core structures were achieved in 15 and 14 steps respectively. Unfortunately, nearly 12 of these 15 steps were targeted to elaborate the tether into a 1,4 dicarbonyl system. Shair's group, on the other hand, inspired by the biosynthesis of lomaiviticins, developed a more convergent approach to the central core of lomaiviticins. Using the rigid oxanorbornanone bicyclic system **1.48**, the hindered central carbon-carbon bond of lomaiviticin A was synthesized by the stereoselective oxidative coupling of the corresponding enolate. Starting from the known oxazolidinone **1.49**, the synthesis lomaiviticin A core structure, was achieved in 12 steps. Finally, Sulikowski's approach to the dideoxy lomaiviticine core structure relied on the stereoselective protonation of the bisenolates, which in turn was obtained by the stereoselective conjugate addition on bisenone **1.61**. It should be mentioned that at this point Sulikowski's approach does not address the total synthesis of lomaiviticins but provides a synthetic route to simplified analogues to evaluate their potential biological activity.

1.1.5 Summary

The unique molecular architecture and impressive biological activity of lomaiviticins A and B made it an attractive target to synthesis. Numerous reports of methodologies targeting the core of lomaiviticins have appeared and several hypotheses have been put forward to explain their mechanism of action. Despite this effort, total synthesis of these molecules has not yet been achieved.

1.1.6 References

1. He, H.; Ding, W.-D.; Bernan, V. s.; Richardson. A. D.; Ireland, C. M.; Greenstein, M.; Ellestad, G. A.; Carter, G. T. *J. Am. Chem. Soc*. **2001**, *123*, 5362-5363.
2. Gould, S. J. *Chem. Rev.* **1997**, 97, 2499-2509.
3. Monks, A.; Scudiero, D.; Skehan, P. *J. Natl. Cancer Inst.* **1991**, *83*, 738-40.
4. Cone, M. C. M.; Melville, C. R.; Gore, M. P.; Gould, S. J. *J. Org. Chem.* **1993**, *58*, 1058.
5. Isolation of kinamycins, their antibiotic activity and the original structure determination: (a) Ito, S.; Matsuya, T.; Omura, S.; Otani, M.; Nakagawa, A.; Takeshima, H.; Iwai, Y.; Ohtani, M.; Hata, T. *J. Antibiot*. **1970**, *23*, 315-317; (b) Hata, T.; Omura, S.; Iwai. Y.; Nakagawa, A.; Otani, M.; Ito, S.; Matsuya, T. *J. Antibiot*. **1971**, *24*, 353-359; (c) Omura, S.; Nakagawa, A.; Yamada, H.; Hata, T.; Furusaki, A.; Watanabe, T. *Chem. Pharm. Bull*. **1971**, *19*, 2429-2430; (d) Omura, S.; Nakagawa, A.; Yamada, H.; Hata, T.; Furusaki, A.; Watanabe, T. *Chem. Pharm. Bull*. **1973**, *21*, 931-940.
6. (a) Gould, S. J.; Tamayo, N.; Cone, M. C. *J. Am. Chem. Soc.* **1994**, *116*, 2207-09 and the references therein. (b) Mithani, S.; Weeratunga, G.; Taylor, N. J.; Dmitrienko, G. I. *J. Am. Chem. Soc.* **1994**, *116*, 2209-10. (c) Sato, S.; Geckle, M.; gould, S. J. *Tetrahedron Lett.* **1985**, *26*, 4019.
7. Arya, D. P. *Top. Heterocyl. Chem* . **2006**, *2*, 129-152.
8. (a) Arya, D. P.; Jebaratnum, D. J. *J. Org. Chem.* **1995**, *60*, 3268. (b) R. S. Laufer, G. I. Dmitrienko, *J. Am. Chem. Soc.* **2002**, *124*, 1854-1855; (c) K. S. Feldman, K.

J. Eastman, *J. Am. Chem. Soc.* **2005**, *127*, 15344-15345; (d) K. S. Feldman, K. J. Eastman, *J. Am. Chem. Soc.* **2006**, *128*, 12562-73

9. (a) Subbe, J.; Kozarich, J. W. *Chem. Rev*. **1987**, *87*, 1107-1136. (b) Murphy, J. A.; Griffiths, J. *Nat. Prod. Rep*. **1993**, 551-564. (c) Dussy, A.; Meggars, E.; Giese, b. *J. Am. Chem. Soc*. **1998**, *120*, 7339-7403.
10. Sugiyama, H.; Fujiwara, T.; Saito, I. *Tetrahedron Lett*. **1994**, *35*, 8825-8828.
11. (a) Nicolaou, K. C.; Li, H.; Nold, A. L.; Pappo, D. P.; Lenzen, A. *J. Am. Chem. Soc*. **2007**, *129*, 10356-10357. (b) Lei, X.; Jr. Porco, J. A. *J. Am. Chem. Soc*. **2006**, *128*, 14790-14791. (b) Nicolaou, K. C.; Li, H. M. *Angew. Chem. Int. Ed*. **2009**, *48*, 5860-5863.
12. Nicolaou, K. C.; Denton, r. M.; Lenzen, A.; Edmonds, D. J.; Li, A.; Milburn, R. R.; Harrison, S. T.; *Angew. Chem. Int. Ed*. **2006**, *45*, 2076-2081.
13. Krygowski, E. S.; Murphy-Benenato, K.; Shair, M. D. *Angew. Chem. Int. Ed*. **2008**, *47*, 1680-1684.
14. Zhang, W. D.; Baranczak, A.; Sulikowski, G. A. *Org. Lett*. **2008**, *10*, 1939-1941.
15. Gholap, S. L.; Woo, C. M.; Ravikumar, P. C. *Org. Lett*. **2009**, *11*, 4322-4325.

1.2 Results and Discussion

1.2.1 Our approach to lomaiviticin core structure

ortho-Quinols and masked *ortho*-benzoquinones (Scheme 1-17) are potential useful building blocks for the enantioselective synthesis of natural products.[1] They are attractive starting points from which numerous total syntheses begin. They are usually generated by oxidation of phenols by a variety of methods and reagents like $Pb(OAc)_4$, $NaIO_4$, Iodine(III) reagents, anodic oxidation, etc.

Scheme 1-17. *ortho*-Quinols and masked *ortho*-benzoquinones

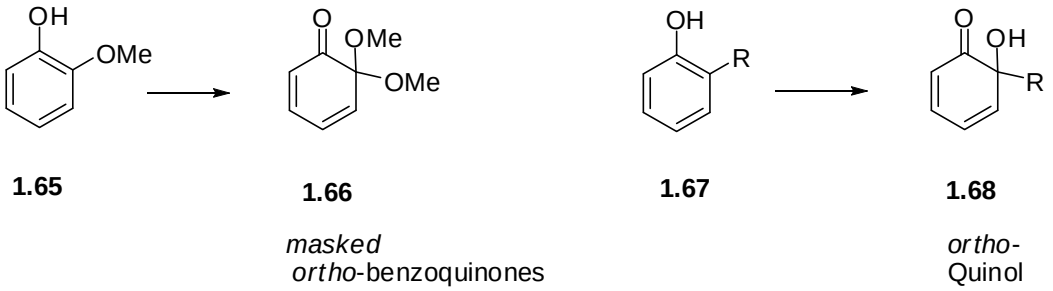

1.65 **1.66** **1.67** **1.68**

masked *ortho*-benzoquinones

ortho-Quinol

To a large extent, the stability and mode of reactivity of these intermediates depends on the type of substitution on the ring.[2] The chemistry of *ortho*-quinols **1.68** and masked *ortho*-benzoquinones **1.66** (Scheme 1-17) is dominated by their propensity toward self dimerization via the intermolecular Diels-Alder reaction. Pioneering studies by Adler showed that this dimerization proceeds with remarkable regio- and stereoselectivity.[3-11] The stereochemical aspect of the self dimerization of *ortho*-quinols is discussed first. Theoretically, 16 diastereomers could be generated during the dimerization of racemic *ortho*-quinols; nevertheless, only one is typically observed,

suggesting the dimerization of the opposite enantiomers is not favorable. In this case, the diene and the dienophile approach via their oxygenated faces as shown in Scheme 1-18. Although the exact reason is not clearly understood, a C_2-symmetric transition state has been invoked by Quideau to explain this facial selectivity.[12] It is pertinent to mention here that the dimerization of *ortho*-quinols is usually considered a nuisance and most efforts were directed so far to harness the reactivity of these compounds toward intermolecular Diels-Alder reaction with external dienes and dienophiles.[13-22]

Scheme 1-18. Self dimerization of *ortho*-quinols

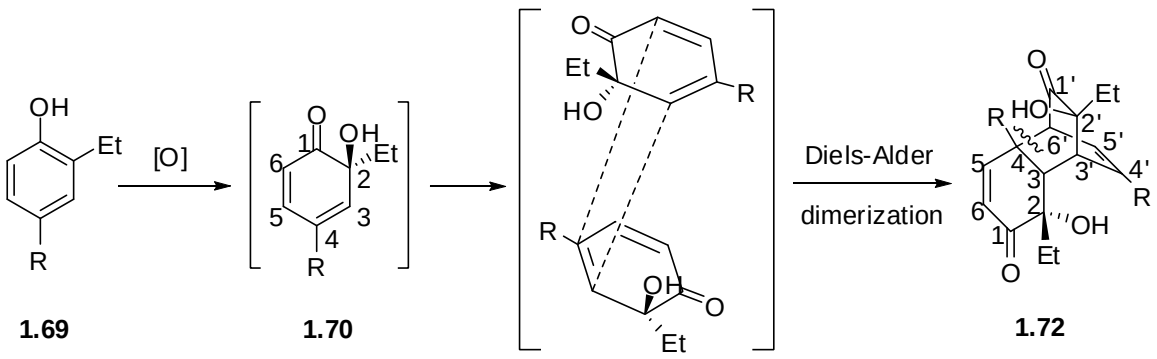

1.69 **1.70** **1.71** **1.72**

In contemplating a novel synthetic strategy toward lomaiviticins, we realized that the central core of lomaiviticin is embedded in these dimeric structures as shown in Scheme 1-19. Remarkably, 4 of the 6 stereocenters are set correctly in the Diels-Alder step, and the remaining two can be easily set by the stereoselective reduction of the carbonyls, capitalizing the facial bias provided by the rigidity of the tricyclic system. Fragmentation of the C4-C6 ′ bond in **1.72** would generate the central core of lomaiviticin.

Scheme 1-19. Central core of lomaiviticins embedded in *ortho*-quinol dimers

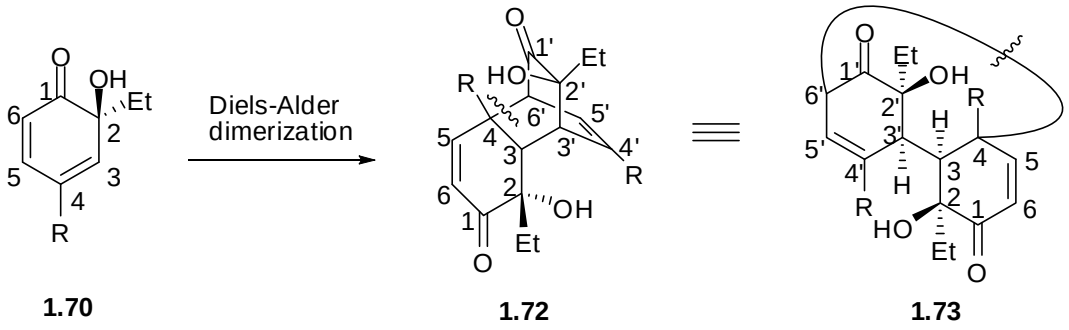

1.70 **1.72** **1.73**

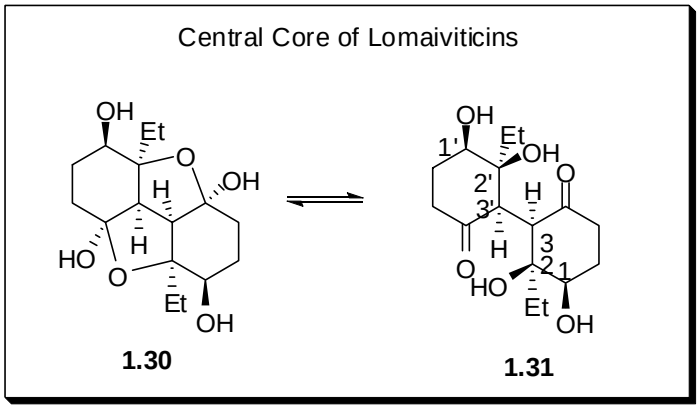

1.30 **1.31**

The chemistry of masked *ortho*-benzoquinones **1.74** is similar to that of *ortho*-quinols **1.69**. The self dimerization of masked *ortho*-benzoquinones is also known to proceed regio- and stereoselectively via the intermolecular Diels-Alder reaction, shown in Scheme 1-20. It should be noted in this case, dimer **1.77** contains 2 of the 6 stereocenters present in the central core of lomaiviticins.

Scheme 1-20. Self dimerization of masked *ortho*-benzoquinones

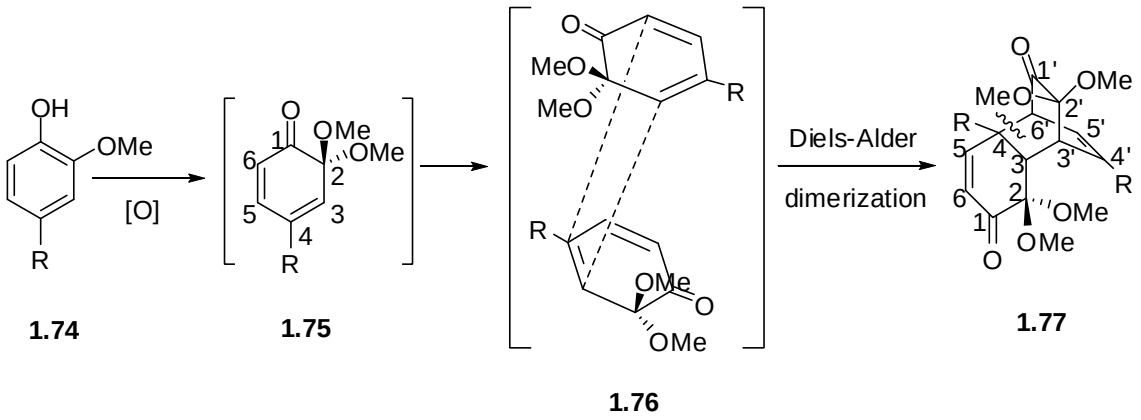

1.2.2 Proposed fragmentation strategies

Unraveling these Diels-Alder dimers into the densely functionalized central core of lomaiviticins required us to consider several fragmentation strategies. The general idea envisaged for the scission the extra *carbon-carbon* bond is illustrated in Scheme 1-21. Both anionic and free radical pathways could potentially be suitable for the scission of the extra bond. It should be mentioned here that this fragmentation could in principle be induced from either end of the tricyclic system depending on the groups X and Y. Examination of 3D models indicated that X-C5, C4-C6′ and C5′-Y bonds involved in this process are nearly antiperiplanar to one another.

Scheme 1-21. Proposed anionic and free radical fragmentation strategies

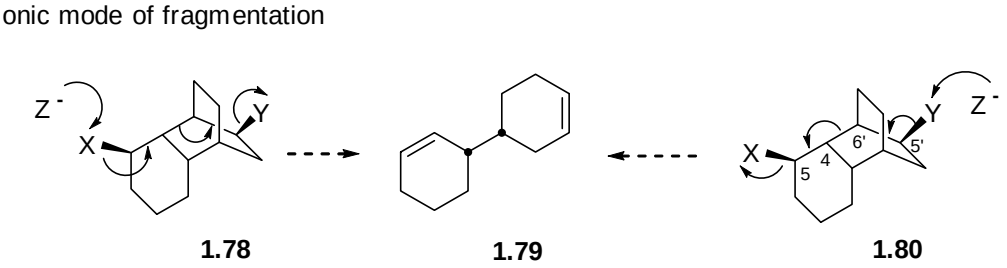

Free radical mode of fragmentation

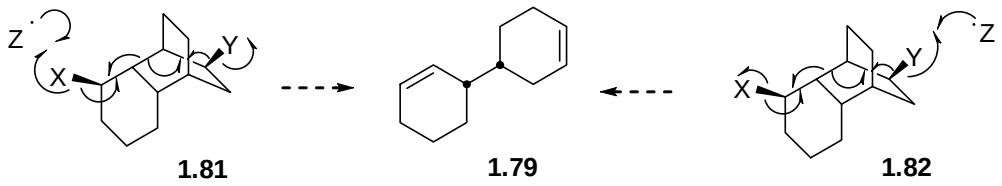

1.81 **1.79** **1.82**

1.2.3 Ionic mode of fragmentation

The ionic mode of fragmentation with X = $SnMe_3$ and Y = I was explored first. The readily accessible *ortho*-quinol dimer **1.83** was chosen for this model study. This was obtained by the oxidation of 2,4-dimethyl phenol using sodium periodate following the protocol by Adler.[3] The synthesis began with the introduction of Me_3Sn- moiety by Michael addition following the protocol by Still as depicted in Scheme 1-22.[23] With access to **1.84**, we focused our attention on the formation of the cyclic ether with the hydroxyl on C2 by a 5-*exo-trig* cyclization onto the tri-substituted double bond. Unfortunately, all attempts to render this cyclization using NBS, NIS, Br_2, I_2, mCPBA only led to decomposition of **1.84**. ^{1}H NMR data suggested that Me_3Sn- moiety competes with the olefin for the electrophile leading to a complex mixture of products presumably via **1.87**. Attempts to use the tetra-ol **1.85** obtained by the $NaBH_4$ reduction of **1.84** also failed, as the decomposition of this compound could not be avoided. It was decided at this point that the installation of Me_3Sn- moiety should be deferred and electrophilic cyclization should be investigated first. Unfortunately, all attempts to effect iodo cyclization on Diels-Alder dimer **1.83** also failed to generate **1.86** and only the starting material was recovered. We attributed this to the poor solubility of **1.83** in common organic solvents.

Scheme 1-22. Attempted synthesis of 1.92

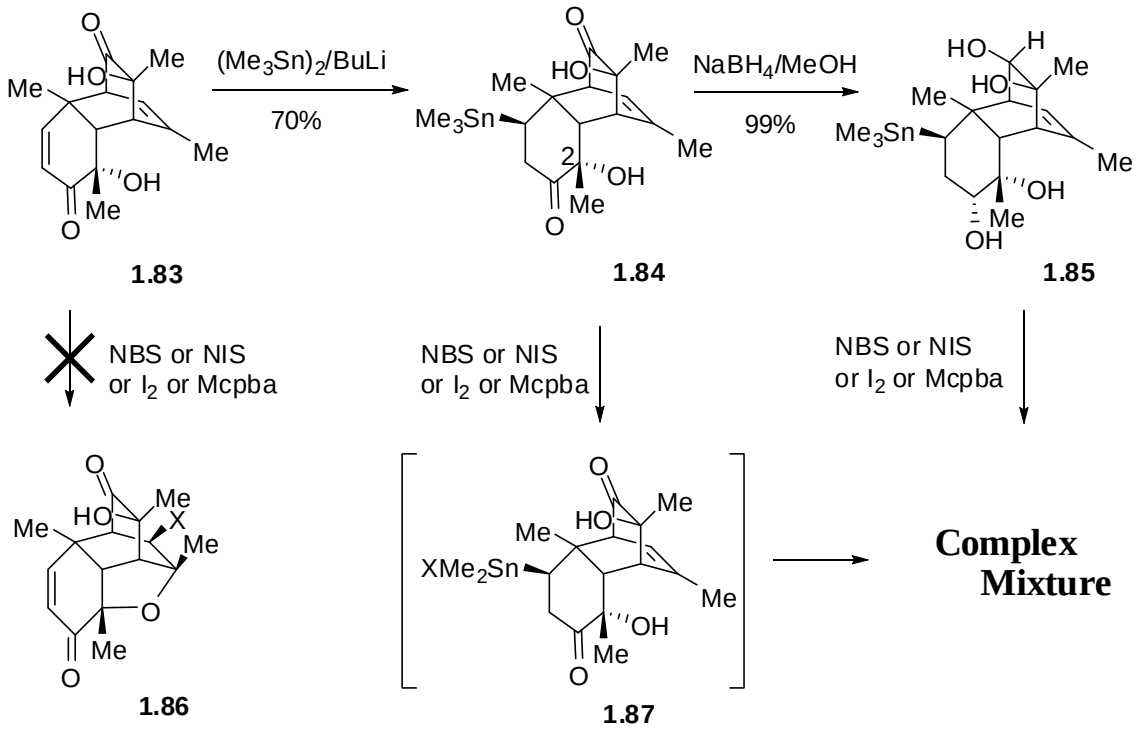

However, when **1.88** was subjected to iodo cyclization **1.89** was isolated in 75% yield as shown in Scheme 1-23. **1.88** was obtained by chemoselective reduction of the conjugated double bond.[3] Having now established a viable route to **1.89**, α,β-unsaturation was introduced in a two step sequence. First, TMS enol ether **1.90** was prepared following the procedure reported by Corey.[24] Saegusa oxidation with $Pd(OAc)_2$ successfully regenerated the α,β-unsaturation.[25] The tertiary alcohol on C2′ remained protected as TMS ether giving **1.91** in 75% yield. To our dismay, addition of Me_3SnLi did not produce **1.92**. Instead, **1.91** underwent opening of the tetrahydrofuran ring via **1.93** producing **1.83** in 30% yield along with 40% recovery of the starting material.

Scheme 1-23. Attempted ionic fragmentation on 1.92

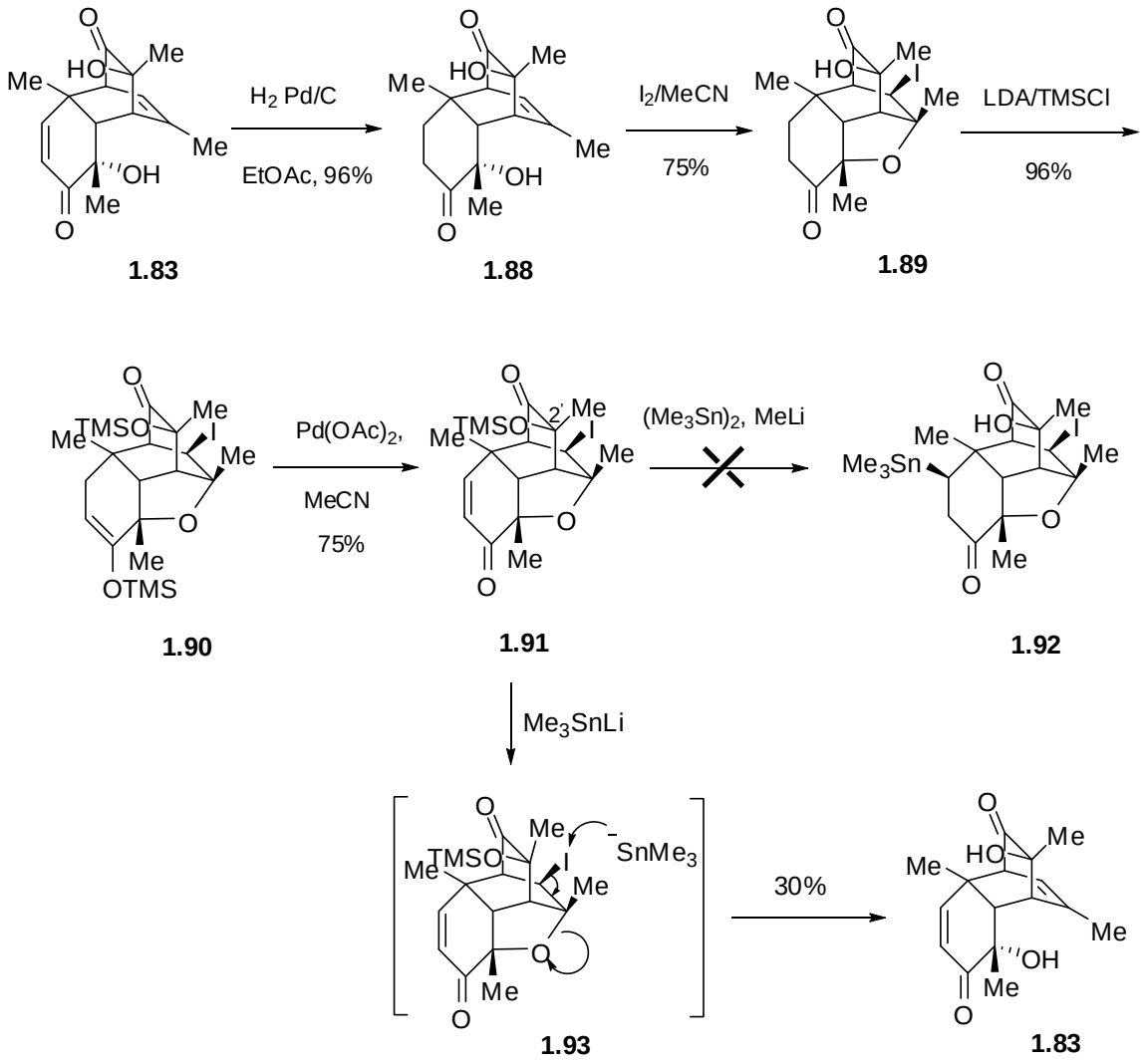

In the end, it was clear that the Me_3Sn- moiety needed to be replaced by a more robust group. Literature search showed PhSe- moiety as a promising candidate. Miyashita and Yoshikoshi showed that PhSeH generated *in situ* by the reduction of $(PhSe)_2$ with $NaBH_4$ followed by the addition of acetic acid, adds to a variety of unsaturated enones in excellent yields.[26] This opened the door to free radical pathway proposed in the previous section, shown in Scheme 1-21.

1.2.4 Free radical mode of fragmentation

At first we attempted Michael addition of PhSeH on **1.83**. Unfortunately, only starting material was recovered. We attributed this to the poor solubility of the dimer and protected it as the diacetate **1.94** with $HClO_4$ and Ac_2O. Michael addition proceeded smoothly to give **1.95** in 90% yield. Global reduction with DIBAL-H in THF gave tetra-ol **1.96**. It should be mentioned that **1.96** contains all the six stereocenters present in the central core of lomaivicitin. Our fears regarding the stability of PhSe- moiety during the iodo cyclization, were soon dispelled when **1.97** was obtained in 58% yield (66% yield BRSM) as shown in Scheme 1-24. More importantly, chemoselective cyclization of the hydroxyl at C2 in preference to the hydroxyl at C1, occurred as planned to generate the 5-membered cyclic ether **1.97**.

Scheme 1-24. Synthesis of fragmentation precursor 1.97

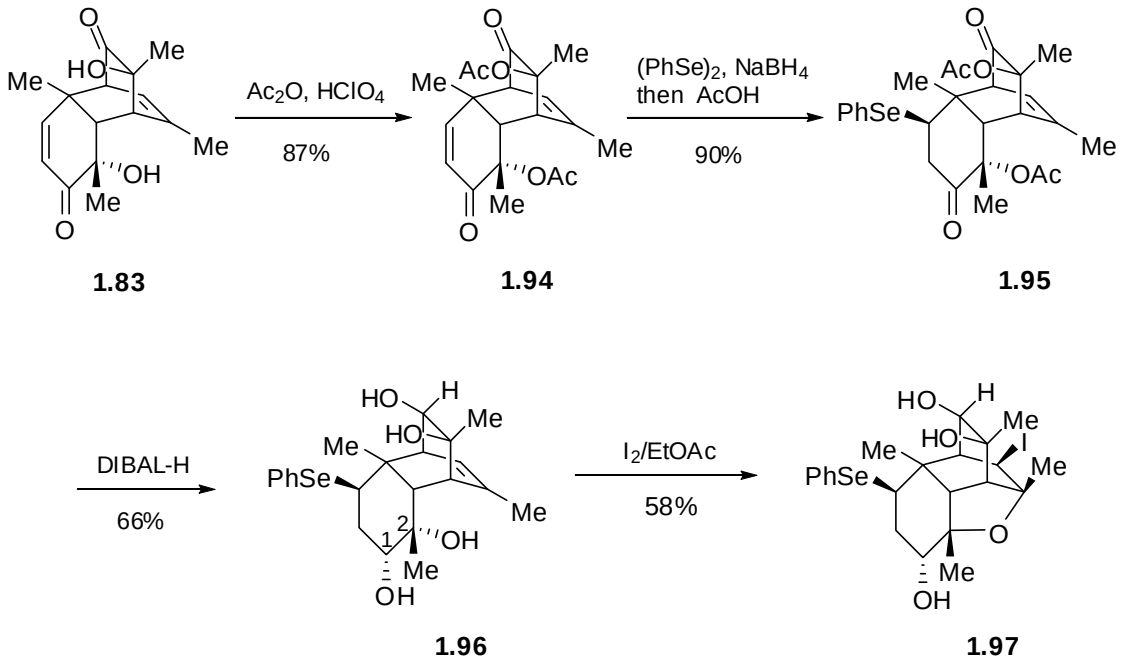

The structure of the tetra-ol **1.96** is confirmed from its experimentally observed NOE interactions shown in Scheme 1-25. A strong NOE between H_{11} and Me_{16} suggested they are on the same side. A strong NOE was observed between H_1 and Me_{14}, H_1 and H_9, H_1 and Me_{15}, and H_1 and H_{2b} indicating they are on the same side of the molecule. On the other hand, H_1 had a weak NOE interaction with H_{2a} indicating they are away from each other. H_{2a} on the other hand, showed a strong NOE with H_3 indicating they are on the same face of the molecule. To summarize, Michael addition of the PhSe- moiety and the global reduction with DIBAL-H proceeded from the convex face of the molecule as expected.

Scheme 1-25. Diagnostic NOE interactions in tetra-ol 1.96

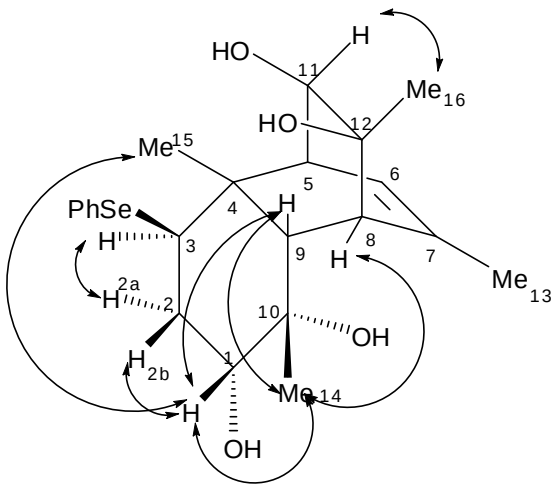

1.96

With access to the key precursor **1.97**, free radical conditions for the scission of the C4-C6´ bond were explored as shown in Scheme 1-26. Under these conditions a single compound, tentatively assigned **"A"**, was isolated in 46% yield. Compound **A** showed a molecular ion peak m/z 280.17 which is consistent with the desired structure

1.98 or **1.99**. However, ^{1}H NMR for the compound **A** (Scheme 1-27) showed only two vinyl hydrogen peaks between 5-6 ppm. If the fragmentation occurred as planned, the product would have the structure **1.98** with three peaks (H_1, H_2 and H_3) in the vinylic region (5-6 ppm) in the ^{1}H NMR. Clearly, this possibility was immediately ruled out.

Scheme 1-26. Results from free radical mode of fragmentation

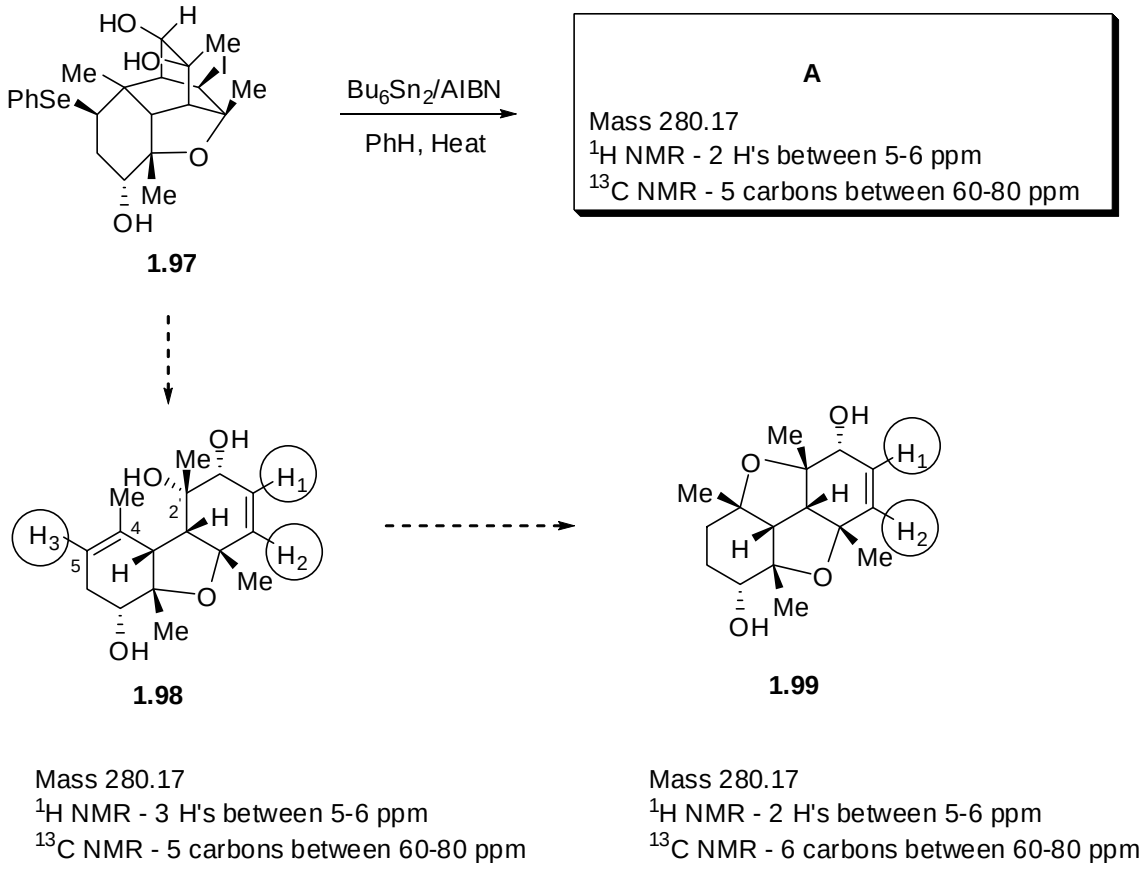

At first, we tried to reconcile our spectroscopic data with structure **1.99**, which could conceivably arise from **1.98**. However, the ^{13}C NMR spectrum of **A** (Scheme 1-28) did not agree with this structural assignment. For example, one would predict that ^{13}C NMR of **1.99** should contain six peaks connected to oxygen in the region 60 to 80 ppm.

Unfortunately, compound **A** showed only five peaks in that region. In the end, it was clear that neither **1.98** nor **1.99** fit the description for **A**. After considering several other structures that did not show promise, it occurred to us that the structural assignment so far has been on the premise that the fragmentation took place and the possibility that the reaction is proceeding via a different pathway should also be considered.

Scheme 1-27. ^{1}H NMR for compound A

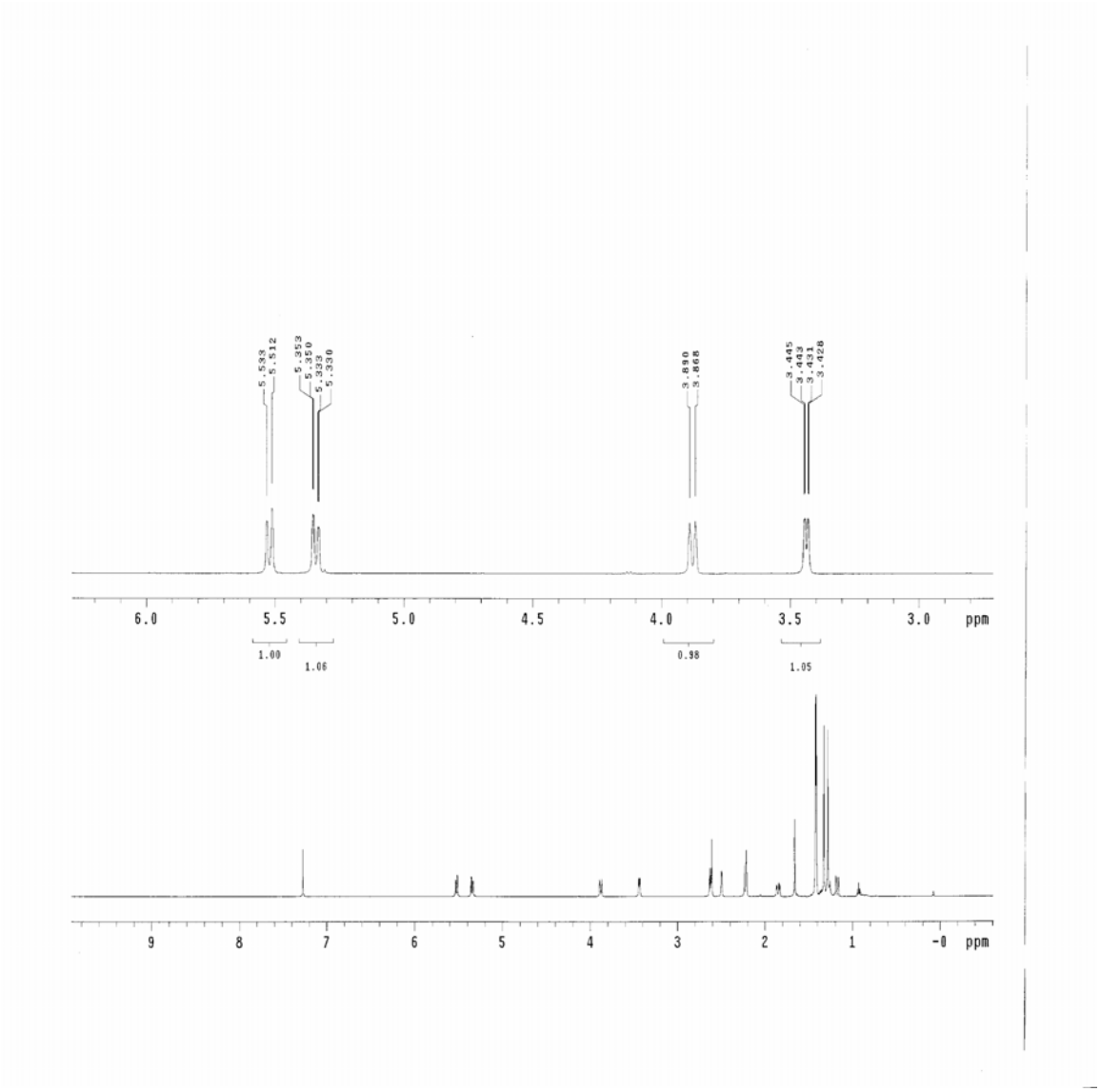

Scheme 1-28. ^{13}C NMR for compound A

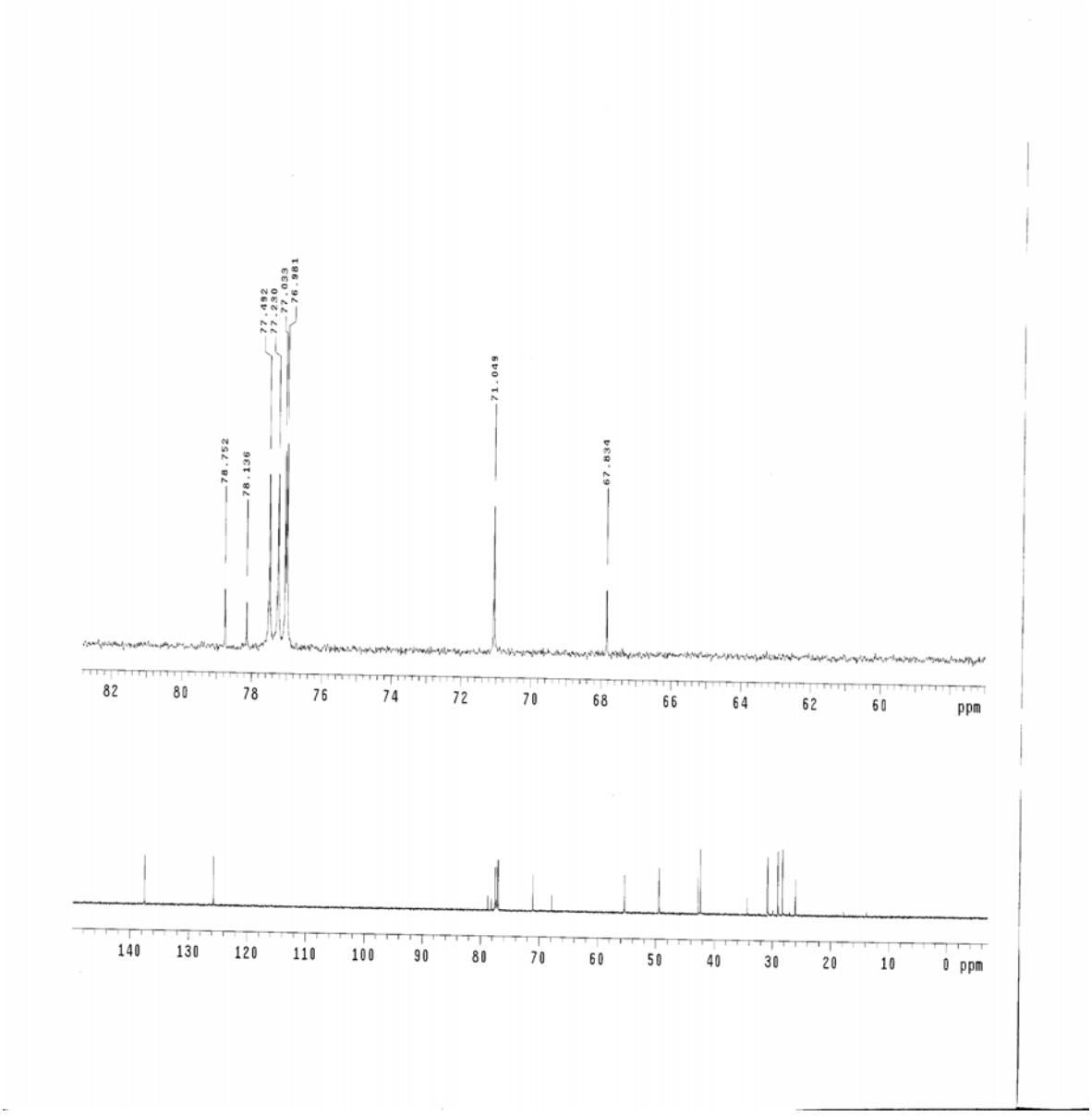

Our proposal was borne from the fact that the difference in mass between **1.97** and compound **A** is 280.86 which corresponds to a loss of PhSeI. We realized that the secondary radical **1.100** generated during the propagation step, might undergo a 1,5 hydrogen abstraction to generate **1.101**. This would be followed by expulsion of the PhSe- moiety to form **1.102** as shown in Scheme 1-29. Predicted ^{1}H and ^{13}C NMR for compound **1.102** seemed to fit the data for compound A.

Scheme 1-29. Mechanistic proposal for the formation of compound A

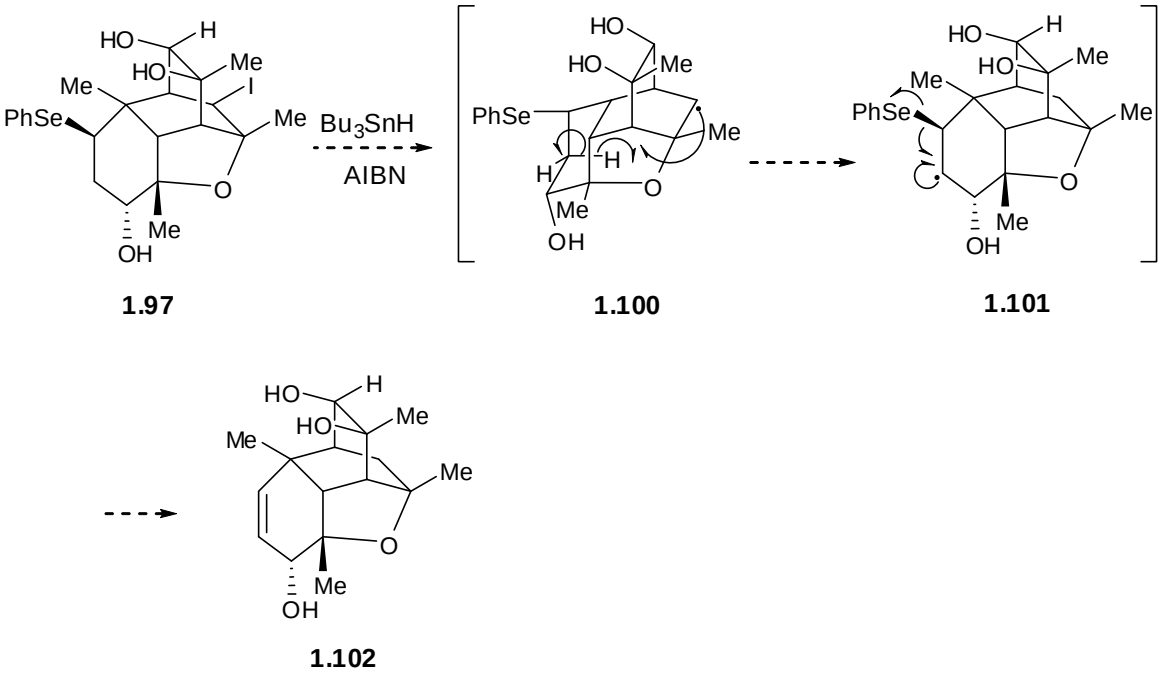

The proposed structure for compound **A** was confirmed by its independent synthesis from **1.97** in two steps shown in Scheme 1-30. H_2O_2 oxidation of **1.97** followed by reduction with Bu_3SnH and AIBN gave **1.102** in 96% yield over two steps. Compound **A** and **1.102** have identical ^{1}H and ^{13}C NMR finally putting this structural ambiguity to rest.

Scheme 1-30. Synthesis of the proposed structure for compound A

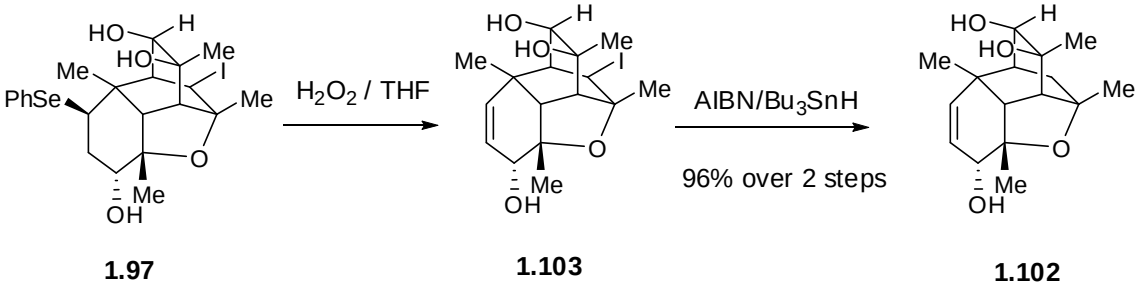

1.2.5 Reductive mode of fragmentation

The reductive mode of fragmentation with Y = SO_2Ar shown in Scheme 1-31 was investigated next. It should be mentioned that this mode of fragmentation is a vinylogous analog of the anionic fragmentation pathway (Scheme 1-21) proposed earlier. Fragmentation can be initiated by chemoselective reduction of the allyl sulfone, which can be achieved with variety of reagents eg., SmI_2, LDDB, Li in naphthalene etc. The *in situ* generated allyl anion **1.107** during this process was expected to fragment *via* the expulsion of sulfinate, as shown in Scheme 1-31. The expulsion of the weaker sulfinate base ($ArSO_2^-$) when compared to the allyl anion **1.107** was expected to provide the driving force for this reaction.

Scheme 1-31. Reductive mode of fragmentation

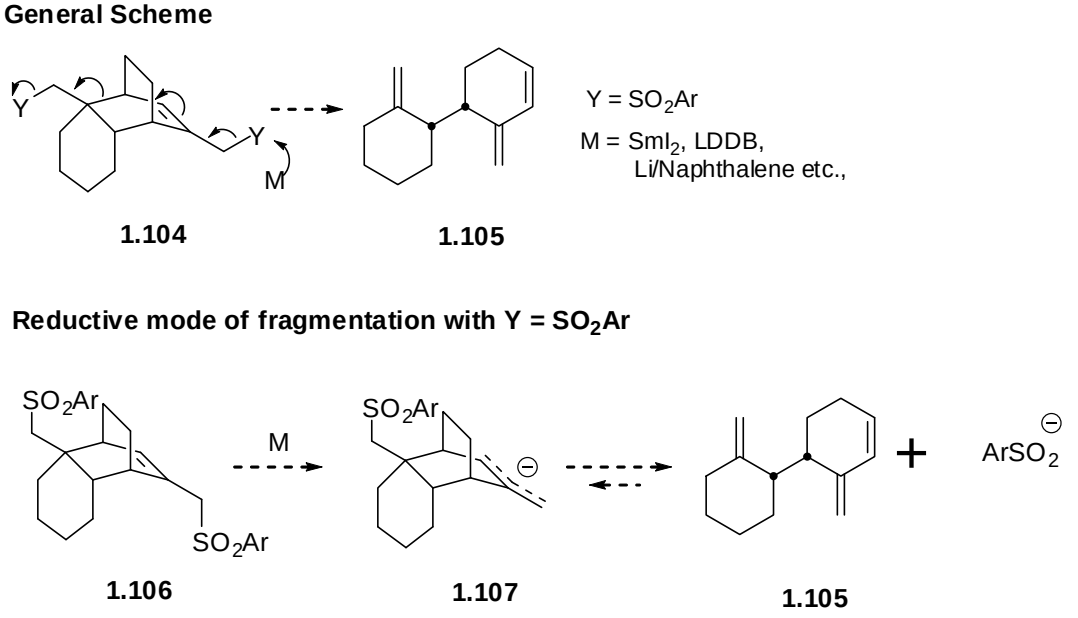

For the sake of experimental convenience, in this case, we decided to use masked *ortho*-benzoquinone Diels-Alder dimers instead of *ortho*-quinol dimers. The synthesis

began by preparing sulfone **1.108** from commercially available vanillyl alcohol and sodium *para*-toluenesulfinate as shown in Scheme 1-32.[27] Oxidation of **1.108** with iodobenzene-diacetate generated masked *ortho*-benzoquinone **1.109** which dimerized spontaneously to give Diels-Alder dimer **1.110** in quantitative yield.[28] Luche reduction followed by hydrolysis of the ketal under mild conditions gave **1.111**.

Scheme 1-32. Attempted addition of ethyl groups to 1.112

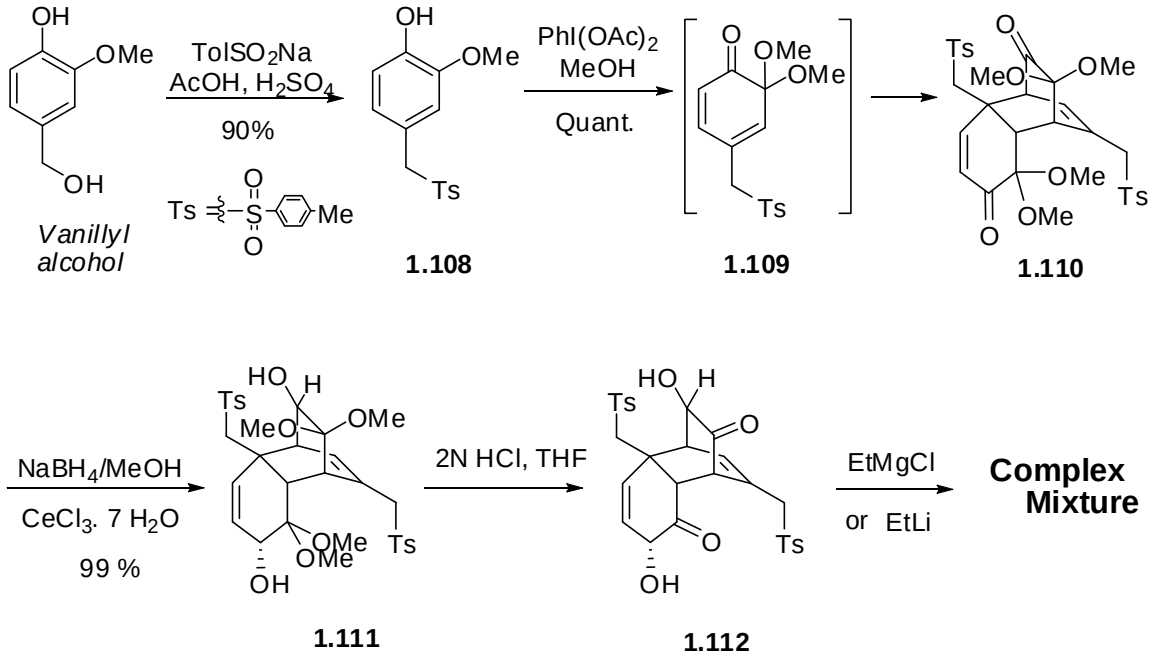

Initial attempts to add the ethyl groups using EtLi or EtMgBr to **1.112** led to the decomposition of the starting material. Suprisingly, ethyl cerium reagent[29] gave rise to **1.114** in 30% yield. The structure of **1.114** was confirmed by its independent synthesis from vanillyl alcohol. We presume that the formation of **1.114** is due to a facile retro Diels-Alder via the formation of ene-diol **1.113** shown in Scheme 1-33.

Scheme 1-33. Retro Diels-Alder reaction decomposition pathway

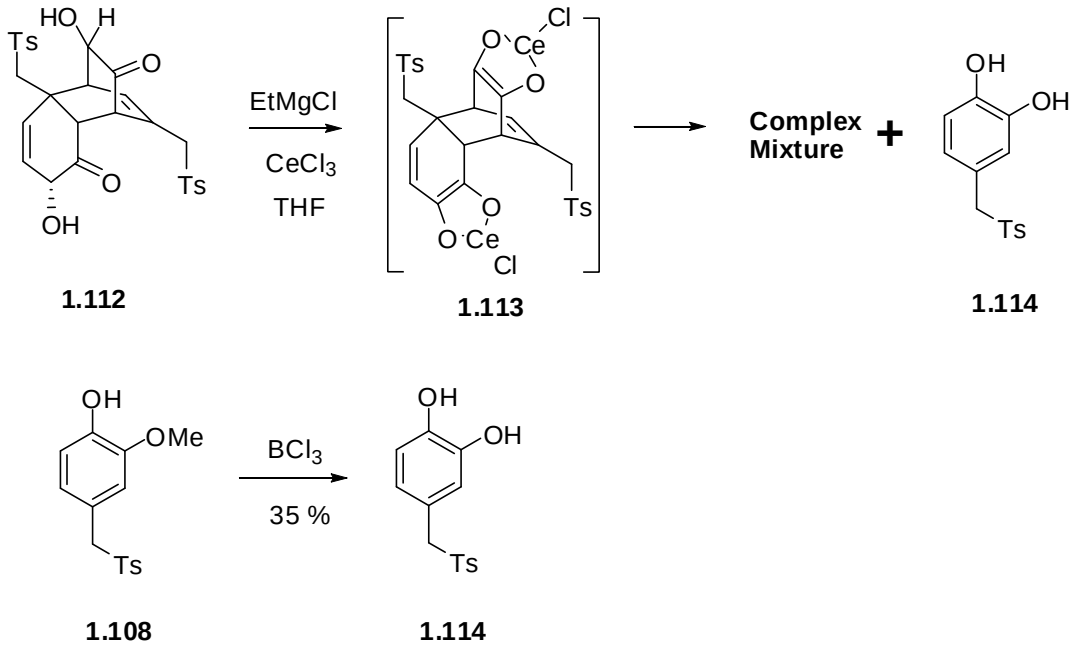

The nucleophilic addition was eventually achieved by adopting a three step sequence as shown in Scheme 1-34. Transient protection of the hydroxyl groups as MIP ethers **1.115**, was achieved with 2-methoxy propene and PPTS. This was followed by the addition of Et_2CeCl[29] to give the diol **1.116**. Further, treatment of crude 3.34 with excess 2-methoxy propene and PPTS afforded the bis acetonide **1.117** in 54% yield over three steps. Our rationale for the stereoselectivity during the nucleophilic addition to the carbonyls was based on the rigidity of the bicyclic system which has a convex and convcave face. As anticipated, the nucleophilic attack on both of the carbonyls occurred from the convex faces in **1.115** setting the remaining two stereocenters in the central core of lomaiviticins.

Scheme 1-34. Successful synthesis of the reductive fragmentation precursor 1.117

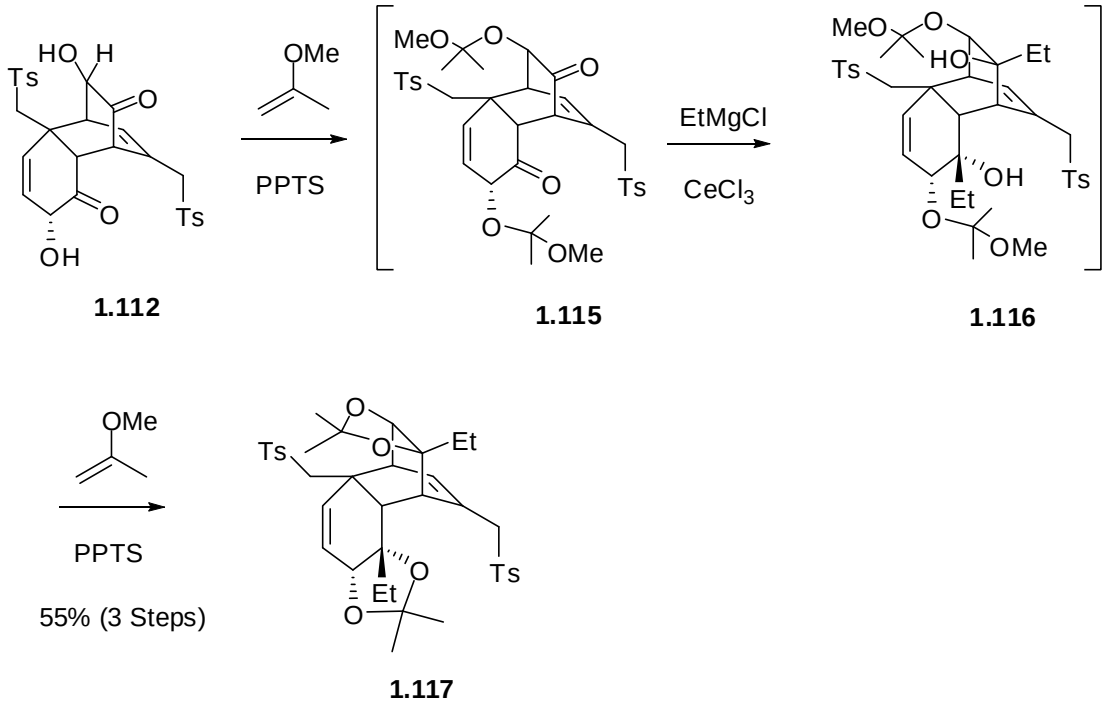

With sufficient quantities of **1.117** in hand, we investigated its reduction with SmI_2 in THF. Only the starting materials were recovered in this case. The reduction of the allyl sulfone moiety proceeded uneventfully upon the addition of three equivalents of degassed HMPA to which SmI_2 in THF was added.[30] To our surprise, the allyl anion **1.118** generated did not fragment the C4-C6′ bond to give **1.120**, instead an inseparable mixture of regioisomers **1.119** were obtained in 68% yield (Scheme 1-35). To eliminate the possibility of quenching the allyl anion **1.118** generated during this process by **1.117**, the order of addition was changed. Accordingly, to a degassed solution of HMPA, SmI_2 in THF was added. To this, a solution of **1.117** in THF was added slowly over 30 minutes. Unfortunately, this did not change the outcome of the reaction and **1.119** was obtained in 70% yield but **1.120** was never observed. Changing the reductant to

Li/naphthalene[31] also did not change the course of this reaction and the allyl anion **1.118** proved reluctant to fragment C4-C6′ bond. In this case, **1.119** was obtained in slightly lower yields (54%).

Scheme 1-35. Failure of the reductive mode of fragmentation

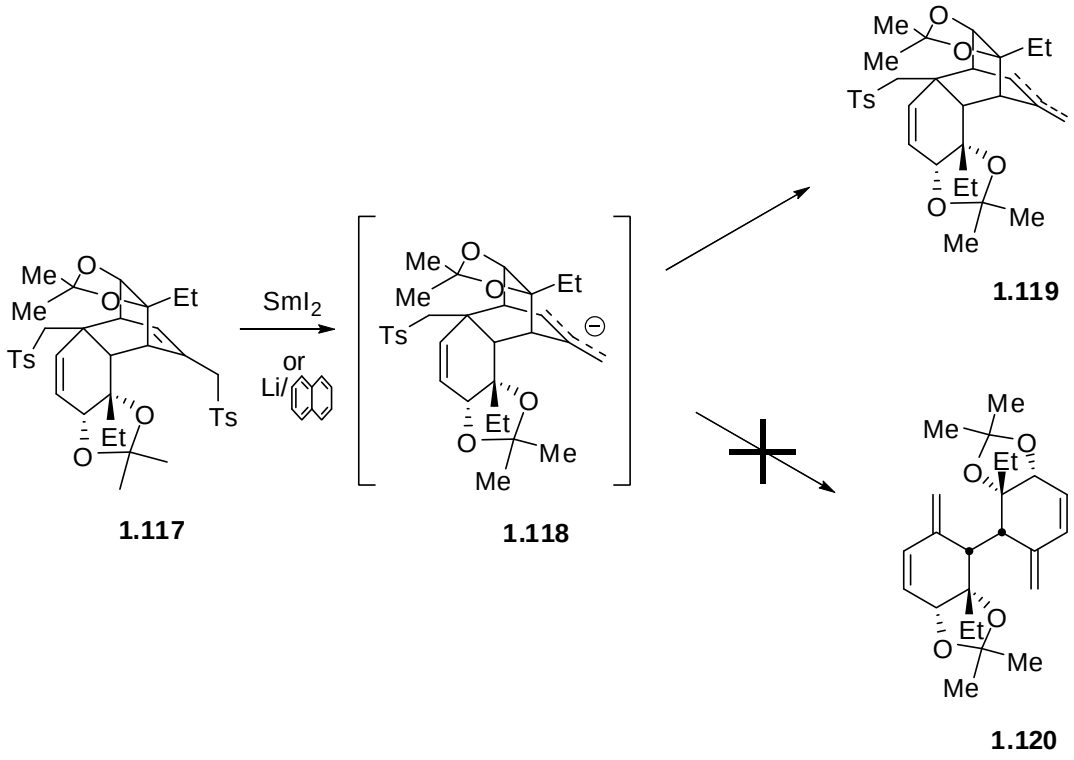

1.2.6 Summary

ortho-Quinols and masked *ortho*-benzoquinone dimers were recognized as suitable starting materials for the construction of the central core of lomaiviticins. We realized that the central core of lomaiviticins was embedded in the *ortho*-quinol and *ortho*-benzoquinone dimers requiring the scission of an extra carbon-carbon bond to be unraveled. Realization of this strategy required us to investigate several modes of fragmentation for the scission of this extra bond. However, all attempts directed to

unravel these dimers into the lomaiviticin core were unsuccessful. The methodology developed for elaborating *ortho*-quinol and *ortho*-quinone monoketal dimers into the central core of lomaiviticins in this project will be useful for further studies in this direction.

1.2.7 References

1. (a) Magdziak, S. J.; Pettus, T. R. R. *Chem. Rev*. **2004**, *104*, 1383-1430. (b) Liao, CC.; Peddinti, K. *Acc. Chem. Res*. **2002**, *35*, 856-866.
2. Liao, C-C.; Chu, C-S.; Lee, T-H.; Rao, P. D.; Ko, S.; Song, L-D.; Shiao, H-C. *J. Org. Chem*. **1999**, *64*, 4102-4110, and references therein. (stability aspects)
3. Adler, E.; Junghahn, L.; Lindberg, U.; Berggren, B.; Westin, G. *Acta. Chem. Scand*. **1960**, *14*, 1261-1273.
4. Adler, E.; Holmberg, K. *Acta. Chem. Scand*. **1971**, *25*, 2775-2776.
5. Karlsson, B.; Gaard, P. K.; Pilotti, A-M.; Weihager, A-C.; Lindgreen, B. O. *Acta. Chem. Scand*. **1973**, *5*, 1428.
6. Adler, E.; Holmberg, K.; *Acta. Chem. Scand. B*. **1974**, *5*, 549-554.
7. Holmberg, K. *Acta. Chem. Scand. B*. **1974**, *28*, 857-865.
8. Holmberg, K.; Kirudd, H.; Westin, G.; *Acta. Chem. Scand. B*. **1974**, *28*, 913-921.
9. Adler, E.; Andersson, G.; Edman, E.; *Acta. Chem. Scand. B*. **1975**, *29*, 909-920.
10. Andersson, G. *Acta. Chem. Scand. B*. **1976**, *30*, 64-70.
11. Karlsson, B.; Lindgreen, B. O.; Pilotti, A-M.; Soderholm, A-C. *Acta. Chem. Scand. B*. **1977**, *31*, 436-438.
12. Gagnepain, J.; Castet, F.; Quideau, S. *Angew. Chem. Int. Ed*. **2007**, *46*, 1533-5.

13. Hsu, D-S.; Liao, CC. *Org. Lett*. **2007**, *9*, 4563-4565.

14. Hsu, D-S.; Liao, CC. *Org. Lett*. **2003**, *5*, 4741-4743.

15. Hsu, D-S.; Hsu, P-Yi, Liao, CC. *Org. Lett*, **2001**, *3*, 263-265.

16. Shiao, H-Y.; Hsieh, H-P.; Liao, CC. *Org. Lett*. **2008**, *10*, 449-452.

17. Liao, CC.; Rao, P. D.; Chen, C-H. *J. Am. Chem. Soc*. **1998**, *120*, 13254-13255.

18. Lin, K-C.; Shen, Y-L, Rao, K.; Liao, CC. J. Org. Chem. 2002, 67, 8157-8165.

19. Chu, C-S.; Lee, T-H.; Rao, P, D.; Song, L-D.; Liao, C-C. *J. Org. Chem*. **1999**, *64*, 4111-4118.

20. Hsu, P-Y.; Peddinti, R. K.; Chittimalla, S. K.; Liao, C-C. *J. Org. Chem*. **2005**, *70*, 9156-9167.

21. Chen, C-H.; Peddinti, R. K.; Rao, K. N. S.; Liao, C-C. *J. Org. Chem*. **2004**, *69*, 5365-5373.

22. Lai, C-H.; Shen, Y-L.; Wang, M-N.; Rao, K. N. S.; Liao, C-C. *J. Org. Chem*. **2002**, *67*, 6493-6502.

23. Still. W.C. *J. Am. Chem. Soc*. **1977**, *99*, 4836-4838.

24. Corey, E. J.; Gross, W. A. *Tetrahedron Lett*. **1984**, *25*, 495-498.

25. Ito, Y.; Hirao, T.; Saegusa, T. *J. Org. Chem*. **1978**, *43*, 1011-1013.

26. Miyashita, M.; Yoshikoshi, A. *Synthesis*, **1980**, *8*, 664-667.

27. Forzelius, S-E.; Jerkeman, P.; Lindberg, B. *Acta. Chem. Scand*. **1963**, *17*, 1470-1471.

28. Liao, C-C.; Chu, C-S.; Lee, T-H.; Rao, D. P.; Ko, S.; Song, L-D.; Shiao, H-C. *J. Org. Chem*. **1999**, *64*, 4102-4110.

29. Imamoto, T.; Takiyama, N.; Nakamura, K.; Hatajima, T.; Kamiya, Y. *J. Am. Chem. Soc*. **1989**, *111*, 4392-4398.

30. Clayden, J.; Julia, M.; *J. Chem. Soc., Chem. Commun*., **1994**, 2261.

31. Feldman, K. S.; Perkins, A. L.; Masters, K. M. *J. Org. Chem.* **2004**, *69*, 7928-7932.

32. Adler, E.; Junghahn, L.; Lindberg, U.; Berggren, B.; Westin, G. *Acta. Chem. Scand*. **1960**, *14*, 1261-1273.

Chapter 2: Studies toward the synthesis of englerin A

2.1. Background

2.1.1. Isolation and biological activity

In 2008 Beutler and co-workers reported the isolation and characterization of two new guaiane sequiterpenes, englerins A **2.1** and B **2.2** shown in Scheme 2-1, from the extracts of the stem bark of *Phyllanthus engleri* in Tanzania.[1] Englerin A demonstrated excellent selectivity for the renal cancer cell line panel, with 5 of 8 renal lines having GI_{50} values under 20 nM, while for most other cell lines the GI_{50} values ranged from 10-20 μM.[1] Although detailed studies regarding the biological acitivity have not been disclosed, the low activity and selectivity of the structural analogue Englerin B, suggested that the substitution at the C-9 position may be important for the observed potency and selectivity. It is also noteworthy that other known glycolic acid containing natural products pleuromutilin,[2] saframycin R,[3] and an ecdysteroid from a Carribean sponge[4] did not show any selectivity to the renal cancer cell lines, suggesting that glycolate substitution alone cannot account for the renal selectivity.[5]

Scheme 2-1. Englerins A and B

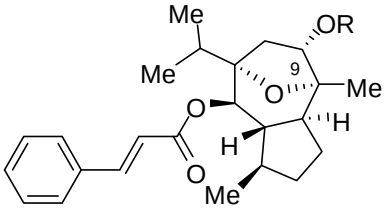

2.1 Englerin A; R = $COCH_2OH$

2.2 Englerin B; R = H

2.3 Englerin B acetate; R = Ac

2.1.2. Biosynthesis of sesquiterpenes

Terpenoids are structurally diverse large family of natural compounds derived from isoprene (C_5) units typically joined in a head to tail fashion. These are further classified based on the number of isoprene units into hemiterpenes (C_5), monoterpenes (C_{10}), sesquiterpenes (C_{15}), diterpenes (C_{20}), sesterterpenes (C_{25}), triterpenes (C_{30}) and tetraterpenes (C_{40}). About 25% of all known terpenoids belong to the group of sesquiterpenes.[6] Encompassing a wide range of nearly 200 distinct skeletal types,[7] sesquiterpenes have rekindled the interest of several research groups all around the world. Over the years a number of reviews, book chapters have appeared in the literature regarding their biogenesis[8] and isolation[9] and it is impossible to assimilate all of it in a single chapter. For this reason, attention in this chapter will focus on the biosynthesis of a specific class of sesquiterpenes, containing the 5,7-hydroazulene ring framework, namely guaianes **2.4**. Other sesquiterpenes belonging to this group are pseudoguaianes **2.5**, lactaranes **2.6**, carotanes **2.7**, aromandranes **2.8**, bourbanes **2.9**, and the β- and γ-patchoulanes **2.10** and **2.11** shown in Scheme 2-2.

Scheme 2-2. Common hydroazulene sesquiterpene frameworks

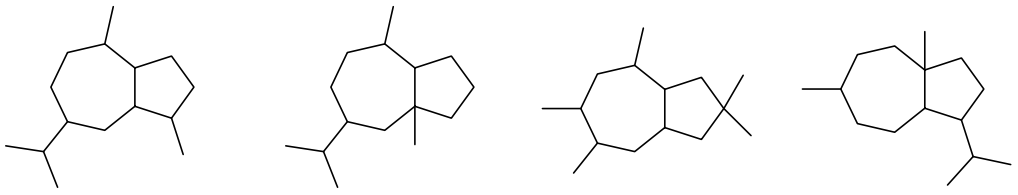

2.4 **2.5** **2.6** **2.7**

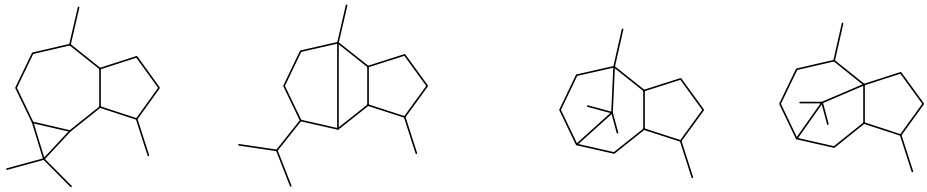

2.8 **2.9** **2.10** **2.11**

The biosynthesis of guaiane sesquiterpenes (Scheme 2-3) is well known to arise from E,E-farnesyl pyrophosphate (FPP) **2.20**, which is in equilibrium with the E,Z-farnesyl pyrophosphate **2.23**, via the corresponding allylic carbocations **2.21** and **2.22**.[10] Farnesyl pyrophosphate has in turn shown to arise from dimethylallyl diphosphate (DMAPP) **2.19**, an intermediate product of both the mevalonic acid (MVA) or 2-*C*-methyl-$_D$-erythritol-4-phosphate (methyl erythritol phosphate; MEP) pathways.[11]

Scheme 2-3. Biosynthesis of farnesyl pyrophosphate

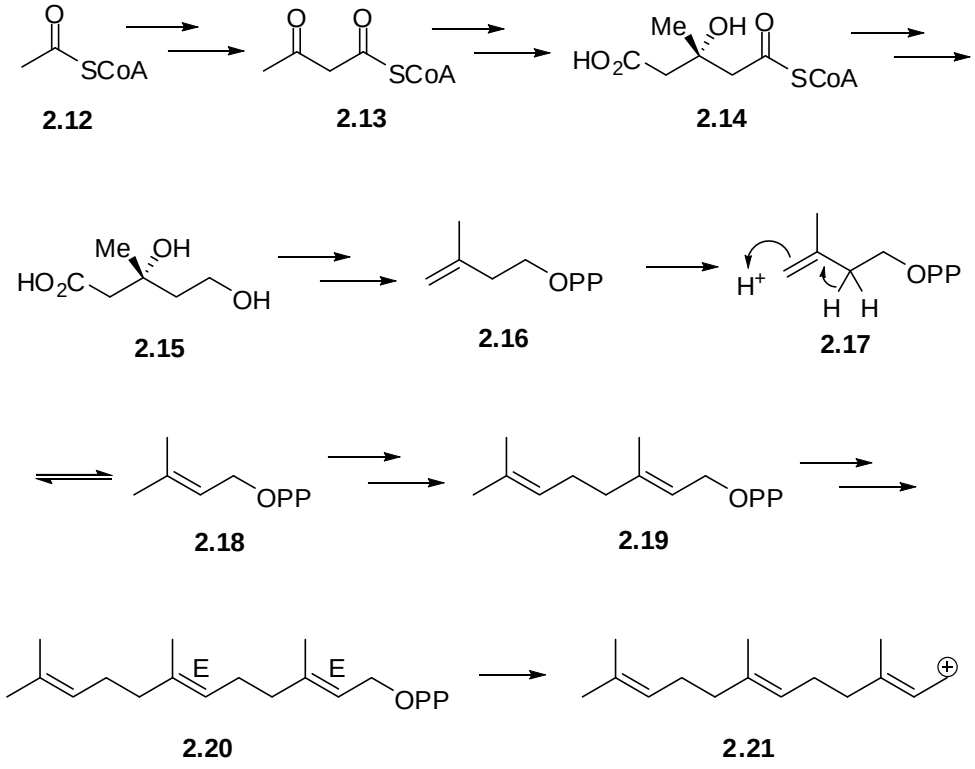

2.12 **2.13** **2.14** **2.15** **2.16** **2.17** **2.18** **2.19** **2.20** **2.21**

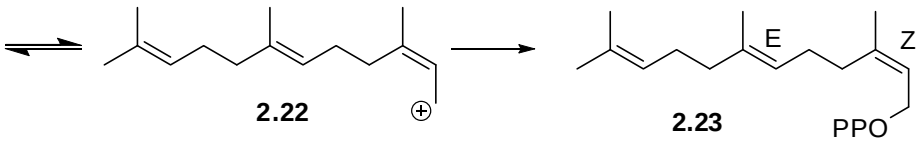

2.22 2.23

Enzyme-mediated solvolysis of the pyrophosphate group in **2.20**, then generates the germacryl carbocation **2.25**,[12] presumably by the assistance of the terminal double bond via the formation of the non-classical carbocation **2.24**.[13] Germacryl carbocation **2.25** is believed to be the biosynthetic precursor for the guaiane and eudesmane classes of sesquiterpenes.[13] Anti-Markovnikov addition of a proton at the more substituted end of a double bond in **2.26** forms the guaiyl cation **2.27** precursor to the guaiane sesquiterpenes. On the other hand, eudesmane class of sesquiterpenes are formed via the eudesmyl carbocation **2.29** as shown in Scheme 2-4.[8c]

Scheme 2-4. Biosynthesis of guaiane and eudesmane sesquiterpenes

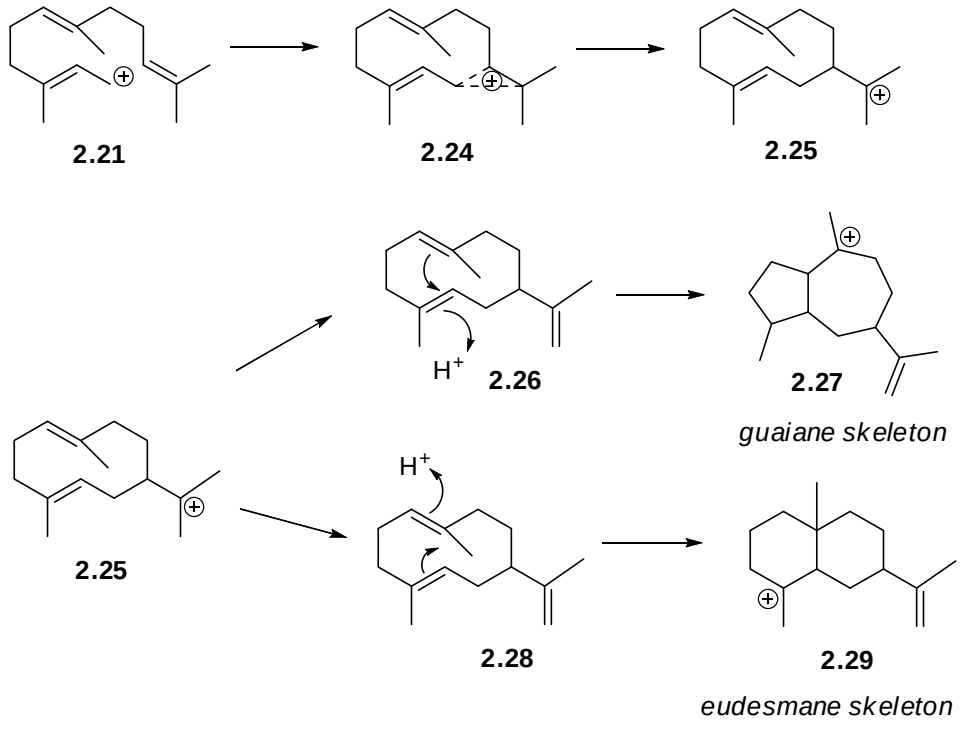

2.1.3. Synthesis of hydroazulene sesquiterpenes

Hydroazulene skeleton (bicyclo[5.3.0]decane) is a common structural motif in hundreds of sesquiterpenes exemplified by its founding members guaianes and pseudoguaianes, whose skeletons differ only in the placement of the single methyl group.[14] These families of sesquiterpenes have garnered considerable attention from the synthetic community once it was recognized that many hydroazulenes possess cytotoxic activities.[15-17] Over the years, several creative approaches have been put forward toward the synthesis of the hydroazulene motif incorporated in these sesquiterpenes. It is beyond the scope of a single chapter to cover this formidable volume of accomplishments.[16] Hence, this chapter will focus on the synthetic approach that is pertinent for this thesis, which is the solvolytic Wagner-Meerwein rearrangement of the hydronapthalene precursors **2.30**. The conceptually similar pinacol rearrangement of hydronaphthalenes **2.33** is also shown in Scheme 2-5.[18]

Scheme 2-5. Hydroazulene synthesis via rearrangement of hydronaphthalenes

Solvolytic Wagner Meerwein Rearrangement

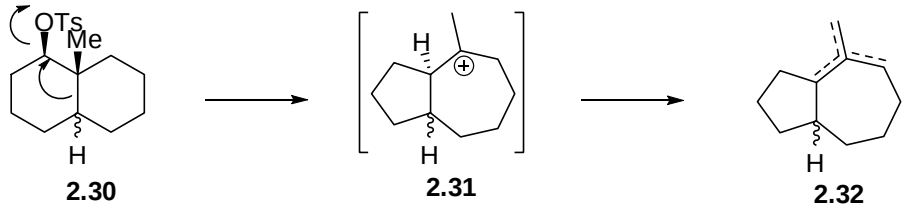

2.30 **2.31** **2.32**

Pinacol Rearrangement

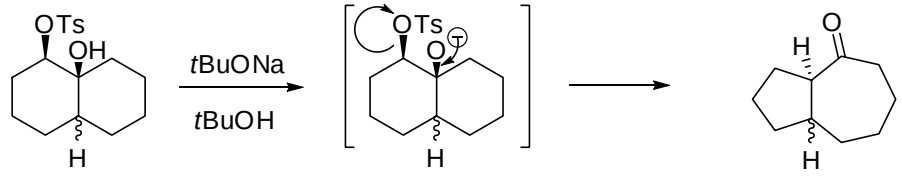

2.33 **2.34** **2.35**

2.1.4. Solvolytic Wagner-Meerwein rearrangement of hydronaphthalenes

2.1.4.1. Studies by Heathcock

In 1968, Heathcock and Ratcliff published their approach to hydroazulenes based on the discovery that both the *trans*- and *cis*-9-methyldecalin-1-toluene-*p*-sulfonates **2.36** and **2.40**, shown in Scheme 2-6, undergo solvolytic rearrangement to the hydroazulenes **2.39** and **2.43**.[19-21] An antiperiplanar relationship between the tosyloxy leaving group and the migrating carbon-carbon bond is a necessary requirement for this rearrangement. This requirement is met in the rigid *trans*-fused system **2.37**, but in the flexible *cis*-fused system, which can exist in two conformers **2.41** and **2.44**, the anticoplanarity can be achieved by only one conformer **2.44**. Hence, only solvolysis of the conformer **2.44** will result in the hydroazulene framework, while the other conformer **2.41** will give rise to the elimination products **2.43**. In this case, ionization and *carbon-carbon* bond migration cannot occur synchronously, because of the gauche orientation of the leaving group and the migrating carbon-carbon bond.

Scheme 2-6. Heathcock's hypothesis

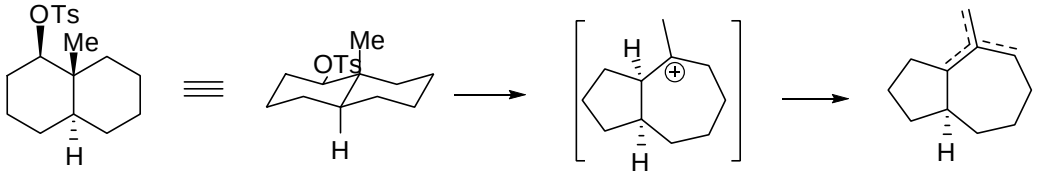

2.36 **2.37** **2.38** **2.39**

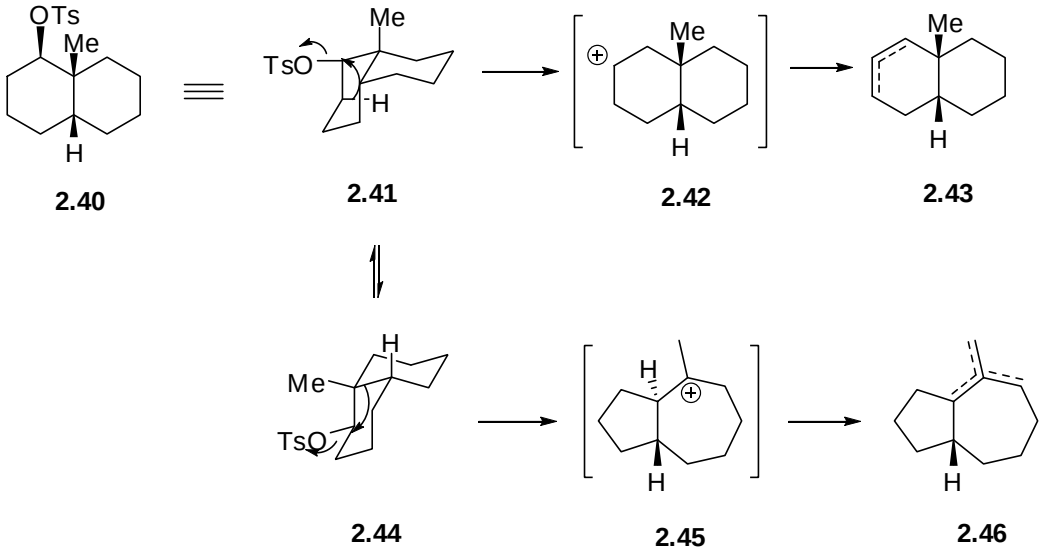

2.40 **2.41** **2.42** **2.43**

2.44 **2.45** **2.46**

Heathcock's group was the first to investigate this methodology to construct the hydroazulene sesquiterpenes. During the course of their studies shown in Scheme 2-7, it was shown that the *trans*-fused keto tosylate **2.47**, obtained from the corresponding alcohol, upon refluxing in acetic acid with two equivalents of potassium acetate produced a mixture of products from which the hydroazulene **2.49** was isolated in 78% yield. This was accompanied by two other products **2.50** and **2.51** in 5% and 10% respective yields. Surprisingly, under similar solvolytic conditions, the *trans*-deoxyketone **2.48**, always gave a higher yield of the rearranged hydroazulene **2.49**. In either case, the methyl migrated products were not detected.

Scheme 2-7. Heathcock's solvolysis results of *trans*-hydronaphthalene tosylates

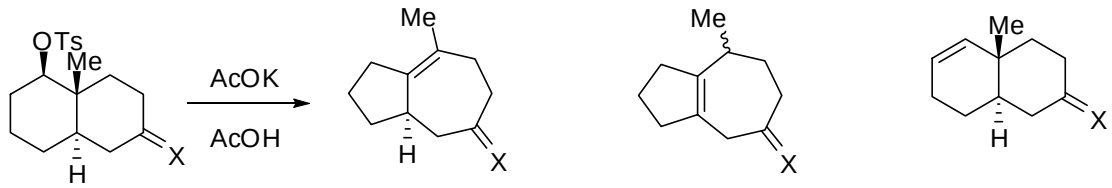

		2.49	**2.50**	**2.51**
2.47	X = O	78%	5%	10%
2.48	X = H_2	80%	15%	—

In contrast to the *trans*-series, a different result was obtained when the *cis*-fused tosylates **2.52** and **2.53** were subjected to similar solvolysis conditions. The *cis*-keto tosylate **2.52** gave an inseparable mixture of nonrearragened double bond regioisomers **2.55** in a total of 87% yield. Only 9% of the rearranged hydroazulene **2.54** was obtained. On the other hand, the *cis*-deoxy tosylate **2.53** gave more of the rearranged olefin compounds **2.50** and **2.54** in a total of 54% yield, accompanied by 39% of the nonrearranged products **2.55**, illustrated in Scheme 2-8.

Scheme 2-8. Heathcock's solvolysis of the *cis*-hydronaphthalene tosylates

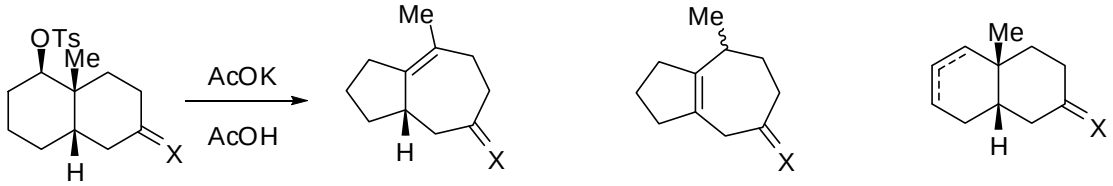

		2.54	**2.50**	**2.55**
2.52	X = O	9%	—	87%
2.53	X = H_2	30%	24%	39%

Comparing these two studies, three interesting trends can be immediately discerned. First, the rearranged hydroazulene compounds are obtained in lower yield during the solvolysis of *cis*-series when compared to the *trans*-series. This was expected, given the conformational flexibility inherent in the *cis*-fused system when compared to the rigidity of the *trans*-fusion, as discussed earlier. Second, a more interesting result is that both the *trans*- and *cis*-deoxy-tosylates **2.48** and **2.53**, underwent solvolysis to give a higher ratio of the rearranged to the nonrearranged products when compared to the keto tosylates **2.47** and **2.52**. Third, this effect was more profound in the *cis*- series than the *trans*-series. Clearly, the distal carbonyl group exerts a marked decelerating effect on the reaction. Heathcock et. al., explained this by invoking field effect due to the carbonyl group.[20] For example, during the solvolysis of the *trans*-keto tosylate **2.47** depicted in Scheme 2-9, it is reasonable to assume that rearrangement would be disfavored as a result of an increased electrostatic repulsion between the newly formed tertiary carbocation **2.58** and the carbonyl group, than the intimate ion pair **2.57** from which it formed.

Scheme 2-9. Field effects during the solvolysis of *trans*-keto tosylate

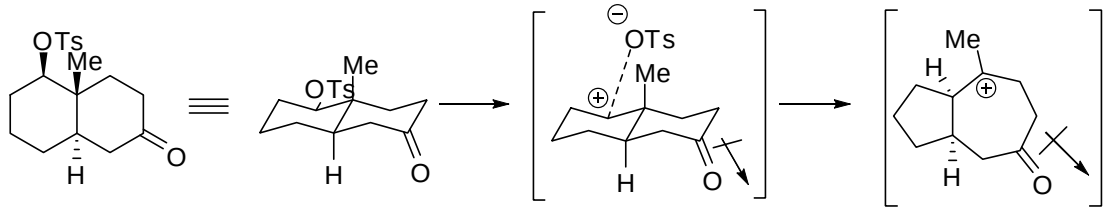

2.47 **2.56** **2.57** **2.58**

In the case of the *cis*-keto tosylate **2.52**, this effect is more pronounced as the developing charge is closer to the positive end of the carbonyl dipole (due to the convex nature of the conformation) in **2.63** (Scheme 2-10) when compared to **2.57**. The

decreased electrostatic repulsion during the formation of **2.61** explains the higher ratio of the elimination products when compared to the rearranged products. Clearly, solvolysis of the analogous *cis*-deoxytosylate **2.53**, lacking the keto group does not suffer from such electrostatic repulsion. Hence, a higher ratio of the rearranged products to the elimination products was obtained.

Scheme 2-10. Field effects during the solvolysis of *cis*-keto tosylate

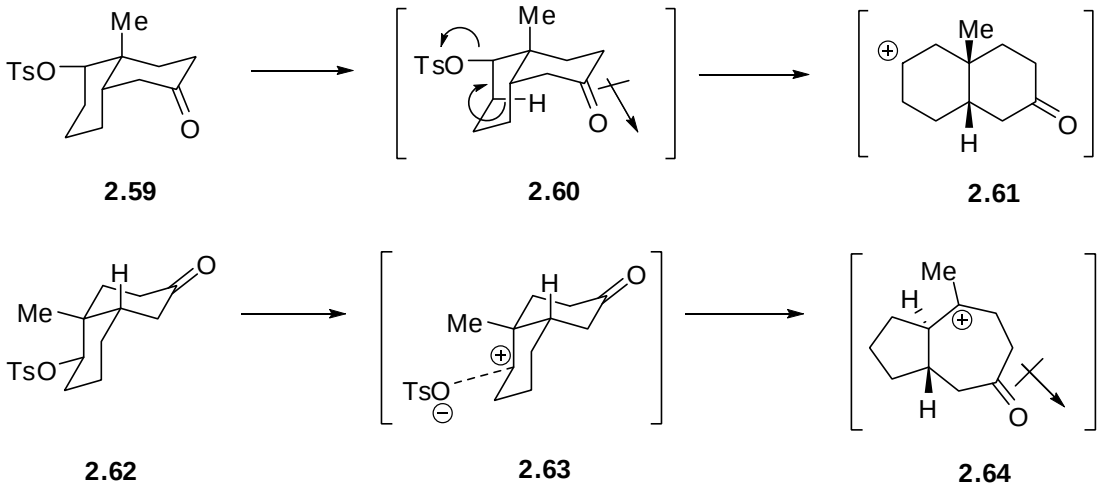

2.1.4.2. Application to the synthesis of bulnesol

Heathcock successfully applied this methodology to the total synthesis of bulnesol and related natural products (Scheme 2-11).[21] Starting from the known Wieland-Miescher ketone **2.65**, the *trans*-decalin tosylate **2.66** was prepared in a series of straightforward steps. The tosylate **2.66**, was then transformed into bulnesol **2.67** in 87% yield, by heating **2.66** in buffered acetic acid. Apart from bulnesol, three other natural products, α-Bulnesene **2.68**, β-bulnesene **2.69** and guaiol **2.70** were also obtained in this reaction in 2%, 2% and 5% yields.

Scheme 2-11. Heathcock's synthesis of Bulnesol

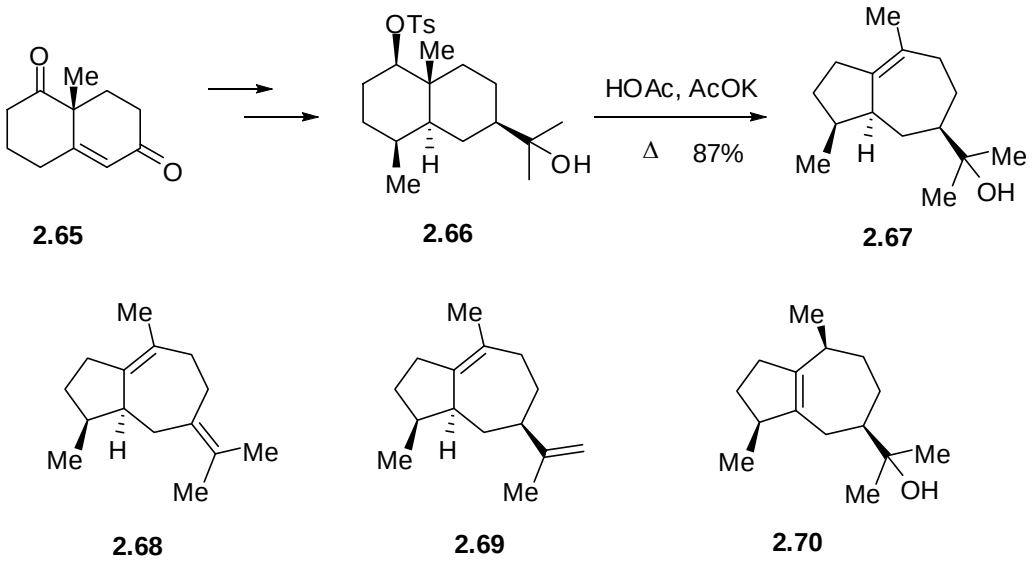

2.1.4.3. Studies by Yoshikoshi

Soon after the pioneering studies by Heathcock, Yoshikoshi's group investigated the solvolytic rearrangement of the analogous 1*β*-tosyloxy-4α,8a*β*-dimethyl- *trans*- and *cis*- decalin derivatives **2.71** and **2.74**.[22] The presence of an additional methyl group on the α-face at C4 on **2.74**, was envisioned to favor the formation of the rearranged hydroazulene products **2.78**, when compared to the parent unsubstituted compound **2.53**. This was expected, because the transition state leading to the elimination products **2.76**, will now be higher in energy due to an unfavorable 1,3 diaxial interaction between the axial methyl at C4 and the methylene on C_6 as shown in Scheme 2-12.

Scheme 2-12. Yoshikoshi's hypothesis

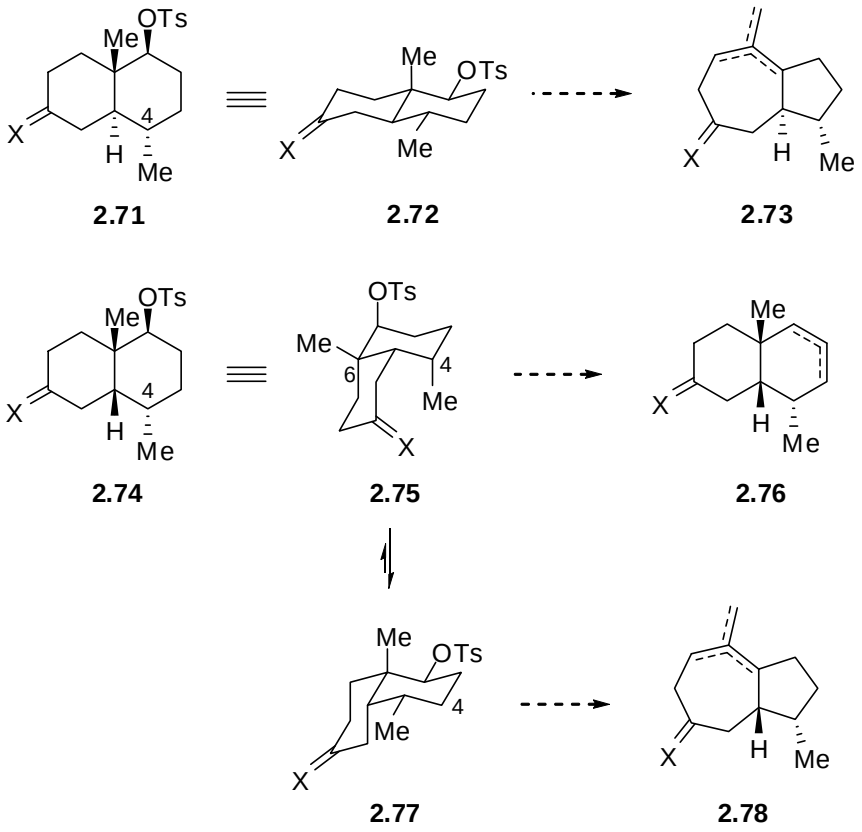

The solvolytic rearrangement of the *trans*- and the *cis*- tosylates **2.79** and **2.81** were investigated by heating them in buffered acetic acid. The results from these studies are shown in Scheme 2-13. The *trans*-keto tosylate **2.79** gave the rearranged product **2.80** in 85% yield, a result comparable to the one obtained by Heathcock during the solvolysis of **2.47** (Scheme 2-7). This was expected, as the *trans*-fused system is already rigid and the additional methyl group at C4 does not affect the conformational equilibrium. The solvolysis of the *cis*-keto tosylate **2.81** on the other hand, showed a marked increase in the ratio of rearranged product to the elimination products, due to the difference in the energies of the transition states leading to them. The rearranged product **2.82** was now obtained in 38% yield when compared to the elimination product **2.83**, isolated in 46%

yield. To conclude, Yoshikoshi's results showed that by judicious choice of groups on the *cis*-fused hydronaphthalene skeleton, one can alter the energy of the transition states and favor the hydroazulene formation.

Scheme 2-13. Yoshikoshi's solvolytic rearrangement results

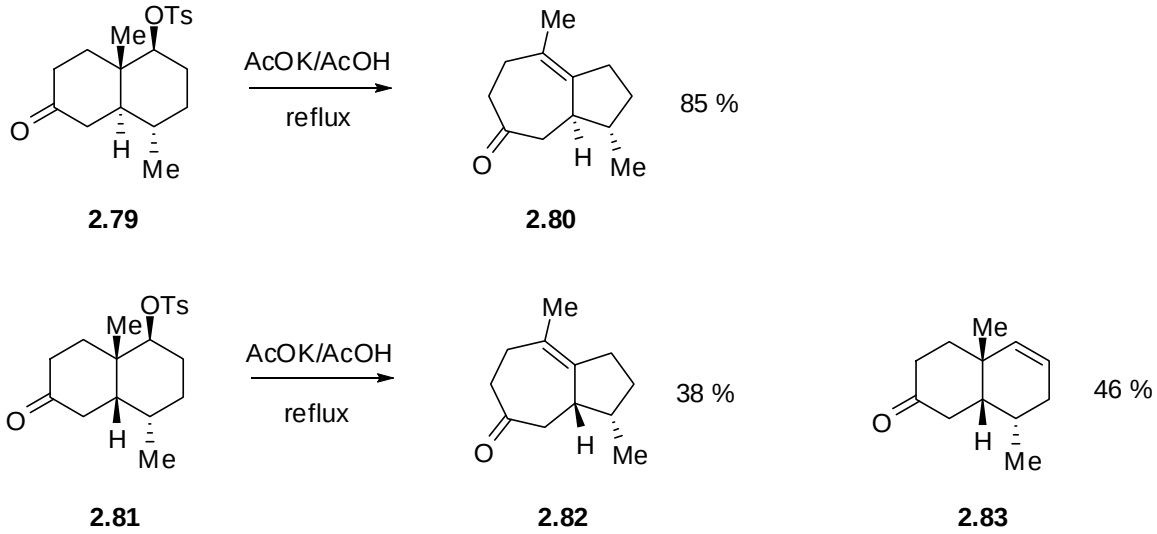

2.1.4.4. Application to the synthesis of bulnesol and kessane

In contrast to Heathcock's synthesis of bulnesol which relied on the rigidity of the *trans*-decalin type system to effect the solvolytic rearrangement, Yoshikoshi's approach utilized the *cis*-fused system.[23] Yoshikoshi's synthesis of bulnesol is shown in Scheme 2-14. The synthesis commenced with the known acetoxy-ketone **2.84** obtained in two steps from Wieland-Miescher ketone **2.65**. This was transformed into the ester **2.85**, in a series of steps, which was eventually transformed into bulnesol **2.86**, via its solvolytic rearrangement. However, the yield of rearrangement product **2.86** was not mentioned and Yoshikoshi's discussion suggested that a mixture of products was obtained. Finally, an

elegant application of this methodology to the synthesis of kessane **2.89** by Yoshikoshi, relevant to our approach to englerin A, will be discussed.[23] Adapting a similar strategy, starting with the β-epimer **2.87**, kessane **2.89** was prepared by an intramolecular trapping of the intermediate carbocation by the tertiary alcohol on the side chain.

Scheme 2-14. Yoshikoshi's synthesis of bulnesol and kessane

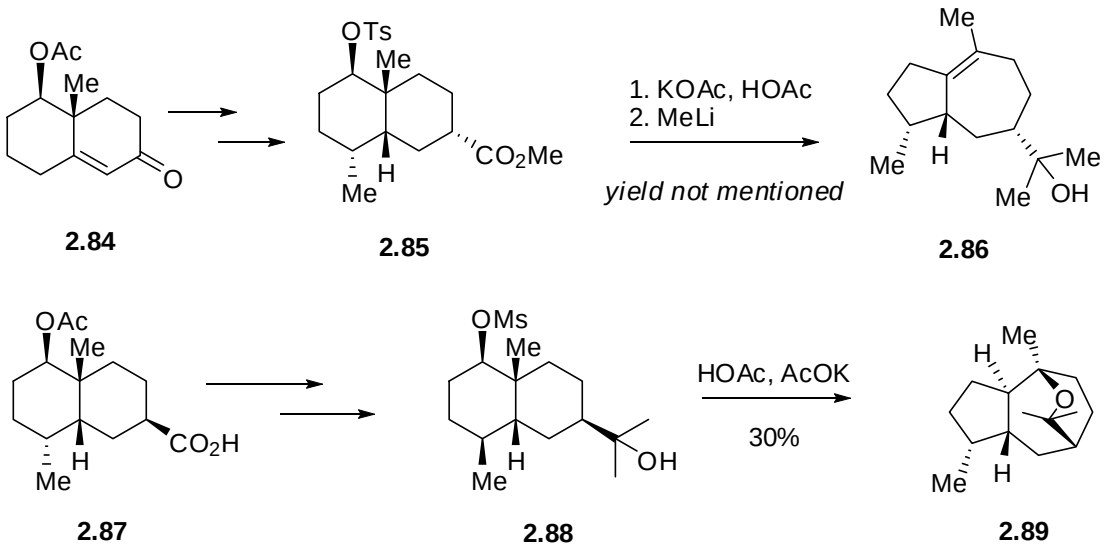

2.1.5. Summary

A novel guaiane sesquiterpene englerin A, containing *trans*-hydroazulene skeleton was isolated in 2008. Preliminary analysis showed that, englerin A exhibited 1000-fold selectivity against 6 of the 8 renal cancer cell lines. Although the exact mechanism of action is not clear at this time, future studies hopefully will be aimed at understanding the site selectivity. Solvolytic Wagner-Meerwein rearrangement of hydronaphthalene tosylates to hydroazulenes has found widespread use in sesquiterpenes

synthesis. Its application to the total synthesis of hydroazulene natural products was discussed.

2.1.6. References

1. Ratnayake, R.; Covell, D.; Ransom, T.T.; Gustafson, K. R.; Beutler, J. A. *Org. Lett*. **2008**, *11*, 57-60.
2. Knauseder, F.; Brandl, E. *J. Antibiot*. **1976**, *29*, 125.
3. Saito, N.; Kameyama, N.; Kubo, A. *Tetrahedron* **2000**, *56*, 9937.
4. Costantino, V.; Dell'Aversano, C.; Fattorsusso, E.; Mangno, A. *Steroids* **2000**, *65*, 138.
5. http://dtp.nci.nih.gov/dtpstandard/cancerscreeningdata/index.jsp.
6. Nuhn, P. *Naturstoffchemie*, 2. Auflage; S. Hirzel: Stuttgart, 1990, pg 481.
7. Croteau, R.; Johnson, M. A. In: *Biosynthesis and Biodegradation of Wood Compounds*; Academic Press: New York, **1985**; pp 379-439.
8. (a) Gonzalez, A. G.; Galindo, A.; Mansilla, H.; Palenzuela, J. A. *Tetrahedron Letters* **1983**, *24*, 969-72. (b) Cordell, G. A. *Chem. Rev.* **1976**, *76*, 425-60. (c) Dewik, P. M.; *Medicinal Natural Products: A Biosynthetic Approach*. 3rd edition; John Wiley & Sons; New York, **2009**; pp 127-186.
9. Fraga, B. M. *Nat. Prod. Rep*. **2008**, *25*, 1180-1209; previous issues listed there in.
10. Cane, D. E. In: *Biosynthesis of Isoprenoid Compounds* (Porter, J. W.; Spurgeon, S. L. eds.) Vol. 1; John wiley & Sons; New York, **1981**; p 283.
11. Rodriguez-Concepcion. M.; Boronat. A.; *Plant Physiol 130*, 1079-1089.

12. Torsell, K. B. G.; *Natural Product Chemistry*; John Wiley & Sons; Chichester, **1983**; p 188.

13. (a) Hendrickson, J. B.; *Tetrahedron* **1959**, *7*, 82. (b) Parker, W.; Roberts, J. S.; Ramage, R. *Quart. Rev*. **1967**, *21*, 311.

14. (a) Gandurin, A., *Berichte*, **1909**, *41*, 4359-4363; (b) Semmler, F. W., Mayer, W. E., *Berichte* **1912**, *45*, 3384-3394.

15. (a) Heathcock, C. H., in *The Total Synthesis of Natural Products*, ApSimon, J., Ed., wiley: New York, 1973, Vol. 2, pp. 197-558; (b) Heathcock, C. H., Graham, S. L., Pirrung, M. C., Plavac, F., White, C. T., in *The Total Synhtesis of Natural Products*, ApSimon, J., Ed., Wiley: New York, 1983, Vol. 5; (c) Pirrung, M. C., Morehead, A. T., Jr., Young, B. C., in *The Total Synthesis of Natural Products*, Goldsmith, D., Ed., Wiley: New York, 2000, Vol. 11.

16. *Terpenes and Steroids*, Specialist Periodical Reports, The Chemical Society/Royal Society of Chemistry: London, 1970-1983, Vols.1-12.

17. Ho, T.-S., *Carbocycle Construction in Terpene Synthesis*. VCH: NY, 1988.

18. Hudlicky, T., Reed, J. W. in *The way of Synthesis*. Wiley-VCH: Weinheim, 2007.

19. Heathcock, C. H., Ratcliffe, R; *Chem. Commun*. **1968**, 994.

20. Heathcock, C. H., Ratcliffe, R. J., Van, J. *J. Org. Chem*. **1972**, *37*, 1796.

21. Heathcock, C. H., Ratcliffe, R. *J. Am. Chem. Soc*. **1971**, *93*, 1746.

22. Kato, M., Kosugi, H., Yoshikoshi, A., *J. Chem. Soc., Chem. Commun*. **1970**, 185-186.

23. Kato, M., Kosugi, H., Yoshikoshi, A., *J. Chem. Soc., Chem. Commun*. **1970**, 934.

2.2. Results and Discussion

2.2.1. Our approach to Englerin A

Inspired by Heathcock's and Yoshikoshi's results, we envisioned a similar strategy to construct the *trans*-hydroazulene framework in englerin A. Our retrosynthetic analysis is outlined in Scheme 2-15. From the outset, englerin A was thought to arise from the alkene **2.91**, by a series of steps involving stereoseletive epoxidation to form the epoxide **2.90**, followed by transannular epoxide opening and cinnamate formation. At the time of writing this thesis, total synthesis of englerin A was accomplished by Christmann's group[1] and a similar end game was utilized. The alkene **2.91**, was in turn envisioned to arise from the tosylate **2.92**, via a hitherto unexplored tandem reaction comprising of solvolytic Wagner-Meerwein rearrangement followed by an intramolecular trapping of the *in situ* generated carbocation by the neighboring ester. The stereochemical aspects of this novel tandem reaction will be discussed in due course. Stereoselective construction of the *cis*-hydronaphthalene **2.93**, was realized to come from the diol **2.94**. The three stereocenters in the diol **2.94** would be set stereoselectively starting with (+)-carvone, a widely used chiral starting material.[2]

Scheme 2-15. Retrosynthetic analysis of englerin A

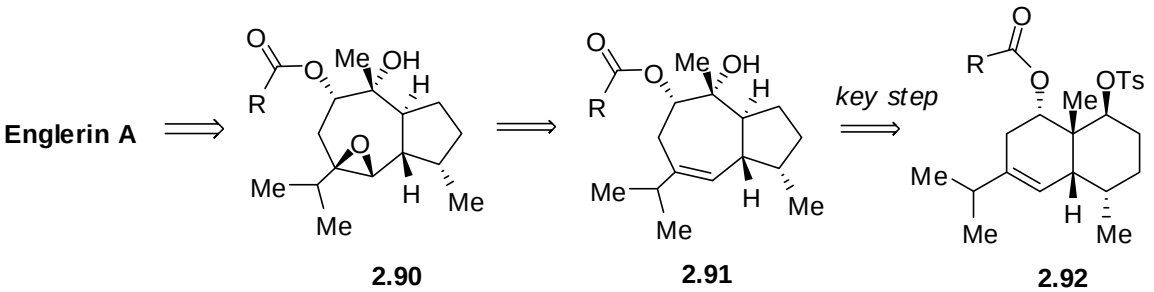

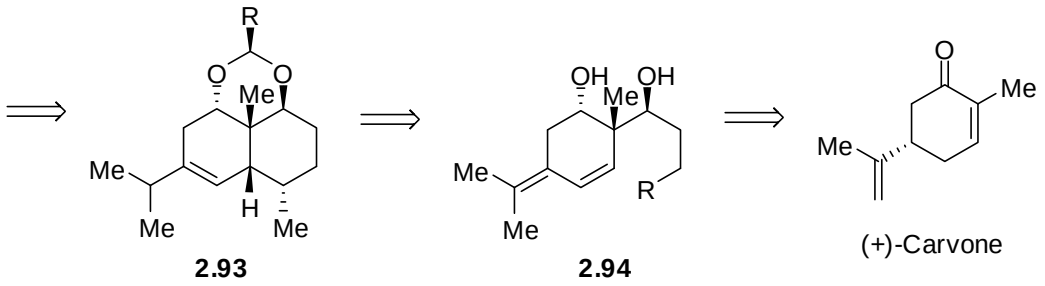

2.93 **2.94**

The stereochemical aspects of the key tandem reaction are shown in Scheme 2-16. Analogous to the solvolytic studies by Yoshikoshi, we expect the solvolysis of the *cis*-hydronaphthalene tosylate **2.92** to proceed via the more reactive conformer **2.96**, in which all the substituents are equatorial. The alternate transition state via the conformer **2.95** would be disfavored because of its higher energy. Migration of the antiperiplanar *carbon-carbon* bond would form the tertiary carbocation **2.97**, which we hope will be trapped by the neighboring ester to form **2.98**. Hydrolysis then furnishes *trans*-hydroazulene **2.91** framework of englerin A. Noteworthy is the fact that the stereochemistry of the tertiary alcohol in **2.91** is set by the chirality of the neighboring ester during the course of this reaction.

Scheme 2-16. Proposed construction of the hydroazulene framework in englerin A

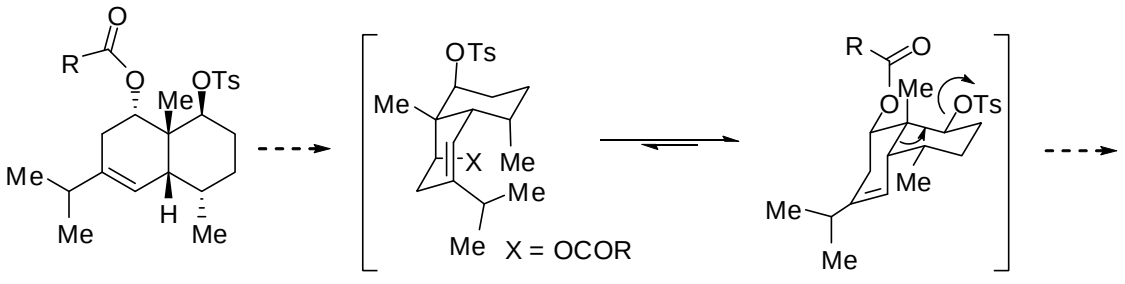

2.92 **2.95** **2.96**

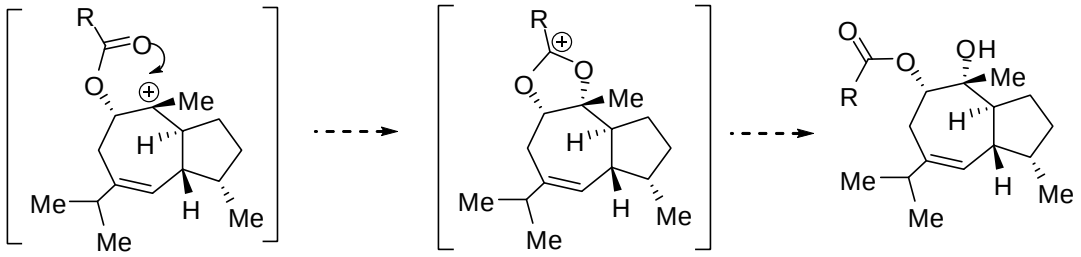

2.97 **2.98** **2.91**

The synthesis of kessane by Yoshikoshi (Scheme 2-14) served as a close precedent for the viability of this methodology. It is pertinent to mention here that the latter part of the hypothesis was inspired by the Woodward-Prevost reaction[3] depicted in Scheme 2-17.

Scheme 2-17. Resemblance to Woodward-Prevost reaction

Woodward-Prevost Reaction

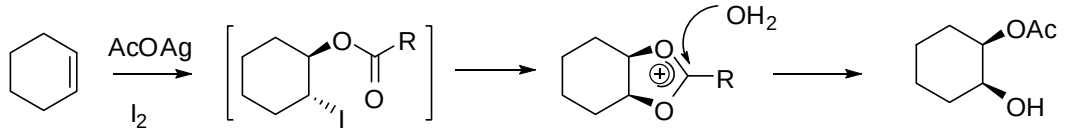

2.99 **2.100** **2.101** **2.102**

Present hypothesis

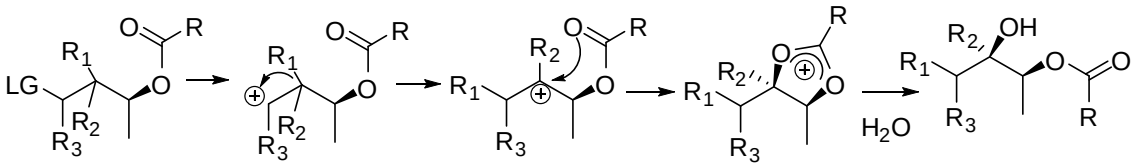

2.103 **2.104** **2.105** **2.106** **2.107**

The proposal for the stereoselective construction of the *cis*-decalin system also deserves a comment. As discussed earlier, we envisioned its synthesis from (+)-carvone,

by two related routes, namely, metal-catalyzed carbocyclization and the 6-exo-trig carbocyclization via the free radical or anionic pathways. The stereochemical aspects of the cyclozirconation to construct the *cis*-hydronaphthalene system will be discussed first. A great deal of effort has been put into understanding the mechanism of the cyclozirconation reaction by several research groups.[4] The general scheme for cyclozirconation is depicted in Scheme 2-18. Carbocylization is usually effected by treating the corresponding dienes with Cp_2ZrCl_2 in presence of Bu_2Mg in THF at 0 °C. This reaction proceeds via the *in situ* generated zirconocene, which coordinates to the olefins **2.109**. Formation of the metallocycle **2.110** and ensuing acidic quench generates the product **2.111** (Eq. 1). The use of conjugated dienes **2.112** is also tolerated and the cyclozirconation produces the corresponding alkene **2.115** shown in (Eq. 2).

Scheme 2-18. General scheme for cyclozirconation of olefins

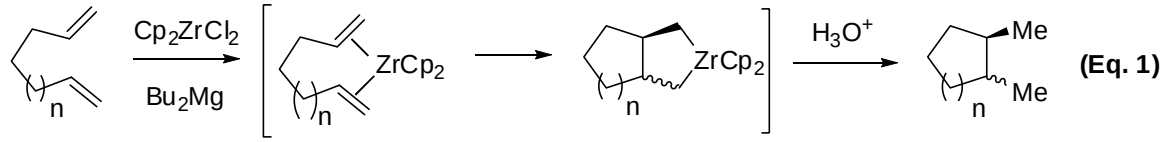

2.108 **2.109** **2.110** **2.111** **(Eq. 1)**

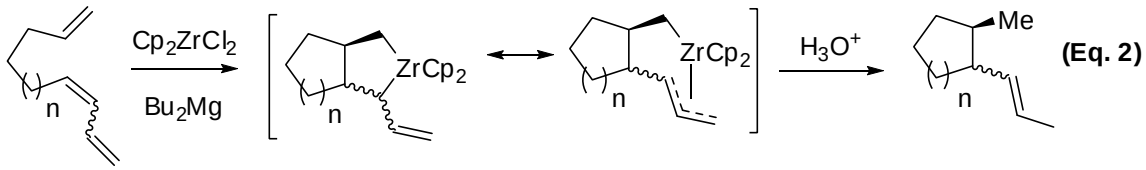

2.112 **2.113** **2.114** **2.115** **(Eq. 2)**

Application of this reaction to the synthesis of natural products pertinent to this project is shown in Scheme 2-19. Blechert and co-workers utilized cyclozirconation as

the key step in the construction of (+)-*trans*-195A.[5] Interestingly, advanced intermediate **2.116** produced the *trans*-hydronaphthalene **2.118** instead of *cis*-hydronaphthalene.

Scheme 2-19. Application of cyclozirconation to the synthesis of (+)-*trans*-195A

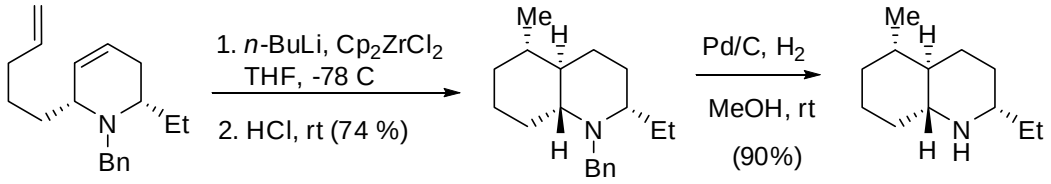

2.116 **2.117** **2.118**

We envisioned a similar type of construction for the *cis*-hydronaphthalene diol **2.93** in the synthesis of englerin A. Scheme 2-20, depicts its construction using cyclozirconation. In comparing our hypothesis with Blechert's studies, we believe that in our case, by constraining the diol as a cyclic acetal **2.119**, the formation of the tetracyclic [6.6.6.5] system with the *cis* junction between B, C and D rings **2.123**, should be favored over the alternate *trans*-tetracyclic compound **2.120**, as a result of higher torsional and ring strain associated with the latter. Acidic quench of the metallacycle **2.124** would then furnish the tricylic compound **2.103** with the methyl group on C4 on the α-face of the molecule.

Scheme 2-20. Proposed carbocyclization via cyclozirconation

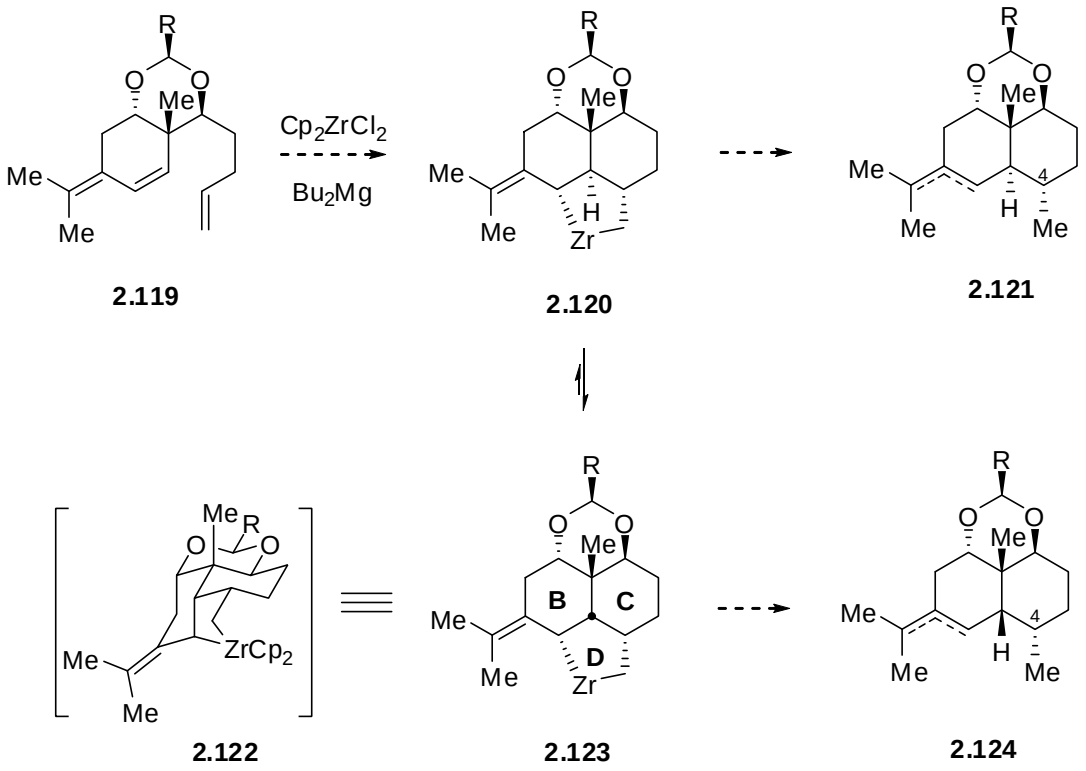

The stereochemical aspects of the analogous 6-exo-trig carbocyclization via free radical pathway will be discussed next. In this case as well, we believe by constraining the diol as an acetal **2.125** (Scheme 2-21), formation of *cis*-hydronaphthalene would be preferred over the *trans*. This is also reflected by the difference in energy of the transition states. The transition state arising from the more reactive conformer **2.126** in which the methyl group would assume the pseudo-equatorial position is expected to be lower in energy compared to the alternate transition state leading to **2.129**, which is plagued by the 1,3 diaxial interaction between the two methyl groups. With all these regio- and stereochemical issues in mind, we embarked on developing a concise route to the synthesis of the appropriate precursors from carvone.

Scheme 2-21. Proposed 6-exo-trig carbocyclization via free radical pathway

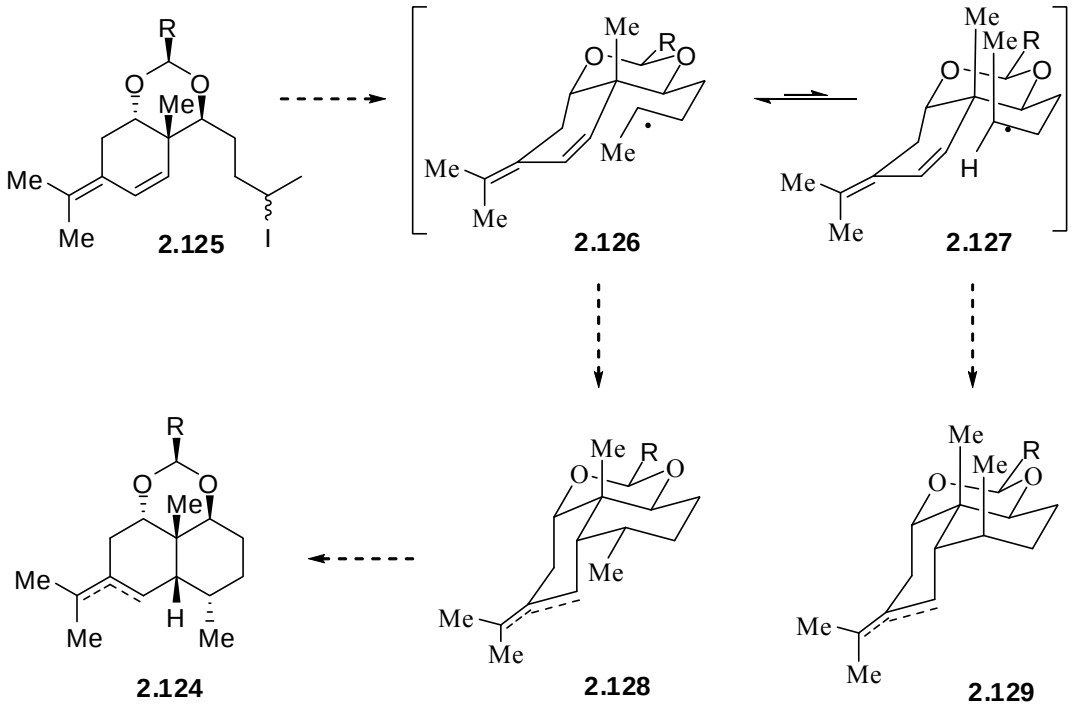

2.2.2. Prior work in our group

In 2008, Curtis Seizert, then an undergraduate student, initiated studies toward the synthesis of englerin A. His plan was to use the cyclozirconation approach to construct the *cis*-hydronaphthalene system as discussed above. As the absolute stereochemistry of englerin A is not known, the less expensive R-(-)-carvone was chosen for our model studies. The synthesis commenced with the tandem Michael-aldol sequence on R-(-)-carvone initiated by the *in situ* generated phenyl selenide. Scheme 2-22, outlines the synthetic route. Developed by Livinghouse,[6] this methodology has not been explored to its fullest potential in the context of total synthesis of natural products. On the other hand, the analogous phenylsulfide Michael-Aldol sequence has been utilized by Floreancig[7a] and Baran[7b] in the total synthesis of natural products. Proceeding with the synthesis, the

sensitive β-hydroxy group in the aldol adduct **2.130**, was protected as the MOM ether[8] **2.131**, which was followed by the oxidation of the selenide with H_2O_2 to generate the β,γ-unsaturated compound **2.132**. $NaBH_4$ reduction gave the secondary alcohol **2.133**, in 90% yield over three steps from the aldol adduct **2.130**. The reader is referred to section **2.2.3.1** for the discussion of the stereochemical aspects of the above reaction sequence. The monoprotected diol **2.133**, was then transformed into a series of compounds, on which the cyclozirconation was tested. Treating **2.133** with TMSOTf afforded cyclic acetal **2.134** in 62% yield.[9] At this juncture, the proposed scheme called for moving the external double bond into conjugation. Based on literature precedents, base-catalyzed reaction was deemed most promising.[10]

Scheme 2-22. Synthesis of the monoprotected diol-triene

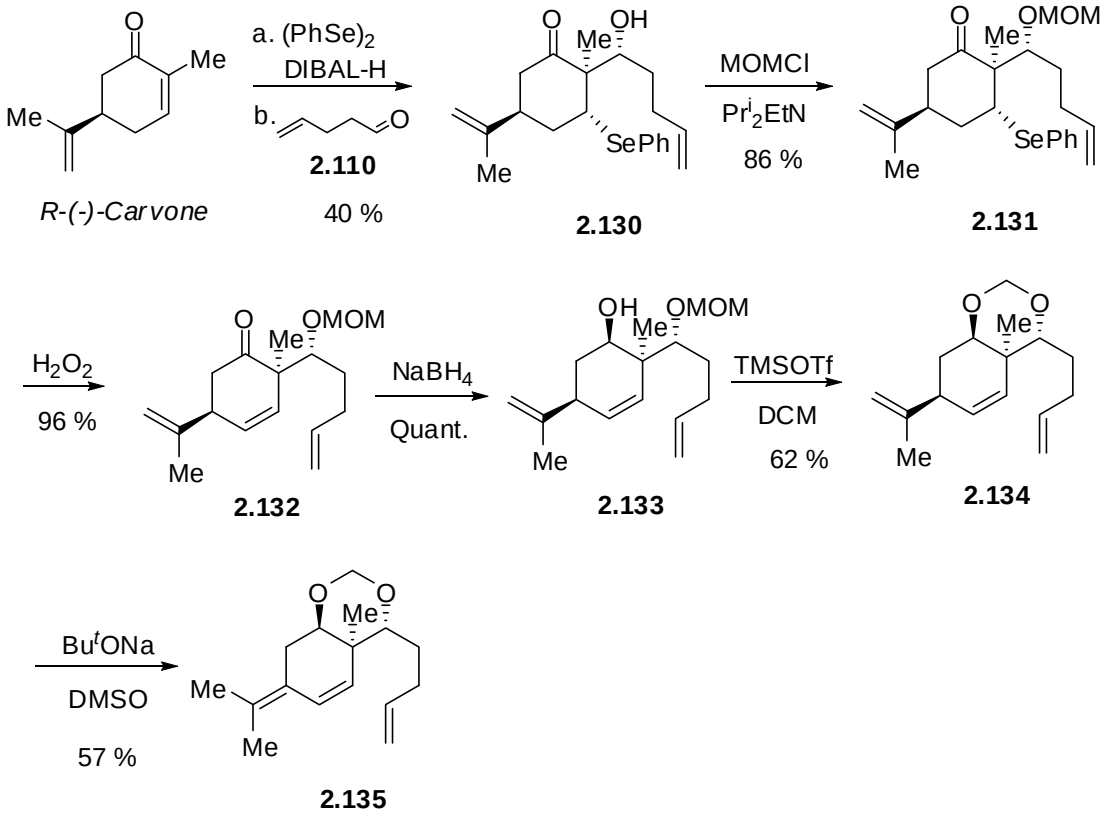

Although the use of *t*-BuOK in DMSO resulted in the formation of **2.135**, the reaction was irreproducible. The conjugated diene **2.135** was eventually obtained by using Bu^tONa in DMSO. Proceeding with the synthesis, the pivotal cyclozirconation was then studied on all four model compounds. Unfortunately, all our attempts to cyclozirconate these substrates under variety of conditions, did not produce the cyclized products, instead, only decomposition was observed. Attempts to heat the reaction mixture in hopes of cyclozirconation only led to decomposition. Scheme 2-23, depicts the results of the cyclozirconation studies and the various conditions investigated.

Scheme 2-23. Failure of the cyclozirconation route

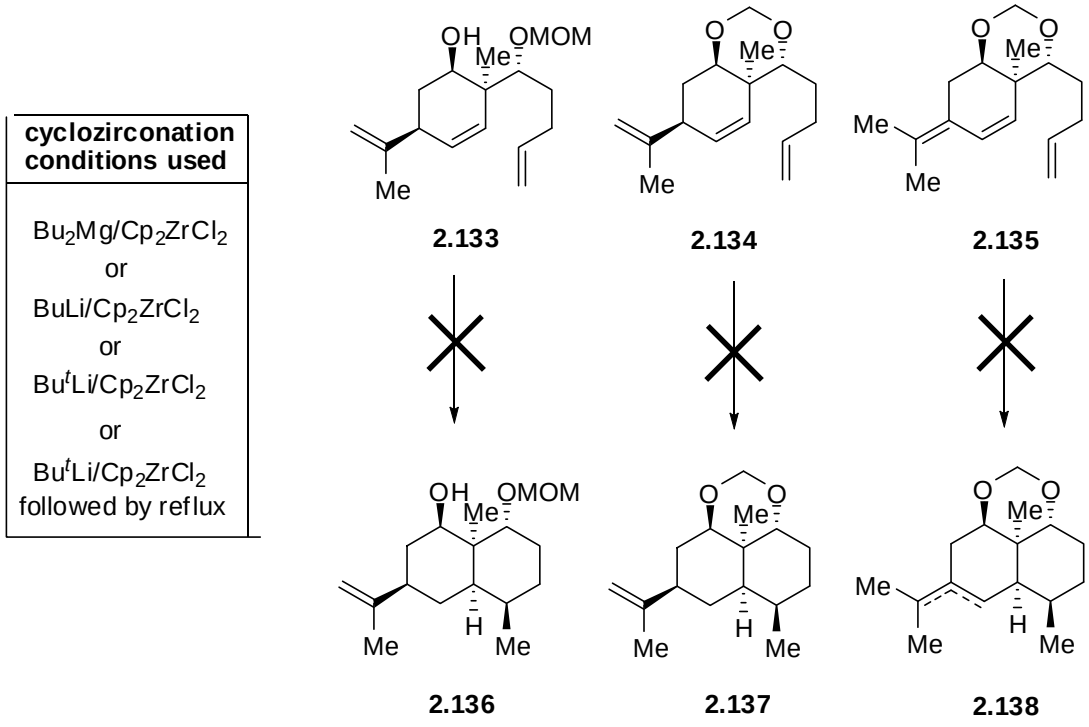

With the failure of the cyclozirconation route, we sought to find alternate ways to construct the *cis*-hydronaphthalene system. At this point, Curtis put his studies on hold

and I took over the project and began investigating alternate ways to prepare the advanced intermediate **2.125** (Scheme 2-21) in order to investigate carbocyclization via free radical and anionic pathways.

2.2.3. My study

2.2.3.1. Synthesis of the carbocyclization precursor

The synthesis began with the preparation of the aldehyde building block **2.142** required for the aldol reaction. This was accomplished in three straightforward steps as shown in Scheme 2-24. Reduction of the commercially available ketone **2.139** was achieved with $NaBH_4$ to give alcohol **2.140** in 98% yield. After considerable experimentation, pivalolyl protection showed promise and accordingly pivalate **2.141** was prepared. Ozonolysis furnished aldehyde **2.142** in 90% yield, over two steps.

Scheme 2-24. Preparation of the side chain aldehyde

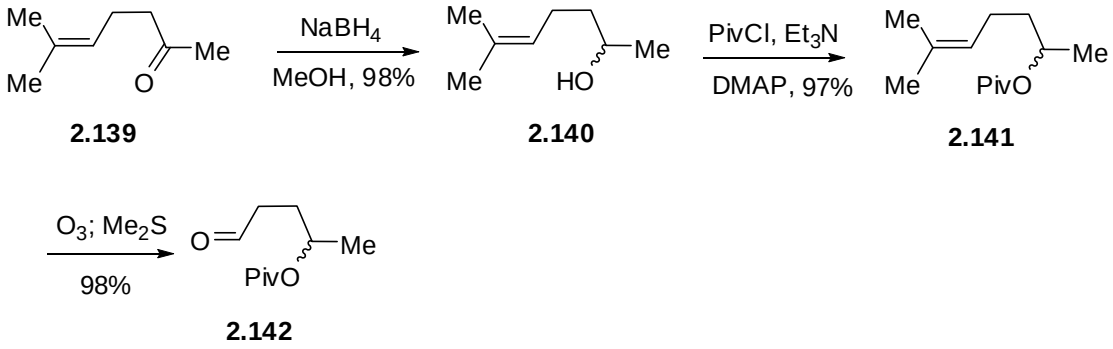

With access to aldehyde **2.142**, we next focused our attention on the stereoselective aldol reaction as shown in Scheme 2-25. This was achieved in one step, following the in-house protocol developed by Curtis, for the cyclozirconation route.

Michael addition of *in situ* generated dibutylaluminum phenylselenide to R-(-)-carvone, produced the aluminum enolate **2.144**, which was subsequently treated with the aldehyde **2.142** to afford the aldol adduct **2.146** in 53% yield. In this tandem one-pot reaction three contiguous stereocenters were put in place with complete stereocontrol. The stereochemistry during the Michael addition can be explained by an axial attack of the *in situ* generated phenylselenide as shown in **2.143** followed by the stereoselective aldol reaction proceeding via Zimmerman-Traxler transition state **2.146**. We found -78 °C to be the optimal temperature for this reaction and higher temperatures led to lower diastereoselectivity and other side products. In any event, even though this reaction was low yielding, we were able to scale it up and multigram quantities of the aldol adduct **2.146** were prepared.

Scheme 2-25. Highly stereoselective tandem Michael-aldol reaction on (-)-carvone

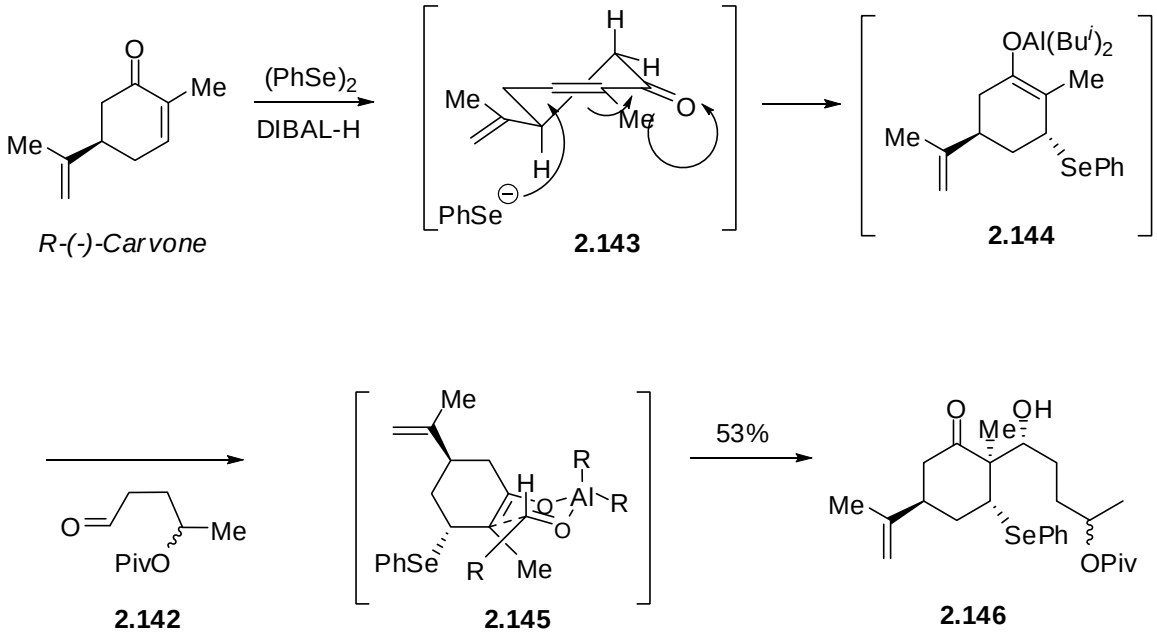

The sensitive β-hydroxy aldehyde **2.146** was protected as the acetate **2.147**, to eliminate the possibility of retroaldol reaction, by treating it with acetic anhydride and pyridine as illustrated in Scheme 2-26. β,γ-unsaturation in **2.147** was then achieved in one step by the *in situ* syn elimination of the selenoxide generated by the H_2O_2 oxidation.

Scheme 2-26. Synthesis of the PMP-acetal 2.151

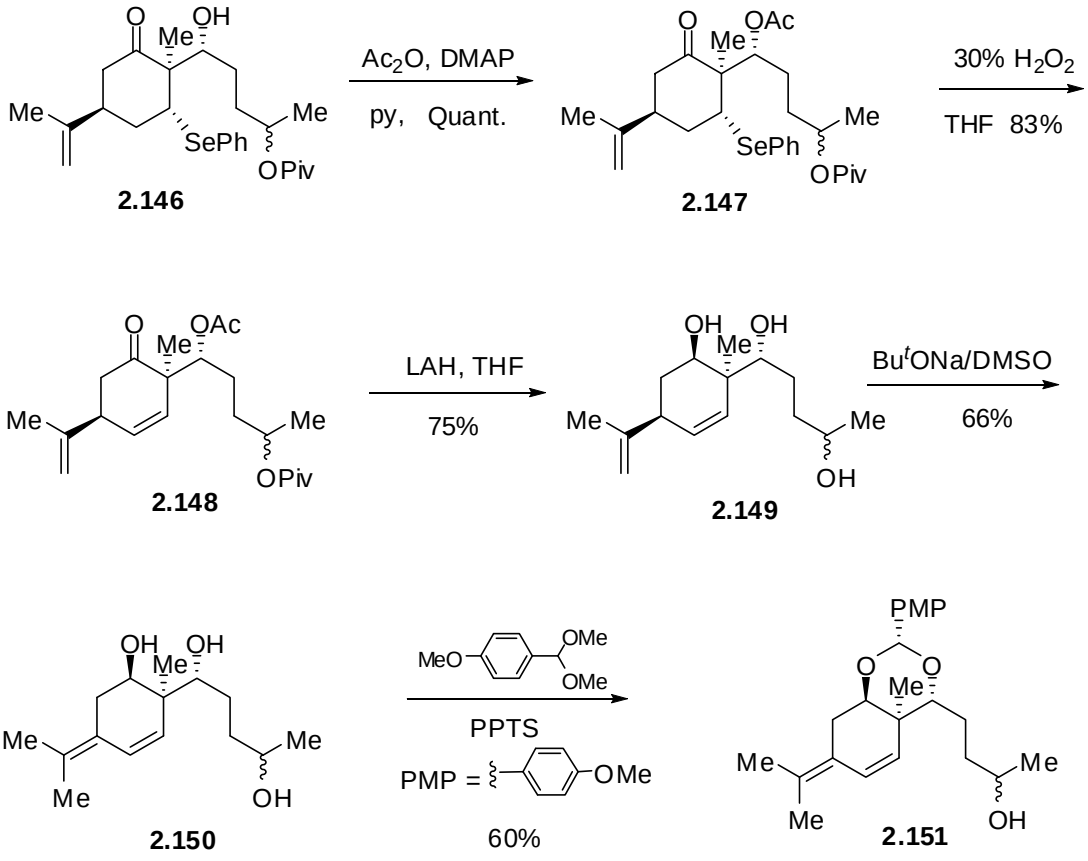

Global reduction with LAH furnished the triol **2.149** in 75% yield. The stereoselectivity observed during the LAH reduction can be explained via an axial attack of the hydride. The conjugated triol **2.150** was obtained in 66% yield by using *t*-BuONa in DMSO. Chemoselective protection of the 1,3-diol was achieved using PPTS and *p*ara-methoxybenzaldehyde dimethylacetal to give **2.151**. Due to the thermodynamic nature of this reaction, **2.151** was obtained as the only compound, presumably with both the *p*ara-methoxyphenyl group and the side chain containing the alcohol in the equatorial position, as depicted in **2.152**.

Scheme 2-27. Unanticipated problems during the preparation of the iodide 2.153

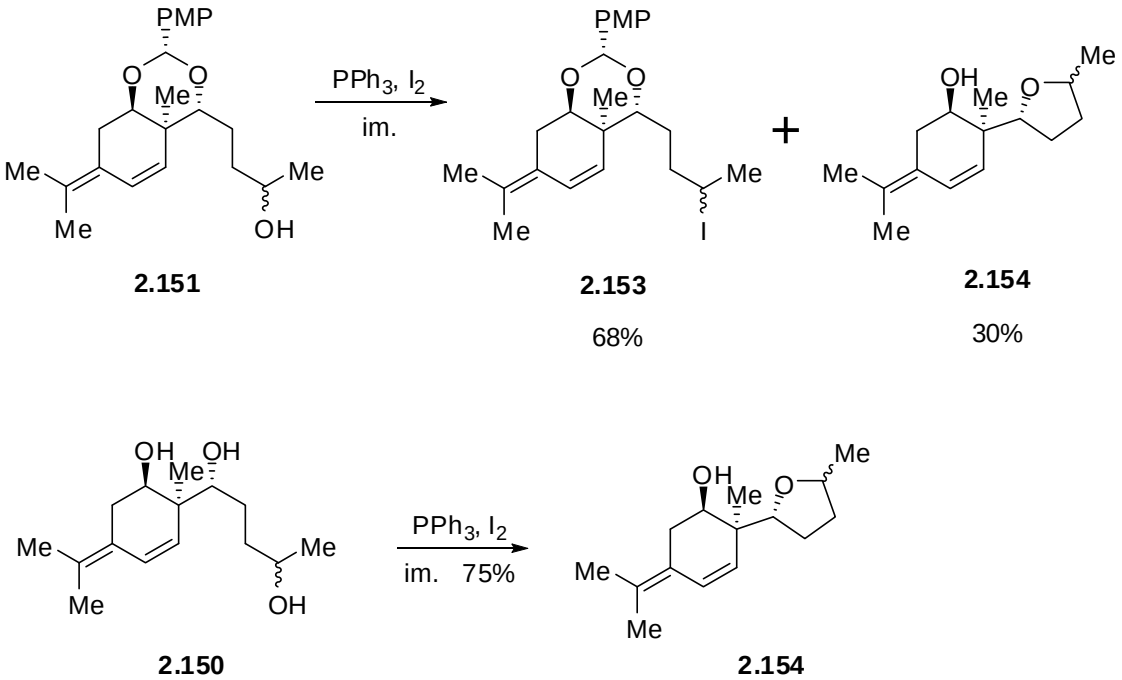

Conversion of the secondary alcohol **2.151** to the iodide **2.153** was attempted next. Unfortunately, treating **2.151** with PPh_3 and I_2 gave **2.153** in a moderate yield, accompanied by the tetrahydrofuran compound **2.154** as an inseparable mixture of

diastereomers. These results are shown in Scheme 2-27. The structure of the latter compound was confirmed by an independent synthesis from the triol **2.150**. In order to eliminate the formation of this side product **2.154**, we decided to use a more robust protecting group. The use of benzaldehyde dimethylacetal instead of the *para*-methoxybenzaldehyde acetal solved this problem. Scheme 2-28, depicts these efforts. In this case as well, the reaction furnished only one compound **2.155**, presumably with the phenyl group and the side chain in the equatorial position. Smooth conversion to the iodide **2.156** ensued, using the previously explored conditions. The more robust benzaldehyde acetal protecting group, as expected, did not produce any of the undesired tetrahydrofuran side products.

Scheme 2-28. Successful preparation of the iodide 2.156

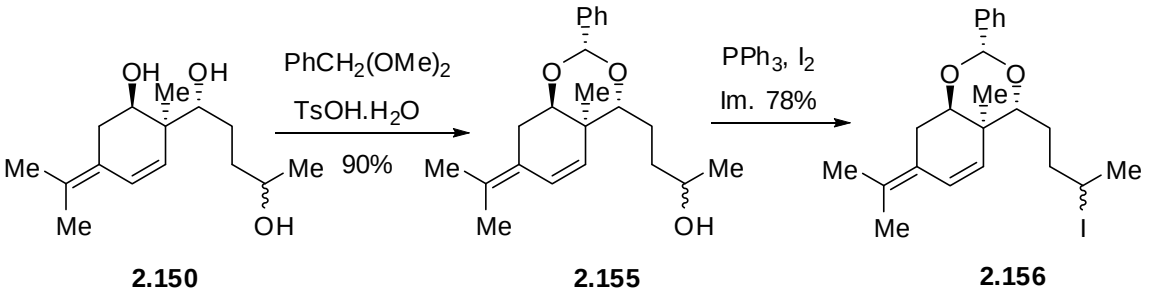

2.150 **2.155** **2.156**

2.2.3.2. Carbocyclization under anionic conditions

Having successfully established a viable synthetic route to the cyclization precursor, we then turned our attention to the key cyclization reaction to generate the *cis*-hydronaphthalene system. To achieve this task, two modes of cyclization were considered, namely anionic and free-radical cyclization. First, anionic mode of cyclization was investigated. In contrast to the wealth of information available on the 5-

exo-trig anionic carbocyclization to generate functionalized cyclopentanes,[11-15] little is known about the analogous 6-exo-trig cyclization, which is not particularly surprising, in light of the slow cyclization rates to form six membered rings. However, it is not entirely unprecedented. Detailed studies by Bailey[16,17] showed that these types of cyclization are under equilibrium and often sluggish, but can be promoted by addition of Lewis bases like TMEDA. Although there have been several reports speculating on the true mechanism operating under these conditions, the possibility of a free-radical mechanism was ruled out by Bailey et. al., when **2.157** did not cyclize under these conditions. However, the unsubstituted alkene **2.158** cyclized in an excellent 89% yield. If the radical mechanism were indeed operative, then one would expect the former substrate to undergo carbocyclization faster due to the formation of the more stable tertiary radical.

Scheme 2-29. Carbocyclization under anionic conditions

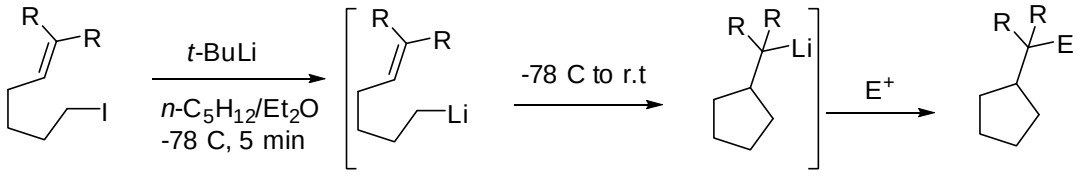

2.157 R= CH_3

2.158 R = H

E = H, D, CO_2H, OH

In our case, we hypothesized that, the formation of the more stable allyl anion **2.160** from the initially generated secondary carbanion **2.159** (Scheme 2-30), might provide the driving force for the formation of the decalin system. With this in mind, we began exploring the anionic carbocyclization using the conditions reported by Bailey[17] with the PMP-protected acetal-iodide **2.153**.

Scheme 2-30. Proposed carbocyclization under anionic conditions

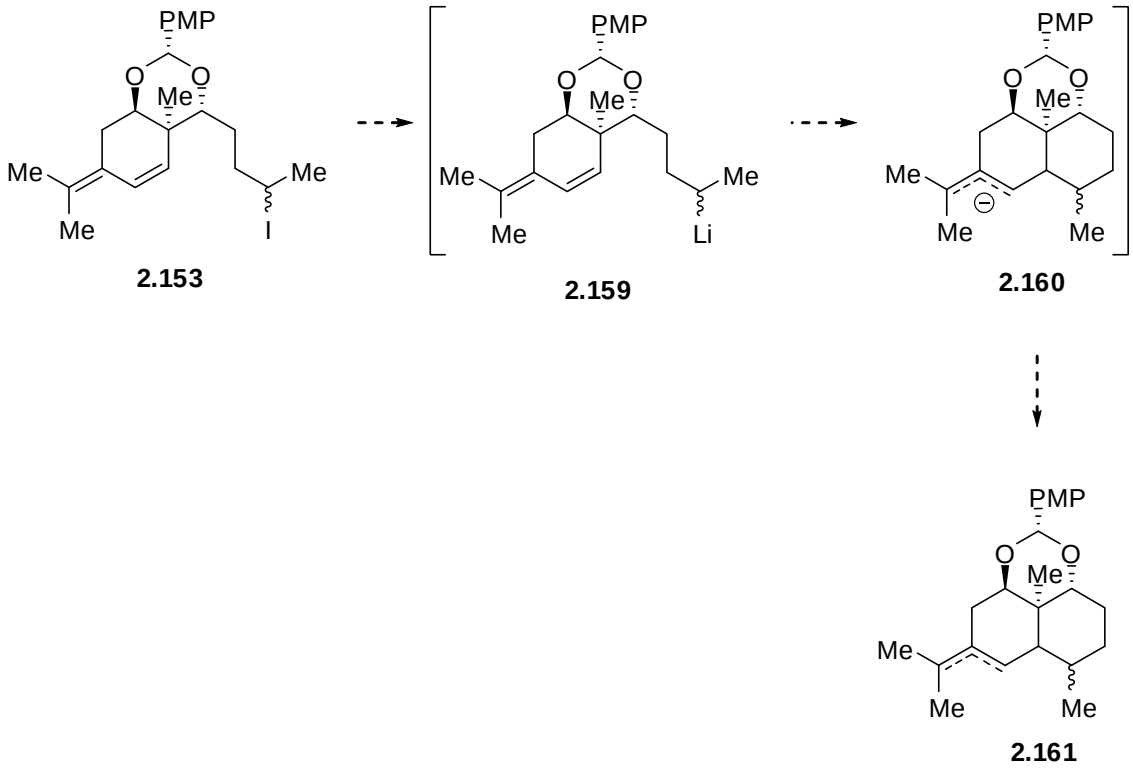

Accordingly, when **2.153** was subjected to halogen-metal exchange with *t*-BuLi at -78 °C in hexanes followed by addition of TMEDA, as shown in Scheme 2-31, a mixture of compounds **2.162** and **2.163** were detected in the crude ^{1}H NMR. Unfortunately, the cyclized product **2.161** was never observed. Bailey also observed formation such side products via Wurtz-type coupling, reduction and elimination, during their studies with secondary iodides.[17] Changing the order of addition of reagents did not alter the outcome of the reaction and products **2.162** and **2.163** via the elimination and reduction prevailed.

Scheme 2-31. Failure of the anionic carbocyclization

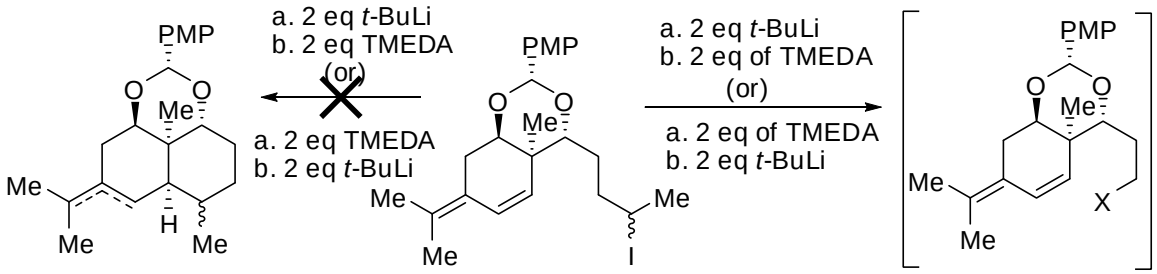

2.161 **2.153**

2.162 X = $CH{=}CH_2$

2.163 X = CH_2CH_3

2.2.3.3. Carbocyclization under free-radical conditions

With the failure of the carbocyclization under anionic conditions, we began to investigate the free-radical mode of cyclization. Due to the instability of the PMP protected acetal-iodide **2.153** to silica, benzaldehyde protected acetal-iodide **2.156** was chosen for subsequent studies. Submission of **2.156** to the standard free-radical conditions using Bu_3SnH and AIBN in benzene, effected a smooth cyclization to the hydronaphthalene products **2.164** as a mixture of diastereomers along with the reduction product **2.165**. The results from this free-radical carbocyclization are shown in Scheme 2-32. However, we were now faced with a new problem separating these compounds. Fortunately, upon hydrolysis with TsOH the cyclized product was isolated as a 3.5:1 inseparable mixture of diastereomers **2.166** in 54% yield over two steps, along with the reduction product **2.167** in 5% yield. It is noteworthy to mention here that this reaction was surprisingly regiospecific and the regioisomeric alkene **2.168** was never isolated.

Scheme 2-32. Attempted 6-exo-trig free radical carbocylization results

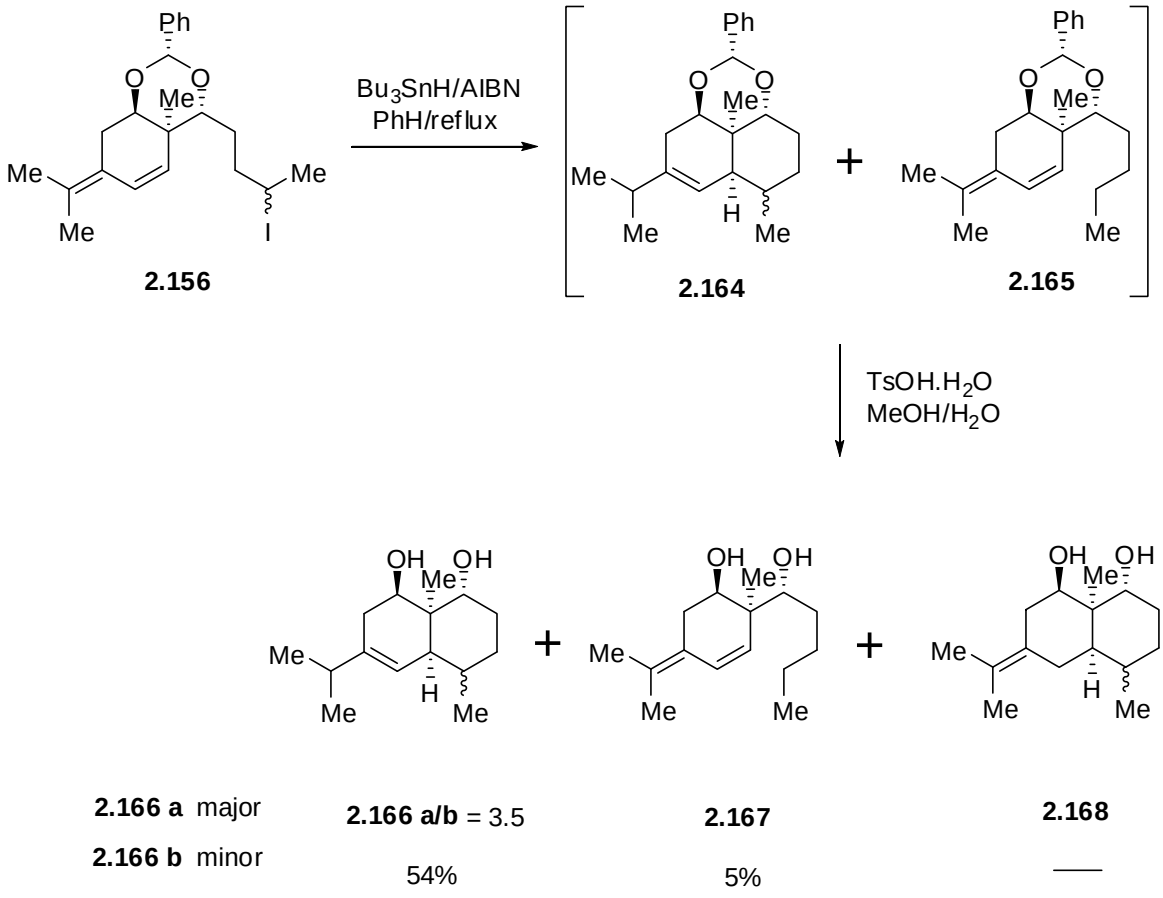

Luckily, the major diastereomer **2.166a** was partially separable and it formed the basis for further studies toward the synthesis of the rearrangement precursor. As discussed in the previous section, the stereochemistry of the ring junction and the newly formed stereogenic center are critical for the solvolytic Wagner-Meerwein rearrangement, for the stereoselective construction of the *trans*-hydroazulene skeleton of Englerin A. Thus, we embarked on the structural elucidation of the major diastereomer using NOE studies. Diagnostic NOE interactions for the major diastereomer are shown in Scheme 2-33.

Scheme 2-33. Diagnostic NOE interactions in the major diastereomer

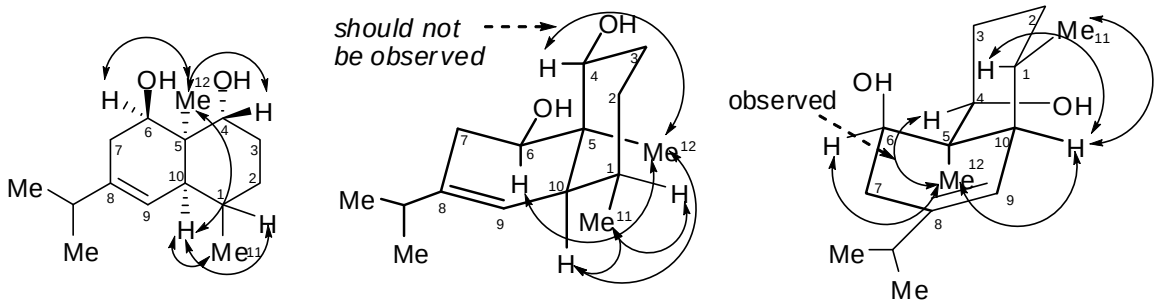

2.166 a **2.169** **2.170**

A strong NOE interaction observed between Me_{12} and H_{10} suggested *cis*-fusion between the rings. We next attempted to reconcile the experimentally observed NOE with the expected diastereomer which would presumably exist in the conformation **2.169** where all the substituents are equatorial. Most of the observed diagnostic NOE interactions for the major diastereomer **2.166a** matched those predicted for **2.169**, except for the interaction between Me_{12} and H_4. Due to the *anti* orientation between Me_{12} and H_4 NOE should not be observed. However, the other diastereomer which would presumably exist in the conformation **2.170**, accounted for all of the above observed NOE interactions. In this case, due to the gauche orientation of Me_{12} and H_4, a strong NOE was expected between them. This conclusion seemed rather surprising given that the transition state leading to the formation of **2.170** would be plagued by 1,3-diaxial interactions of Me_{11} and Me_{12} (See Scheme 2-21). Attempts to corroborate this structural assignment based on the predicted multiplicity of H_1 were unsuccessful due to the overlap of signals from H_2. After much deliberation, we decided to continue with the synthesis as planned hoping that we would be able to solve this structural ambiguity at a later stage. Moreover, in the event that the structural assignment proved correct, the

chemistry developed in the course of this study would potentially be useful for the minor diastereomer as well.

2.2.3.4. Synthesis of the solvolytic precursor of the major diastereomer

Accordingly, chemoselective mono-protection of the major diastereomeric diol **2.166a**, as the *para*-methoxybenzoate **2.171** was investigated. After considerable experimentation, it was found that the treatment of **2.166a** with two equivalents of BuLi/THF at -78 °C, followed by the addition of *para*-methoxybenzoyl chloride produced a mixture of compounds, from which the mono-protected *para*-methoxybenzoate **2.171** was isolated in 44% yield (Scheme 2-34). In addition to **2.171**, bis-*para*-methoxybenzoate **2.173**, and the mono *para*-methoxybenzoate **2.172** were obtained in 33% and 5% yields respectively, along with the unreacted diol **2.166a** in 13% yield. The structure of the mono *para*-methoxybenzoate **2.171** was established unambiguously from its single crystal X-ray structure (Scheme 2-35). The ORTEP diagram of **2.171**, showed that the molecule has a *cis*-fusion as expected from the NOE studies, but more importantly, the methyl group Me_{11} is on the α face of the molecule.

Scheme 2-34. Chemoselective mono-protection of the major diastereomer

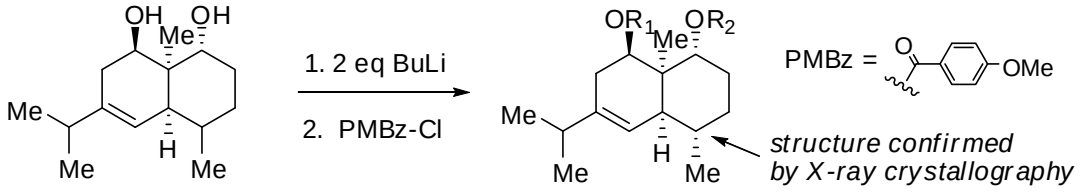

2.166 a

2.171	R_1 = PMBz; R_2 = H	44%
2.172	R_1 = H; R_2 = PMBz	5%
2.173	R_1 = R_2 = PMBz	33%

In light of these results, two things needed to be addressed. First, the free-radical cyclization clearly favored the formation of the diastereomer in which the methyl group Me_{11}, is on the α-face of the molecule. Although an exact rationale cannot be provided at this moment, we speculate that the transition state leading to the other diastereomer **2.174**, suffers from the allylic strain arising due to the steric interactions between the methyl group Me_{11} and the H_9, as shown in Scheme 2-36. The alternate transition state, in which the methyl group is pointed away from H_9 **2.177**, does not suffer from this steric interaction and can account for the surprising diastereoselectivity observed during the cyclization. To the best of our knowledge, this is the first example of a 6-exo-trig free radical cyclization initiated from a secondary radical.

Scheme 2-35. X-ray crystal structure of the mono *para*-methoxybenzoate 2.171

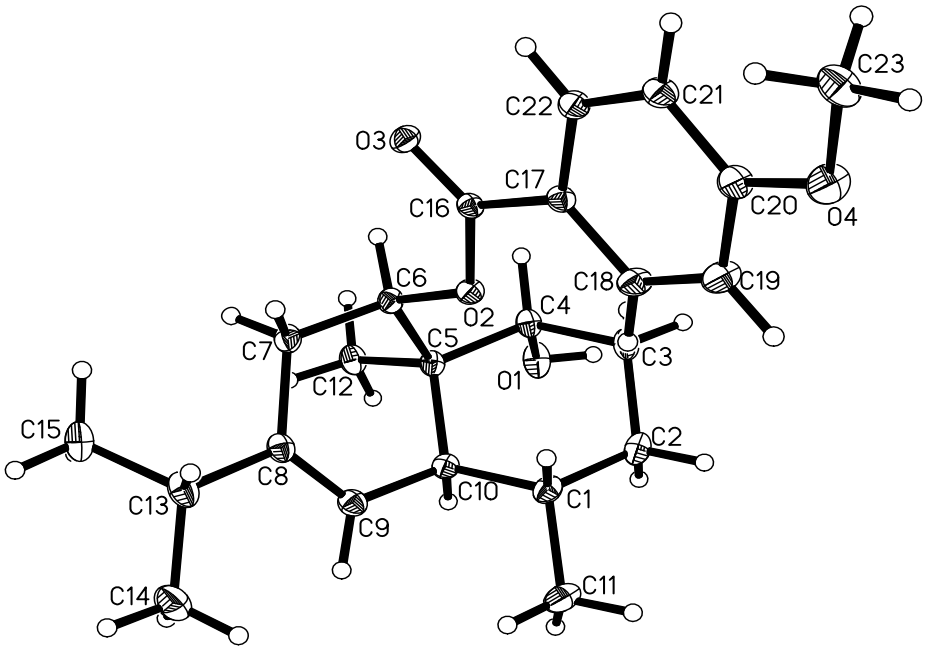

Scheme 2-36. Hypothetical transition state for the unexpected selectivity

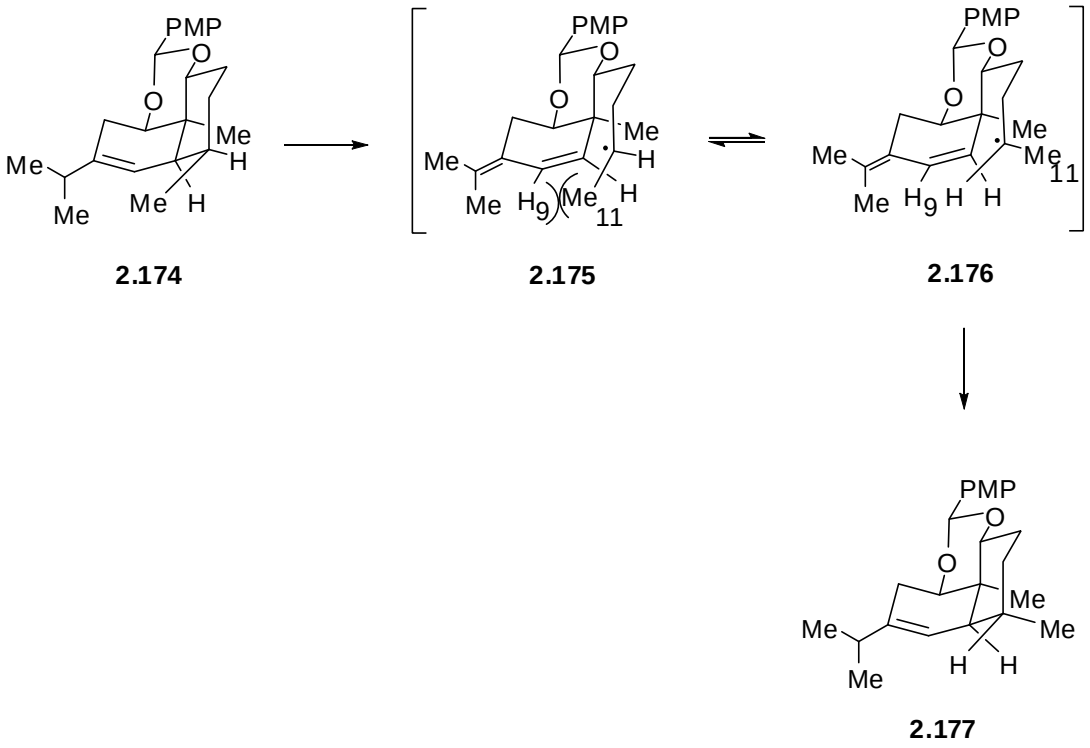

2.174 **2.175** **2.176**

2.177

Secondly, the chemoselectivity during the mono-protection of the diol **2.166a**, with *para*-methoxybenzoyl chloride also deserves a comment. We observed that this surprising selectivity eroded, on treating **2.171**, with KHMDS at -78 °C, suggesting that it is kinetic rather than thermodynamic in origin. In any event, having come thus far in the project, and fully aware that the stereochemistry of the methyl group Me_{11} on the major diastereomer, is not what we needed, we decided to continue as planned and investigate the solvolytic rearrangement of the major diastereomer. To this end, the synthesis of the tosylate **2.178** was accomplished, using KHMDS and TsCl in 75% yield, as shown in Scheme 2-37. It should be mentioned that, to prevent the equilibration of the *para*-methoxybenzoate **2.171**, deprotonation was conducted in presence of excess TsCl. With

the key precursor **2.178** at hand, solvolytic rearrangement of the tosylate was then investigated under several sets of conditions.

Scheme 2-37. Tosylation of the *para*-methoxybenzoate of the major diastereomer

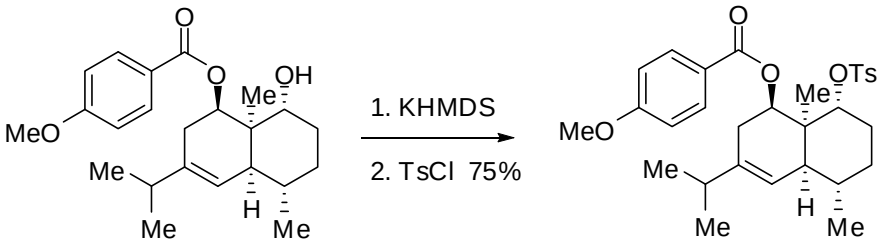

2.171 **2.178**

2.2.3.5. Solvolytic studies on the major diastereomer

Our first attempt in this connection, utilized 2,2,2-trifluoroethanol as the solvent owing to its non-nucleophilicity and high dielectric constant. Heating **2.178** in trifluoroethanol afforded an inseparable mixture of regioisomers **2.179** and **2.180**, differing in the position of the double bond as shown in Scheme 2-38. Similar products were also observed by Heathcock and Yoshikoshi (discussed in section **2.1.4**), during the solvolytic studies. Next, the solvolysis in AcOH with varying amounts of AcOK was attempted to understand the effect of the solvent on the rearrangement. However, under these conditions, a mixture of compounds was obtained, from which a new compound **2.181** was isolated, arising presumably by the displacement of the axial tosylate by the *para*-methoxybenzoate *via* **2.183**. A plausible mechanism for the formation of these products is shown in Scheme 2-39. In all the cases investigated, the rearranged product was never observed.

Scheme 2-38. Solvolytic rearrangement of the tosylate of the major diastereomer

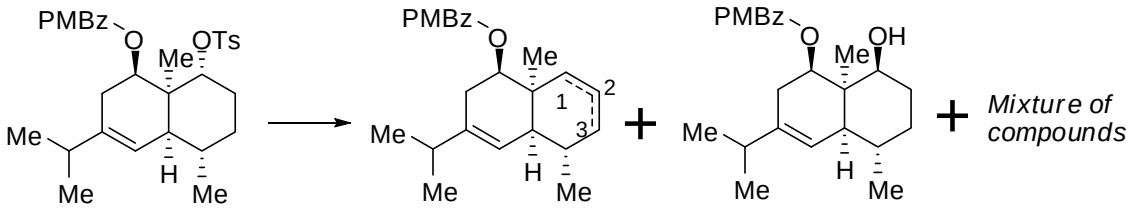

2.178 **2.179** $\Delta^{1,2}$ **2.180** $\Delta^{2,3}$ **2.181**

CF_3CH_2OH	80%	———
0.5 N AcOK/AcOH	62%	14%
2 eq. AcOK/AcOH	40%	18%
AcOH	40%	21%

These results are not surprising in light of Heathcock and Yoshikoshi's results, because of the gauche relationship between the migrating carbon-carbon bond and the leaving group in the more reactive conformer **2.183**. Noteworthy is the observation that longer reaction times led to decomposition of the starting material. We surmise that the decomposition might be due to the competing solvolysis of the axial *para*-methoxybenzoate, as the amount of *para*-methoxybenzoic acid isolated increased upon continued heating in all cases. Although this study with the major diastereomer **2.166a**, did not lead to the skeletal rearrangement, we gained a great deal of information and experience regarding the solvolytic rearrangement.

Scheme 2-39. Proposed mechanism of formation of 2.152

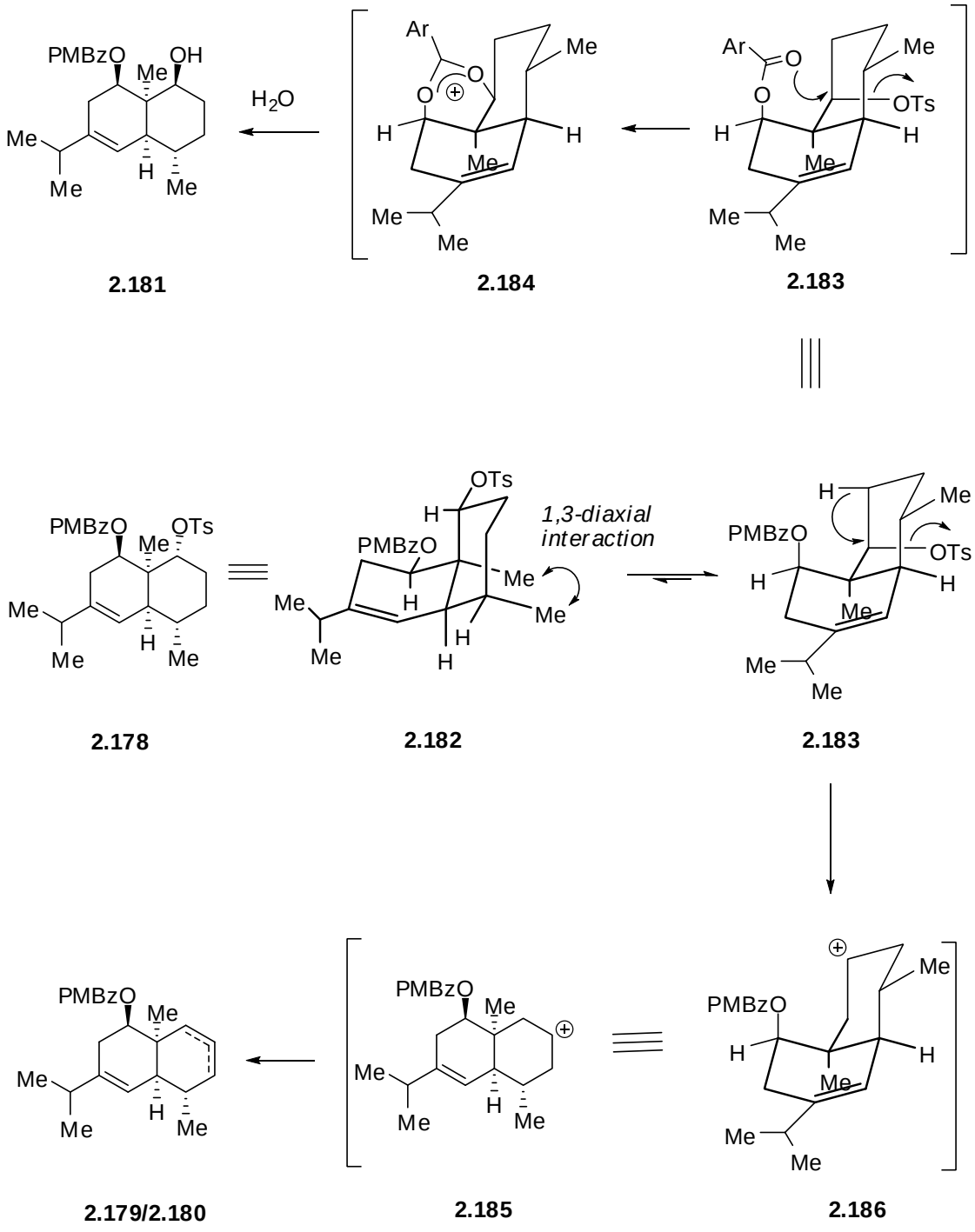

2.2.3.6. Synthesis of the solvolytic precursor of the minor diastereomer

At this juncture, isolation of the minor diastereomer in order to investigate its transformation into the *trans*-hydroazulene skeleton of englerin A was our next objective. Initial efforts in this regard explored the feasibility of mono-protection of the mixture of diastereomeric diols **2.166a/b** as the *para*-methoxybenzoates. When this mixture of diols was subjected to the same monoprotection conditions explored before, four compounds were isolated. Scheme 2-40 illustrates the results from this experiment. Fortunately, the chemoselectivity observed during the monoprotection of the major diastereomer prevailed in this case as well, and an inseparable mixture enriched with mono *para*-methoxybenzoate of the minor diastereomer **2.187**, contaminated with trace amounts of impurities was obtained. The latter products were identified as bis-*para*-methoxybenzoates **2.173** and **2.189**, mono *para*-methoxybenzoates **2.172** and **2.188**. The chemoselectivity observed during the course of this monoprotection of the diol is remarkable, as both the major and minor diastereomer underwent benzoylation on the same hydroxyl group, despite the similar steric environment.

Scheme 2-40. Chemoselective mono protection of the mixture of diastereomeric diols

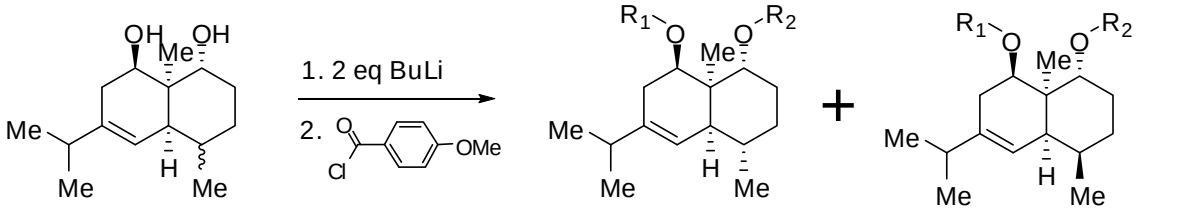

2.166 a/b

2.171	R_1 = PMBz, R_2 = H	**2.187**	R_1 = PMBz, R_2 = H
2.172	R_1 = H, R_2 = PMBz	**2.188**	R_1 = H, R_2 = PMBz
2.173	R_1 = R_2 = PMBz	**2.189**	R_1 = R_2 = PMBz

Unfortunately, when **2.187** was subjected to tosylation only the starting material was recovered. We suspect that this could probably due to the difference in sterics between an axial and equatorial hydroxyl group. Mesylation on the other hand (Scheme 2-41) proceeded uneventfully with MsCl and Et_3N[18] at 0 °C to give pure **2.190** in 35% yield.

Scheme 2-41. Mesylation of the *para*-methoxybenzoate of the minor diastereomer

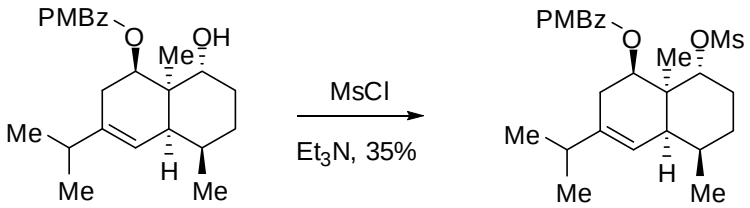

2.187 **2.190**

Extensive NMR analysis confirmed the structure of this compound. The key NOE interactions are shown in Scheme 2-42. Strong NOE between Me_{12} and H_6 and Me_{12} and H_1, indicate they are on the same side. Weak NOE between Me_{12} and H_4 suggest they are on the opposite side. A strong NOE was also observed between H_{10} and Me_{11}, H_{10} and H_1 indicating the structural assignment so far for the minor diastereomer to be correct.

Scheme 2-42. Key NOE interactions in the minor diastereomer mesylate 2.190

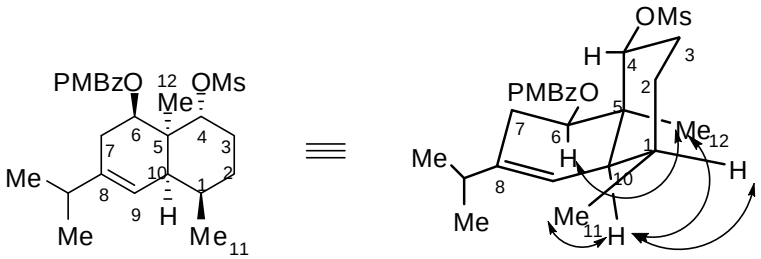

2.190 **2.191**

2.2.3.7. Solvolytic studies on the minor diastereomer

With access to the mesylate **2.190**, we then eagerly proceeded to explore the solvolysis of this substrate. Our enthusiasm was short lived, as heating **2.190** in AcOH for 36 hours gave alkene **2.1940** in 75% yield along with 5% of the unreacted starting material. Unfortunately, using milder solvolytic conditions (3M $LiClO_4$/THF) also furnished **2.194**, albeit in lower yield (50%). Under no circumstances was the rearranged product produced. It should be mentioned that in contrast to the short reaction times (1-3 hours) required for the solvolysis of **2.178** (Scheme 2-38), solvolysis of the mesylate **2.165** required 36 hrs. This could be due to the significant difference in the rates of solvolysis of axial vs equatorial mesylates or tosylates. The results from these solvolytic studies are shown in Scheme 2-43.

Scheme 2-43. Solvolysis of the tosylate of the minor diastereomer

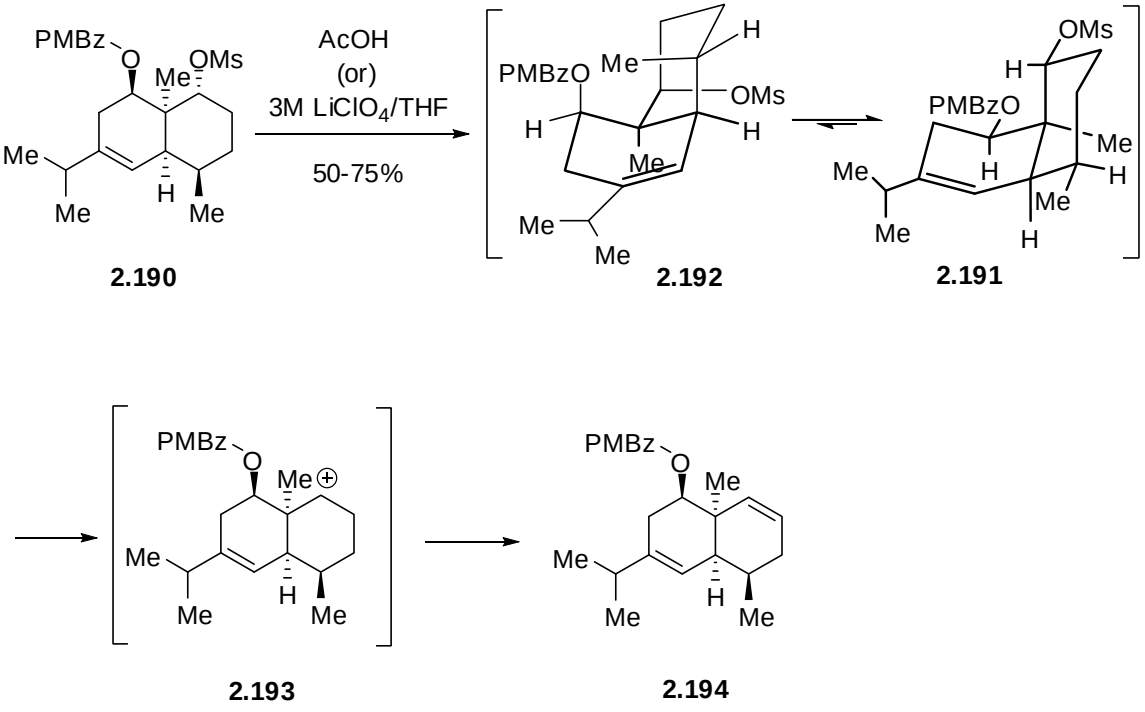

2.190 **2.192** **2.191**

2.193 **2.194**

This result came as a surprise to us, as in related studies by Yoshikoshi (Scheme 2-13) with **2.81**, the rearranged hydroazulene product was isolated, albeit in a low yield (38%). Comparing our results with Yoshikoshi's, we suspect that this could be due to the presence of the negative inductive effect of the *para*-methoxybenzoate at C_6. We presume that it retards the skeletal rearrangement, by disfavoring the formation of the carbocation on the *vicinal* carbon. Heathcock et. al. encountered a similar situation during the solvolytic studies of **2.52** (Section **2.1.4.1**), and invoked field effects due to the distal carbonyl group, which explained the higher ratio of the elimination products to the rearranged products. Unfortunately, further studies to understand the effect of the *para*-methoxybenzoate on this skeletal rearrangement would require the synthesis of deoxy-*para*-methoxybenzoate of **2.199**, access to which is not straightforward from the present route. Although a slight variation of the current scheme might lead to the synthesis of this compound, the low yield of the minor diastereomer coupled with problems with its separation from the major diastereomer, necessitates an alternate route toward the construction of this material. Scheme 2-44 depicts an alternate route for its synthesis.[19] Future studies along this line will address this issue.

Scheme 2-44. Proposed scheme to prepare deoxy-*para*-methoxybenzoate

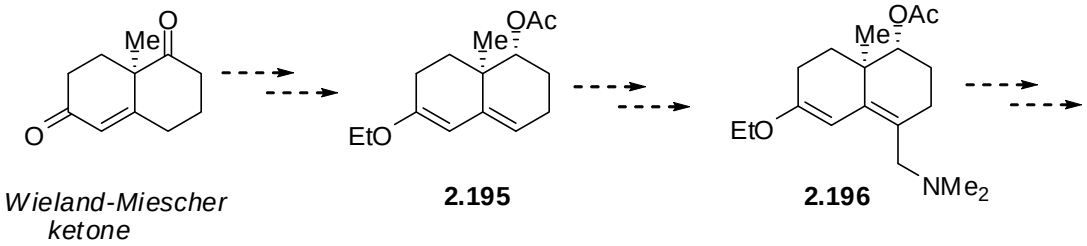

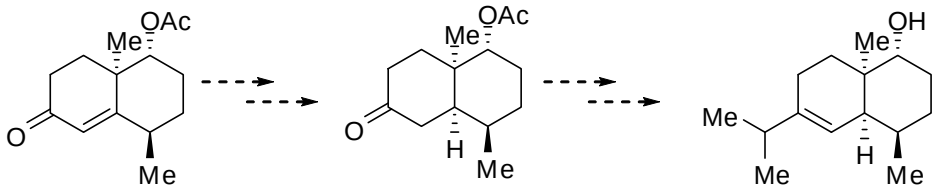

2.197 **2.198** **2.199**

2.2.4. Summary

In summary, we have investigated a synthetic route to the antitumor natural product Englerin A based on the proposed cationotropic shift/stereoselective cation trapping tandem. Several key features from this study should be highlighted. The key eudesmane intermediate *en route* to the guaiane skeleton was synthesized in seven steps starting from the commercially available (-)-carvone. Its construction was achieved using an unprecedented 6-exo-trig cyclization of a secondary radical producing, unfortunately, the undesired diastereomer as the major compound. Contrary to our expectations, the key solvolytic Wagner-Meerwein rearrangement of the *cis*-hydronaphthalene precursor to the hydroazulene skeleton did not take place. However, the concept of solvolytic Wagner-Meerwein rearrangement followed by intramolecular trapping of the *in situ* generated carbocation deserves further study in the context of other targets.

2.2.5. References

1. Willot, M.; Radtke, L.; Konning, D.; Frohlich, R.; gessner, V.; Strohmann, C.; Christmann, M. *Angew. Chem. Int. Ed*. **2009**, *48*, 9105-9108.
2. Ho, T.-L. *Enantioselective Synthesis, Natural Products from Chiral Terpenes*; Wiley Interscience: New York. 1992; 123-183.
3. Woodward, R. B.; *Jr*. Brutcher, F. V. *J. Am. Chem. Soc*. **1958**, *80*, 209-211.

4. (a) Taber, D. F., Louey, J. P., Wang, Y., Nugent, W. A., Dixon, D. A., Harlow, R. L. *J. Am. Chem. Soc*. **1994**, *116*, 9457-9463; (b) Nugent, W. A., Taber, D. F. *J. Am. Chem. Soc*. **1989**, *111*, 6435-6437; (c) RajanBabu, T. V., Nugent, W. A., Taber, D. F., Fagan, P. J., *J. Am. Chem. Soc*. **1988**, *110*, 7128-7135.
5. Holub, N.; Neidhofer, J.; Blechert, S. *Org. Lett*. **2005**, *7*, 1227-1229.
6. Leonard, W. R.; Livinghouse, T. *Tetrahedron Lett*. **1985**, *26*, 6431-6434.
7. (a) Lee, C. A.; Floreancig, P. E.; *Tetrahedron Lett*. **2004**, *45*, 7193-7196. (b) Ritcher, J. M., Ishihara, Y., Masuda, T., Whitefield, B. W., Llamas, T., Phjakallio, A., Baran, P. S., *J. Am. Chem. Soc*.**2008**, *130*, 17938-17954.
8. Fuji, K., Nakano, S., Fujita, E. *Synthesis* **1976**, 276.
9. Matsuda, F., Kawasaki, M., Terashima, S. *Tetrahedron Lett*. **1985**, *26*, 4639.
10. Chapman, O. L., Engel, M. R., Springer, J. P., Clardy, J. C. *J. Am. Chem. Soc.* **1971**, *93*, 6696-6698.
11. Barluenga, J., Sanz, R., Fananas, F. J., *Tetrahedron Lett*., **1997**, *38*, 2763.
12. Chamberlin, A. R., Bloom, S. H., Cervini, L. A., Fotsch, C. H. *J. Am. Chem. Soc*. **1988**, *110*, 4788-4796.
13. Cohen, T., Gibney, H., Ivanov, R., Yeh, E. A.-H., Marek, I., Curran, D. *J. Am. Chem. Soc*. **2007**, *129*, 15405-15409.
14. Deng, K., Bouguerra, B. A., Whetstone, J., Cohen, T., *J. Org. Chem*. **2006**, *71*, 2360-2372.
15. Liu, H., Deng, K., Cohen, T., Jordan, K. D., *Org. Lett*. **2007**, *9*, 1911-1914.
16. Bailey, W. F., Khanolkar, A. D., Gavaskar, K., Ovaska, T. V., Rossi, K., Theil, Y., Wiberg, K. B., *J. Am. Chem. Soc*. **1991**, *113*, 5720.

17. Bailey, W. F., Nurmi, T. T., Patricia, J. J., Wang, W. *J. Am. Chem. Soc*. **1987**, *109*, 2442-2448.

18. Yoshida, Y., Sakakura, Y., Aso, N., Okada, S., Tanabe, Y. *Tetrahedron*. **1999**, *55*, 2183-2192.

19. Kato, M., Kosugi, H., Yoshikoshi, A., *J. Chem. Soc., Chem. Commun*. **1970**, 185-186.

Chapter 3: Experimental

General: All reagents were purchased and used as received from commercial sources, unless otherwise specified. EM Science 60 F Silica Gel plates were used for monitoring the reactions by thin layer chromatography (TLC) and ICN Ecochrom silica gel silica gel (32-63 μm) was used to conduct flash chromatography. Reactions requiring anhydrous conditions were performed in vacuum heat-dried glassware under argon atmosphere. All anhydrous solvents were distilled just before use. Anhydrous tetrahydrofuran was obtained by distillation from sodium and benzophenone. Anhydrous dichloromethane was obtained by distillation after drying with CaH_2. ^{1}H NMR spectra were recorded using a Varian Unity Plus-300 NMR Spectrometer at 300 MHz, a Varian Unity Inova-500 NMR Spectrometer at 500 MHz or a Varian Unity Inova-600 NMR Spectrometer at 600 MHz. ^{13}C NMR spectra were recorded using a Varian Unity Plus-300 NMR Spectrometer at 75 MHz, a Varian Unity Inova-500 NMR Spectrometer at 125 MHz or a Varian Unity Inova-600 NMR Spectrometer at 150 MHz. The chemical shifts were reported as δ values (ppm) relative to TMS. Infrared spectra were recorded on a Perkin-Elmer Spectrophotometer Bx using think film technique and NaCl plates. High-resolution mass spectral analyses were performed on a Kratos MS-50TA spectrometer using Finnigan LCQ-Classic Ion-Trap mass spectrometer using electrospray ionization method (ESI). Melting points were measured on a Thomas-Hoover capillary melting point apparatus and were uncorrected.

3.1 Supporting information for lomaiviticins A and B

3.1.1. Oxidation of 2,4-dimethyl phenol:

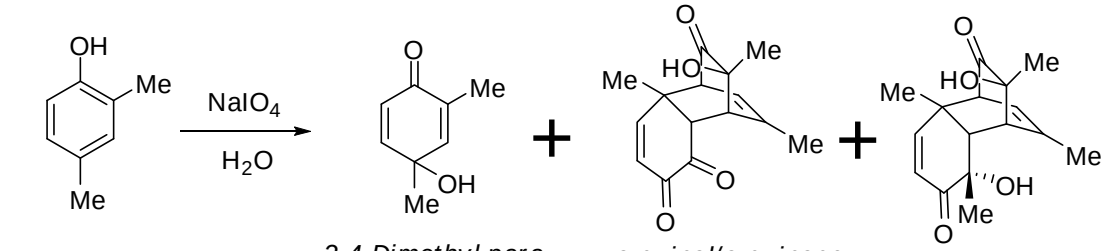

2,4-dimethylphenol | *2,4-Dimethyl-para -benzoquinol* | *o-quinol/o-quinone Diels Alder dimer* | **1.83**

These compounds were prepared following the protocol by Adler[1] and is reproduced here with the spectral data for the reader's convenience. To a stirred solution of 2,4-dimethyl-phenol (19.8 mL, 0.164 mol) in H_2O (3.5 L) was added aqueous solution of sodium meta-periodate (70 g, 0.327 mol). After stirring for 5 minutes, ethylene glycol (18 mL, 0.322 mol) was added in order to reduce the excess periodate. A light-brown amorphous precipitate (0.8 g) was removed by filtration and the orange-red solution was repeatedly extracted with dichloromethane. The combined organic extracts were dried over Na_2SO_4 and concentrated under vacuum to leave a reddish-brown, partly crystalline product from which three compounds were isolated.

2,4-Dimethyl-*para*-benzoquinol 3.1

The crude reaction product was treated with ether, in which a minor part of the product dissolved. Concentration of the red ether extract gave a light-red crystalline solid, which was recrystallised several times from benzene-hexane to afford **3.1** as colorless needles and flat prisms, 10.61 g (47% yield).

^{1}H NMR (300 MHz, $CDCl_3$) δ 6.76-6.81 (dd, J = 9.9 Hz, J = 3 Hz, 1H), 6.58-6.60 (m, J = 1.5 Hz, 1H), 5.95-5.99 (d, J = 9.9 Hz, 1H), 1.78 (d, J = 1.5 Hz, 3H), 1.38 (s, 3H); **^{13}C NMR** (75 MHz, $CDCl_3$) δ 186.59, 152.72, 148.43, 133.28, 126.68, 67.38, 26.94, 15.60.

Diels-Alder dimer 3.2

When the yellow alkaline extract obtained from the crude periodate oxidation product was poured into excess acetic acid, a colorless substance precipitated. Slow neutralization of the alkaline solution with acetic acid, however, produced a yellow crystalline product, which after recrystallization from ethyl acetate gave **3.2** as colorless needles, 3.2 g (15% yield)

^{1}H NMR (300 MHz, CD_3OD) δ 6.99 (d, J = 1.2 Hz, 1H), 5.78-5.75 (dt, J = 6.3 Hz, J = 1.8 Hz, 1H), 4.05 (d, J = 1.8 Hz, 1H), 3.10-3.08 (d, J = 6 Hz,1H), 1.83 (s, 3H), 1.39 (s, 3H), 1.36 (s, 3H); **^{13}C NMR** (75 MHz, CD_3OD) δ 210.43, 185.38, 155.25, 147.60, 145.24, 137.71, 134.30, 121.24, 72.11, 59.21, 56.08, 55.44, 50.00, 45.41, 30.59, 25.39, 21.35, 15.88.

***ortho*-quinol dimer 1.83**

The residue obtained from the ether extraction of the crude product was treated with 0.5N aqueous NaOH (10 mL per 1 g of solids). The nearly white insoluble residue was filtered off and washed with water. Recrystallization from benzene gave **1.83** as colorless prisms 1.77 g (16% yield)

^{1}H NMR (500 MHz, DMSO) δ 6.27-6.25(d, J = 10 Hz, 1H), 5.91-5.89 (d, J = 10 Hz, 1H), 5.542 (br, 1H), 5.40-5.39 (dd, J = 3 Hz, 1H), 5.0 (br, 1H), 2.92 (s, 1H), 2.73-2.70 (d,

J= 6.5 Hz, 1H), 2.69-2.69 (d, J = 1.5 Hz, 1H), 1.64 (s, 3H), 1.29 (s, 3H), 1.29 (s, 3H), 1.01 (s, 3H); **^{13}C NMR** (125 MHz, DMSO) δ 211.09, 201.33, 151.72, 145.22, 125.81, 121.74, 73.29, 71.04, 59.08, 50.65, 48.25, 44.05, 32.58, 25.72, 24.60, 21.43.

3.1.2. Me_3Sn- Michael adduct 1.84

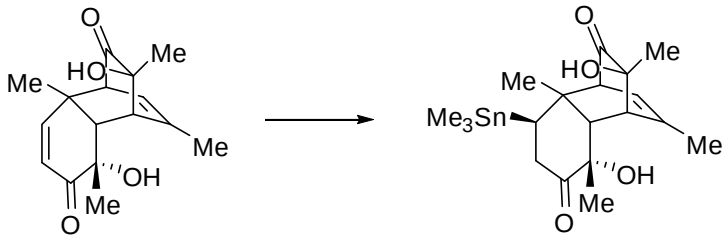

1.83 **1.84**

To Me_6Sn_2 (0.9 mL, 17.36 mmol) in THF (9 mL) at 0 °C, 1.35M BuLi (3.0 mL, 4.04 mmol) was added dropwise. After stirring for 20 minutes the reaction mixture was cooled to -78 °C and **1.83** (300 mg, 1.086 mmol) in THF (20 ml) was added dropwise and continued to stir for another 30 minutes at that temperature. After the consumption of the starting material (check by TLC) the reaction was quenched with 1N HCl and the organic phase was extracted with dichloromethane. The organic phase was washed with Brine, dried over Na_2SO_4, filtered and concentrated under vacuum. Chromatography (Hexanes: EthylAcetate-5:2) gave **1.84** as an off-white solid, 342 mg (70% yield).

^{1}H NMR (300 MHz, CD_3OD) δ 5.58-5.61 (dt, J = 6.3 Hz, J = 1.5 Hz, 1H), 2.98-2.91 (dd, J = 13.5 Hz, J = 6.9 Hz), 2.78-2.7 (m, 2H), 2.6-2.58 (d, J = 6.3 Hz, 1H), 2.5-2.4 (dd, J = 18.1 Hz, J = 13.5 Hz, 2.21-2.20 (d, J = 1.2 Hz, 1H), 2.02 (d, J = 1.2 Hz, 1H), 1.27 (s, 3H), 1.26 (s, 3H), 0.97 (s, 3H), 0.13 (s, 3H); **^{13}C NMR** (75 MHz, CD_3OD) δ 216.89, 215.28, 148.77, 118.92, 76.81, 72.64, 62.48, 53.40, 53.31, 50.00, 40.35, 30.79, 27.44, 25.04,

23.10, 22.92, -8.98; **IR** (film, cm^{-1}) 3423, 2973, 2942, 1714; **HRMS** (ESI) m/z [$(M+H)^+$] ($C_{19}H_{30}O_4Sn$) calculated 442.1166, found 442.1064; mp 170-172 °C.

3.1.3. tetra-ol 1.85

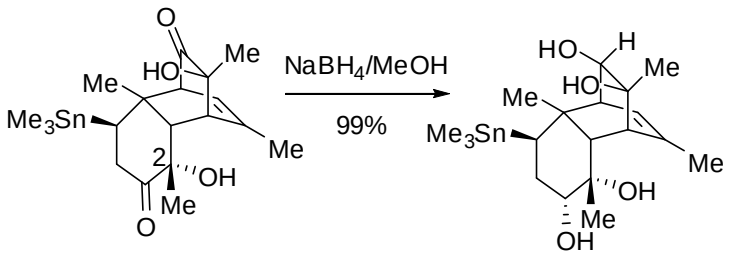

1.84 **1.85**

To **1.84** (32 mg, 0.073 mmol) in EtOH (0.8 mL) at 0 °C was added $NaBH_4$ (6 mg, 0.145 mmol) portionwise. The reaction mixture was slowly warmed to room temperature and stirred for 30 minutes at that temperature. At this time, the reaction mixture was concentrated under vacuum and DCM (10 mL) was added. The organic phase was then washed with water, dried over $MgSO_4$ and concentrated under vacuum to give **1.85** as an off-white solid, 32 mg (99% yield).

^{1}H NMR (600 MHz, CD_3OD) δ 5.62-5.49 (d, J = 6.6 Hz, 1H), 3.87-3.84 (m, 1H), 3.36-3.33 (m, 1H), 2.67 (s, 1H), 2.43-2.41 (dd, J = 3.6 Hz, 1H), 2.21 (s, 1H), 2.06-2.03 (dd, 1H, J = 13.2 Hz, 6 Hz, 1H), 1.89 (s, 1H), 1.93-1.86 (m, 1H), 1.79-1.74 (td, j = 13.8 Hz, 5.4 Hz, 1H), 1.36-1.16 (m, 2H), 1.33 (s, 3H), 1.27 (s, 3H), 1.26 (s, 3H), 0.08 (t, J = 25 Hz, 9H), 0.06 (d, J = 25 Hz, 1H); **^{13}C NMR** (150 MHz, CD_3OD) δ 143.94, 126.23, 84.86, 83.19, 76.40, 74.33, 50.944, 50.17, 49.22, 48.97, 48.72, 44.12, 34.25, 34.25, 32.86, 31.87, 28.58, 26.63, 22.42, -8.84; **IR** (film, cm^{-1}) 3443, 3031, 2928; **HRMS** (ESI) m/z [$(M+H)^+$] ($C_{19}H_{34}O_4Sn$) calculated 446.1479, found 446.1388; mp 280-282 °C.

3.1.4. Dihydro-dimer 1.88

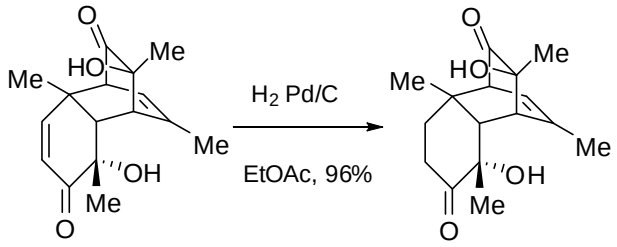

1.83 **1.88**

This compound was prepared following the protocol by Adler[1] and is reproduced here with the spectral data for the reader's convenience. To **1.83** (25 mg, 0.09 mmol) in ethanol (2.5 mL) was added 5% Pd/C (50 mg) and stirred for 5 hours under H_2 at atmospheric pressure. After the consumption of starting material (check by TLC) the reaction mixture was filtered over celite. This was rinsed with ethyl acetate and the filtrate was concentrated under vacuum to yield **1.88** as a white solid, 24 mg (95% yield). **^{1}H NMR** (500 MHz, CD_3OD) δ 5.70-5.68 (dt, J = 6.6 Hz, 1.5 Hz, 1H), 3.31-3.30 (dd, J = 2.5 Hz, 2 Hz, 1H), 2.62-2.61 (d, J = 6 Hz, 1H), 2.60-2.53 (m, 1H), 2.45-2.44 (d, 2Hz, 1H), 2.40-2.34 (q, J = 7 Hz, 1H), 2.36-2.33 (m, 1H), 1.86-1.85 (d, J= 2 Hz,1H), 1.72-1.69 (q, J = 7 Hz, 1H); **^{13}C NMR** (125 MHz, CD_3OD) δ 215.14, 213.99, 146.98, 121.45, 76.88, 72.13, 62.53, 52.92, 51.20, 40.55, 35.22, 33.50, 29.27, 25.68, 24.92, 22.50.

3.1.5. tetrahydrofuran 1.89

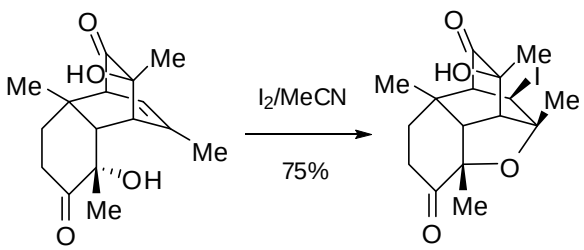

1.88 **1.89**

1.88 (300mg, 1.08 mmol), $NaHCO_3$ (370 mg, 4.4 mmol), Iodine (550 mg, 2.2 mmol) in acetonitrile (3 mL) were stirred at room temperature for 72 hrs. At this time saturated $Na_2S_2O_3$ was added. The aqueous phase was washed successively with DCM and Et_2O. The combined organic extracts were dried and concentrated under vacuum. Recystallization from MeCN gave **1.89** as a white solid, 245 mg (75% yield).

^{1}H NMR (600 MHz, CD_3OD) δ 4.84-4.82 (d, J = 4.2 Hz, 1H), 2.73-2.72 (d, J = 3Hz, 1H), 2.59-2.523 (td, J = 15.6 Hz, 4.8 Hz, 1H), 2.39-2.38 (d, J = 3Hz, 1H), 2.31-2.30 (d, J = 3.6 Hz, 1H), 2.29-2.26 (m, 1H), 2.06-2.01 (t, J = 14.4 Hz, 1H), 1.62 (s, 3H), 1.50-1.48 (m, 1H), 1.47 (s, 3H), 1.21 (s, 3H), 1.16 (s, 3H); **^{13}C NMR** (150 MHz, CD_3OD) δ 211.30, 208.40, 81.69, 79.03, 68.54, 63.31, 56.46, 49.49, 36.50, 35.03, 33.19, 32.19, 30.97, 29.07, 25.73, 21.54; **IR** (film, cm^{-1}) 3432, 2937, 1722; **HRMS** (ESI) m/z [$(M+H)^+$] ($C_{16}H_{21}IO_4$) calculated 404.0485, found 404.0386; mp 240-242 °C.

3.1.6. TMS-enol ether 1.90 and unsaturated diketone 1.91

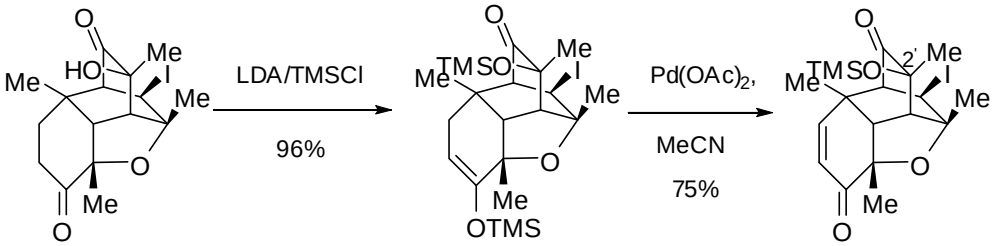

1.89 **1.90** **1.91**

TMS-enol ether 1.90: To THF (0.4 mL) under N_2 at 0 °C was added diisopropylamine (0.04 mL, 0.28 mmol). n-BuLi (0.1 mL, 0.25 mmol) was added dropwise and stirred at that temperature for 30 min. This was then cooled to -78 °C and TMSCl (0.07 mL, 0.5 mmol) was added dropwise and stirred for 30 min at that temperature. At this time **1.89** (40 mg, 0.1 mmol) in THF (1.0 mL) was added dropwise at -78 °C and stirred for another

1 hr at that temperature. After the consumption of starting material (check by TLC) Et_3N (0.4 mL), saturated $NaHCO_3$ (3 mL) was added and quickly extracted with Et_2O (2x 15 mL) washed with H_2O, 0.1N citric acid. The Et_2O layer was dried, filtered and concentrated under vacuum to yield **1.90** as a colorless liquid, 52 mg (96% yield). This compound was used without further purification in the next step.

Unsaturated diketone 1.91: The crude product from the above was subjected to saegusa oxidation by stirring with $Pd(OAc)_2$ (21mg, 0.091 mmol) in CH_3CN (1.5 mL) under argon atmosphere overnight. After the consumption of starting material (check by TLC) the reaction mixture was filtered through celite. The filtrate was concentrated and DCM was added. This was then washed with aqueous saturated $NaHCO_3$, dried over Na_2SO_4 and then concentrated under vacuum to yield **1.91** as an off-white solid, 32 mg (74% yield).

^{1}H NMR (300 MHz, $CDCl_3$) δ 6.31-6.28 (d, J = 10.5 Hz, 1H), 6.13-6.09 (d, J = 10.5 Hz, 1H), 4.51-4.50 (d, 1H, J = 3.9 Hz, 1H), 2.86-2.85 (d, J = 3.6 Hz, 1H), 2.56-2.55 (d, J = 1Hz, 1H), 1.75 (s, 3H), 1.66 (s, 3H), 1.38 (s, 3H), 1.31 (s, 3H), 0.11 (s, 9H); **^{13}C NMR** (75 MHz, $CDCl_3$) δ 207.33, 194.32, 152.14, 125.77, 82.33, 76.81, 71.76, 62.57, 60.31, 51.67, 39.38, 32.63, 30.48, 29.05, 25.23, 21.03, 2.67; **IR** (film, cm^{-1}) 2958, 1745, 1689; **HRMS** (ESI) m/z $[(M+H)^+]$ ($C_{22}H_{37}IO_4Si_2$) calculated 474.0723, found 474.0625; mp 130-135 °C.

3.1.7. diacetate 1.94

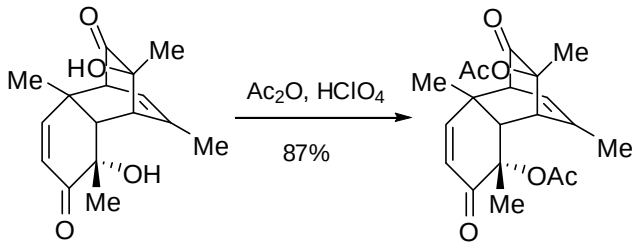

1.83 **1.94**

This compound was prepared following the protocol by Adler[1] and is reproduced here with the spectra data for the reader's convenience. To **1.83** (200 mg, 1.085 mmol), 2M Ac_2O/Ethyl Acetate/1.15% $HClO_4$ (3 mL) was added in one portion and stirred for 10 minutes. At this time, water was added and the reaction mixture was diluted with DCM. The organic phase was washed with 1N NaOH, water and filtered over Na_2SO_4, concentrated and dried under vacuum to give **1.94** as white solid in 343 mg, (87% yield). **^{1}H NMR** (300 MHz, $CDCl_3$) δ 6.05-6.01 (d, J = 10.2 Hz, 1H), 5.92-5.89 (d, 10.2 Hz, 1H), 5.50-5.47 (dt, J = 6.3 Hz, J = 1.8 Hz, 1H), 3.5-3.49 (t, J = 1.8 Hz, 1H), 3.02 (s, 1H), 2.80-2.78 (d, J = 6.3 Hz, 1H), 2.13 (s, 3H), 2.04 (s, 3H), 1.78 (s, 3H), 1.74-1.73 (d, J = 1.8 Hz, 3H), 1.49 (s, 3H), 1.36 (s, 3H); **^{13}C NMR** (75 MHz, $CDCl_3$) δ 205.48, 194.36, 169.95, 149.44, 144.02, 127.28, 123.16, 82.87, 80.18, 58.92, 46.94, 46.89, 44.64, 27.13, 26.02, 22.04, 22.02, 21.75, 20.01.

3.1.8. PhSe-diacetate 1.95

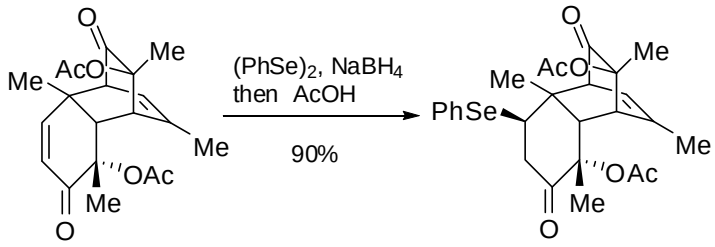

1.94 **1.95**

To $(PhSe)_2$ (30 mg, 0.094 mmol) in EtOH (2 mL) at 0 °C, $NaBH_4$ (8 mg, 0.190 mmol) was added portionwise. After stirring for 15 minutes at that temperature, acetic acid (0.03 mL) was added and stirred for 10 more minutes. At this time, **1.94** (52 mg, 0.144 mmol) in DCM (5 mL) was added and slowly warmed to room temperature and stirred for 3 hrs. After completion of starting material (check by TLC), the reaction mixture was diluted with DCM, quenched with 1N HCl and the organic phase was dried over Na_2SO_4 and concentrated under vacuum. Chromatography (Hexanes: Ethyl Acetate-3:1) gave **1.95** as a white solid, 44 mg (90% yield).

^{1}H NMR (300 MHz, $CDCl_3$) δ 7.50-7.47 (dd, J = 7.5 Hz, J = 1.8 Hz, 2H), 7.28-7.20 (m, 3H), 5.27-5.23 (dt, J = 6.6 Hz, J = 1.5 Hz, 1H), 3.99-9.92 (dd, J = 12.6 Hz, J = 8.4 Hz, 1H), 3.84 (s, 1H), 3.39-3.37 (d, J = 6.6 Hz, 1H), 2.98-2.72 (dd, J = 1.8 Hz, 1H), 1.96 (s, 3H), 1.92-1.91 (d, J = 1.8 Hz, 3H), 1.60-1.59 (d, J = 1.5 Hz, 1H), 1.49 (s, 3H), 1.38 (s, 3H), 1.02 (s, 3H); **^{13}C NMR** (75 MHz, $CDCl_3$) δ 205.27, 205, 169.99, 169.71, 154.16, 145.69, 135.11, 129.60, 128.48, 119.53, 83.83, 80.61, 57.57, 51.24, 47.41, 47.17, 45.57, 44.75, 23.31, 22.85, 22.04, 20.083, 19.67, 18.82; **IR** (film, cm^{-1}) 3032, 2943, 1738; **HRMS** (ESI) m/z $[(M+H)^+]$ ($C_{26}H_{30}O_6Se$) calculated 518.1208, found 518.1100; mp 178-180 °C.

3.1.9. PhSe-tetra-ol 1.96

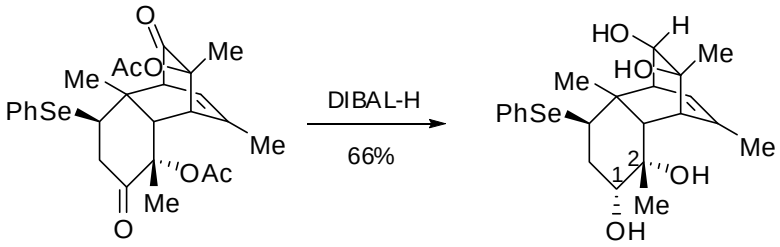

1.95 **1.96**

To **1.95** (522 mg, 1.01 mmol) in THF (15 mL), 1M DIBAL-H/THF (8.07 mL, 8.07 mmol) was added slowly at room temperature. After stirring for 1 hr, the reaction mixture was cooled to 0 °C and diluted with Et_2O and quenched slowly with H_2O (0.5 mL), 15% NaOH (0.5 ml), stirred for 15 minutes and $MgSO_4$ was added and continued to stir for another 15 minutes. Further dilution with Ethyl Acetate the reaction mixture was filtered over celite and the filtrate concentrated. Recrystallization from acetonitrile gave **1.96** as a white solid, 292 mg (66% yield).

^{1}H NMR (300 MHz, CD_3OD) δ 7.56-7.50 (m, 2H), 7.25-7.21 (m, 3H), 5.20-5.17 (dt, J = 6.6 Hz, 1.5 Hz, 1H), 3.96-3.90 (dd, J = 10.8 Hz, 8.4 Hz, 1H), 2.78-2.74 (dd, J = 6.6 Hz, 3 Hz, 1H), 2.45-2.33 (m, 2H), 2.19-2.18 (d, J = 1.5 Hz, 1H), 1.99-1.89 (m, 1H), 1.78-1.77 (d, J = 1.5 Hz, 3H), 1.30 (s, 3H), 1.23 (s, 3H), 1.15 (s, 3H); **^{13}C NMR** (75 MHz, CD_3OD) δ 143.19, 135.54, 132.05, 129.97, 128.04, 125.13, 75.58, 75.47, 73.82, 69.46, 51.79, 50.62, 50.28, 49.98, 49.60, 44.20, 39.26, 30.20, 26.17, 25.50, 22.77; **IR** (film, cm^{-1}); **HRMS** (ESI) m/z [$(M+H)^+$] ($C_{22}H_{30}O_4Se$) calculated 438.1309, found 438.1211; mp 195-198 °C.

3.1.10. PhSe-triol 1.97

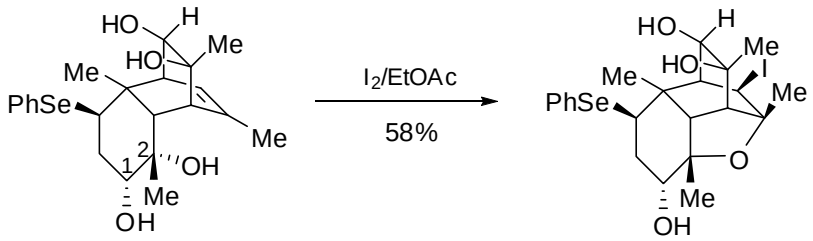

1.96 **1.97**

To **1.96** (100mg, 0.23 mmol) in Ethyl Acetate (2 mL) was added $NaHCO_3$ (77 mg, 0.92 mmol) and I_2 (117 mg, 0.46 mmol) and heated at 40 °C for 24 hrs. At this time, the reaction was quenched with saturated $Na_2S_2O_3$ and washed with water. The organic phase was dried over $MgSO_4$ and concentrated under vacuum. Chromatography (DCM: MeOH-10:1) gave **1.97** as a faint yellow color solid, 46 mg (58% yield) (66% BRSM).

^{1}H NMR (300 MHz, $CDCl_3$) δ 7.57-7.53 (m, 2H), 7.32-7.26 (m, 3H), 4.89-4.87 (d, J = 4.2 Hz, 1H), 4.47 (s, br, 3H), 3.76-3.70 (dd, J = 13.2 Hz, 2.7 Hz, 1H), 3.64-3.61 (dd, J = 5.4 Hz, 4.8 Hz, 1H), 2.94 (s, 1H), 2.94-2.91 (d, J = 6.9 Hz, 1H), 2.56-2.54 (d, J = 5.7 Hz, 1H), 2.44-2.42 (d, J = 3.3 Hz, 1H), 2.04 (m, 3H), 1.71-1.62 (m, 1H), 1.61 (s, 3H), 1.47 (s, 3H), 1.46 (s, 3H), 1.24 (s, 3H); **^{13}C NMR** (150 MHz, $CDCl_3$) δ 134.23, 130.48, 129.61, 127.75, 82.19, 77.75, 75.07, 72.55, 67.09, 55.30, 51.00, 47.06, 46.76, 44.38, 42.34, 38.07, 36.31, 33.32, 31.11, 28.50, 25.05; **IR** (film, cm^{-1}) 3367, 2928; **HRMS** (ESI) m/z $[(M+H)^+]$ ($C_{22}H_{29}IO_4Se$) calculated 564.0276, found 564.0169; mp 110-112 °C.

3.1.11. allyl alcohol-iodide 1.103

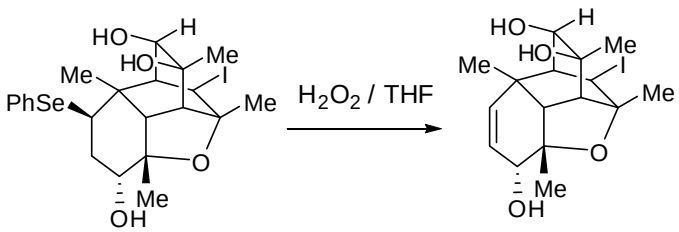

1.97 **1.103**

To **1.97** (5 mg, 8.8 μmol) in THF (3 mL), 30% H_2O_2 (0.2 mL) is added dropwise at 0 °C and slowly warmed to room temperature and stirred for 2 hrs. At this time, saturated $NaHCO_3$ is added and the organic phase is extracted with Ethyl Acetate, washed with water, brine and dried over $MgSO_4$, concentrated under vacuum. Chromatography (Hexanes: Ethyl Acetate-3:1) gave **1.103** as a colorless viscous liquid, 3.5 mg (98% yield).

^{1}H NMR (300 MHz, $CDCl_3$) δ 5.65-5.61 (dd, J = 10.5 Hz, 1.8 Hz, 1H), 5.39-5.35 (dd, J = 10.5 Hz, 2.1 Hz, 1H), 4.67-4.66 (dd, J = 3.9 Hz, 0.9 Hz, 1H), 4.31-4.28 (dd, J = 6.9 Hz, 1.8 Hz, 1H), 3.91-3.86 (dt, J = 11.1 Hz, 2.4 Hz, 1H), 2.71 (s, 1H), 2.47-2.46 (d, J = 3.9 Hz, 1H), 2.45-2.42 (d, J = 7.2 Hz, 1H), 2.27-2.25 (d, J = 3.3 Hz, 1H), 2.11-2.07 (d, J = 11.4 Hz, 1H), 2.04 (s, 1H), 1.59 (s, 3H), 1.46 (s, 3H), 1.40 9s, 3H), 1.31(s, 3H); **^{13}C NMR** (75 MHz, $CDCl_3$) δ 136.65, 127.01, 78.76, 74.31, 70.84, 67.04, 55.22, 51.13, 49.16, 43.66, 35.09, 33.62, 30.71, 29.88, 28.73, 25.07; **IR** (film, cm^{-1}) 3381, 2925; **HRMS** (ESI) m/z [$(M+H)^+$] ($C_{16}H_{23}IO_4$) calculated 406.0641, found 406.0543.

3.1.12. allyl alcohol 1.102

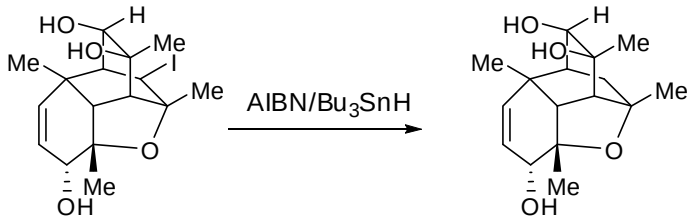

1.103 **1.102**

To **1.103** (10 mg, 0.025 mmol), Bu_3SnH (66 μL, 0.25 mmol), AIBN (2 mg, 0.012 mmol) and benzene (4 mL) was degassed and then heated to reflux for 2 hrs. After this time, the reaction mixture is cooled to room temperature and concentrated under vacuum. Chromatography (Hexanes: Ethyl Acetate-20:1) gave **1.102** as a colorless viscous liquid, ~7 mg (98% yield).

^{1}H NMR (500 MHz, $CDCl_3$) δ 5.52-5.50 (d, J = 10 Hz, 1H), 5.34-5.32 (dd, J = 10 Hz, 1.5 Hz, 1H), 3.88-3.85 (d, J = 11 Hz, 1H), 3.43-3.41 (dd, J = 7 Hz, 1Hz, 1H), 2.62-2.61 (d, j = 6.5 Hz, 1H), 2.59 (s, 1H), 2.49-2.48 (d, J = 3Hz, 1H), 2.22-2.20 (d, J = 11 Hz, 1H), 2.20 (s, 1H), 1.85-1.82 (dd, J = 14.5 Hz, 4.5 Hz, 1H), 1.65 (s, 1H), 1.41 (s, 3H), 1.40 (s, 3H), 1.39-1.24 (m, 2H), 1.31 (s, 3H), 1.27 (s, 3H); **^{13}C NMR** (125 MHz, $CDCl_3$) δ 137.48, 125.70, 78.75, 78.13, 77.03, 71.04, 67.83, 55.39, 49.42, 42.78, 42.38, 34.31, 30.83, 29.05, 28.27, 26.06; **IR** (film, cm^{-1}) 3379, 2960, 2926, 1670; **HRMS** (ESI) m/z $[(M+H)^+]$ ($C_{16}H_{24}O_4$) calculated 280.1675, found 280.1573.

3.1.13. 2-methoxy-4-(tosylmethyl) phenol 1.108

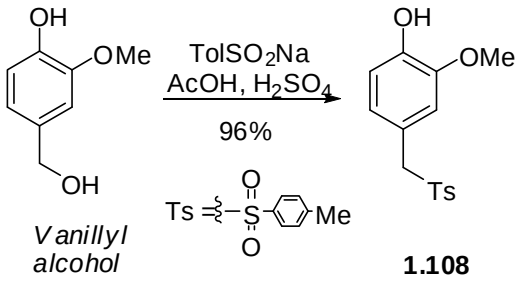

1.108

To vanillyl alcohol (2 g, 0.013 mmol) was added sodium *para*-toluenesulfinate (3.24 g), 3M AcOH (80 mL), concentrated H_2SO_4 (4 drops) and heated to reflux for 3 hrs, after which it was cooled to 0 °C and then the precipitate was collected, dried under vacuum to give **1.108** as a white solid, 6.8 g (90% yield).

^{1}H NMR (300 MHz, $CDCl_3$) δ 7.53-7.50 9d, J = 7.8 Hz, 2H), 7.25-7.23 (d, J = 7.8 Hz, 2H), 6.76-6.73 (dd, J = 8.1 Hz, 1.5 Hz, 1H), 6.64 (s, 1H), 6.47-6.45 (d, J = 8.1 Hz, 1H), 5.75 (s, 1H), 3.77 (s, 3H), 2.41 (s, 3H); **^{13}C NMR** (75 MHz, $CDCl_3$) δ 146.62, 146.30, 144.76, 135.10, 129.64, 128.84, 124.29, 119. 99, 114.47, 113.18, 62.84, 56.03, 21.75; **IR** (film, cm^{-1}) 3422, 1597, 1519; **HRMS** (ESI) m/z [$(M+H)^+$] ($C_{15}H_{16}O_4S$) calculated 292.0769, found 292.0664; mp 165-168 °C.

3.1.14. MOB-dimer 1.110

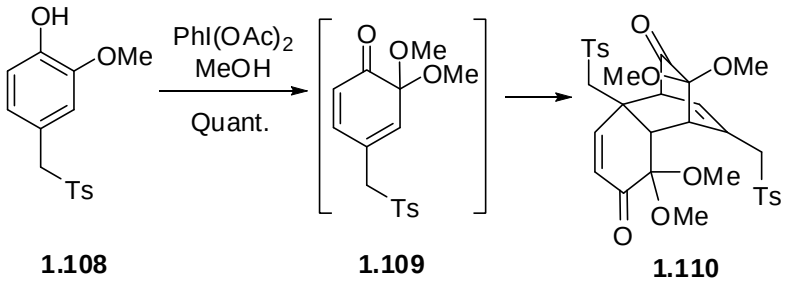

1.108 **1.109** **1.110**

To **1.108** (530 mg, 1.82 mmol) and $PhI(OAc)_2$ (642 mg, 2.0 mmol) under anhydrous MeOH (18 mL) was stirred overnight. After this time, the reaction mixture was

concentrated under vacuum. Chromatography (Hexanes: Ethyl Acetate -1:1) gave **1.110** as a faint yellow color solid, 589 mg (99% yield).

^{1}H NMR (300 MHz, $CDCl_3$) δ 7.82-7.80 (d, J = 8.1 Hz, 2H), 7.77-7.74 (d, J = 8.1 Hz, 2H), 7.39-7.37 9d, J = 8.1 Hz, 2H0, 7.33-7.31 (d, J = 8.1 Hz, 2H), 7.06-7.03 (d, J = 10.5 Hz, 1H0, 6.01-5.97 (d, J = 10.5 Hz, 1H), 5.90-5.88 (d, J = 6.3 Hz, 1H), 4.11-4.09 (d, J = 6.9 Hz, 1H), 3.77-3.67 (m, 3H), 3.31 (s, 3H), 3.29 (s, 3H), 3.28 (s, 3H), 3.21-3.16 (d, J = 14.4 Hz, 1H), 3.06 (s, 3H), 3.03 (s, 3H), 2.73 (s, 1H), 2.46 (s, 3H), 2.43 (s, 3H); **^{13}C NMR** (75 MHz, $CDCl_3$) δ 200.15, 193.06, 147.11, 145.35, 144.88, 137.68, 136.24, 134.30, 130.44, 130.21, 129.77, 128.52, 127.92, 127.84, 98.04, 94.59, 62.79, 60.48, 55.57, 51.45, 50.12, 48.86, 47.50, 47.14, 44.81, 21.74; **IR** (film, cm^{-1}) 2945, 1740, 1707; **HRMS** (ESI) m/z [$(M+H)^+$] ($C_{32}H_{36}O_{10}S_2$) calculated 644.1750, found 644.1657; mp 110-115 °C.

3.1.15. diol 1.111

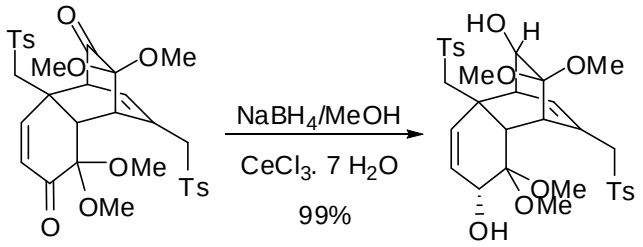

1.110 **1.111**

To **1.110** (100 mg, 0.155 mmol) and $CeCl_3.7H_2O$ (116 mg, 0.30 mmol) in DCM (1 mL) at 0 °C was added $NaBH_4$ (12 mg, 0.155 mmol). MeOH (1 mL) was added dropwise slowly and the reaction was continued to stir for 3-4 hrs slowly warming to room temperature. At this time the reaction mixture was concentrated and DCM was added and

the filtered over celite. The filtrate was then concentrated to give **1.111** as a faint yellow color solid, 100 mg (99% yield).

^{1}H NMR (300 MHz, $CDCl_3$) δ 7.97-7.94 (d, J= 8.4 Hz, 2H), 7.94-7.91 (d, J = 8.4 Hz, 2H), 7.52-7.50 9d, J = 8.4 Hz, 2H), 7.50-7.47 (d, J = 8.4 Hz, 2H), 6.56-6.54 (d, J = 6.6 Hz, 1H), 6.01-5.96 (dd, J = 9.9 Hz, 5.7 Hz, 1H), 5.47 (s, 1H), 4.39-4.35 (d, J = 13.5 Hz, 1H), 4.08 (s, br, 3H), 3.97 (s, 1H), 3.71 (s, 1H), 3.59-3.54 (d, J = 13.2 Hz, 1H), 3.48 (s, 3H), 3.43 9s, 3H), 3.22 (s, 3H), 3.17 (s, 3H), 3.07-3.06 (d, J = 3 Hz, 1H), 2.95 (s, 1H), 2.60 (2s, 6H), 2.35 (s, 1H); **^{13}C NMR** (75 MHz, $CDCl_3$) δ 144.84, 144.50, 138.64, 137.25, 134.50, 131.94, 129.86, 128.50, 127.90, 127.67, 124.10, 101.61, 99.96, 71.69, 63.65, 63.21, 59.82, 48.83, 48.50, 46.96, 45.03, 43.40, 42.98, 40.12, 21.69; **IR** (film, cm^{-1}) 3492, 2945, 1597; **HRMS** (ESI) m/z [$(M+H)^+$] ($C_{32}H_{40}O_{10}S_2$) calculated 648.2063, found 648.1965; mp 115-118 °C.

3.1.16. diketone 1.112

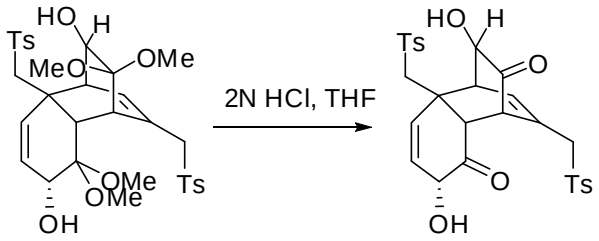

1.111 **1.112**

To **1.111** (135 mg, 0.21 mmol) in THF (20 mL) was added 2N HCl (30 mL) dropwise at 0 °C. After warming to room temperature and stirred overnight, the organic phase was extracted with Ethyl Acetate and washed with Brine, dried over $MgSO_4$ and concentrated under vacuum to give **1.112** as a colorless viscous liquid, 110 mg (~ 95% pure, 94% yield). The crude product was taken to the next step without further purification.

^{1}H NMR (300 MHz, $CDCl_3$) δ 7.64-7.61 (d, J = 6.4 Hz, 2H), 7.60-7.58 (d, J = 8.4 Hz, 2H), 7.27-7.25 (d, J = 6.4 Hz, 2H), 7.24-7.22 (d, J = 6.4 Hz, 2H), 6.12-6.09 (d, J = 6.9 hz, 1H), 5.59 (s, 1H), 5.07-5.06 (d, J = 2.7 Hz, 1H), 3.99-3.94 (d, J = 13.8 Hz, 1H), 3.87-3.80 (m, 2H), 3.77-3.68 (m, 2H), 3.51-3.46 (m, 2H), 3.37-3.35 (m, 2H), 3.11 (s, 1H), 3.27-3.20 (m, 1H), 3.02-2.89 (m, 1H), 2.36 (s, 3H), 2.34 (s, 3H); **^{13}C NMR** (75 MHz, $CDCl_3$) δ 208.95, 205.42, 145.48, 145.22, 137.80, 135.60, 131.99, 131.71, 130.20, 129.91, 129.61, 128.45, 128.20, 127.75, 73.29, 70.09, 63.16, 61.44, 55.38, 51.59, 49.54, 47.34, 21.81; **IR** (film, cm^{-1}) 3417, 1643.

3.1.17. bis-acetonide

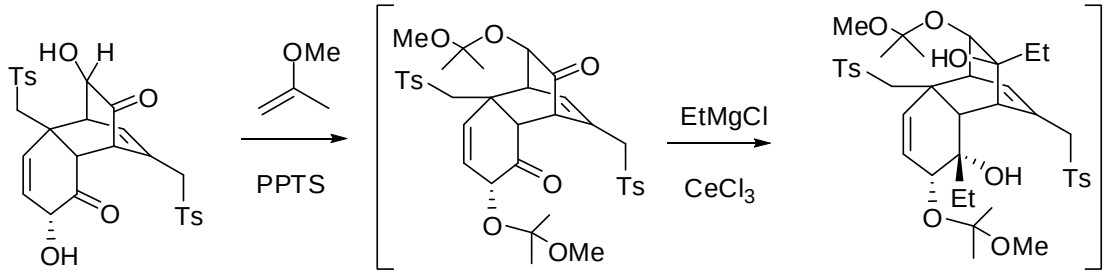

1.112 **1.115** **1.116**

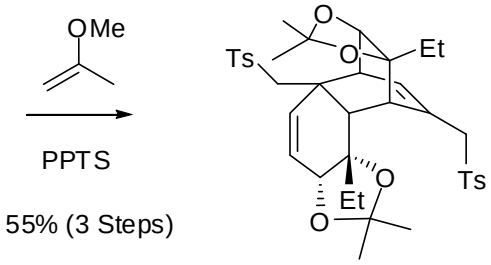

1.117

bis-MIP ether 1.115

To **1.112** (255 mg, 0.46 mmol) in $CDCl_3$ (2 mL), PPTS (16 mg, 0.063 mmol) and 2-methoxy propene (0.3 mL, 3.145 mmol) was added in one shot and stirred for 15 minutes. The reaction mixture was quenched with saturated $NaHCO_3$ and extracted with DCM. The organic layers were combined, dried over Na_2SO_4 and concentrated under vacuum to give **1.115** as a pale yellow solid, 322 mg (~ 99% pure) in nearly quantitative yield. No attempt was made to purify this material and it was used directly for the subsequent reaction.

Diol 1.116

The crude product from the above step without purification was then subjected to the nucleophilic addition. Anhydrous $CeCl_3$ (1 g, 4 mmol) purchased from Aldrich was heated at 160 °C for 3 hours under vacuum and while it is hot fill the flask with argon and cooled to 0 °C. Freshly distilled cold THF (10 mL) (addition of hot THF forms pebbles) was added and stirred vigorously overnight. After cooling to 0 °C, 2M EtMgCl (2 mL, 0.46 mmol) was added dropwise and stirred for 2 hours at that temperature. At this time, **1.115** (322 mg, 0.46 mmol) in THF (2 mL) was added dropwise and stirred for another 3 hours at 0 °C. The reaction was quenched by addition of water and then the filtered. The filtrate was then washed with brine, water and dried with Na_2SO_4, filtered and concentrated under vacuum to give **1.116** as a white solid, 244 mg (70% yield). No attempt was made to purify this material and it was used directly in the subsequent reaction.

Bis-acetonide 1.117

The crude product **1.116** from the above step (244 mg, 0.32 mmol) was dissolved in $CDCl_3$ (1 mL) and 2-methoxy propene (0.2 mL, 2.09 mmol) and PPTS (80 mg, 0.32 mmol) was added and stirred for 30 minutes at room temperature. After this time, the reaction mixture was quenched with addition of saturated $NaHCO_3$ and extracted with DCM. The organic phase was extracted and washed with brine, water, dried over Na_2SO_4, filtered and concentrated under vacuum. Chromatography (Hexanes: Ethyl Acetate -3:1) gave **1.117** as a pale yellow solid, 179 mg (56% yield, over 3 steps).

^{1}H NMR (600 MHz, $CDCl_3$) δ 7.84-7.82 (d, J = 8.4 Hz, 2H), 7.82-7.81 (d, J = 8.4 Hz, 2H), 7.43-7.42 (d, J = 8.4 Hz, 2H), 7.39-7.38 (d, J = 8.4 Hz, 2H), 6.45-6.43 (d, J = 7.8 Hz, 1H), 5.78-5.77 (d, J = 10.2 Hz, 1H), 5.46-5.44 (d, J = 9.6 Hz, 1H), 4.72-4.70 (d, J = 13.8 Hz, 1H), 4.20-4.16 (d, J = 21.6 Hz, 1H), 4.16 (s, 1H), 4.03-4.01 (t, J = 4.2 Hz, 1H), 3.94-3.93 (d, J = 3.6 Hz, 1H), 3.76-3.74 (d, J = 16.8 Hz, 1H), 3.10-3.08 (d, J = 13.2 Hz, 1H), 2.82 (s, 1H), 2.63 (s, 1H), 2.53 (s, 3H), 2.51 (s, 3H), 2.07-2.02 (quintet, J = 6.6 Hz, 1H), 1.66-1.61 (quintet, J = 7.8 Hz, 1H), 1.56-1.48 (m, 2H), 1.53 (s, 3H), 1.45 (s, 3H), 1.42 (s, 3H), 1.42 (s, 3H), 1.05-1.03 (t, J = 7.2 Hz, 3H), 1.02-1.00 (t, J = 7.2 Hz, 3H); **^{13}C NMR** (150 MHz, $CDCl_3$) δ 144.85, 144.28, 139.20, 137.36, 135.37, 132.89, 130.03, 129.95, 129.68, 127.94, 127.71, 111.53, 108.32, 86.96, 84.80, 82.77, 76.62, 76.60, 64.18, 60.09, 45.49, 45.46, 44.55, 44.18, 40.55, 35.54, 32.61, 29.90, 29.09, 27.02, 26.82, 21.72, 21.68, 8.77, 7.10; **IR** (film, cm^{-1}) 2978, 2936, 1597; **HRMS** (ESI) m/z $[(M+H)^+]$ ($C_{38}H_{48}O_8S_2$) calculated 696.2791, found 696.2705; mp 118-120 °C.

3.1.18. Reductive fragmentation conditions

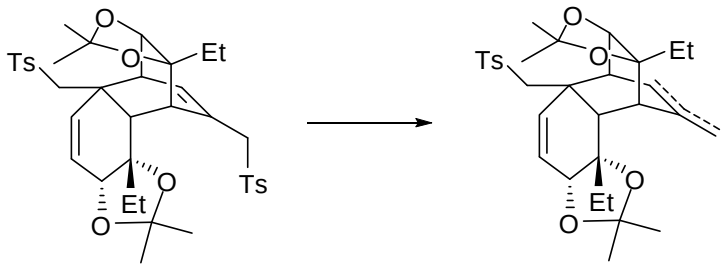

1.117 **1.119**

Procedure A:

1.117 (11.4 mg, 0.0163 mmol) and HMPA (0.04 mL, 0.228 mmol) were degassed and 1M SmI_2/THF (0.57 mL, 0.574 mmol) was added dropwise. The reaction mixture was stirred for 5 hours and quenched with water and extracted with DCM. The organic phase was washed with 1N HCl, water, dried over $MgSO_4$, filtered and concentrated under vacuum. Chromatography (Hexanes: Ethyl Acetate-4:1) gave **1.119** as a colorless viscous liquid, 6.1 mg (68% yield) as a mixture of inseparable regioisomers.

Procedure B:

1M SmI_2/THF (0.57 mL, 0.574 mmol) was added to degassed HMPA (0.04 mL, 0.228 mmol). To this mixture **1.117** (11.4 mg, 0.0163 mmol) in THF (0.5 mL) was added dropwise over 30 minutes and stirred at room temperature for 5 hours. After the disappearance of the purple color, the reaction was quenched and worked up as above to give **1.119** in nearly the same yield.

Procedure C:

To Naphthalene (1.28 g, 1 mmol) and Li (0.07 g, 1 mmol), THF (25 mL) was added under argon atmosphere and sonicated for 3 hours. Titration of this solution was done

with *s*-BuOH/Toluene following the literature procedure.[2] This solution was added carefully and dropwise to **1.117** (11.4 mg, 0.0163 mmol) at -78 °C and stirred for another 5 hours. At this time the reaction mixture was quenched by addition of 1N HCl and extracted in to organic phase using DCM. Concentration under vacuum gave **1.119** in lower yield (54%).

Alkene 1.119

^{1}H NMR (600 MHz, $CDCl_3$) δ 7.73-7.72 (d, J = 7.8 Hz, 2H), 7.65-7.63 (d, J = 9Hz, 2H), 7.23-7.22 (2d, J = 9 Hz, 4H), 5.82-5.80 9d, J = 10.2 Hz, 1H), 5.65-5.52 (d, J = 10.2 Hz, 1H), 5.54-5.52 (d, J = 7.2 Hz, 1H), 5.41-5.40 (d, J = 10.2 Hz, 1H), 5.31-5.29 9d, J = 10.2 Hz, 1H), 4.84 (s, 1H), 4.71 (s, 1H), 4.61-4.59 9d, J = 13.8 Hz, 1H), 4.51-4.49 (d, J = 14.4 Hz, 1H), 4.00 (s, 1H), 3.90 (s, 1H), 3.87-3.86 (d, J = 4.2 Hz, 1H), 3.81-3.80 9d, J = 4.2 Hz, 1H), 3.26-3.24 (m, 1H), 2.92-2.89 (d, J = 13.2 Hz, 1H), 2.75 (s, 1H), 2.72 (s, 1H), 2.73-2.71 (d, J = 13.8 Hz, 1H0, 2.43-2.40 (dd, J = 16.8 Hz, 4.8 Hz, 1H), 2.42 (s, 1H), 2.35 (2s, 6H), 2.23 (s, 1H), 1.90-1.86 (m, 2H), 1.77-1.74 (d, J = 18 Hz, 1H), 1.68 (s, 3H), 1.60-1.55 (quintet, J = 6.6 Hz, 2H), 1.50 (s, 3H), 1.48-1.42 (quintet, J = 6.6 Hz, 2H), 1.40 (s, 3H), 1.38 (s, 3H), 1.37-1.29 (m, 2H), 1.33 (s, 3H), 1.29 (s, 3H), 1.21-1.11 (m, 2H), 1.14 (s, 3H), 1.11 (s, 3H); **^{13}C NMR** (600 MHz, $CDCl_3$) δ 145.46, 144.01, 143.92, 139.82, 139.35, 139.25, 133.42, 131.61, 129.57, 129.51, 129.46, 127.57, 127.53, 127.20, 123.48, 113.91, 111.26, 108.86, 108.48, 108.22, 87.09, 84.49, 84.03, 83.98, 83.61, 83.48, 77.23, 76.56, 64.38, 64.28, 44.97, 44.51, 44.27, 44.12, 40.52, 39.96, 38.37, 37.75, 35.74, 34.33, 32.80, 32.52, 29.65, 29.31, 29.11, 29.09, 28.34, 27.95, 27.02, 26.74, 26.44, 26.13,

21.54, 21.53, 21.08, 8.45, 7.63, 7.18, 6.36; **IR** (film, cm^{-1}) 3018, 2984, 2936; **HRMS** (ESI) m/z [$(M+H)^+$] ($C_{31}H_{42}O_6S$) calculated 542.2702, found 542.2777.

3.1.19. phenol 1.114

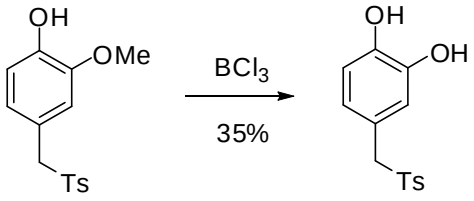

Vanillyl alcohol

1.114

To **1.108** (133 mg, 0.455 mmol) in DCM (0.5 mL) at 0 °C was added 1M BBr_3 (0.91 mL, 0.91 mmol) dropwise. After stirring for 1 hour at that temperature, the reaction mixture was quenched with water and the organic phase was extracted with DCM, dried over Na_2SO_4 and filtered and concentrated under vacuum. Chromatography (Hexanes: Ethyl Acetate-1:2) gave **1.114** as a white solid, 44 mg (35% yield).

^{1}H NMR (300 MHz, CD_3OD) δ 7.53-7.50 (d, J = 8.1 Hz, 2H), 7.33-7.30 (d, J = 8.4 Hz, 2H), 6.58 (s, 1H), 6.61-6.59 (d, J = 8.1 Hz, 1H), 6.38-6.35 (dd, J = 8.4 Hz, 2.1 Hz, 1H), 4.88 (s, 1H), 4.26 (s, 2H), 2.40 (s, 3H); **^{13}C NMR** (75 Hz, CD_3OD) δ 147.19, 146.39, 146.29, 136.62, 130.71, 129.85, 123.97, 120.96, 119.10, 116.20, 63.08, 21.67; **IR** (film, cm^{-1}) 3384, 1597, 1520; **HRMS** (ESI) m/z [$(M+H)^+$] ($C_{14}H_{14}O_4S$) calculated 278.0613, found 278.0512; mp 180-182 °C.

3.2 Supporting information for englerin A

3.2.1. 6-methylhept-5-en-2-yl pivalate 2.141

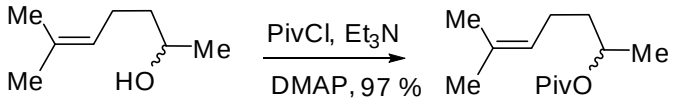

2.140 **2.141**

Trimethylacetyl chloride (18 mL, 0.146 mol) was added drop wise to a stirred solution of 6-methyl-5-hepten-2-ol **2.140** (20.05mL, 0.132 mol), triethylamine (28 mL, 0.2 mol) and 4-(dimethylamino) pyridine (1.61 g, 0.0132mol) in dichloromethane (130 mL) under argon atmosphere. After the completion of reaction (monitored by TLC), the reaction mixture was concentrated under vacuum. Diethylether (100 mL) and 1N HCl (100 mL) were added. The organic layer was further extracted with diethylether (2x 50 mL). The combined organic extracts were washed with 1N NaOH (60 mL) and H_2O (60 mL) three times and finally washed with brine. The organic phase was dried over $MgSO_4$, filtered and concentrated under vacuum to afford of **2.141** as colorless liquid, 27.19 g (97% yield).

^{1}H NMR (300 MHz, $CDCl_3$) δ 5.12-5.06 (t, J = 6.6 Hz, 1H), 4.91-4.81 (septet, J = 6.6 Hz, 1H), 2.07-1.96 (m, 2H), 1.67 (s, 3H), 1.64-1.40 (m, 2H), 1.58 (s, 3H), 1.18(s, br, 12H); **^{13}C NMR** (75 MHz, $CDCl_3$) δ 178.16, 132.06, 123.75, 70.29, 38.84, 36.21, 27.29, 25.81, 24.17, 20.00, 17.68; **IR** (film, cm^{-1}) 2972, 2931, 1727; **HRMS** (ESI) m/z $[(M+H)^+]$ ($C_{13}H_{24}O_2$) calculated 212.1776, found 213.1849.

3.2.2. 5-oxopentan-2-yl pivalate 2.142

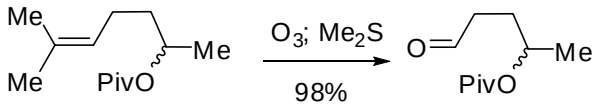

2.141 **2.142**

A solution of alkene **2.141** (42.594 g, 200.6 mmol) in MeOH (400 mL) was cooled to 0 °C in a brine/ice bath and bubbled with ozone while stirring vigorously. A thermometer measuring the solution temperature was used to make sure the reaction mixture stayed below 10 °C. Completion of the reaction was marked by disappearance of starting material on TLC. When treatment with ozone was complete, the solution was kept cold and added slowly (over approximately 20 min) to a refluxing solution of dimethyl sulfide (40 mL, ~2.5 equiv) in MeOH (100 mL) by using positive pressure of nitrogen to force it through a cannula of Teflon tube. The solution was refluxed for 3 hours and concentrated *in vacuo*. The remaining liquid was dissolved in pentane (250 mL) and washed with water (2x200 mL) followed by brine (100 mL). The organic layer was dried with $MgSO_4$ and concentrated to furnish 36.642 g of 2-(5-oxopentyl) pivalate **2.142** as a colorless liquid, 36.58 g (98% yield).

^{1}H NMR (300 MHz, $CDCl_3$) δ 9.72-9.71 (t, J = 1.2 Hz, 1H), 4.89-4.79 (sextet, J = 6.6 Hz, 1H), 2.46-2.41 (t, J = 7.2 Hz, 2H), 1.93-1.75 (m, 2H), 1.17-1.15 (d, J = 6.6 Hz, 3H), 1.12 (s, 3H); **^{13}C NMR** (75 MHz, $CDCl_3$) δ 201.51, 178.12, 69.75, 40.09, 38.87, 28.25, 27.23, 19.96; **IR** (film, cm^{-1}) 2976, 2715, 1727; **HRMS** (ESI) m/z $[(M+H)^+]$ ($C_{10}H_{18}O_3$) calculated 186.1256, found 186.1148.

3.2.3. Michael-Aldol adduct 2.146

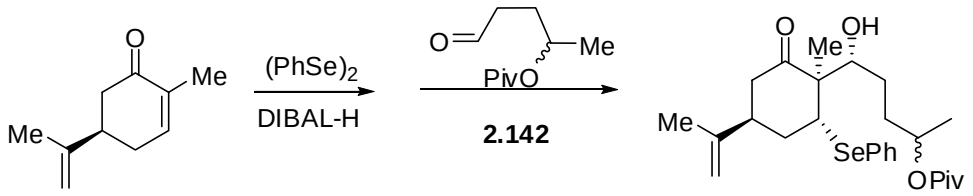

R-(-)-Carvone **2.146**

To a well stirred solution of PhSeSePh (13.84 g, 44.34 mmol) in THF (40 mL) at -78 °C was added DIBAL-H (1.5M in toluene, 59 mL, 88.5 mmol). The yellow solution became clear and (R)-carvone (15.2 mL, 97.0 mmol) was added over 20 minutes. The solution was stirred for 90 minutes after the completion of the addition and 2-(5-oxopentyl) pivalate **2.142** (13.63 g, 80.55 mmol) was added over 15 minutes. The solution was stirred for 30 minutes at -78 °C and quenched by adding a solution of 1M HCl (100 mL) and MeOH (50 mL) over 2 minutes without removing the cooling bath. When the addition was complete, the reaction mixture was allowed to warm slowly to room temperature and was diluted with Et_2O (100 mL) and 1M HCl (100 mL). The organic layer was separated and the aqueous layer extracted with CH_2Cl_2 (3x50 mL). The combined organic extracts were washed with brine (200 mL), dried with $MgSO_4$, and concentrated *in vacuo*. The resulting yellow oil was split into two equal portions, and each portion was purified separately by flash column chromatography (silica gel, 2" dia x 7-8" h, step-up gradient elution with 500 mL each 19:1 hexanes-Et_2O, 9:1 hexanes-Ethyl Acetate, 17:3 hexanes-Ethyl Acetate, 4:1 hexanes-Ethyl Acetate, 3:1 hexanes-Ethyl Acetate). The rapid execution of this step was necessary to obtain maximum yields, and a maximum of 20 minutes was allowed between application of the sample to silica gel and elution. As such, each column was run at its maximum flow rate, approximately 4 mL/s. To ensure that a minimum amount of time would elapse during the changing of

the eluent, the required solutions were premixed before running the column. Evaporation of the desired fractions furnished the pure Michael-aldol adduct **3.8** as yellow viscous oil 21.118 g (53% yield), which was stored in a refrigerator before use.

^{1}H NMR (300 MHz, $CDCl_3$) δ 7.56-7.54 (m, 2H), 7.30-7.25 (m, 3H), 4.99-4.88 (m, 1H), 4.77 (s, 1H), 4.66 (s, 1H), 4.21-4.08 (m, 1H), 3.82-3.78 (m, 1H), 2.90-2.80 (m, 1H), 2.70-2.50 (m, 1H), 2.17-1.40 (m, 4H), 1.54 (s, 3H), 1.21-1.18 (s, br, 16H); **^{13}C NMR** (75 MHz, $CDCl_3$) δ 212.35, 212.24, 178.39, 178.30, 146.31, 135.23, 135.19, 129.37, 129.34, 128.97, 128.91, 128.14, 128.16, 111.21, 75.03, 74.16, 70.83, 69.84, 57.48, 57.42, 49.21, 49.17, 42.53, 42.45, 41.26, 38.79, 33.76, 32.91, 31.65, 31.45, 28.17, 27.67, 27.20, 21.11, 21.03, 20.15, 16.72, 16.59; **IR** (film, cm^{-1}) 3484, 2972, 1717; **HRMS** (ESI) m/z $[(M+H)^+]$ ($C_{26}H_{38}O_4Se$) calculated 494.1935, found 495.2008.

3.2.4. PhSe-acetate 2.147

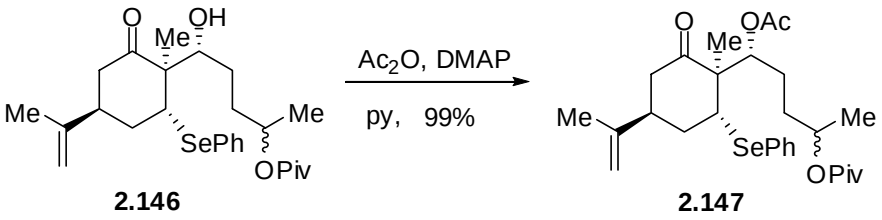

2.146 **2.147**

Acetic anhydride (2.7 mL, 28.23 mmol) and pyridine (2.3 mL, 28.23 mmol) was added to a stirred solution of aldol **2.146** (4.65 g, 9.41 mmol) and 4-(dimethylamino) pyridine (120 mg, 0.941 mmol) in dichloromethane (10mL) at room temperature. After stirring for 30 minutes the reaction was quenched by addition of water (10 mL). The aqueous layer was extracted with dichloromethane (2x 10 mL) and the combined organic extracts were dried over Na_2SO_4, filtered and concentrated to yield acetate protected Michael-aldol adduct **2.147** as a yellow viscous liquid (5.26 g, 99% yield).

^{1}H NMR (300 MHz, $CDCl_3$) δ 7.49-7.46 (dd, J = 7.5 Hz, 1.5 Hz, 2H), 7.25-7.16 (m, 3H), 5.67-5.58 (m, 1H), 4.93-4.90 (m, 1H), 4.79-4.75 (m, 1H), 4.69 (s, 1H), 4.63 (s, 1H), 3.74-3.70 (dd, J = 7.8 Hz, 7.5 Hz, 1H), 2.86-2.81 (m, 1H), 2.76-2.66 (td, J = 15 Hz, 5.1 Hz, 1H), 2.37-2.29 (m, 1H), 2.37 (m, 6 H), 1.94 (s, 3H), 1.53-1.51 (d, J = 4.8 Hz, 3H), 1.19-1.10 (s, br, 15H); **^{13}C NMR** (75 MHz, $CDCl_3$) δ 210.12, 210.05, 177.76, 177.68, 170.43, 170.38, 146.24, 146.22, 135.35, 135.32, 129.22, 129.19, 128.65, 128.58, 128.16, 128.13, 110.66, 74.93, 73.96, 69.97, 69.11, 56.14, 56.01, 49.87, 42.18, 42.09, 41.05, 40.91, 38.59, 32.86, 32.18, 30.76, 30.59, 27.03, 25.35, 25.01, 20.72, 20.69, 20.61, 20.39, 20.16, 19.95, 16.48, 16.37; **IR** (film, cm^{-1}) 2974, 1730, 1722; **HRMS** (ESI) m/z $[(M+H)^+]$ ($C_{28}H_{40}O_5Se$) calculated 536.2041, found 537.2113.

3.2.5. Keto-Diene 2.148

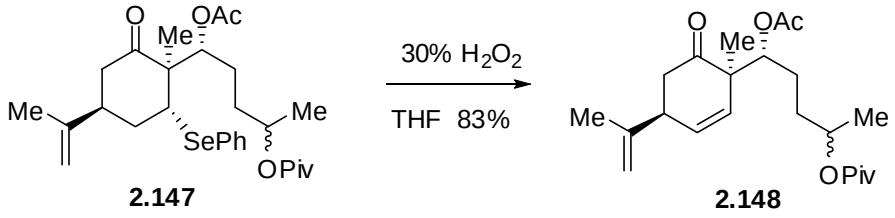

2.147 **2.148**

30% Hydrogen Peroxide (8 mL) was added drop wise to selenide **2.147** (5.26 g, 9.41 mmol) in tetrahydrofuran (30 mL) at room temperature. Stirring was continued until the yellow color disappears (30 min). $NaHCO_3$ (5 g) was added and the reaction was refluxed for 2-3 hours. The reaction mixture was poured in to water (20 mL) and diethylether (20 mL). The organic layer was extracted with diethylether (2x 20 mL). The combined organic extracts were washed with brine and dried over $MgSO_4$, filtered and concentrated to yield keto-diene **3.10** as a pale yellow viscous liquid 3 g (83% yield).

^{1}H NMR (300 MHz, $CDCl_3$) δ 5.84-5.79 (dd, J = 10 Hz, 2.1 Hz, 1H), 5.61-5.57 (d, J = 10 Hz, 1H), 5.15-5.09 (t, J = 10Hz, 1H), 4.85-4.77 (sextet, J = 7Hz, 1H), 4.81 (s, 3H), 4.77 (s, 3H), 3.19-3.14 (dd, J = 7.5 Hz, 1H), 2.65-2.57 (m, 2H), 2.05 (s, 3H), 1.74 (s, 3H), 1.57-1.37 (m, 4H), 1.16 (s, br, 12H), 1.13-1.11 (d, J = 7 Hz, 3H); **^{13}C NMR** (75 MHz, $CDCl_3$) δ 211.51, 178.18, 170.79, 146.40, 132.02, 131.96, 130.89, 111.72, 77.39, 76.93, 70.29, 69.84, 52.50, 45.33, 42.98, 38.93, 32.92, 32.65, 27.36, 26.25, 26.11, 21.21, 20.76, 20.59, 20.09; **IR** (film, cm^{-1}) 2973, 1739, 1723; **HRMS** (ESI) m/z [$(M+H)^+$] ($C_{22}H_{34}O_5$) calculated 378.2406, found 378.2302.

3.2.6. Diene-triol 2.149

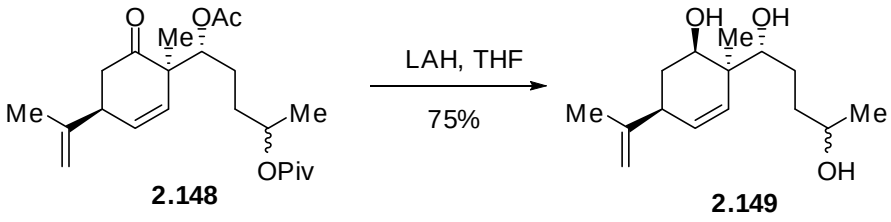

2.148 **2.149**

To the keto-diene **2.148** (3 g, 7.93 mmol) in tetrahydrofuran (16 mL) at 0 °C under argon was added LAH (32 mL, 7.93 mmol, 1M) drop wise. The reaction was slowly warmed to room temperature over 30 minutes and cooled to 0 °C. The reaction was diluted with diethylether (20 mL) and was added water (0.7 mL), 15% NaOH (0.7 mL) and water (0.7 mL) in that order. The reaction was warmed to room temperature and stirred for 30 minutes and $MgSO_4$ was added. After stirring for 30 minutes, the crude was filtered. The filtrate was concentrated under vacuum to yield diene-triol **2.149** as a faint yellow viscous liquid, 1.54 g (75% yield).

^{1}H NMR (300 MHz, CD_3OD) δ 5.58-5.57 (d, J = 10.2 Hz, 1H), 5.49-5.45 (dd, J = 10.2 Hz, 1.5 Hz, 1H), 3.99-3.91 (m, 1H), 3.84-3.74 (m, 2H), 3.06-3.00 (m, 1H), 2.05-1.76 (m,

2H), 1.74 (s, 3H), 1.71-1.44 (m, 4H), 1.25-1.23 (s, br, 6H); **^{13}C NMR** (75 MHz, CD_3OD) δ 149.43, 134.93, 131.17, 110.94, 79.05, 77.55, 77.47, 68.91, 68.67, 46.11, 43.02, 37.37, 37.27, 34.47, 29.06, 28.74, 23.78, 23.74, 20.50, 19.60, 19.56; **IR** (film, cm^{-1}) 3296, 2962, 2928; **HRMS** (ESI) m/z [$(M+H)^+$] ($C_{15}H_{26}O_3$) calculated 254.1882, found 255.1987.

3.2.7. Conjugated diene-triol 2.150

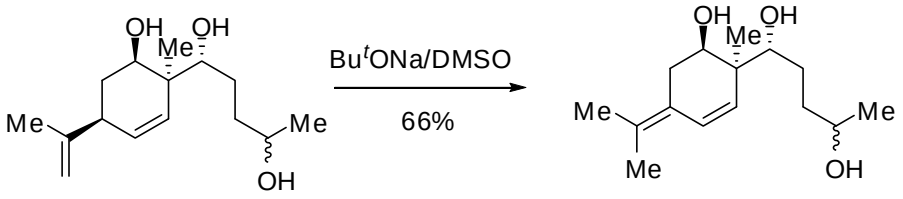

2.149 **2.150**

To a stirred suspension of sodium *tert*-butoxide (3.2 g, 33.25 mmol) in DMSO (30 mL) under argon diene-triol **2.149** (1.54 g, 6.05 mmol) in DMSO (5 mL) was added dropwise at 0° C. The reaction was heated to 100° C overnight and then quenched carefully with 1N HCl. It was then extracted with ethylacetate (6x 30 mL) dried over $MgSO_4$, filtered and concentrated under vacuum to yield crude conjugated diene-triol **2.150** as a colorless viscous liquid, 1.01 g (66% yield).

^{1}H NMR (300 MHz, CD_3OD) δ 6.43-6.39 (d, J = 10.2 Hz, 1H), 5.32-5.28 (d, J = 10.2 Hz, 1H), 3.78-3.69 (m, 3H), 2.66-2.65 (dd, J = 15.6 Hz, 4.5 Hz, 1H), 2.48-2.40 (dd, J = 15.6 Hz, 10.8 Hz, 1H), 1.78 (s, 3H), 1.76 (s, 3H), 1.73-1.33 (m, 4H), 1.61-1.15 (d, J = 6.9 Hz, 3H), 1.10 (s, 3H); **^{13}C NMR** (75 MHz, CD_3OD) δ 132.75, 130.13, 127.40, 126.53, 77.59, 77.51, 77.33, 68.95, 68.67, 43.27, 37.49, 37.35, 33.30, 29.24, 28.97, 23.80, 21.09, 20.08, 20.06, 20.01; **IR** (film, cm^{-1}) 3337, 3031, 2964, 1636; **HRMS** (ESI) m/z [$(M+H)^+$] ($C_{15}H_{26}O_3$) calculated 254.1882, found 254.1775.

3.2.8. PMP-acetal 2.151

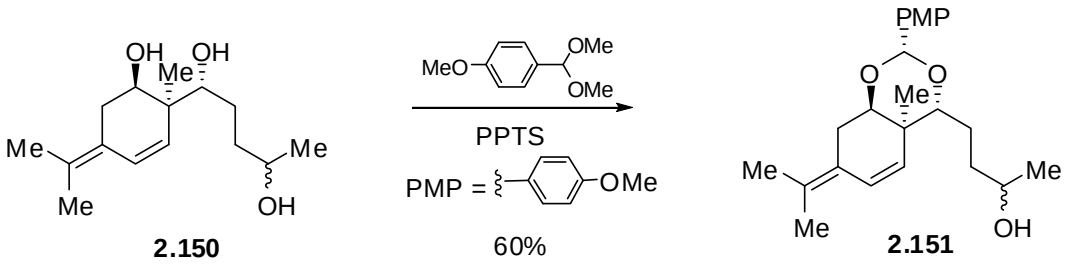

To the conjugated diene-triol **2.150** (571 mg, 2.25 mmol), *para*-anisaldehyde dimethyl acetal (0.8 mL, 4.41 mmol) and pyridinium *p*-toluenesulfonate (60 mg, 0.225mmol) were stirred in dichloromethane (2.5mL) overnight. The reaction mixture was washed with saturated $NaHCO_3$ (10 mL), water (10 mL), dried over Na_2SO_4, filtered and concentrated under vacuum. The crude product was chromatographed (Hexanes: EthylAcetate-6:1) to yield PMP acetal **2.151** as a colorless viscous liquid, 497 mg (60% yield).

^{1}H NMR (300 MHz, $CDCl_3$) δ 7.46-7.43 (d, J = 8.4 Hz, 2H), 6.90-8.87 (d, J = 8.4 Hz, 2H), 6.45-6.42 (d, J = 7.8 Hz, 2H), 5.92 (s, 1H), 5.32-5.29 (d, J = 7.8 Hz, 2H), 3.92-3.86 (m, 2H), 3.77 (s, 3H), 3.70-3.72 (m, 1H), 3.07-2.98 (dd, J = 13.5 Hz, 1H), 2.71-2.65 (dd, J = 14.7 Hz, 5.1 Hz, 1H), 1.80 (s, 3H), 1.78 (s, 3H), 1.70-1.38 (m, 4H), 1.32 (s, 3H), 1.14-1.12 (d, J = 6 Hz, 3H); **^{13}C NMR** (75 MHz, $CDCl_3$) δ 160.02, 159.96, 131.52, 131.32, 130.60, 130.50, 130.13, 130.00, 127.63, 127.56, 126.36, 126.30, 126.04, 126.00, 113.72, 95.11, 95.01, 80.34, 80.27, 79.35, 67.99, 67.50, 55.30, 37.56, 36.76, 36.47, 26.17, 26.13, 26.10, 25.49, 23.54, 20.92, 20.45, 20.01; **IR** (film, cm^{-1}) 3412, 2962, 1614, 1516; **HRMS** (ESI) m/z $[(M+H)^+]$ ($C_{23}H_{32}O_4$) calculated 372.2301, found 372.2197.

3.2.9. PMP-acetal-iodide 2.153

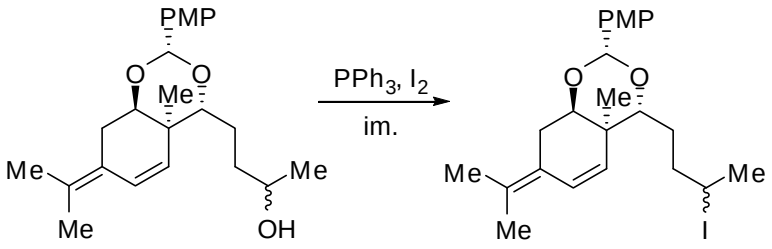

2.151 **2.153**

2.151 (93 mg, 0.26 mmol), triphenylphosphine (106 mg, 0.27 mmol) and imidazole (55 mg, 0.27 mmol) in dichloromethane (1.0 mL) was cooled to 0 °C and iodine (137 mg, 0.27 mmol) was slowly added under argon. After 15 minutes the reaction was quenched with $Na_2S_2O_3$. The reaction mixture was extracted with dichloromethane and washed with water, brine, dried over Na_2SO_4, filtered and concentrated under vacuum. The crude product was chromatographed (Hexanes: EthylAcetate-25:1) to yield the iodide **2.153** as a faint yellow viscous liquid, 82 mg (68% yield) and tetrahydrofuran **2.154** 18 mg, (30% yield).

^{1}H NMR (500 MHz, $CDCl_3$) δ 7.48-7.46 (d, J = 8.5 Hz, 2H), 6.92-6.91 (d, J = 8.5 Hz, 2H), 6.48-6.46 (d, J = 9.5 Hz, 1H), 5.91 (s, 1H), 5.37-5.33 (dd, J = 9.5 Hz, 1H), 4.24-4.12 (m, 1H), 3.95-3.86 (m, 2H), 3.81 (s, 3H), 3.06-3.01 (t, J = 14 Hz, 1H), 2.14-2.08 (m, 2H), 1.93-1.91 (t, J = 6 Hz, 3H), 1.83 (s, 3H), 1.80 (s, 3H), 1.79-1.53 (m, 4H), 1.35 (s, 3H); **^{13}C NMR** (125 MHz, $CDCl_3$) δ 160.09, 160.06, 131.65, 130.51, 130.33, 130.30, 127.70, 127.66, 126.53, 126.09, 113.82, 113.79, 95.16, 95.09, 79.68, 79.44, 78.99, 55.48, 40.32, 39.67, 37.62, 34.82, 31.41, 30.54, 30.20, 29.47, 29.36, 28.90, 26.28, 26.29, 21.06, 20.66, 20.63, 20.17, 20.13, 14.32; **IR** (film, cm^{-1}) 3028, 2915, 1614, 1516; **HRMS** (ESI) m/z $[(M+H)^+]$ ($C_{23}H_{31}IO_3$) calculated 482.1318, found 482.1388.

3.2.10. tetrahydrofuran 2.154

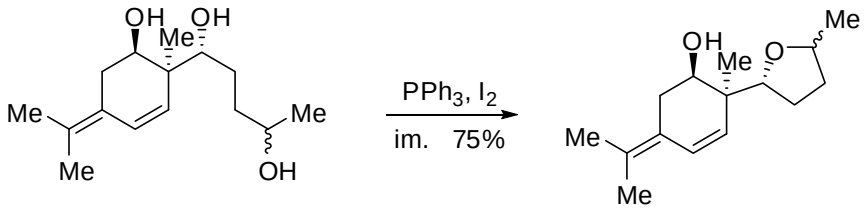

2.150 **2.154**

2.150 (130 mg, 0.47 mmol), triphenylphosphine (135 mg, 0.47 mmol) and imidazole (155 mg, 0.47 mmol) in dichloromethane (1.5 mL) was cooled to 0 °C and iodine (36 mg, 0.47 mmol) was added in one portion under argon. After 45 minutes the reaction was quenched with $Na_2S_2O_3$. The reaction mixture was extracted with dichloromethane and washed with water, brine, dried over Na_2SO_4, filtered and concentrated under vacuum. The crude product was chromatographed (Hexanes, Hexanes: EthylAcetate-25:1) to yield the iodide furan **2.154** as yellow colored viscous liquid, 83 mg (75% yield).

^{1}H NMR (500 MHz, $CDCl_3$) δ 6.43-6.37 (2d, J = 10.2 Hz, 2H), 5.27-5.19 (2d, J = 10.2 Hz, 2H), 4.31-4.28 (d, J = 8 Hz, 1H), 4.25-4.23 (d, J = 10 Hz, 1H), 4.20-4.08 (m, 2H), 4.03-3.93 (m, 2H), 3.75-3.62 (m, 2H), 2.71-2.59 (td, J = 15.3 Hz, 4.8 Hz, 2H), 2.47-2.32 (m, 2H), 2.05-1.81 (m, 6H), 1.77 (s, 3H), 1.74 (s, 3H), 1.47-1.33 (m, 2H), 1.22-1.20 (2d, J = 6 Hz, 6H), 1.09 (s, 3H), 1.07 (s, 3H); **^{13}C NMR** (125 MHz, $CDCl_3$) δ 131.09, 130.93, 130.19, 130.09, 128.54, 126.68, 126.38, 126.26, 126.14, 83.71, 82.39, 77.74, 76.82, 76.15, 76.12, 75.39, 42.00, 41.46, 33.62, 32.98, 32.81, 32.51, 28.04, 26.52, 21.63, 21.27, 21.14, 20.15, 20.12, 19.92, 19.51; **IR** (film, cm^{-1}) 3490, 3028, 2873, 1636; **HRMS** (ESI) m/z $[(M+H)^+]$ ($C_{15}H_{24}O_2$) calculated 236.1776, found 236.1669.

3.2.11. Ph-acetal 2.156

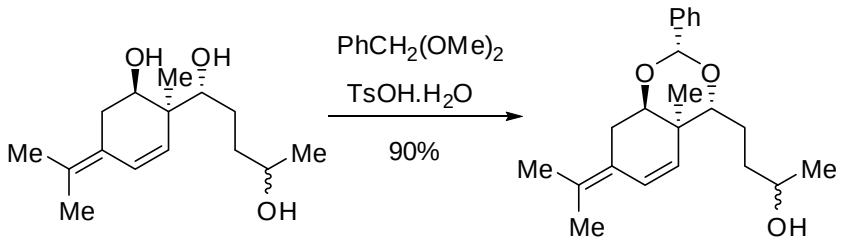

2.150 **2.155**

To **2.150** (571 mg, 2.25 mmol), benzaldehyde dimethylacetal (0.66 mL, 4.41 mmol) and *para*-toluenesulfonic acid monohydrate (171 mg, 0.9 mmol) were stirred in dichloromethane (2.5 mL) overnight. The reaction mixture was washed with saturated $NaHCO_3$ (10 mL), water (10 mL), dried over Na_2SO_4, filtered and concentrated under vacuum. The crude product was chromatographed (Hexanes: Ethylacetate-10:1) to yield benzaldehyde-acetal **2.155** as a yellow colored viscous liquid, 693 mg (90% yield).

^{1}H NMR (300 MHz, $CDCl_3$) δ 7.58-7.56 (d, J = 7.5 Hz, 2H), 7.42-7.35 (m, 3H), 6.51-6.46 (d, J = 10.2 Hz, 1H), 6.00 (s, 1H), 5.38-5.34 (d, J = 10.2 Hz, 2H), 3.99-3.90 (m, 2H), 3.74-3.68 (m, 1H), 3.13-3.04 (dd, J = 14.1 Hz, 1H), 2.77-2.64 (dd, J = 14.1 Hz, 5.4 Hz), 1.85 (s, 3H), 1.83 (s, 3H), 1.78-1.42 (m, 4H), 1.38 (s, 3H), 1.16-1.14 (d, J = 6.3 Hz, 3H); **^{13}C NMR** (75 MHz, $CDCl_3$) δ 138.88, 138.74, 130.43, 130.35, 129.91, 129.81, 128.70, 128.66, 128.15, 126.23, 126.17, 125.89, 125.86, 95.07, 94.99, 80.17, 80.12, 79.22, 67.60, 67.33, 37.48, 36.36, 36.23, 26.00, 25.74, 25.42, 23.41, 23.37, 20.80, 20.35, 19.89; **IR** (film, cm^{-1}) 3400, 3064, 2858; **HRMS** (ESI) m/z [$(M+H)^+$] ($C_{22}H_{30}O_3$) calculated 342.2195, found 342.2095.

3.2.12. Ph-acetal-iodide 2.156

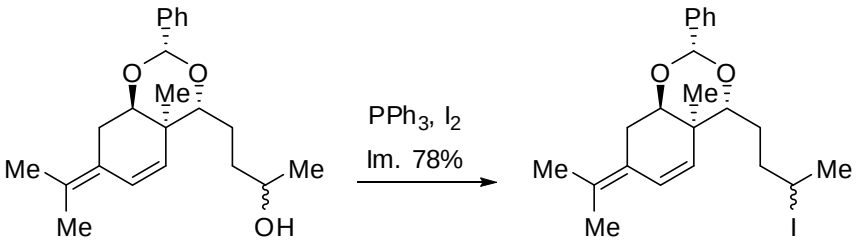

2.155 **2.156**

2.155 (2.45 g, 7.173 mmol), triphenylphosphine (1.975 g, 8.61 mmol) and imidazole (1.02 g, 15.06 mmol) in dichloromethane (14.0 mL) was cooled to 0 °C and iodine (2.73 g, 10.75 mmol) was slowly added under argon. After 15 minutes the reaction was quenched with $Na_2S_2O_3$. The reaction mixture was extracted with dichloromethane and washed with water, brine, dried over Na_2SO_4, filtered and concentrated under vacuum. The crude product was chromatographed (Hexanes then Hexanes: EthylAcetate-25:1) to yield the iodide **2.156** as yellow viscous oil, 2.54 g (78% yield).

^{1}H NMR (300 MHz, $CDCl_3$) δ 7.61-7.58 (d, J = 7.5 Hz, 2H), 7.47-7.40 (m, 3H), 6.55-6.51 (d, J = 10.2 Hz, 1H), 6.01 (s, 1H), 5.43-5.38 (d, J = 10.2 Hz, 1H), 4.31-4.16 (m, 1H), 4.02-3.93 (m, 2H), 3.14-3.05 (t, J = 14.1 Hz, 1H), 2.80-2.73 (dd, J = 14.1 Hz, 5.1 Hz, 1H), 1.99-1.96 (m, 3H), 1.88 (s, 3H), 1.86 (s, 3H), 2.22-1.60 (m, 4H); **^{13}C NMR** (75 MHz, $CDCl_3$) δ 139.09, 130.43, 130.32, 128.92, 128.88, 128.42, 128.39, 126.54, 126.40, 126.36, 126.04, 95.28, 95.18, 79.73, 79.44, 79.03, 40.30, 39.64, 37.64, 31.27, 30.48, 30.10, 29.84, 29.54, 29.32, 28.89, 26.24, 21.06, 20.64, 20.62, 20.16; **IR** (film, cm^{-1}) 3064, 2916, 2857; **HRMS** (ESI) m/z [$(M+H)^+$] ($C_{22}H_{29}IO_2$) calculated 452.1212, found 452.1266.

3.2.13. Carbocyclization under anionic conditions

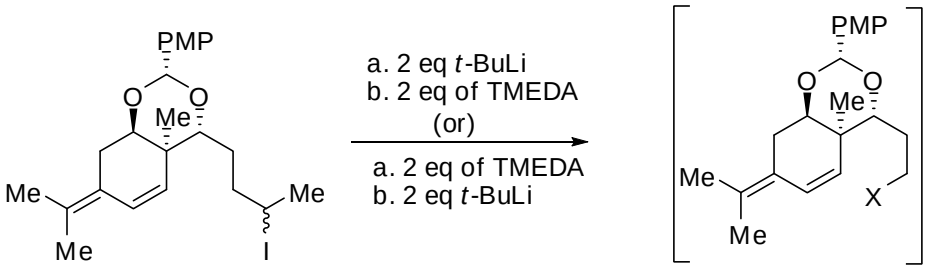

2.153

2.162 X = $CH{=}CH_2$

2.163 X = CH_2CH_3

1. To **2.153** (35 mg, 0.0725 mmol) in THF (0.3 mL) was added *t*-BuLi (0.13 mL, 0.218 mmol) in one portion at -78 °C and stirred for 15 minutes at that temperature. The reaction mixture was quenched by careful addition of H_2O dropwise and extracted with DCM, dried over Na_2SO_4, filtered and concentrated under vacuum. Crude ^{1}H NMR indicated **2.162** and **2.163** in 1:3 ratio.

2. To degassed TMEDA (70 μL, 0.155 mmol) was added *t*-BuLi (0.28 mL, 0.155 mmol) in one portion at -78 °C. To this was added **2.153** (75 mg, 0.155 mmol), Et_2O (1.55 mL) at that temperature dropwise. The reaction mixture was slowly warmed to room temperature and continued stirring for another 45 minutes to 3 hours, after which the reaction was quenched by addition of H_2O, followed by workup as above. Crude ^{1}H NMR indicated a similar ratio of compounds.

3. To **2.153** (75 mg, 0.155 mmol) and Et_2O (1.55 mL) at -78 °C was added *t*-BuLi (0.28 mL, 0.155 mmol) dropwise. To this was added degassed TMEDA (70 μL, 0.155 mmol) at the same temperature and continued stirring for another 4 hours

slowly warming to room temperature. The reaction was quenched and worked up as above to give the same result.

3.2.14. Free Radical cyclization procedure:

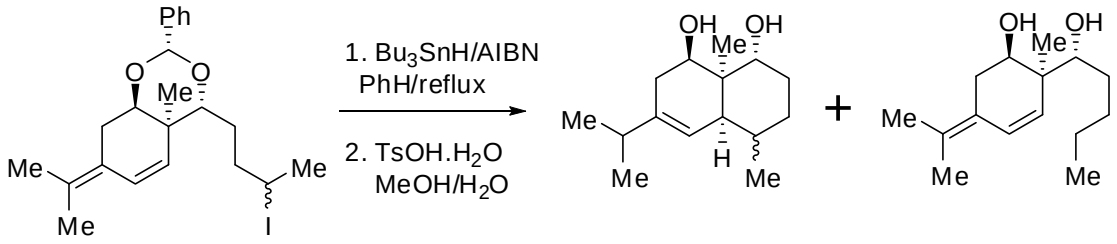

2.156

2.166 a major

2.166 b minor

2.166 a/b = 3.5

2.167

Bu_3SnH (1.4 mL, 5.18 mmol), AIBN (142 mg, 0.86 mmol) and **2.156** (1.954 g, 4.321 mmol) in benzene (430 mL) were degassed by freeze-pump-thaw (3x). This was then heated to reflux for 1.5 hrs and additional AIBN (284 mg, 1.73 mmol) was added gradually in four portions over 1 hour. After refluxing overnight, benzene was removed by concentrating under vacuum. $TsOH.H_2O$ (150 mg), DCM (10 mL), H_2O (25 mL) and MeOH (15 mL) were added and refluxed overnight. The reaction mixture was extracted with DCM, dried over Na_2SO_4, filtered and concentrated under vacuum. The crude product was chromatographed (Hexanes: Ethyl Acetate-6:1) gave **2.167** as viscous colorless liquid, 35 mg (~ 4% yield) and **2.166 a/b** as a viscous liquid, 560 mg (54% yield) as a 3.5:1 mixture of diastereomers. (After the separation on silica the major diastereomer was isolated 291 mg along with 203 mg of the mixture of diastereomers).

Mixture of diols 2.166 a/b

^{1}H NMR (300 MHz, CD_3OD) δ 5.28 (s, 1H), 5.02 (s, 2.4H), 3.95-3.87 (m, 3.6H), 3.63-3.55 (m, 3.42H), 2.41-1.37 (m, 35H), 1.21 (s, 9H), 1.19-1.16 (m, 12H), 1.04-0.96 (m, 26H); **^{13}C NMR** (75 MHz, CD_3OD) δ 141.88, 140.35, 125.10, 116.58, 77.54, 77.12, 70.52, 69.44, 49.10, 47.62, 40.63, 40.09, 34.95, 34.71, 34.53, 32.24, 31.66, 30.35, 29.75, 28.41, 26.40, 25.44, 21.96, 21.57, 21.17, 21.09, 19.19, 17.87, 15.79; **IR** (film, cm^{-1}) 3349, 2956, 2845; **HRMS** (ESI) m/z $[(M+H)^+]$ ($C_{15}H_{26}O_2$) calculated 238.1933, found 238.1833.

Major diastereomer diol 2.166a

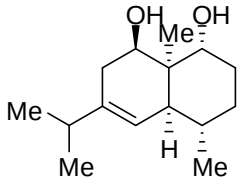

^{1}H NMR (300 MHz, $CDCl_3$) δ 4.92 (s, 1H), 3.95-3.88 (dt, J = 10.8 Hz, 3.3 Hz, 1H), 3.66-3.58 (dt, J = 99.9 Hz, 6.3 Hz, 1H), 3.28-3.26 (d, J = 6.3 Hz, 1H), 3.09-3.08 (d, J = 2.7 Hz, 1H), 2.34-2.27 (dd, J = 16.8 Hz, 4.8 Hz, 1H), 2.19-2.10 (m, 2H), 2.01 (s, 1H), 1.79-1.77 (m, 1H), 1.73-1.30 (m, 3H), 1.24 (s, 3H), 1.17-1.14 (d, J = 7.8 Hz, 3H), 0.98-0.96 (d, J = 6.9 Hz, 3H); **^{13}C NMR** (75 MHz, CD_3OD) δ 140.49, 125.26, 70.71, 49.25, 40.31, 34.85, 34.67, 31.81, 26.55, 25.69, 22.09, 21.70, 21.24, 17.94; **IR** (film, cm^{-1}) 3337, 2931, 2872; **HRMS** (ESI) m/z $[(M+H)^+]$ ($C_{15}H_{26}O_2$) calculated 238.1933, found 238.1833.

Reduction product 2.167

^{1}H NMR (300 MHz, $CDCl_3$) δ 6.45-6.42 (d, J = 11 Hz, 1H), 5.36-5.32 (d, J = 11 Hz, 1H), 3.89-3.83 (dd, J = 12 Hz, 5.8 Hz, 1H), 3.74-3.71 (d, J = 10.5 Hz, 1H), 3.01 (s, 1H), 2.84-2.82 (d, J = 5.8 Hz, 1H), 2.58 (s, 1H), 2.55 (s, 1H), 1.80 (s, 3H), 1.76 (s, 3H), 1.76-1.30 (m, 6H), 1.07 (s, 3H), 0.93-0.88 (t, J – 6.8 Hz, 3H); **^{13}C NMR** (75 MHz, $CDCl_3$) δ 131.53, 130.80, 125.42, 125.02, 75.85, 42.79, 32.27, 31.47, 29.91, 29.13, 23.01, 21.08, 20.35, 20.13, 14.31; **IR** (film, cm^{-1}) 3310, 3100, 1600; **HRMS** (ESI) m/z [$(M+H)^+$] ($C_{15}H_{26}O_2$) calculated 238.1933, found 238.1898.

3.2.15. Chemoselective protection of the major diastereomer

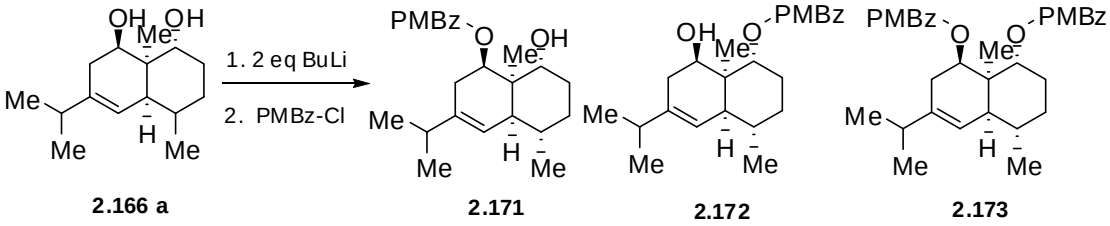

2.166 a **2.171** **2.172** **2.173**

2.166a (291 mg, 1.22 mmol) in THF (2 mL) was cooled to -78 °C and 2.5M *n*-BuLi (1.1 mL, 2.68 mmol) was added dropwise under argon and stirred for 15 minutes. *para*-methoxybenzoyl chloride (0.18 mL,1.34 mmol) in THF (2 mL) was added dropwise over 15 minutes. The reaction mixture was then stirred for 2 hours at -78 °C and it was quenched with 1N HCl and extracted with DCM. The organic phase was washed with H_2O, brine and dried over Na_2SO_4 and concentrated under vacuum. Chromatography (Hexanes:Ethyl Acetate-8:1) gave **2.171** as white solid, 200 mg (44% yield), **2.172** as a colorless viscous liquid, 22 mg (5% yield), **2.173** as a colorless viscous liquid, 191 mg (33% yield) and **2.166 a** (53 mg, 13%).

Mono *para*-methoxybenzoate 2.171

^{1}H NMR (300 MHz, $CDCl_3$) δ 7.96-7.93 (d, J = 9 Hz, 2H), 6.95-6.92 (d, J = 9 Hz, 2H), 5.24 (s, 1H), 5.21-5.17 (dd, J = 7.8 Hz, 5.7 Hz, 1H), 3.98-3.94 (dd, J = 8.1 Hz, 4.8 Hz, 1H), 2.55-2.47 (m, 2H), 2.27-2.18 (m, 2H), 2.06 (s, br, 1H), 1.93-1.85 (m, 1H), 1.74-1,55 (m, 3H), 1.45-1.37 (m, 1H), 1.18-1.15 (d, J = 7.5 Hz, 3H), 1.03-1.01 (d, J = 6.9 Hz, 3H), 1.02-1.00 (d, J = 6.9 Hz, 3H), 1.15 (s, 3H); **^{13}C NMR** (75 MHz, $CDCl_3$) δ 165.94, 163.63, 139.19, 131.62, 123.95, 122.65, 113.97, 78.64, 70.56, 55.57, 48.11, 40.35, 34.73, 34.48, 28.99, 27.24, 26.42, 21.71, 21.56, 21.33, 18.88; **IR** (film, cm^{-1}) 3503, 2957, 2869, 1706, 1606; **HRMS** (ESI) m/z $[(M+H)^+]$ ($C_{23}H_{32}O_4$) calculated 372.2301, found 372.2203; mp 95-97 °C.

Mono *para*-methoxybenzoate 2.172

^{1}H NMR (300 MHz, $CDCl_3$) δ 8.00-7.97 (d, J = 9.3 Hz, 2H), 6.93-6.90 (d, J = 9.3 Hz, 2H), 5.38 (s, 1H), 5.32-5.29 (dd, J = 7.8 Hz, 3.6 Hz, 1H), 3.85 (s, 3H), 3.69-3.63 (dd, J = 7.8 Hz, 5.7 Hz, 1H), 2.44-2.36 (d, J = 18 Hz, 1H), 2.23-2.16 (quintet, J = 6.9 Hz, 1H), 2.09-2.02 (m, 2H), 1.86-1.76 (m, 3H), 1.70-1.62 (m, 2H), 1.10 (s, 3H), 1.11-1.09 (d, J = 6.9 Hz, 3H), 1.02-1.00 (d, J = 6.9 Hz, 3H); **^{13}C NMR** (150 MHz, CD_3OD) δ 167.56, 165.21, 139.95, 132.67, 124.64, 122.79, 114.93, 77.49, 74.70, 56.13, 45.75, 41.52, 36.34, 35.57, 34.10, 30.03, 28.60, 22.04, 22.00, 21.95, 21.92; **IR** (film, cm^{-1}) 3502, 2927, 1705, 1606; **HRMS** (ESI) m/z $[(M+H)^+]$ ($C_{23}H_{32}O_4$) calculated 372.2301, found 372.2193.

Bis-*para*-methoxybenzoate 2.173

^{1}H NMR (300 MHz, $CDCl_3$) δ 8.03-8.00 (d, J = 9.3 Hz, 2H), 7.76-7.73 (d, J = 9.3 Hz, 2H), 6.92-6.89 (d, J = 9.3 Hz, 2H), 6.67-6.64 (d, J = 9.3 Hz, 2H), 5.39-5.36 (m, 2H), 5.21-5.17 (t, J = 5.7 Hz, 1H), 3.86 (s, 3H), 3.78 (s, 3H), 2.47-2.26 (qd, J = 18 Hz, 5.4 Hz, 1H), 2.26-2.17 (septet, J = 6.9 Hz, 1H), 2.10-2.02 (m, 1H), 2.02-1.93 (m, 1H), 1.83-1.77 (q, J = 6.6 Hz, 2H), 1.73-1.63 (m, 1H), 1.59 (s, br, 1H), 1.49-1.36 (m, 1H), 1.20-1.18 (d, J = 6.9 Hz, 3H), 1.17 (s, 3H), 1.02-1.00 (2d, J = 6.9 Hz, 3H each); **^{13}C NMR** (75 MHz, $CDCl_3$) δ 166.36, 165.50, 163.41, 163.27, 139.60, 131.93, 131.80, 123.74, 122.98, 122.52, 113.78, 113.57, 77.65, 77.17, 76.80, 76.75, 76.63, 73.70, 55.65, 55.48, 48.15, 39.97, 34.82, 34.76, 29.67, 27.96, 26.18, 21.69, 21.59, 20.54; **IR** (film, cm^{-1}) 2930, 2957, 1707, 1606; **HRMS** (ESI) m/z [$(M+H)^+$] ($C_{30}H_{36}O_5$) calculated 506.6298, found 506.2578.

3.2.16. tosylate 2.178

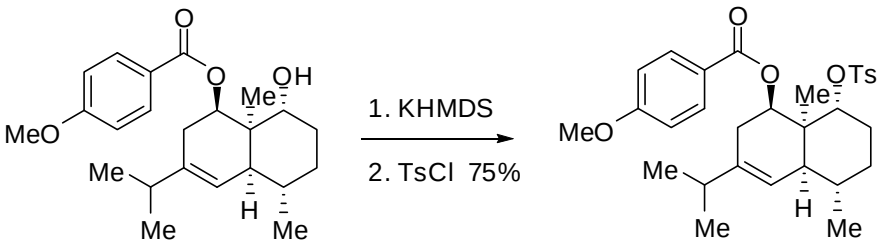

2.171 **2.178**

2.171 (200 mg, 0.54 mmol), TsCl (309 mg, 0.54 mmol) in THF (10 mL) was cooled to -78 °C and 0.5N KHMDS (3.24 mL, 0.54 mmol) was added dropwise. Stirring was continued for another 30 minutes after which the reaction mixture was allowed to warm up to 0 °C in 10 minutes and then stirred at this temperature for another 20 minutes. The reaction was quenched with 1N HCl and extracted with DCM. The organic phase was

washed with H_2O, dried and concentrated under vacuum. Chromatography (Hexanes:Ethyl Acetate-10:1) gave **2.178** as a colorless viscous liquid, 213 mg (75% yield).

^{1}H NMR (300 MHz, $CDCl_3$) δ 7.95-7.92 (d, J = 8.1 Hz, 2H), 7.78-7.76 (d, J = 8.1 Hz, 2H), 7.29-7.27 (d, J = 8.1 Hz, 2H), 6.93-6.90 (d, J = 8.1 Hz, 2H), .547 (s, 1H), 5.05-5.02 (dd, J = 4.5 Hz, 1H), 4.69-4.66 (dd, J = 5.4 Hz, 3.6 Hz, 1H), 3.84 (s, 3H), 2.45-2.37 (m, 1H), 2.41 (s, 3H), 2.20-2.11 (quintet, J = 6.6 Hz, 1H), 2.09-2.01 (dd, J = 18.3 Hz, 3.3 Hz, 1H), 1.88-1.63 (m, 4H), 1.54-1.23 (m, 3H), 1.08-1.06 (d, J = 6.3 Hz, 3H), .96-0.92 (m, 6H), 0.96 (s, 3H); **^{13}C NMR** (75 MHz, $CDCl_3$) δ 166.201, 163.596, 144.588, 138.35, 134.83, 131.88, 129.89, 127.94, 122.87, 121.03, 113.93, 85.28, 75.36, 55.61, 46.49, 39.99, 46.49, 39.99, 34.82, 34.23, 31.74, 29.83, 27.90, 27.62, 22.81, 21.77, 21.53, 21.41, 21.36; **IR** (film, cm^{-1}) 2958, 2869, 1707, 1606; **HRMS** (ESI) m/z [$(M+H)^+$] ($C_{30}H_{38}O_6S$) calculated 526.2389, found 526.2286.

3.2.17. Solvolytic conditions for tosylate 2.178

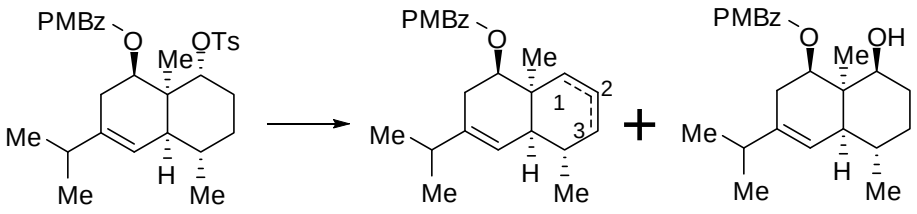

2.178 **2.179** $\Delta^{1,2}$ **2.181**

2.180 $\Delta^{2,3}$

1. **2.178** (40 mg, 0.076 mmol) in CF_3CH_2OH (0.5 mL) was heated to reflux for 1 hr. The reaction mixture was concentrated under vacuum and chromatography

(Hexanes: Ethyl Acetate-4:1) gave an inseparable mixture **2.179/2.180** as a viscous liquid (21 mg, 80% yield).

2. **2.178** (40 mg, 0.076 mmol) in 0.5N AcOH/AcOK (24 mg/0.5 mL), was heated to reflux for 3 hours. The reaction mixture was washed with H_2O and extracted with DCM. The organic phase was dried over Na_2SO_4 and concentrated under vacuum. Chromatography gave **2.179/2.180** (~ 17 mg, 62% yield), **2.181** as a colorless viscous liquid (~ 4 mg, 14% yield).
3. **2.178** (40 mg, 0.076 mmol) in 2eq AcOK/AcOH (15 mg/0.5 mL), was heated to reflux for 3 hours. Workup and isolation as above gave **2.179/2.180** (~ 11 mg, 40% yield), **2.181** (~ 5 mg, 18% yield).
4. **2.178** in AcOH was heated to reflux for 3 hours. The reaction mixture was subjected to the same work up as above. Isolated yield was **2.179/2.180** (~ 11 mg, 40% yield), **2.181** (~ 6 mg, 21% yield).

alkene 2.179/2.180

^{1}H NMR (300 MHz, $CDCl_3$) δ 7.98-7.95 (d, J = 9 Hz, 2H), 7.89-7.86 (d, J = 9Hz, 2H), 6.92-6.87 (m, 2H), 5.66-5.54 (m, 2H), 5.56-5.44 (m, 0.34H), 5.40-5.37 (d, J = 10.2 Hz, 1H), 5.10-5.07 (dd, J = 4.5 Hz, 2.4 Hz, 1H), 3.86 (s, 0.6H), 3.84 (s, 3H), 2.45-2.36 (dm, J = 19.2 Hz, 1H), 2.27-1.96 (m, 4H), 1.92-1.61 (M, 2H), 1.25-1.16 (m, 2H), 1.08-1.06 (d, J = 6.6 Hz, 3H), 1.04 (s, 3H), 1.02-1.00 (d, J = 4.2 Hz, 3H), 0.99-0.98 (d, J = 4.2 Hz, 3H), 0.95-0.08 (m, 1H); **^{13}C NMR** (75 MHz, $CDCl_3$) δ 166.38, 163.25, 138.02, 133.52, 131.81, 131.71, 131.21, 126.50, 124.35, 123.87, 123.69, 120.10, 113.74, 78.13, 76.80, 74.90, 55.61, 47.21, 45.81, 37.91, 37.27, 35.18, 34.77, 33.93, 31.82, 30.40, 29.91, 29.52,

28.79, 26.72, 25.45, 22.27, 21.73, 21.40, 20.74; **IR** (film, cm^{-1}) 2959, 1707, 1606; **HRMS** (ESI) m/z [$(M+H)^+$] ($C_{23}H_{30}O_3$) calculated 354.2195, found 354.2087.

mono *para*-methoxybenzoate 2.181

^{1}H NMR (600 MHz, $CDCl_3$) δ 7.94-7.92 (d, J = 9 Hz, 2H), 6.94-6.92 (d, J = 9 Hz, 2H), 5.72-5.71 (d, J = 3.6 Hz, 1H), 5.54-5.53 (d, J = 4.8 Hz, 1H), 3.86 (s, 3H), 3.42-3.38 (m, 1H), 2.75-2.73 (d, J = 10.2 Hz, 1H), 2.44-2.40 (d, br, J = 21.6 Hz, 1H), 2.28-2.23 (quintet, J = 6.6 Hz, 1H), 2.09-2.06 (d, J = 19.2 Hz, 1H), 1.76-1.66 (m, 2H), 1.59-1.51 (m, 2H), 1.46-1.43 (dd, J = 11.4 Hz, 5.7 Hz, 1H), 1.35-1.21 (m, 1H); **^{13}C NMR** (150 MHz, $CDCl_3$) δ 167.61, 163.80, 137.86, 132.10, 123.18, 120.29, 114.05, 79.08, 71.93, 55.67, 48.89, 40.59, 35.22, 35.09, 33.72, 32.35, 30.81, 29.91, 26.90, 21.82, 21.46, 21.41; **IR** (film, cm^{-1}) 2923, 1699, 1606; **HRMS** (ESI) m/z [$(M+H)^+$] ($C_{23}H_{32}O_4$) calculated 372.2301, found 372.2188.

3.2.18. Mono *para*-methoxybenzoate 2.187

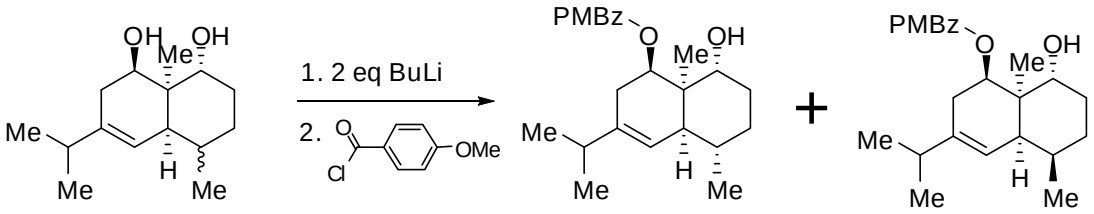

2.166 a/b **2.171** **2.187**

To the mixture of diastereomers **2.166 a/b** (297 mg, 1.25 mmol) in THF (3 mL) at -78 °C, *n*-BuLi (1.8 mL, 2.75 mmol) was added dropwise under argon and stirred for 15 minutes at that temperature. *para*-methoxybenzoyl chloride (319 mg, 2.25 mmol) in THF (1.5 mL) was added dropwise over 15 minutes. The reaction mixture was then stirred for

2 hours at -78 °C and it was quenched with 1N HCl and extracted with dichloromethane. The organic phase was washed with H_2O, brine and dried over Na_2SO_4 and concentrated under vacuum. Chromatography (Hexanes: Ethyl Acetate-8:1). This reaction furnished **2.171** (112 mg, 24%) and **2.187** as a viscous liquid, 112 mg (24% yield) contaminated with **2.172**, **2.173**, **2.188**, **2.189** was obtained.

^{1}H NMR (300 MHz, $CDCl_3$) δ 7.93-7.90 (d, J = 8.7 Hz, 2H), 6.93-6.90 (d, J = 8.7 Hz, 2H), 5.30 (s, 1H), 5.22-5.16 (dd, J = 10.5 hz, 6.3 Hz, 1H), 4.09-4.04 (dd, J = 10.8 Hz, 4.5 Hz, 1H), 3.85 (s, 3H), 2.69 (s, 1H), 2.61-2.53 (dd, J = 17.1 Hz, 5.7 Hz, 1H), 2.31-2.19 (m, 2H), 2.14 (s, 1H), 2.00-1.96 (m, 1H), 1.78-1.73 (m, 1H), 1.62 (s, 1H), 1.55-1.42 (m, 2H), 1.24-1.07 (m, 1H), 1.11 (s, 3H), 1.01-.98 (m, 9H); **^{13}C NMR** (75 MHz, $CDCl_3$) δ 165.73, 163.78, 141.59, 131.63, 122.48, 117.18, 114.08, 80.87, 68.89, 68.17, 55.69, 48.11, 41.26, 35.11, 29.90, 29.10, 21.81, 21.32, 19.30, 15.63; **IR** (film, cm^{-1}) 2956, 1709, 1606.

3.2.19. mesylate 2.190

2.187 **2.190**

To **2.187** (80 mg, 0.215 mmol), Et_3N (0.15 mL, 1.075 mmol) in DCM (0.5 mL) at 0 °C, was added MsCl (0.09 mL, 1.075 mmol) dropwise. The reaction mixture was stirred for 30 minutes and quenched with 1N HCl and extracted with DCM, dried and concentrated under vacuum. Chromatography (Hexanes: Ethyl Acetate-12:1) gave **2.190** as a pale yellow viscous liquid, 35 mg (36% yield).

^{1}H NMR (600 MHz, $CDCl_3$) δ 8.06-8.04 (d, J = 8.7 Hz, 2H), 6.86-6.84 (d, J = 8.7 hz, 2H), 5.22 (s, 1H), 5.07-5.04 (dd, J = 10.8 Hz, 6 Hz, 1H), 5.01-4.98 (dd, J = 12Hz, 5.4 Hz, 1H), 3.78 (s, 3H), 2.93 (s, 3H), 2.49-2.39 (m, 2H), 2.23-2.17 (septet, J = 6.6 Hz, 1H), 2.17 (s, 1H), 2.06-2.03 (m, 1H), 1.98-1.93 (m, 1H), 1.79-1.72 (qd, J = 12.6 Hz, 4.6 Hz, 1H), 1.51 (s, 1H), 1.45-1.42 (d, J = 13.8 Hz, 1H), 1.13 (s, 3H), 0.98-0.96 (2d, J = 6.8 Hz, 3H each), 0.94-0.92 (d, J = 6.8 Hz, 3H); **^{13}C NMR** (150 MHz, $CDCl_3$) δ 166.60, 163.41, 143.39, 131.94, 122.89, 116.00, 13.58, 80.38, 77.92, 55.43, 49.22, 41.46, 39.85, 34.84, 29.15, 29.12, 28.57, 28.28, 21.58, 21.17, 18.73, 15.60; **IR** (film, cm^{-1}) 2958, 2872, 1707, 1606; **HRMS** (ESI) m/z $[(M+H)^+]$ ($C_{24}H_{34}O_6S$) calculated 450.2076, found 450.1972.

3.2.20. Solvolytic conditions for mesylate 2.190

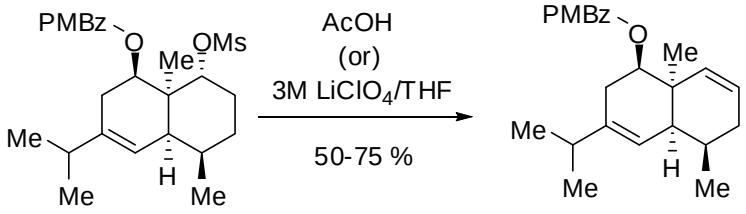

2.190 **2.194**

1. **2.190** in AcOH was heated to reflux for 3 hours. The reaction mixture was subjected to the same work up shown earlier with the major diastereomer. Isolated yield was **2.194** as a viscous liquid (~ 10 mg, 75% yield)

2. 5M $LiClO_4$ in THF (2 mL) was added to **2.190** under argon and then refluxed for 4 hours. Isolated yield was 50%.

alkene 2.194

^{1}H NMR (600 MHz, $CDCl_3$) δ 8.04-8.03 (d, J = 9.6 Hz, 2H), 6.94-6.93 (d, J = 9.6 Hz, 2H), 5.74-5.71 (dd, J = 10.2 Hz, 1H), 5.68-5.66 (d, J = 10.2 Hz, 1H), 5.24 (s, 1H), 5.08-5.05 (dd, J = 10.8 Hz, 7.2 Hz, 1H), 3.87 (s, 3H), 2.24-2.09 (m, 6H), 1.82-1.77 (dt, J = 17.4 Hz, 4.8 Hz, 1H), 1.75-1.70 (dd, J = 17.4 Hz, 11.4 Hz, 1H), 1.56 (s, 3H), 1.26-1.24 (m, 1H), 1.25 (s, 3H), 1.15 (s, 3H), 1.06-1.05 (d, J = 6.6 Hz, 3H), 0.97-0.96 (d, J = 6.6 Hz, 6H); **^{13}**C NMR (150 MHz, CDCl3) δ 166.24, 163.51, 142.77, 131.79, 129.20, 128.54, 123.44, 116.49, 113.83, 77.82, 55.66, 46.35, 40.48, 35.28, 30.50, 29.19, 29.37, 27.95, 24.94, 21.79, 21.30, 19.40; **IR** (film, cm^{-1}) 2958, 2925, 1711, 1606; **HRMS** (ESI) m/z $[(M+H)^{+}]$ ($C23H_{30}O3$) calculated 354.2195, found 354.2092.

3.3. References

1. Adler, E., Junghahn, L., Lindberg, U., Berggren, B., Westin, G. *Acta. Chem. Scand*. **1960**, *14*, 1261-1273.
2. Screttas, C. G., Screttas, M. M. *J. Org. Met Chem*. **1983**, *252*, 263.

STANDARD PROTON PARAMETERS

Pulse Sequence: s2pul

Solvent: dmso
Temp. 25.0 C / 298.1 K
File: 2-16-7-DAadduct-HNMR
INOVA-500 "fao"

Relax. delay 1.000 sec
Pulse 32.4 degrees
Acq. time 1.538 sec
Width 5199.9 Hz
4 repetitions
OBSERVE H1, 499.8911735 MHz
DATA PROCESSING
FT size 16384
Total time 0 min, 10 sec

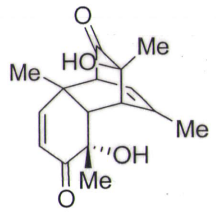

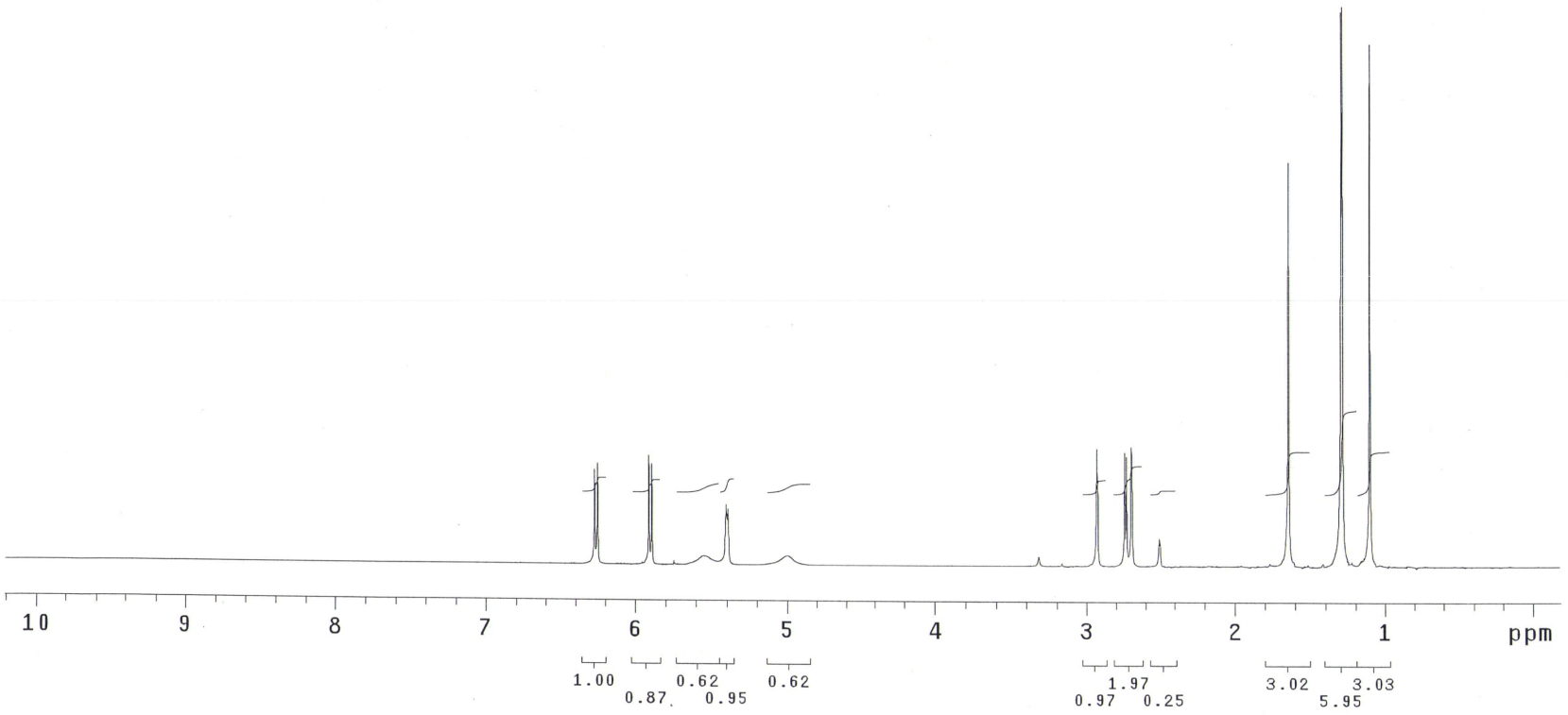

STANDARD CARBON PARAMETERS

Pulse Sequence: s2pul

Solvent: dmso
Temp. 25.0 C / 298.1 K
User: 1-14-87
File: 2-16-7-DAadduct-DMSO
INOVA-500 "fao"

Relax. delay 1.000 sec
Pulse 129.8 degrees
Acq. time 0.500 sec
Width 32000.0 Hz
192 repetitions
OBSERVE C13, 125.6977731 MHz
DECOUPLE H1, 499.8936756 MHz
Low power 10 dB atten.
continuously on
WALTZ-16 modulated
DATA PROCESSING
Line broadening 2.0 Hz
FT size 32768
Total time 4191 hr, 25 min, 55 sec

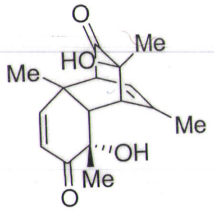

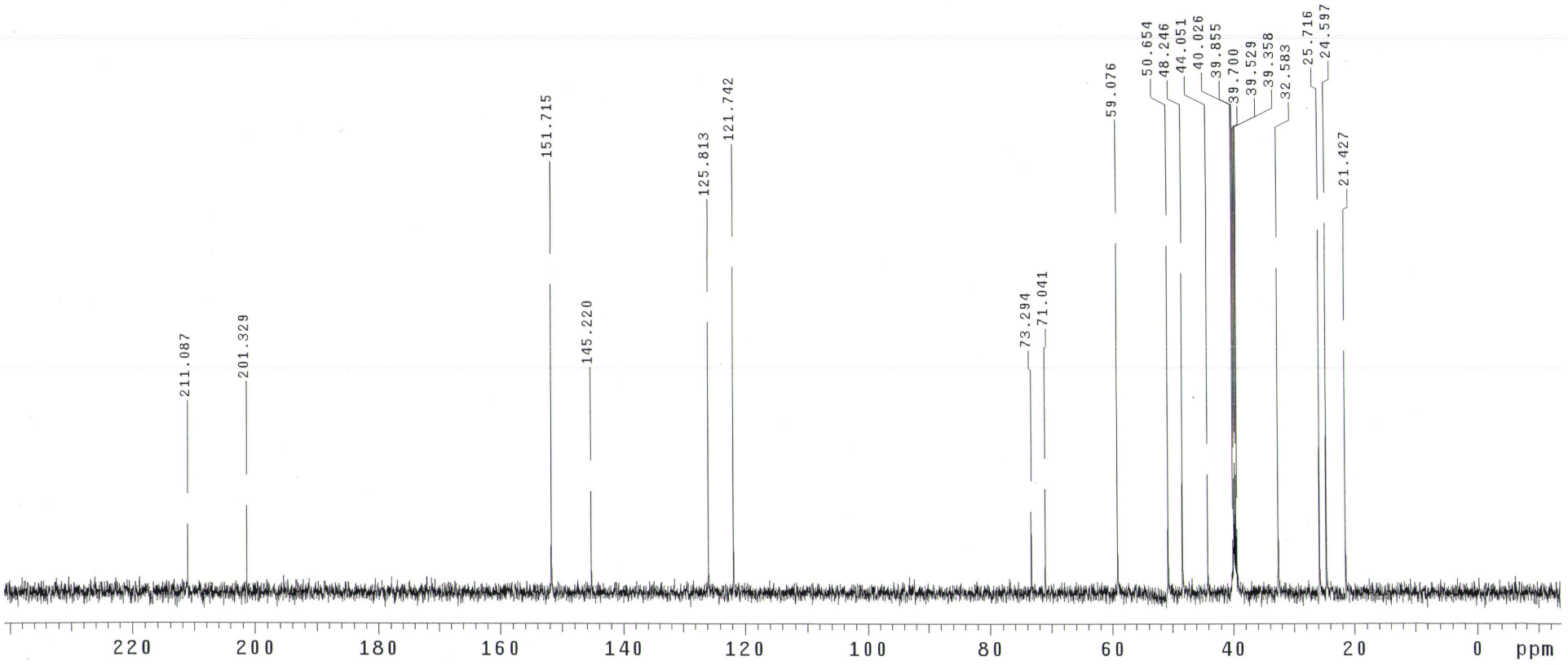

thesis-33-cd3od-HNMR

Pulse Sequence: s2pul

Solvent: CD3OD
Ambient temperature
Operator: vnmr_vb
File: thesis-33-cd3od-HNMR
INOVA-500 "fao"

Relax. delay 1.000 sec
Pulse 64.3 degrees
Acq. time 1.995 sec
Width 4506.5 Hz
16 repetitions
OBSERVE H1, 300.1187817 MHz
DATA PROCESSING
FT size 32768
Total time 0 min, 54 sec

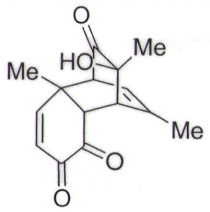

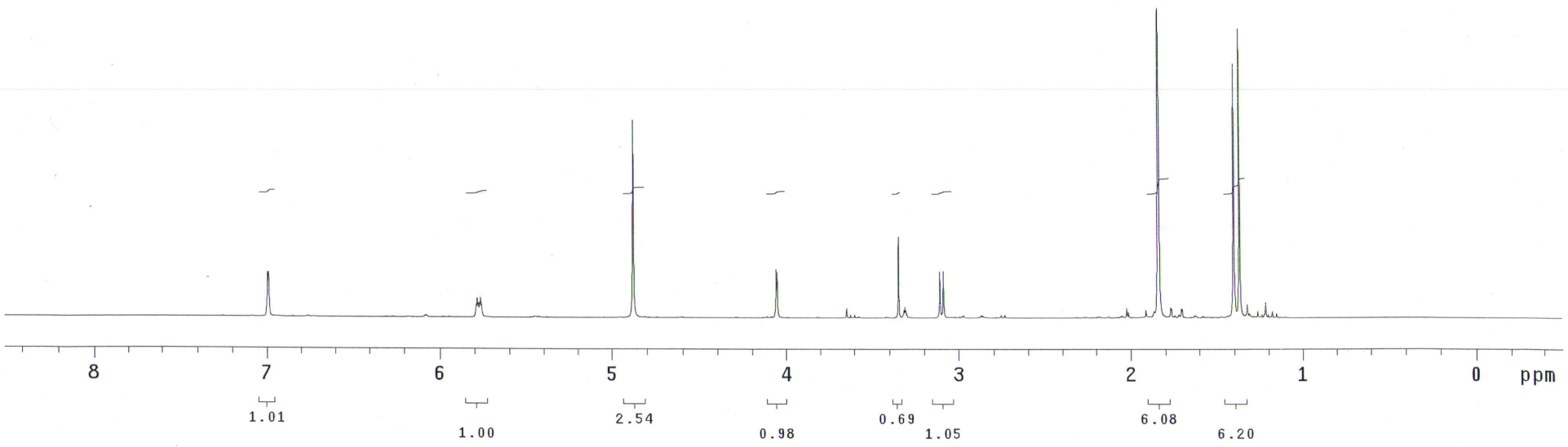

thesis-33-cd3od-CNMR

Pulse Sequence: s2pul

Solvent: CD3OD
Ambient temperature
Operator: vnmr_vb
File: thesis-33-cd3od-CNMR
INOVA-500 "fao"

Relax. delay 1.000 sec
Pulse 43.3 degrees
Acq. time 1.815 sec
Width 18761.7 Hz
384 repetitions
OBSERVE C13, 75.4648110 MHz
DECOUPLE H1, 300.1202380 MHz
Low power 1023 dB atten.
continuously on
WALTZ-16 modulated
DATA PROCESSING
Line broadening 1.0 Hz
FT size 131072
Total time 7 hr, 50 min, 36 sec

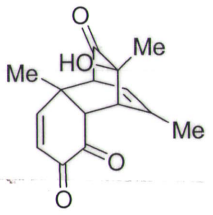

thesis-34-cdcl3-HNMR

Pulse Sequence: s2pul

Solvent: CDCl3
Ambient temperature
Operator: vnmr_vb
File: thesis-34-cdcl3-HNMR
INOVA-500 "fao"

Relax. delay 1.000 sec
Pulse 18.4 degrees
Acq. time 1.995 sec
Width 4506.5 Hz
16 repetitions
OBSERVE H1, 300.1176007 MHz
DATA PROCESSING
FT size 32768
Total time 0 min, 54 sec

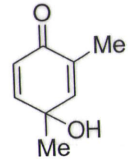

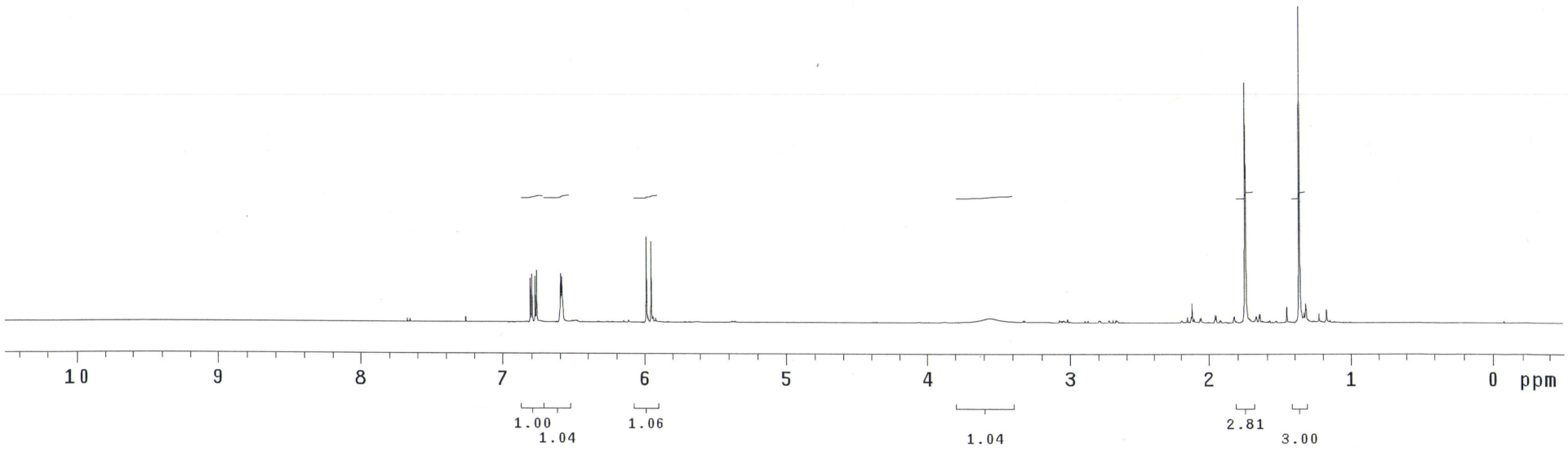

thesis-34-cdcl3-HNMR

Pulse Sequence: s2pul

Solvent: CDCl3
Ambient temperature
Operator: vnmr_vb
File: thesis-34-cdcl3-CNMR
INOVA-500 "fao"

Pulse 43.3 degrees
Acq. time 1.815 sec
Width 18761.7 Hz
64 repetitions
OBSERVE C13, 75.4646233 MHz
DECOUPLE H1, 300.1190556 MHz
Low power 1023 dB atten.
continuously on
WALTZ-16 modulated
DATA PROCESSING
Line broadening 1.0 Hz
FT size 131072
Total time 31 min, 7 sec

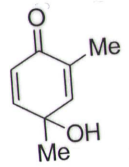

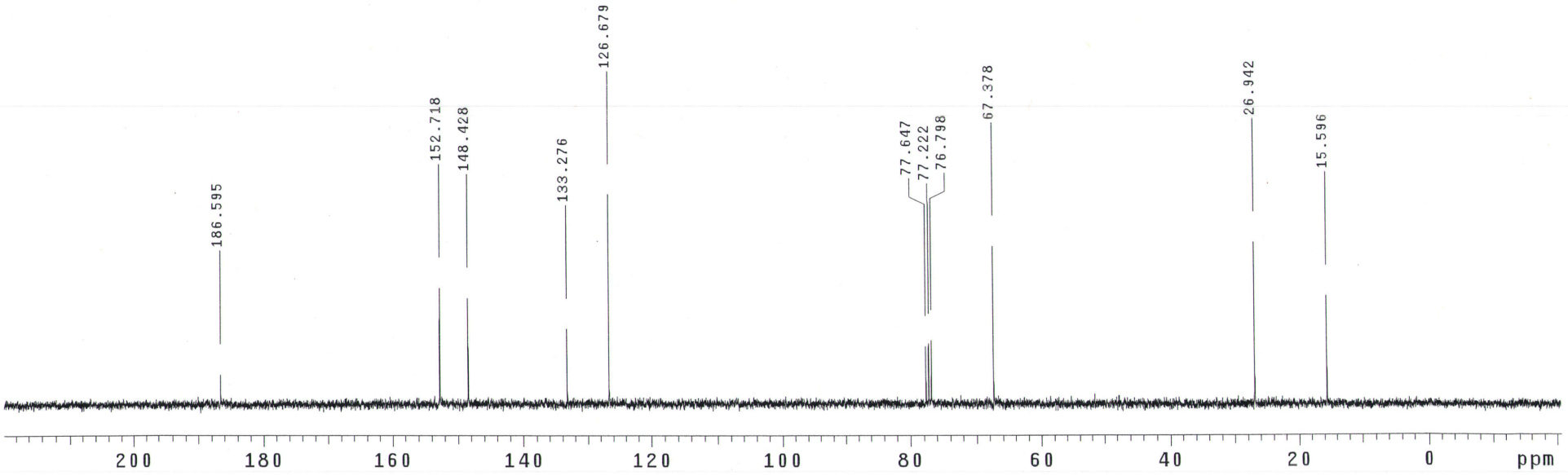

thesis-35-cd3od-HNMR

Pulse Sequence: s2pul

Solvent: Cd3OD
Ambient temperature
Operator: vnmr_vb
File: thesis-35-cd3od-HNMR
INOVA-500 "fao"

Relax. delay 1.000 sec
Pulse 64.3 degrees
Acq. time 1.995 sec
Width 4506.5 Hz
16 repetitions
OBSERVE H1, 300.1187817 MHz
DATA PROCESSING
FT size 32768
Total time 0 min, 54 sec

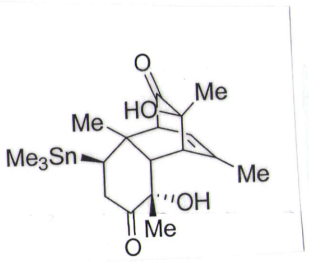

thesis-35-cd3od-CNMR

Pulse Sequence: s2pul

Solvent: CD3Od
Ambient temperature
Operator: vnmr_vb
File: thesis-35-cd3od-CNMR
INOVA-500 "fao"

Relax. delay 2.000 sec
Pulse 105.4 degrees
Acq. time 1.815 sec
Width 20000.0 Hz
480 repetitions
OBSERVE C13, 75.3763428 MHz
DECOUPLE H1, 299.7684327 MHz
Low power 5 dB atten.
continuously on
WALTZ-16 modulated
DATA PROCESSING
Line broadening 1.0 Hz
FT size 131072
Total time 10 hr, 37 min, 19 sec

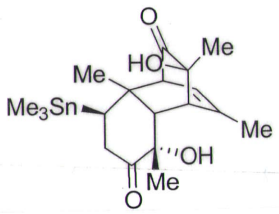

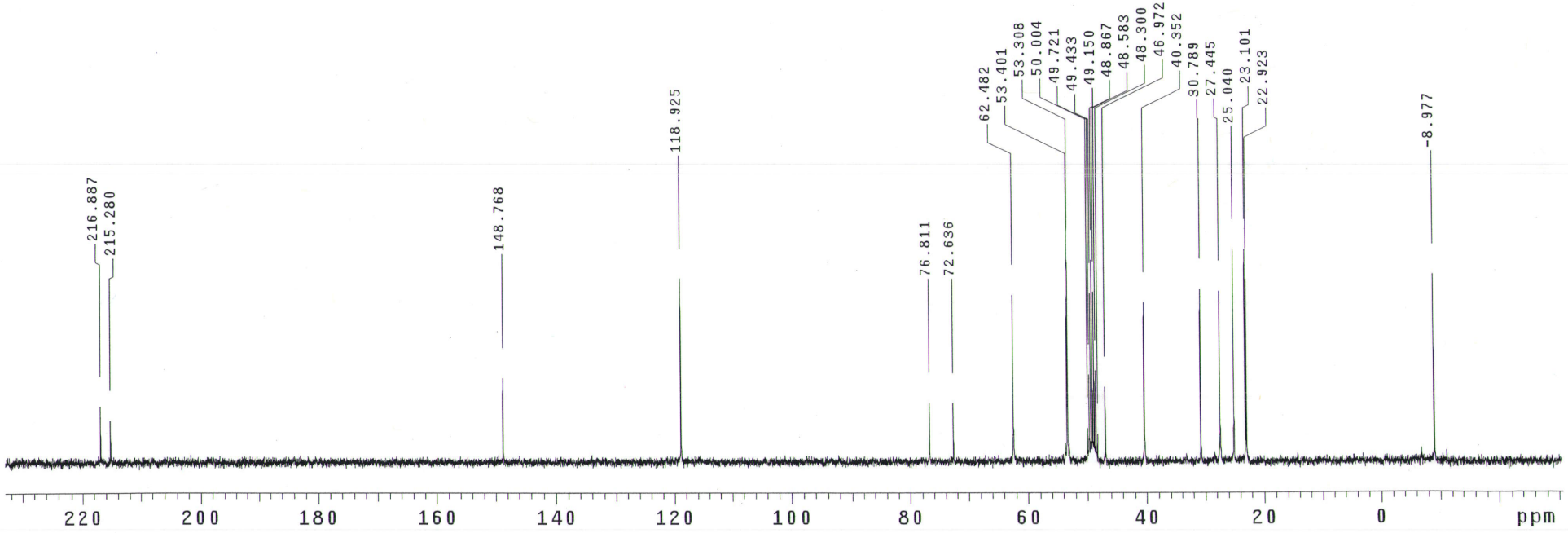

thesis-36-cd3od-HNMR

Pulse Sequence: s2pul

Solvent: cd3od
Temp. 25.0 C / 298.1 K
Operator: vnmr_jk
File: h1
INOVA-500 "fao"

Relax. delay 10.000 sec
Pulse 78.0 degrees
Acq. time 0.870 sec
Width 9199.6 Hz
4 repetitions
OBSERVE H1, 599.7455673 MHz
DATA PROCESSING
Line broadening 1.0 Hz
FT size 16384
Total time 0 min, 43 sec

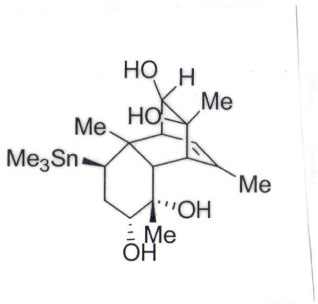

-8.844
22.420
26.638
28.583
31.877
32.860
34.252
44.124
48.721
48.867
48.976
49.006
49.151
49.224
49.290
49.435
49.574
50.179
50.944
74.331
76.400
83.191
84.866
126.235
143.947
ppm
0
20
40
60
80
100
120
140
160
Me
Me
H
HO
HO
OH
Me
OH
Me
Me3Sn

thesis-37-cd3od-HNMR

Pulse Sequence: s2pul

Solvent: cd3od
Temp. 25.0 C / 298.1 K
File: thesis-37-cd3od-HNMR
INOVA-500 "fao"

Relax. delay 1.000 sec
Pulse 32.4 degrees
Acq. time 1.538 sec
Width 5199.9 Hz
4 repetitions
OBSERVE H1, 499.8907743 MHz
DATA PROCESSING
FT size 16384
Total time 0 min, 10 sec

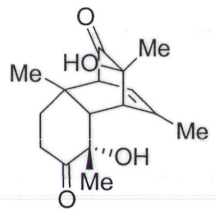

STANDARD CARBON PARAMETERS

Pulse Sequence: s2pul

Solvent: cd3od
Temp. 25.0 C / 298.1 K
User: 1-14-87
File: 2-16-7-hydrogenation-13C-Cd3od
INOVA-500 "fao"

Relax. delay 1.000 sec
Pulse 129.8 degrees
Acq. time 0.500 sec
Width 32000.0 Hz
560 repetitions
OBSERVE C13, 125.6974598 MHz
DECOUPLE H1, 499.8932706 MHz
Low power 10 dB atten.
continuously on
WALTZ-16 modulated
DATA PROCESSING
Line broadening 2.0 Hz
FT size 32768
Total time 41hr, 25 min, 55 sec

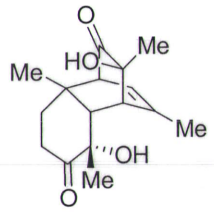

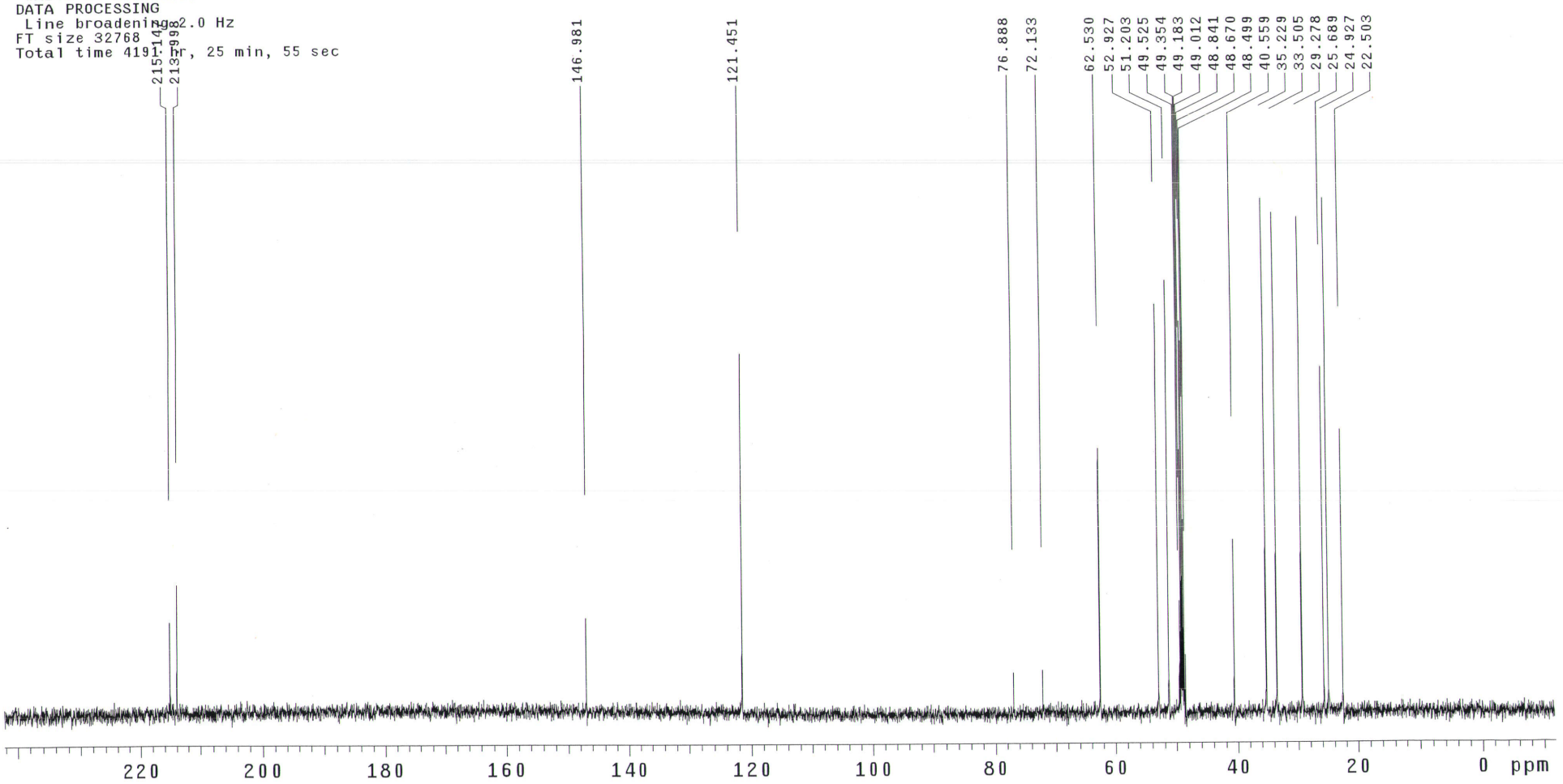

thesis-38-DMSO-HNMR

Pulse Sequence: s2pul

Solvent: dmso
Temp. 25.0 C / 298.1 K
File: thesis-38-DMSO-HNMR
INOVA-500 "fao"

Relax. delay 1.000 sec
Pulse 78.0 degrees
Acq. time 1.274 sec
Width 6277.5 Hz
4 repetitions
OBSERVE H1, 599.7459242 MHz
DATA PROCESSING
FT size 16384
Total time 0 min, 13 sec

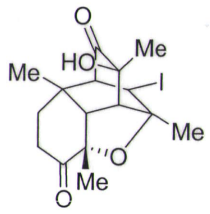

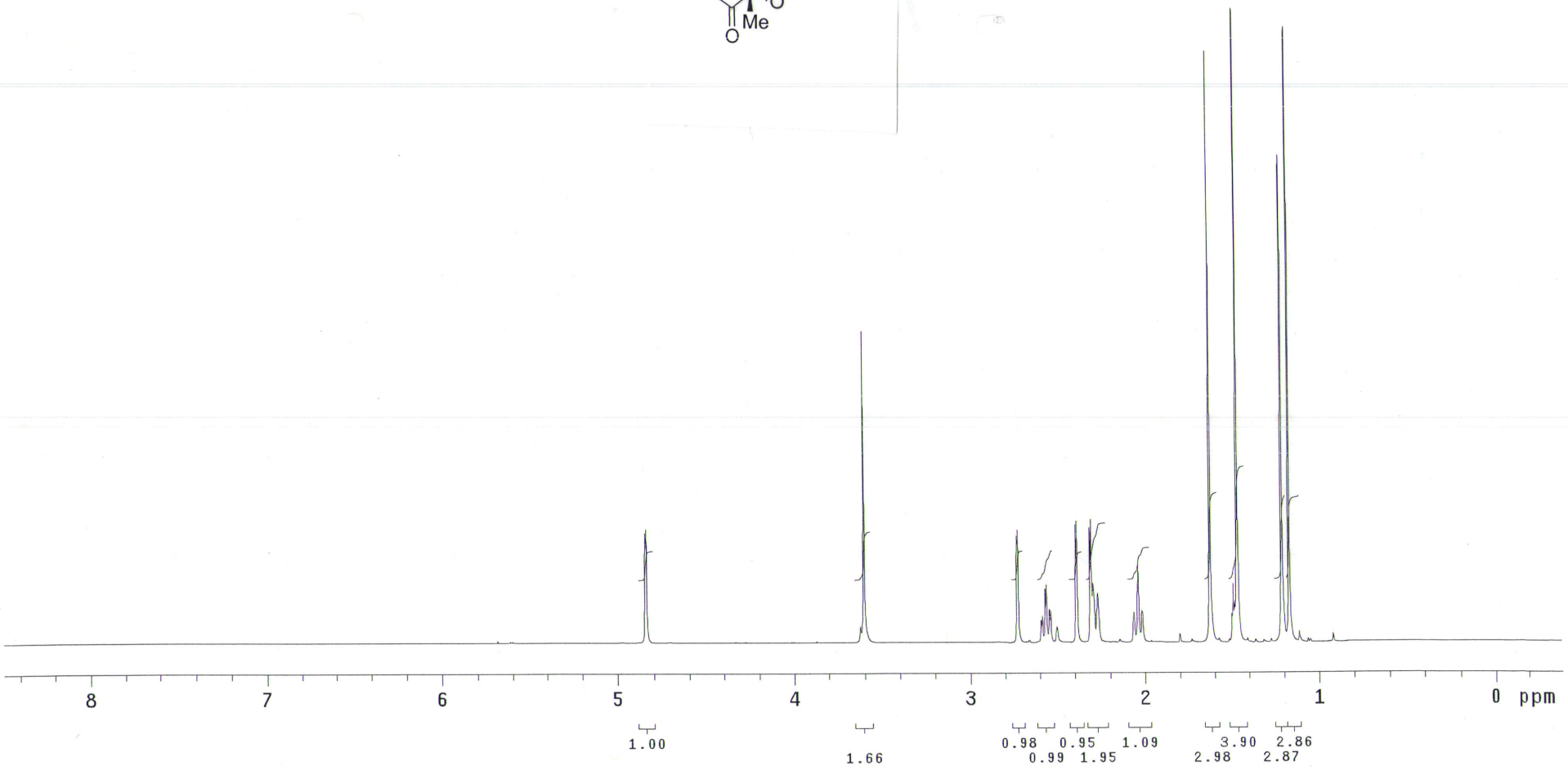

thesis-38-DMSO-CNMR

Pulse Sequence: s2pul

Solvent: dmso
Temp. 25.0 C / 298.1 K
User: 1-14-87
File: thesis-38-DMSO-CNMR
INOVA-500 "fao"

Relax. delay 1.000 sec
Pulse 86.5 degrees
Acq. time 0.421 sec
Width 38004.8 Hz
624 repetitions
OBSERVE C13, 150.8062549 MHz
DECOUPLE H1, 599.7496711 MHz
Low power 10 dB atten.
continuously on
WALTZ-16 modulated
DATA PROCESSING
Line broadening 1.0 Hz
FT size 32768
Total time 2 hr, 32 min, 34 sec

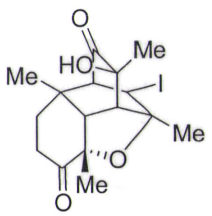

ACH-III-Pg101-crude-cd3cn pure

Pulse Sequence: s2pul

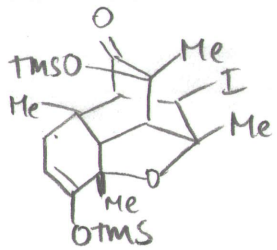

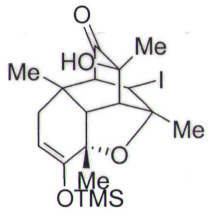

thesis-39-cdcl3-HNMR

Pulse Sequence: s2pul

Solvent: CDCl3
Ambient temperature
Operator: vnmr_vb
File: thesis-39-cdcl3-HNMR
INOVA-500 "fao"

Relax. delay 1.000 sec
Pulse 64.3 degrees
Acq. time 1.995 sec
Width 4506.5 Hz
16 repetitions
OBSERVE H1, 300.1176007 MHz
DATA PROCESSING
FT size 32768
Total time 0 min, 54 sec

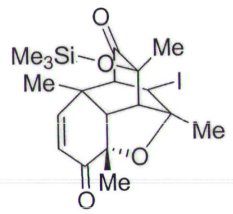

thesis-39-cdcl3-CNMR

Pulse Sequence: s2pul

Solvent: CDCl3
Ambient temperature
Operator: vnmr_vb
File: thesis-39-cdcl3-CNMR
INOVA-500 "fao"

Relax. delay 2.000 sec
Pulse 105.4 degrees
Acq. time 1.815 sec
Width 24775.5 Hz
1088 repetitions
OBSERVE C13, 75.3761486 MHz
DECOUPLE H1, 299.7672516 MHz
Low power 5 dB atten.
continuously on
WALTZ-16 modulated
DATA PROCESSING
Line broadening 1.0 Hz
FT size 131072
Total time 106 hr, 13 min, 15 sec

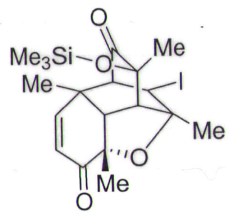

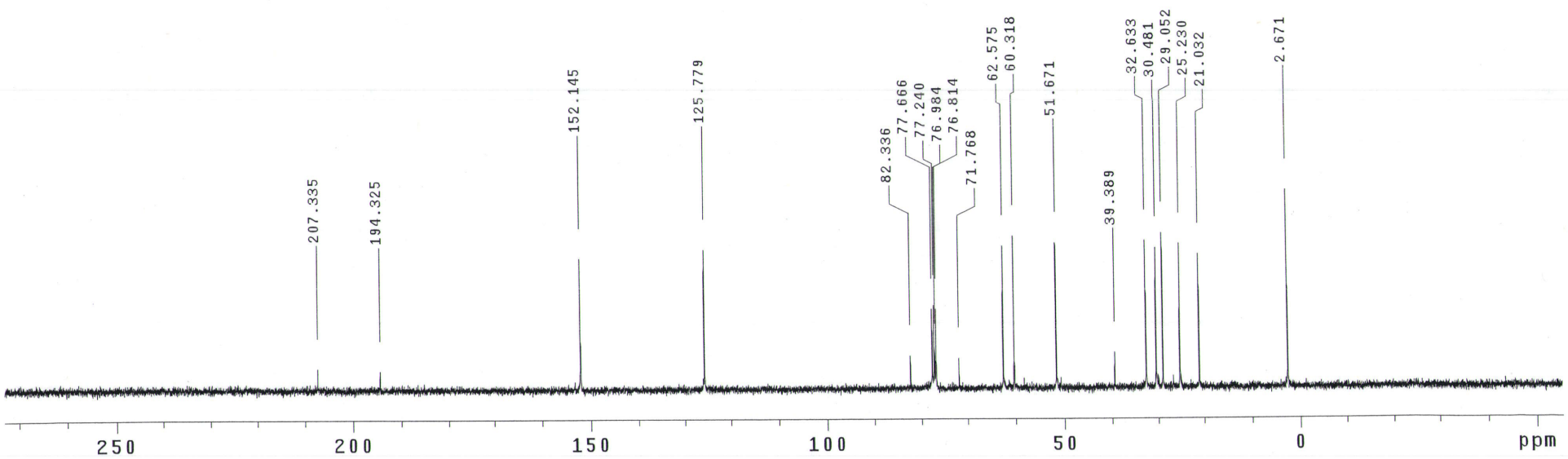

thesis-40-cdcl3-HNMR

Pulse Sequence: s2pul

Solvent: CDCl3
Ambient temperature
Operator: vnmr_vb
File: thesis-40-cdcl3-HNMR
INOVA-500 "fao"

Relax. delay 1.000 sec
Pulse 18.4 degrees
Acq. time 1.995 sec
Width 4506.5 Hz
16 repetitions
OBSERVE H1, 300.1176007 MHz
DATA PROCESSING
FT size 32768
Total time 0 min, 54 sec

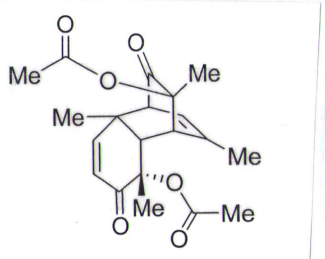

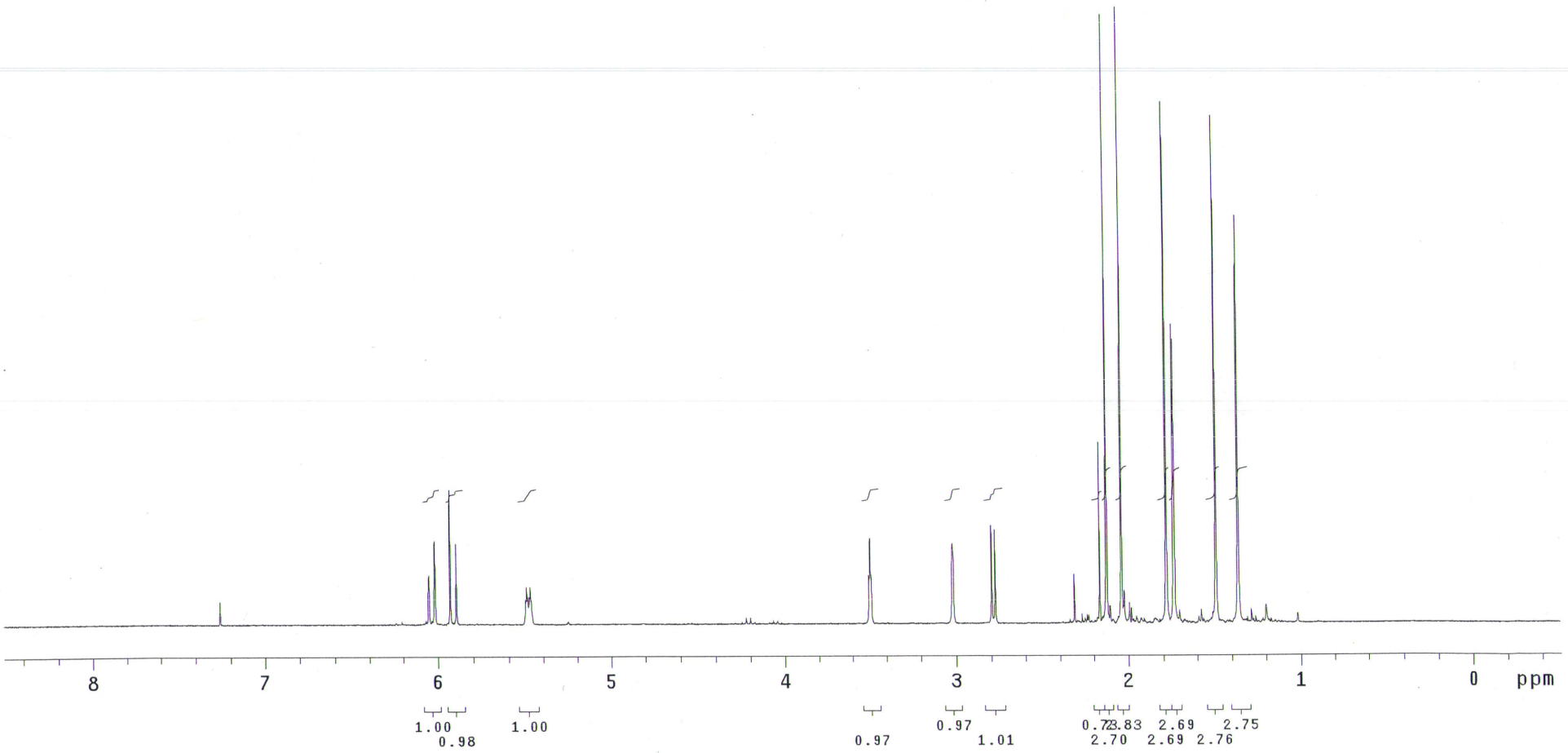

thesis-40-cdcl3-CNMR

Pulse Sequence: s2pul

Solvent: CDCl3
Ambient temperature
Operator: vnmr_vb
File: thesis-40-cdcl3-CNMR
INOVA-500 "fao"

Relax. delay 1.000 sec
Pulse 105.4 degrees
Acq. time 1.815 sec
Width 30360.5 Hz
80 repetitions
OBSERVE C13, 75.3761500 MHz
DECOUPLE H1, 299.7672516 MHz
Low power 5 dB atten.
continuously on
WALTZ-16 modulated
DATA PROCESSING
Line broadening 1.0 Hz
FT size 131072
Total time 7 hr, 50 min, 39 sec

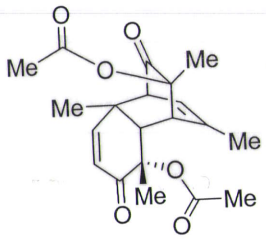

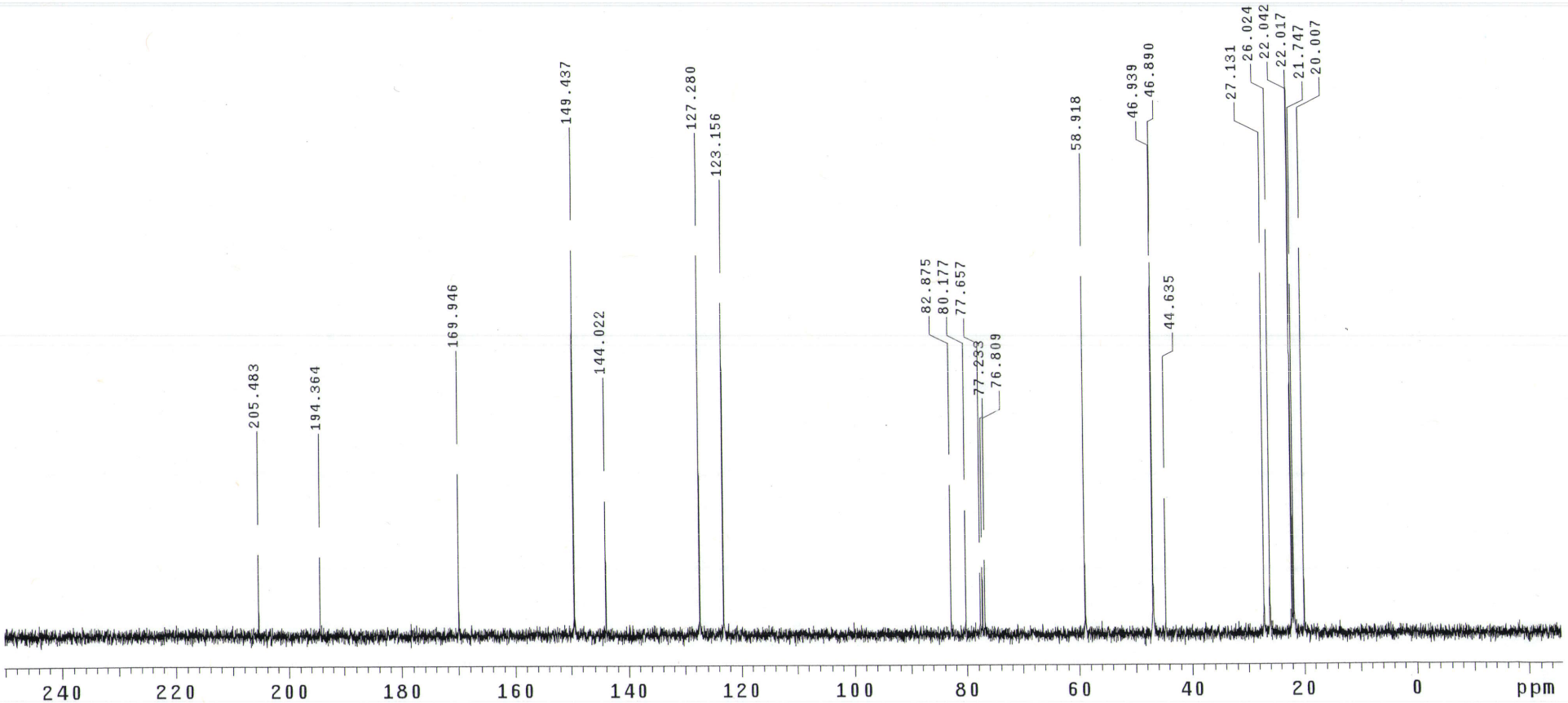

thesis-41-cdcl3-HNMR

Pulse Sequence: s2pul

Solvent: CDCl3
Ambient temperature
Operator: vnmr_vb
File: thesis-41-cdcl3-HNMR
INOVA-500 "fao"

Relax. delay 1.000 sec
Pulse 18.4 degrees
Acq. time 1.995 sec
Width 4506.5 Hz
16 repetitions
OBSERVE H1, 300.1176007 MHz
DATA PROCESSING
FT size 32768
Total time 0 min, 54 sec

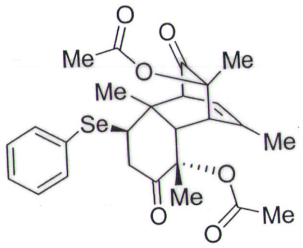

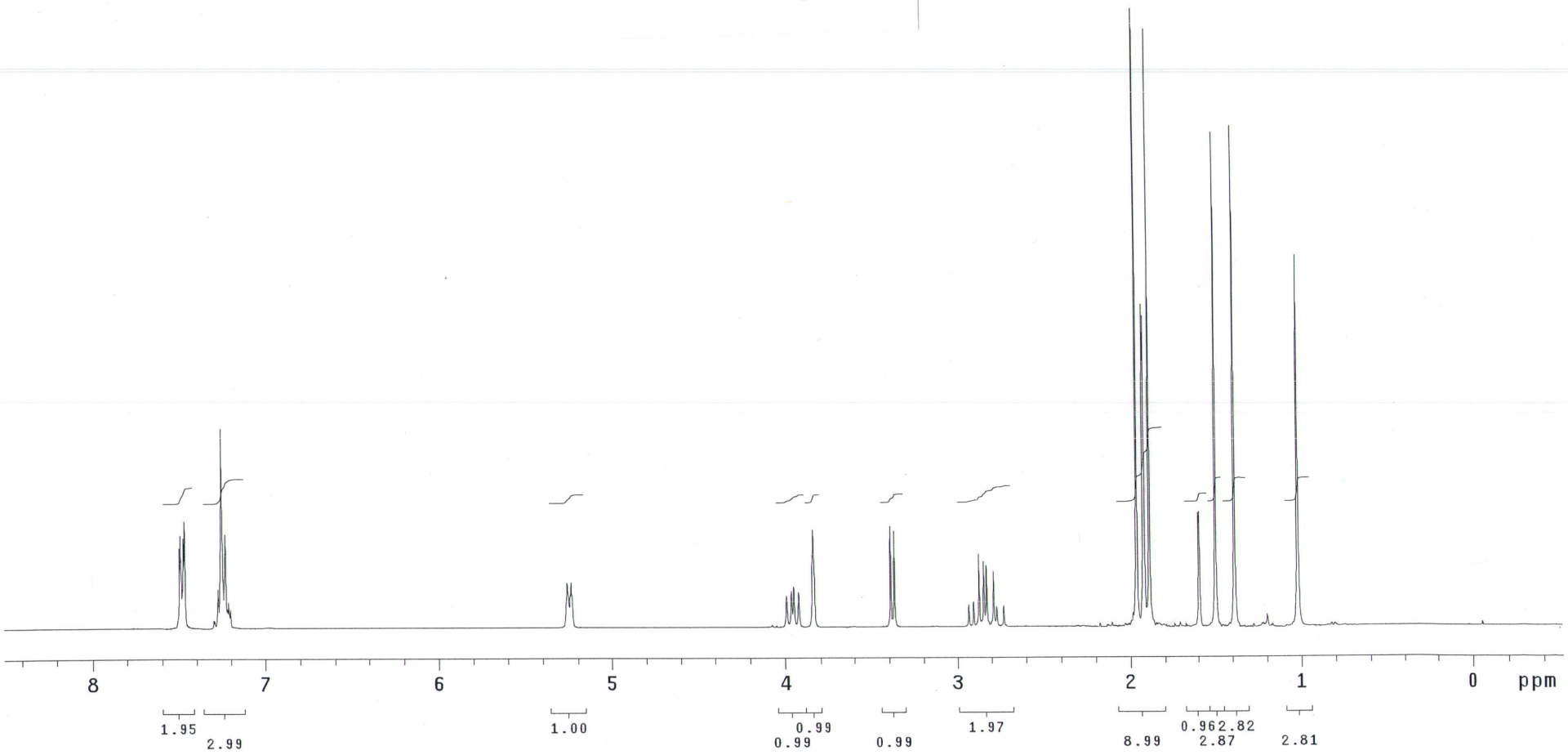

thesis-41-cdcl3-CNMR

Pulse Sequence: s2pul

Solvent: CDCl3
Ambient temperature
Operator: vnmr_vb
File: thesis-41-cdcl3-CNMR
INOVA-500 "fao"

Pulse 43.3 degrees
Acq. time 1.815 sec
Width 25000.0 Hz
160 repetitions
OBSERVE C13, 75.4646235 MHz
DECOUPLE H1, 300.1190556 MHz
Low power 1023 dB atten.
continuously on
WALTZ-16 modulated
DATA PROCESSING
Line broadening 1.0 Hz
FT size 131072
Total time 31 min, 7 sec

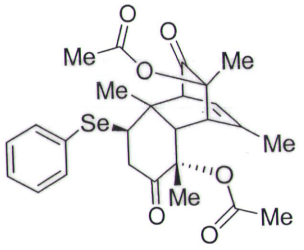

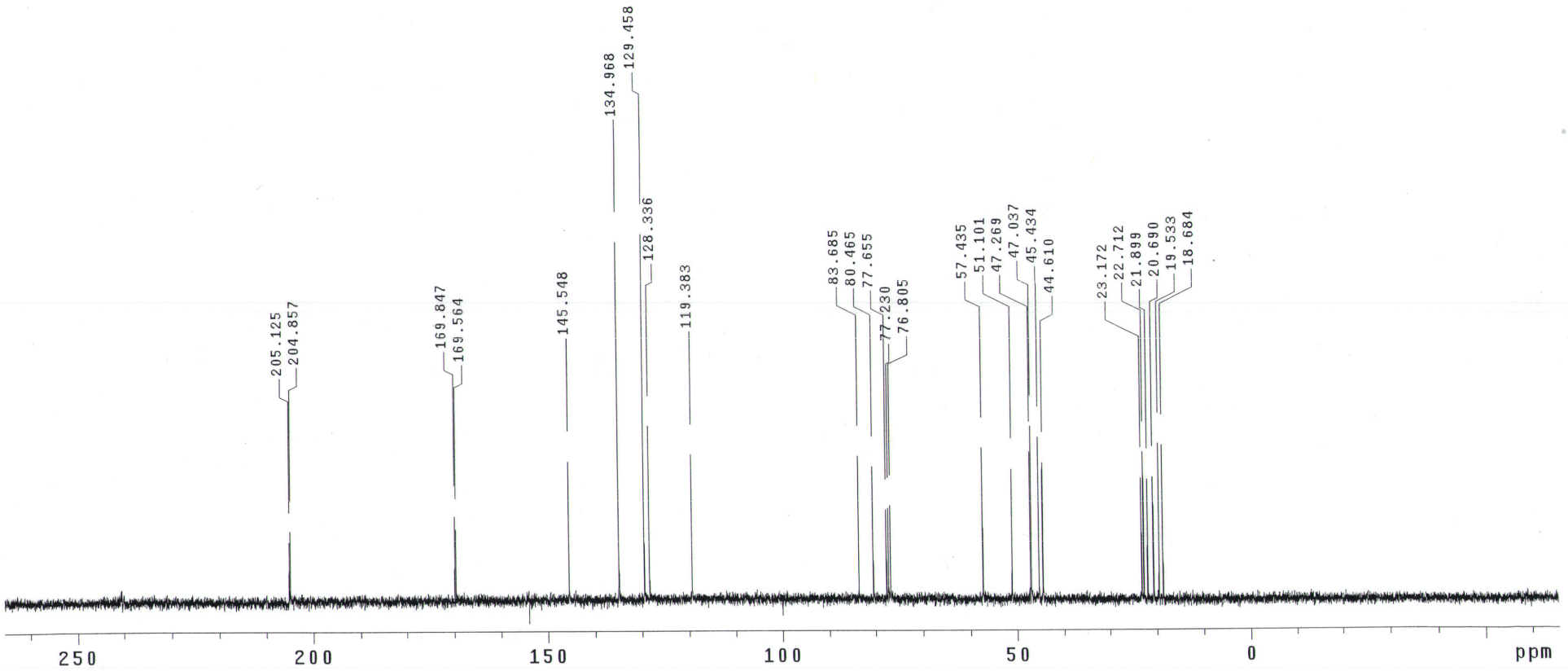

thesis-42-cd3od-HNMR

Pulse Sequence: s2pul

Solvent: cd3od
Temp. 25.0 C / 298.1 K
File: h1
INOVA-500 "fao"

Relax. delay 1.000 sec
Pulse 4.0 usec
Acq. time 1.520 sec
Width 5261.4 Hz
4 repetitions
OBSERVE H1, 499.8907736 MHz
DATA PROCESSING
Line broadening 1.0 Hz
FT size 16384
Total time 0 min, 10 sec

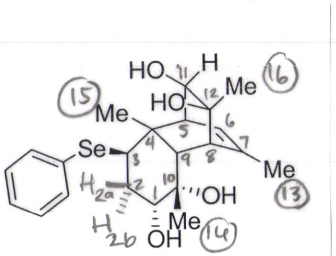

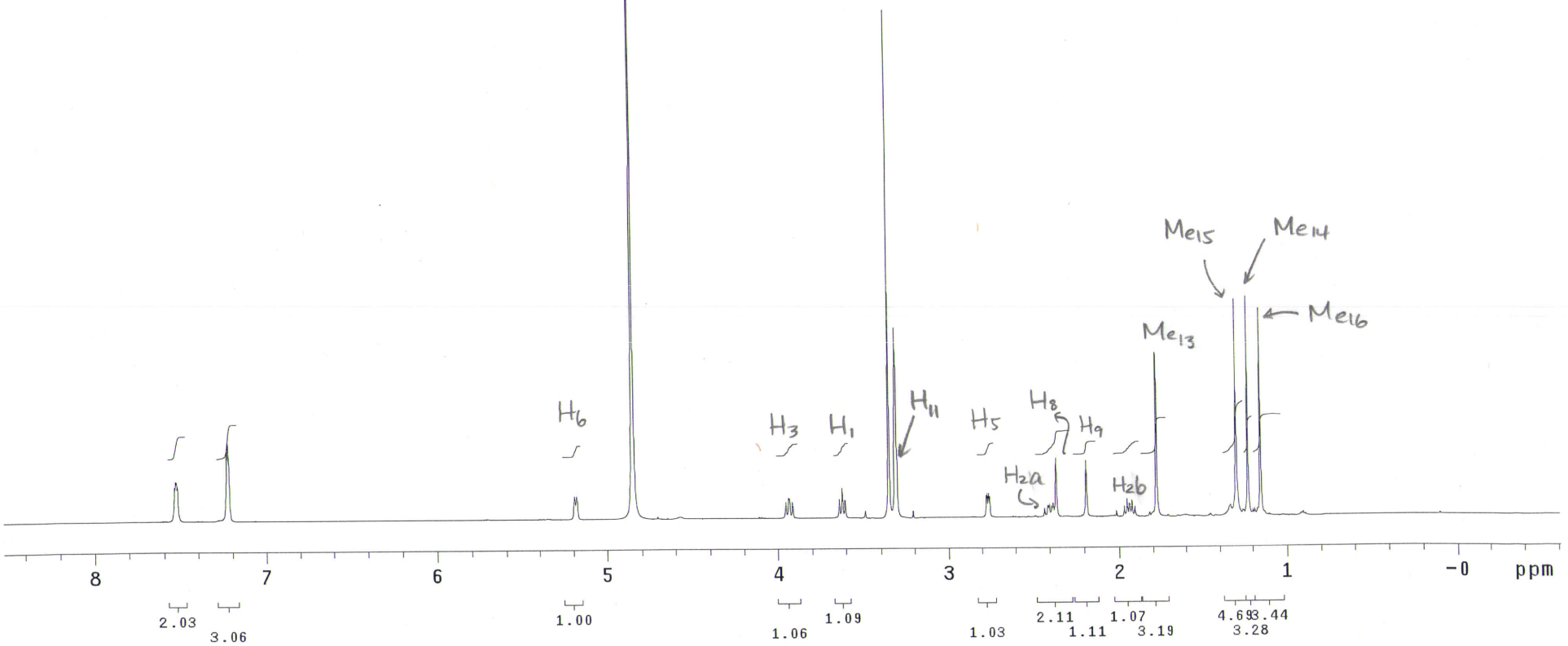

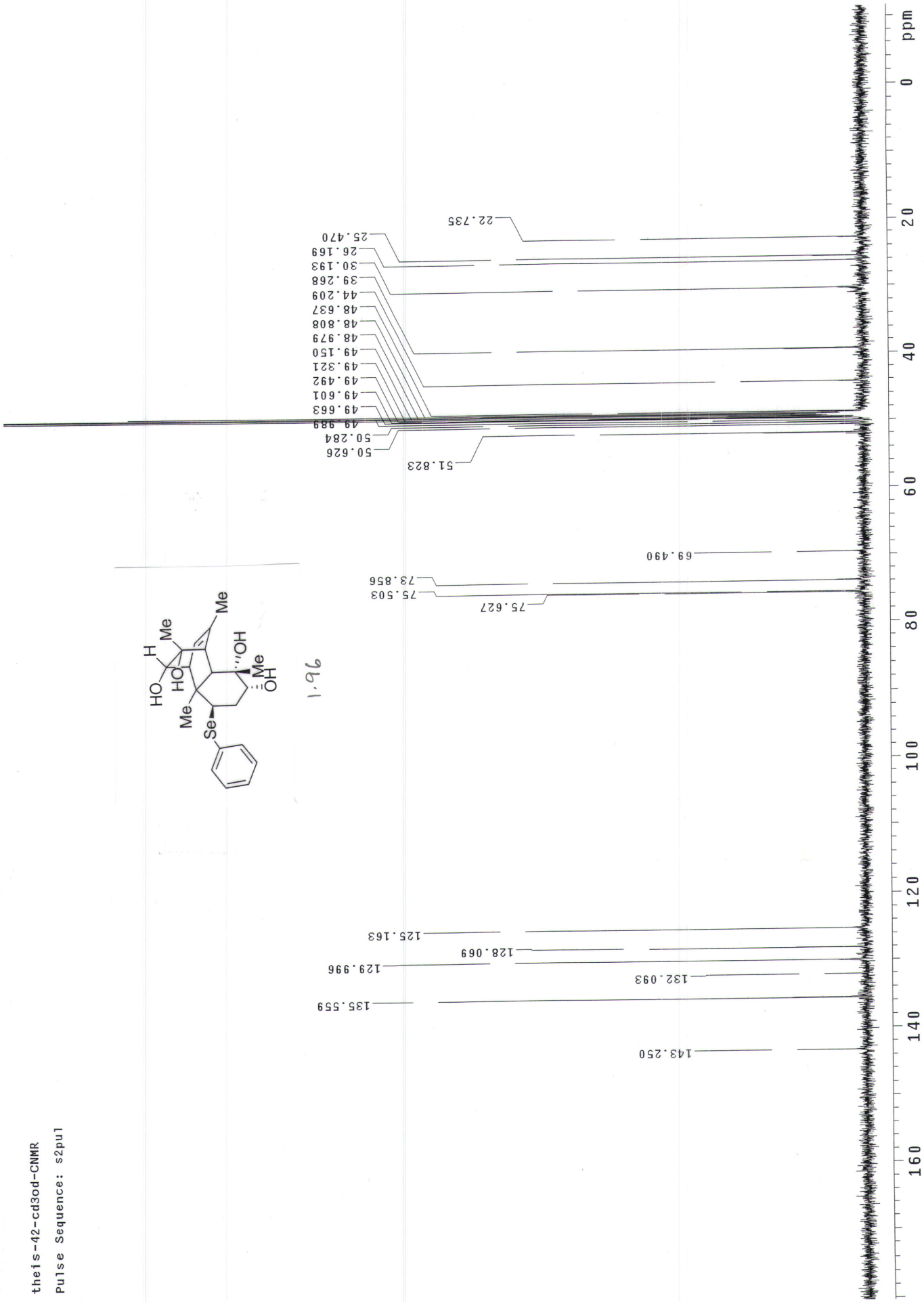
22.735
25.470
26.169
30.193
39.268
44.209
48.637
48.808
48.979
49.150
49.321
49.492
49.601
49.663
49.989
50.284
50.626
51.823
69.490
73.856
75.503
75.627
125.163
128.069
129.996
132.093
135.559
143.250
ppm
0
20
40
60
80
100
120
140
160
Me
Me
H
HO
HO
Me
Se
OH
Me
1.96
theis-42-cd3od-CNMR
Pulse Sequence: s2pul

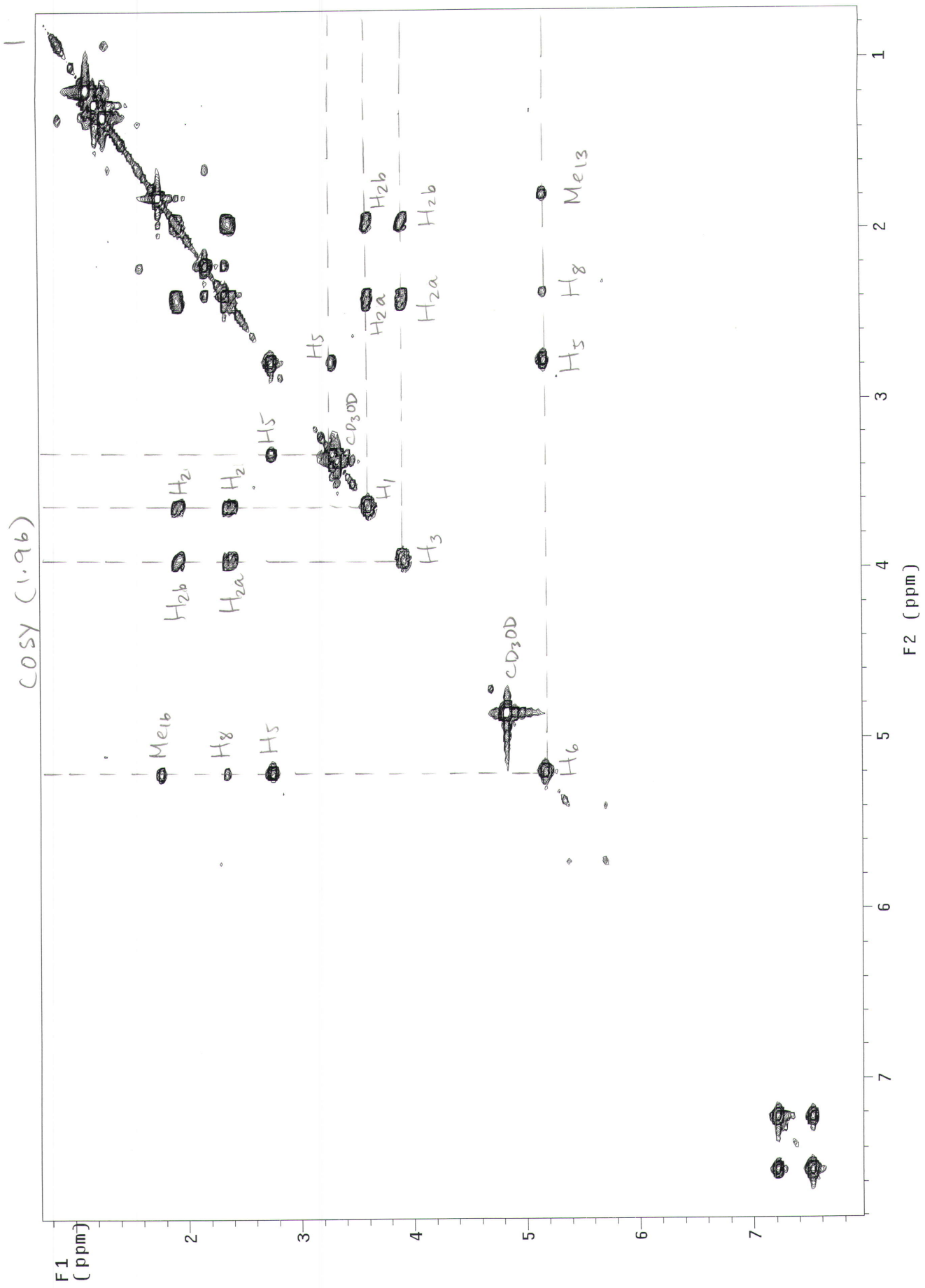
1
COSY (1.96)
F1 (ppm)
F2 (ppm)
Me16
H8
H5
H2b
H2a
H2
H2
H5
H5
CD3OD
H1
H3
H2a
H2b
H2a
H2b
CD3OD
H6
H3
H8
Me13

TOSY (1.96) 2

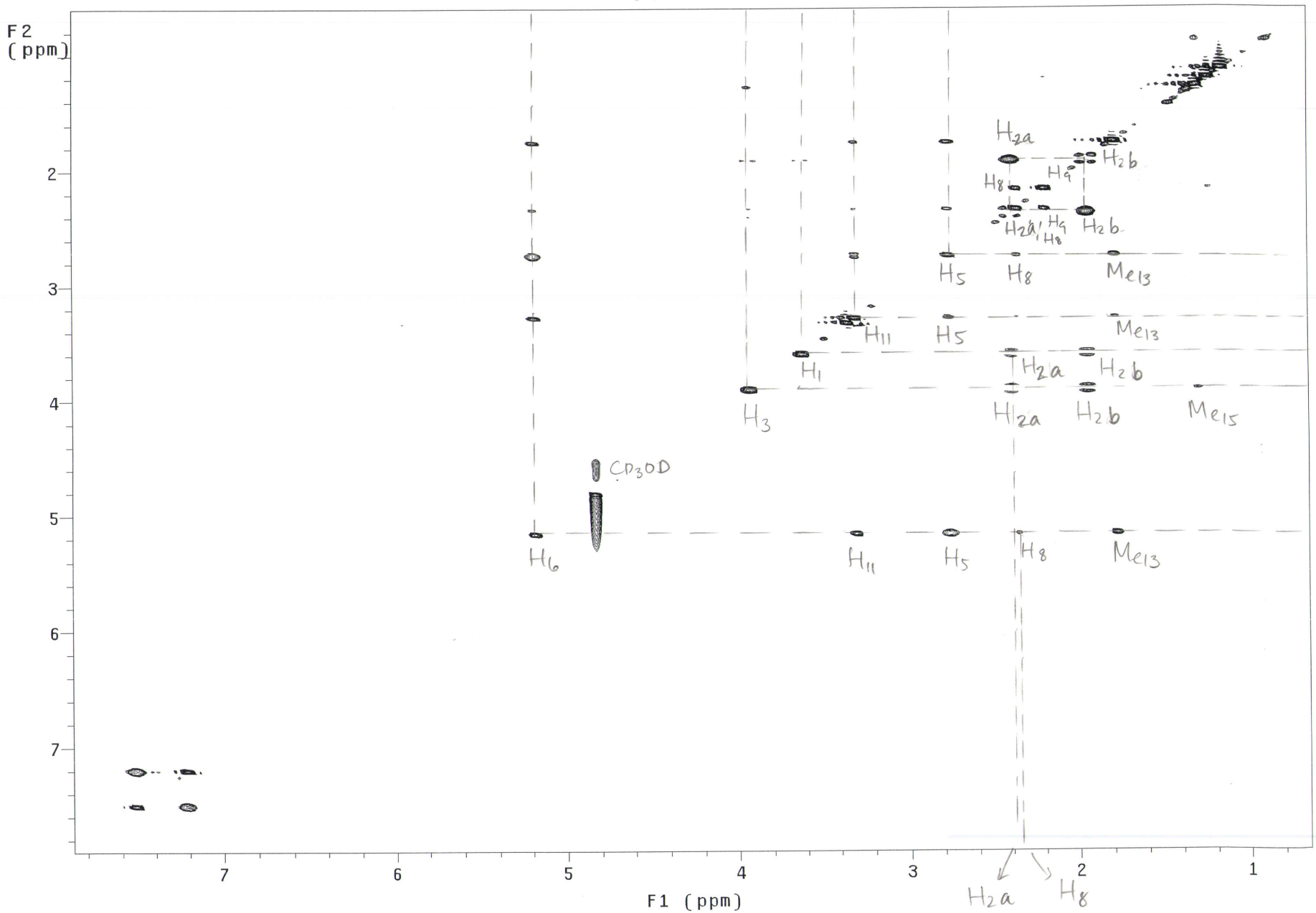
F2 (ppm)
F1 (ppm)
H2a
H2b
H9
H8
H2a'
H5
H8
Me13
H11
H1
H3
Me15
CD3OD
H6
H11
H5
H8
Me13
H2a
H8

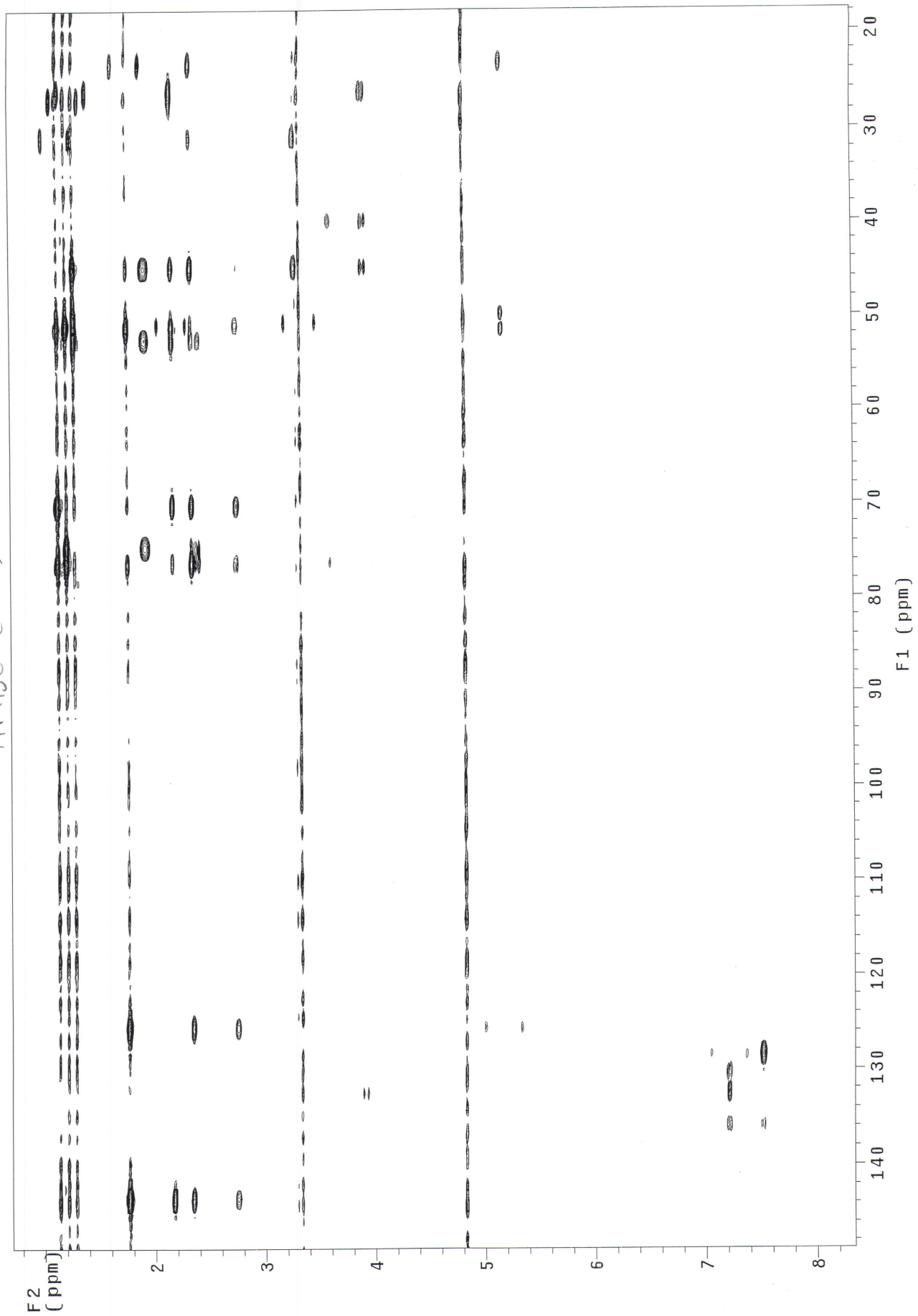
3a
HMBC (196)
F2 (ppm)
F1 (ppm)

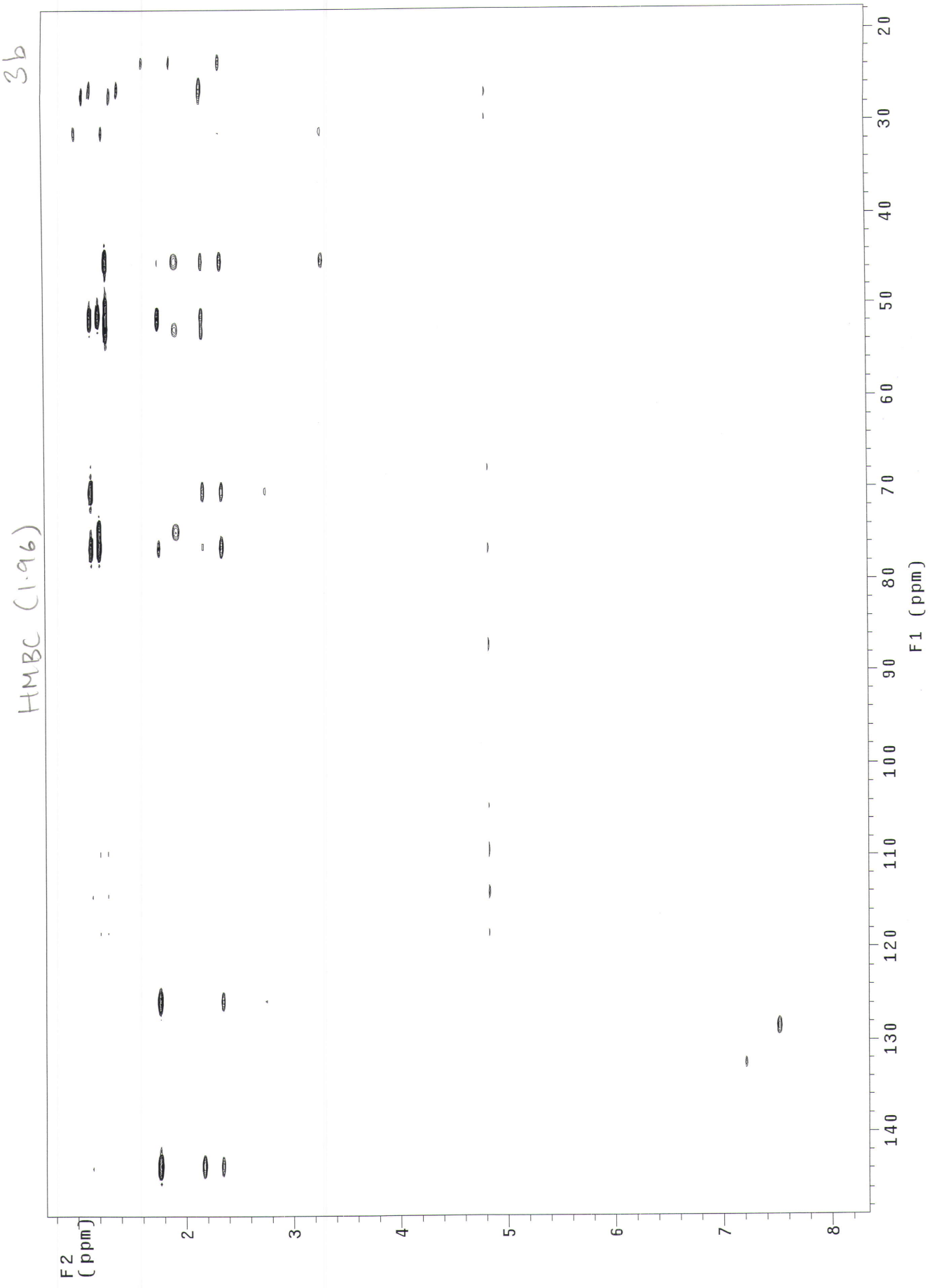
36
HMBC (1.96)
F2 (ppm)
F1 (ppm)

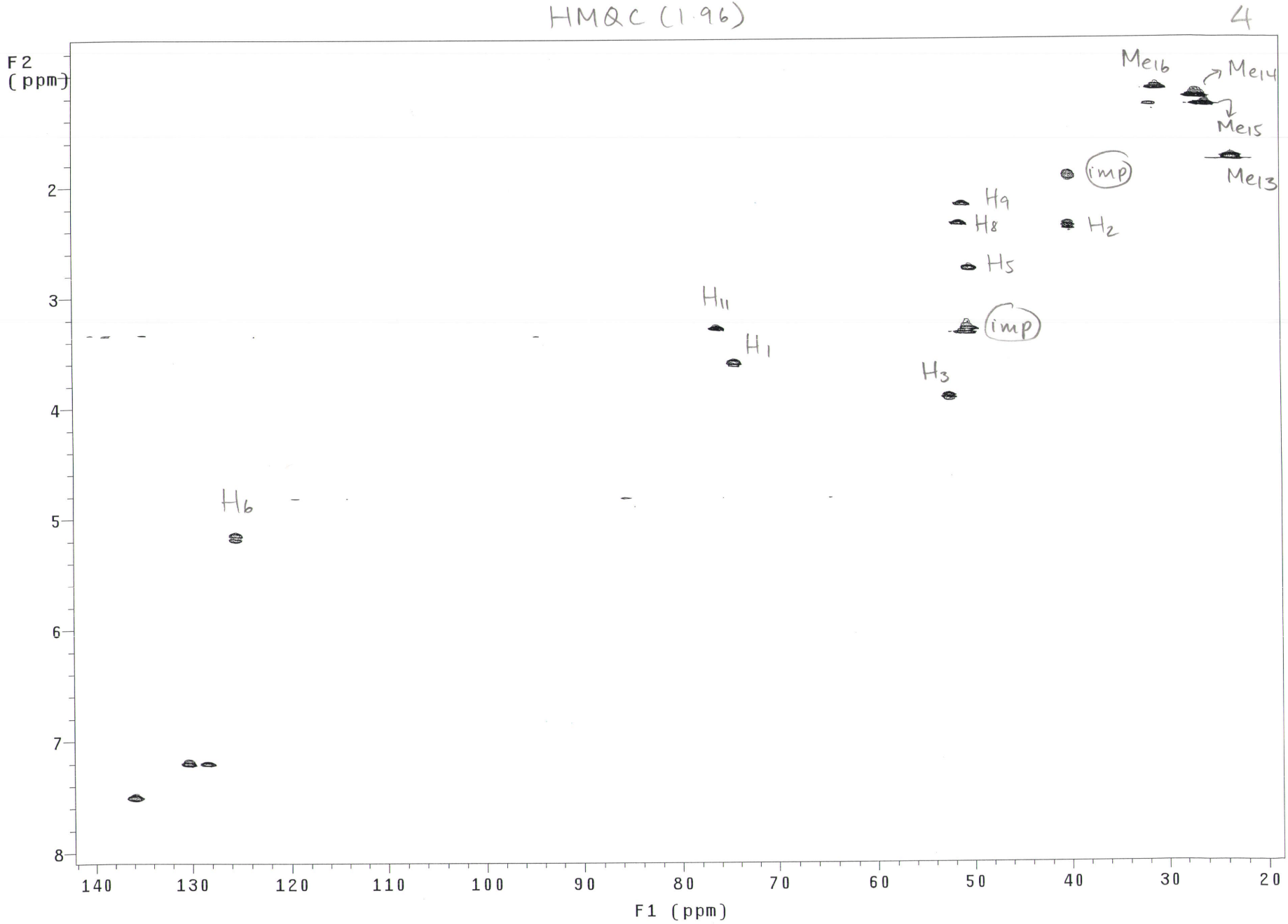
HMQC (1.96)
F2 (ppm)
F1 (ppm)
Me16
Me14
Me15
Me13
imp
H9
H8
H2
H5
H11
imp
H1
H3
H6
2
3
4
5
6
7
8
140
130
120
110
100
90
80
70
60
50
40
30
20

NOE (1.96)

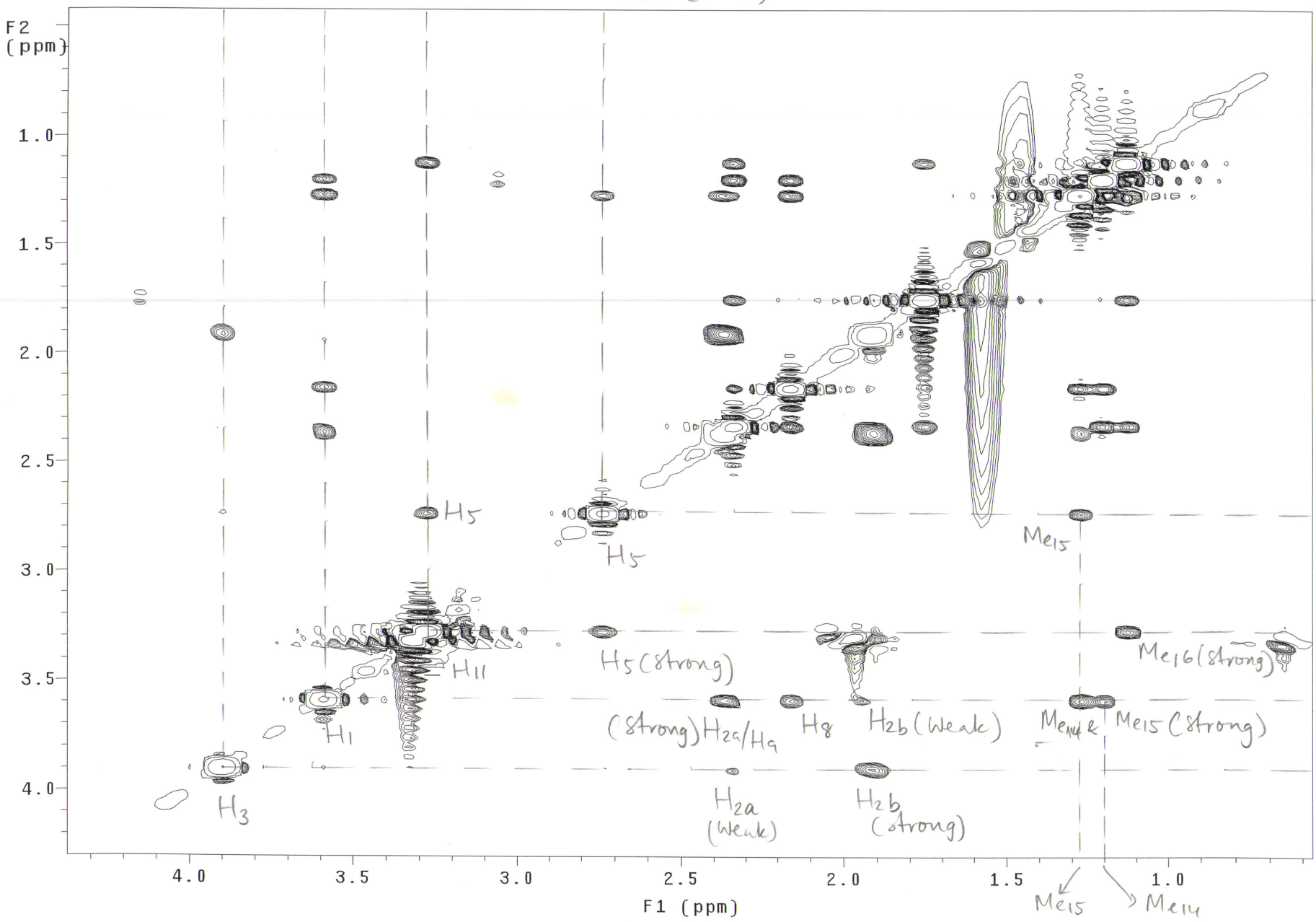
F2 (ppm)
1.0
1.5
2.0
2.5
3.0
3.5
4.0
4.0
3.5
3.0
2.5
2.0
1.5
1.0
F1 (ppm)
H5
H5
Me15
H11
H1
H3
H5 (strong)
Me16 (strong)
(strong) H2a/H9
H8
H2b (weak)
Me14 & Me15 (strong)
H2a (weak)
H2b (strong)
Me15
Me14

thesis-43-cdcl3-HNMR-1

Pulse Sequence: s2pul

Solvent: CDCl3
Ambient temperature
Operator: vnmr_vb
File: thesis-43-cdcl3-HNMR-1
INOVA-500 "fao"

Relax. delay 1.000 sec
Pulse 64.3 degrees
Acq. time 1.995 sec
Width 4506.5 Hz
16 repetitions
OBSERVE H1, 300.1176007 MHz
DATA PROCESSING
FT size 32768
Total time 0 min, 54 sec

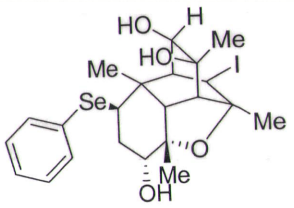

thesis-43-cdcl3-CNMR

Pulse Sequence: s2pul

Solvent: cdcl3
Temp. 25.0 C / 298.1 K
Operator: vnmr_jk
File: thesis-43-cdcl3-CNMR
INOVA-500 "fao"

Relax. delay 1.000 sec
Pulse 86.5 degrees
Acq. time 0.484 sec
Width 33071.5 Hz
13280 repetitions
OBSERVE C13, 150.8054870 MHz
DECOUPLE H1, 599.7456303 MHz
Low power 10 dB atten.
continuously on
WALTZ-16 modulated
DATA PROCESSING
Line broadening 1.0 Hz
FT size 32768
Total time 4146 hr, 25 min, 4 sec

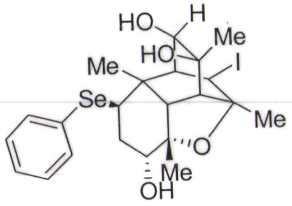

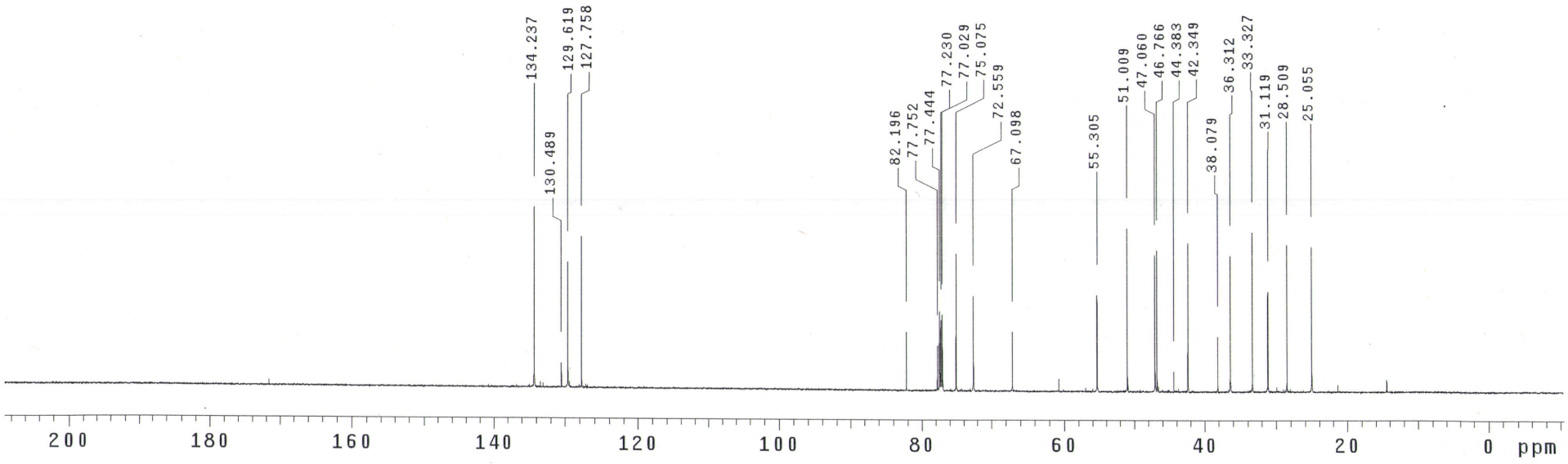

thesis-44-cdcl3-HNMR-2

Pulse Sequence: s2pul

Solvent: CDCl3
Ambient temperature
Operator: vnmr_vb
File: thesis-44-cdcl3-HNMR-2
INOVA-500 "fao"

Relax. delay 1.000 sec
Pulse 64.3 degrees
Acq. time 1.995 sec
Width 4506.5 Hz
16 repetitions
OBSERVE H1, 300.1176007 MHz
DATA PROCESSING
FT size 32768
Total time 0 min, 54 sec

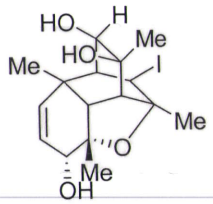

thesis-44-cdcl3-CNMR

Pulse Sequence: s2pul

Solvent: CDCl3
Ambient temperature
Operator: vnmr_vb
File: thesis-44-cdcl3-CNMR
INOVA-500 "fao"

Relax. delay 2.000 sec
Pulse 105.4 degrees
Acq. time 1.815 sec
Width 16501.7 Hz
656 repetitions
OBSERVE C13, 75.3761470 MHz
DECOUPLE H1, 299.7672516 MHz
Low power 5 dB atten.
continuously on
WALTZ-16 modulated
DATA PROCESSING
Line broadening 3.0 Hz
FT size 65536
Total time 106 hr, 13 min, 14 sec

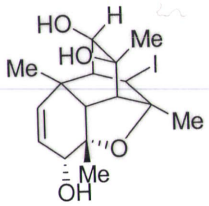

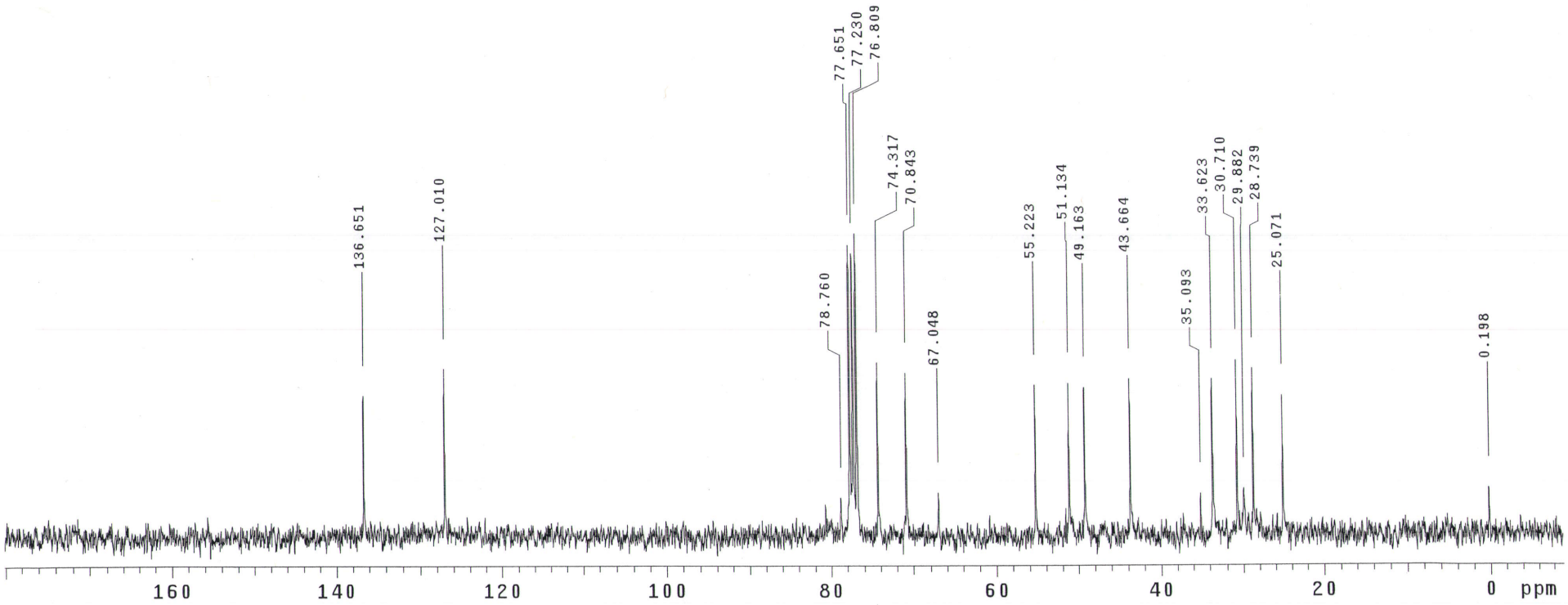

STANDARD PROTON PARAMETERS

Pulse Sequence: s2pul

Solvent: cdcl3
Temp. 25.0 C / 298.1 K
File: h1
INOVA-500 "fao"

Relax. delay 1.000 sec
Pulse 4.0 usec
Acq. time 1.520 sec
Width 5261.4 Hz
4 repetitions
OBSERVE H1, 499.8888021 MHz
DATA PROCESSING
Line broadening 1.0 Hz
FT size 16384
Total time 0 min, 10 sec

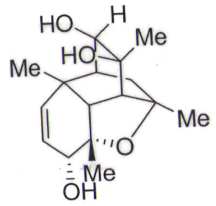

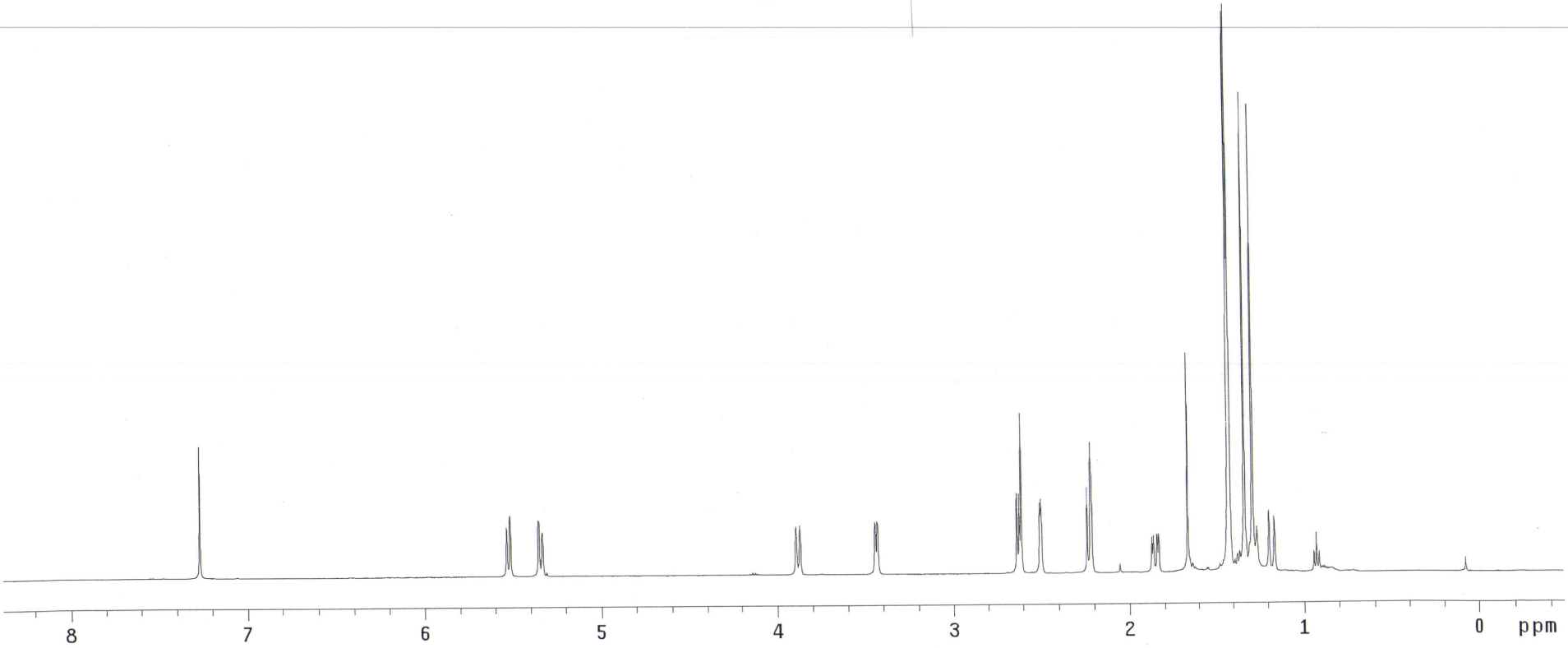

STANDARD CARBON PARAMETERS

Pulse Sequence: s2pul

Solvent: cdcl3
Temp. 25.0 C / 298.1 K
User: 1-14-87
File: c13
INOVA-500 "fao"

Relax. delay 1.000 sec
Pulse 129.8 degrees
Acq. time 0.592 sec
Width 27027.0 Hz
12480 repetitions
OBSERVE C13, 125.6971105 MHz
DECOUPLE H1, 499.8911601 MHz
Low power 10 dB atten.
continuously on
WALTZ-16 modulated
DATA PROCESSING
Line broadening 1.0 Hz
FT size 32768
Total time 4446 hr, 59 min, 15 sec

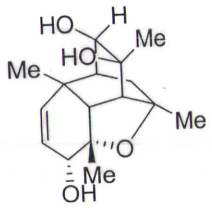

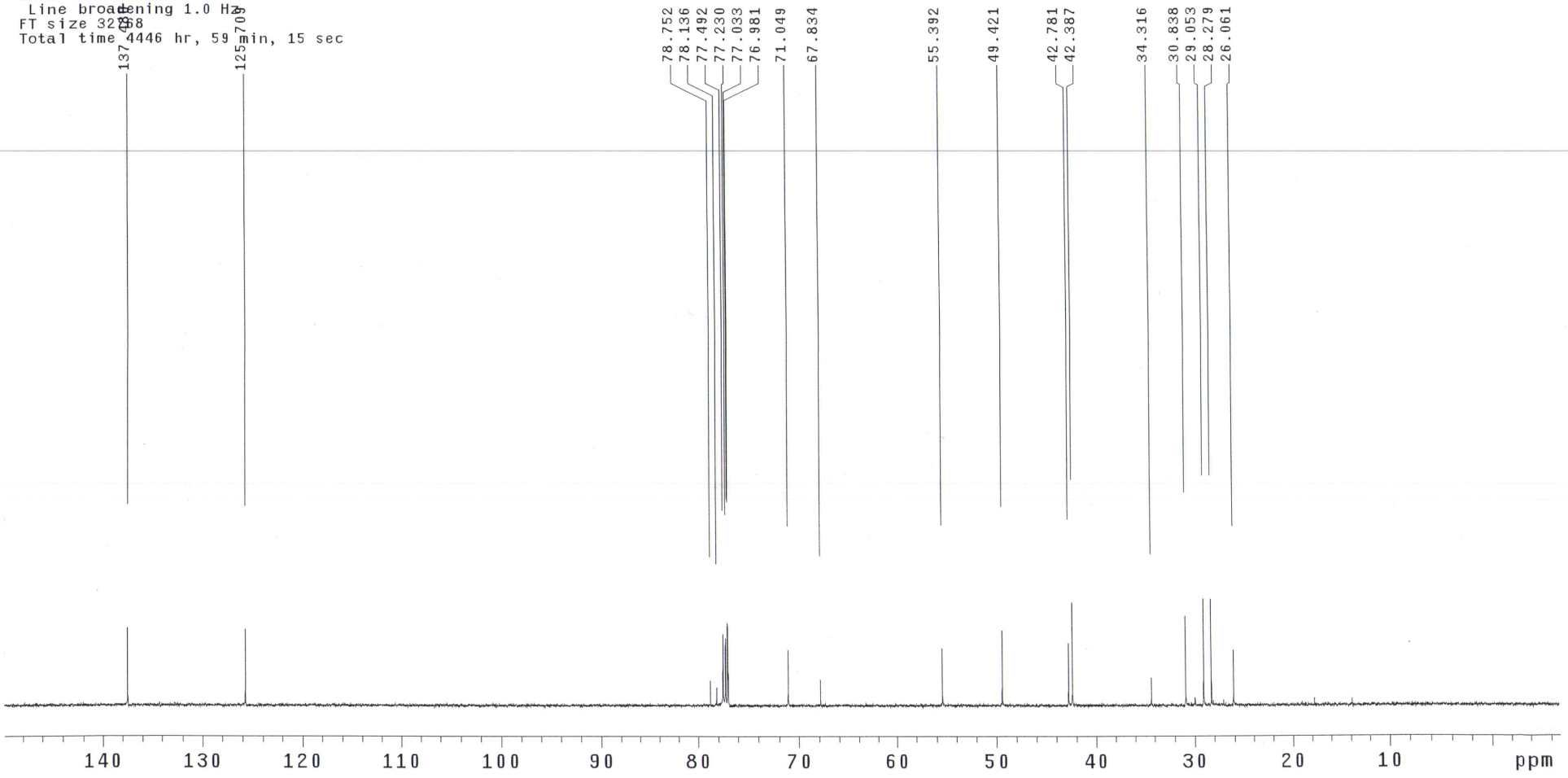

thesis-46-cdcl3-HNMR

Pulse Sequence: s2pul

Solvent: CDCl3
Ambient temperature
Operator: vnmr_vb
File: thesis-46-cdcl3-HNMR
INOVA-500 "fao"

Pulse 58.9 degrees
Acq. time 3.744 sec
Width 4000.0 Hz
16 repetitions
OBSERVE H1, 299.7657645 MHz
DATA PROCESSING
FT size 32768
Total time 1 min, 7 sec

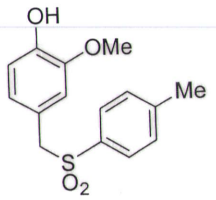

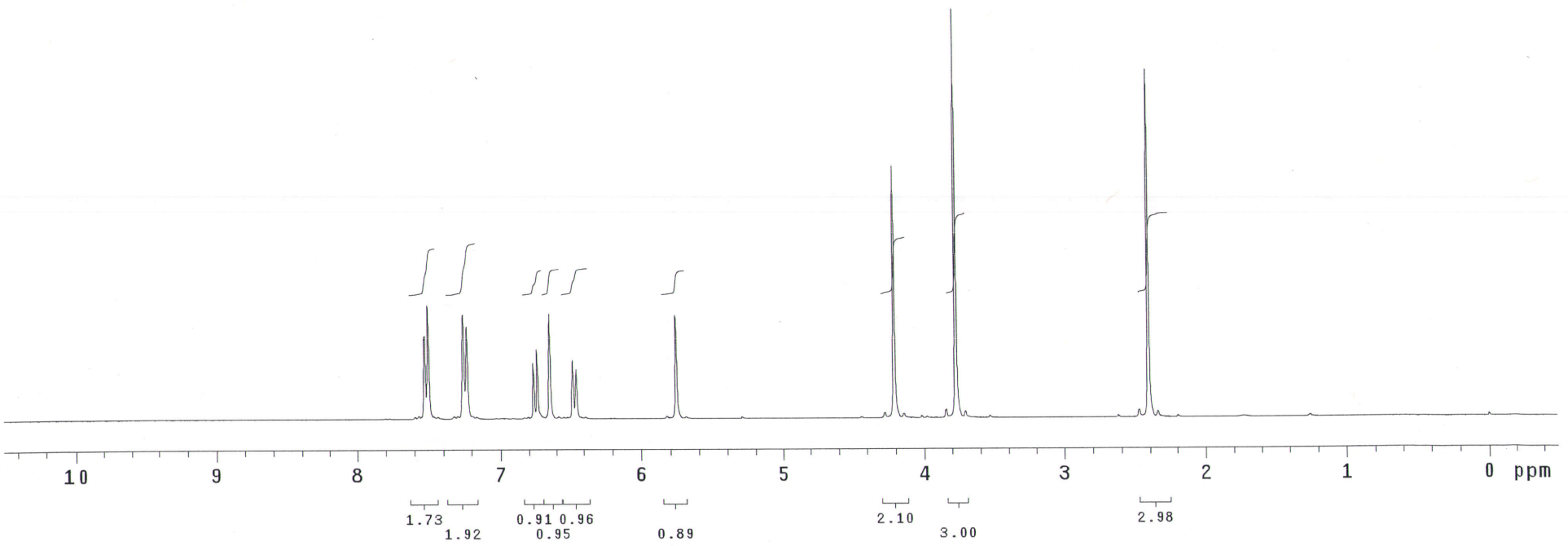

thesis-46-cdcl3-CNMR

Pulse Sequence: s2pul

Solvent: CDCl3
Ambient temperature
Operator: vnmr_vb
File: thesis-46-cdcl3-CNMR
INOVA-500 "fao"

Pulse 105.4 degrees
Acq. time 1.815 sec
Width 16501.7 Hz
448 repetitions
OBSERVE C13, 75.3761515 MHz
DECOUPLE H1, 299.7672516 MHz
Low power 5 dB atten.
continuously on
WALTZ-16 modulated
DATA PROCESSING
Line broadening 1.0 Hz
FT size 65536
Total time 31 min, 7 sec

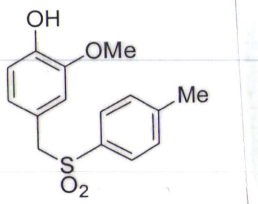

thesis-47-cdcl3-HNMR

Pulse Sequence: s2pul

Solvent: CDCl3
Ambient temperature
Operator: vnmr_vb
File: thesis-47-cdcl3-HNMR
INOVA-500 "fao"

Relax. delay 1.000 sec
Pulse 18.4 degrees
Acq. time 1.995 sec
Width 4506.5 Hz
16 repetitions
OBSERVE H1, 300.1175890 MHz
DATA PROCESSING
FT size 32768
Total time 0 min, 54 sec

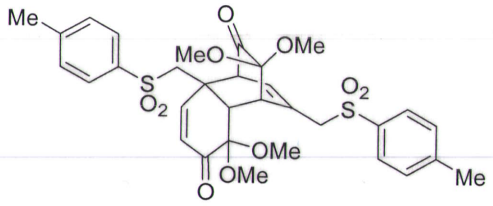

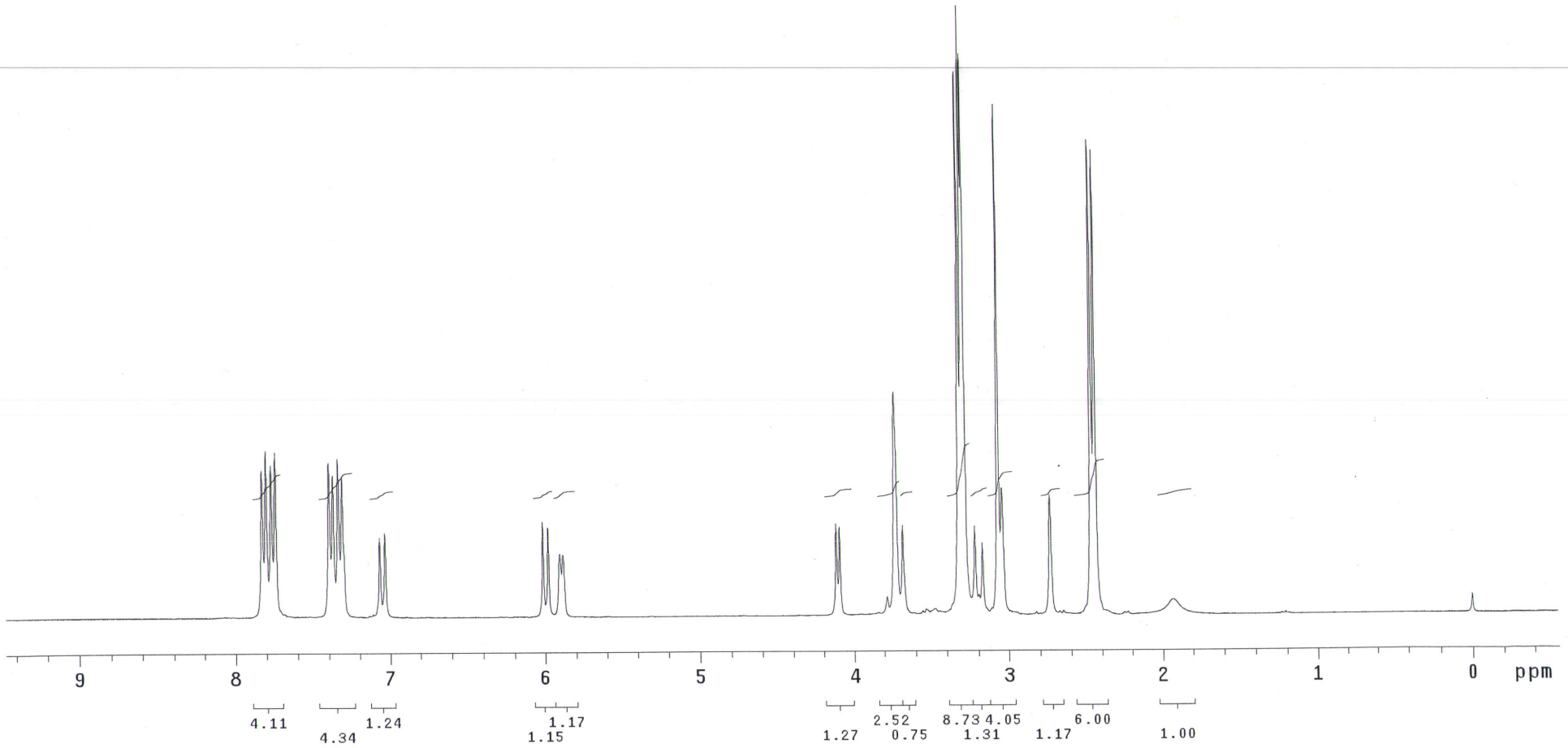

thesis-47-cdcl3-CNMR

Pulse Sequence: s2pul

Solvent: CDCl3
Ambient temperature
Operator: vnmr_vb
File: thesis-47-cdcl3-CNMR
INOVA-500 "fao"

Relax. delay 1.000 sec
Pulse 105.4 degrees
Acq. time 1.815 sec
Width 22497.2 Hz
256 repetitions
OBSERVE C13, 75.3761528 MHz
DECOUPLE H1, 299.7672516 MHz
Low power 5 dB atten.
continuously on
WALTZ-16 modulated
DATA PROCESSING
Line broadening 2.0 Hz
FT size 131072
Total time 48 min, 11 sec

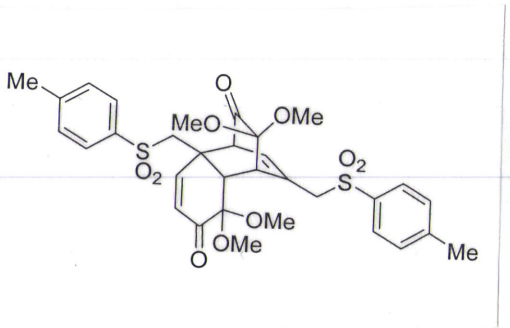

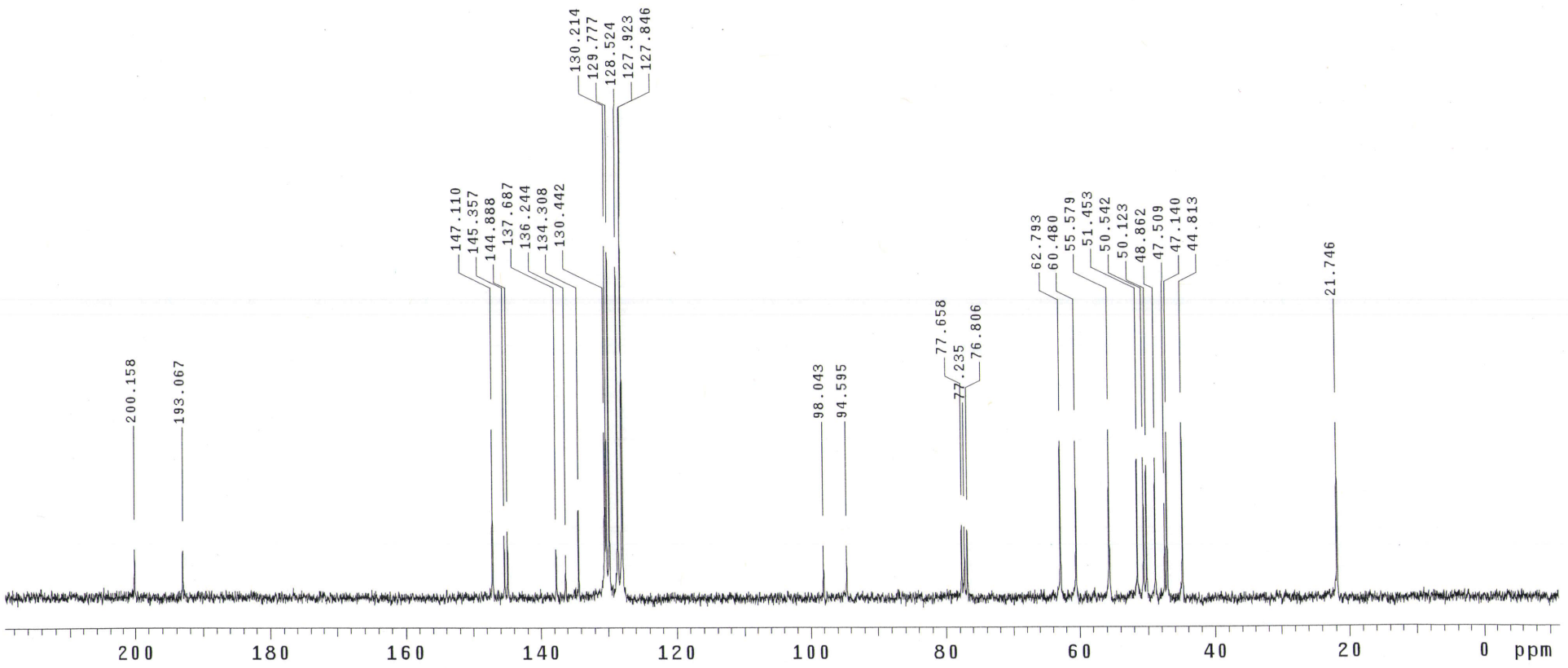

thesis-48-cdcl3-HNMR

Pulse Sequence: s2pul
 Solvent: CDCl3
 Ambient temperature
Operator: vnmr_vb
File: thesis-48-cdcl3-HNMR
INOVA-500 "fao"

 Relax. delay 1.000 sec
 Pulse 18.4 degrees
 Acq. time 1.995 sec
 Width 4506.5 Hz
 16 repetitions
OBSERVE   H1, 300.1176007 MHz
DATA PROCESSING
FT size 32768
Total time 0 min, 54 sec

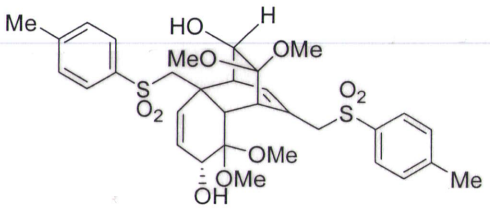

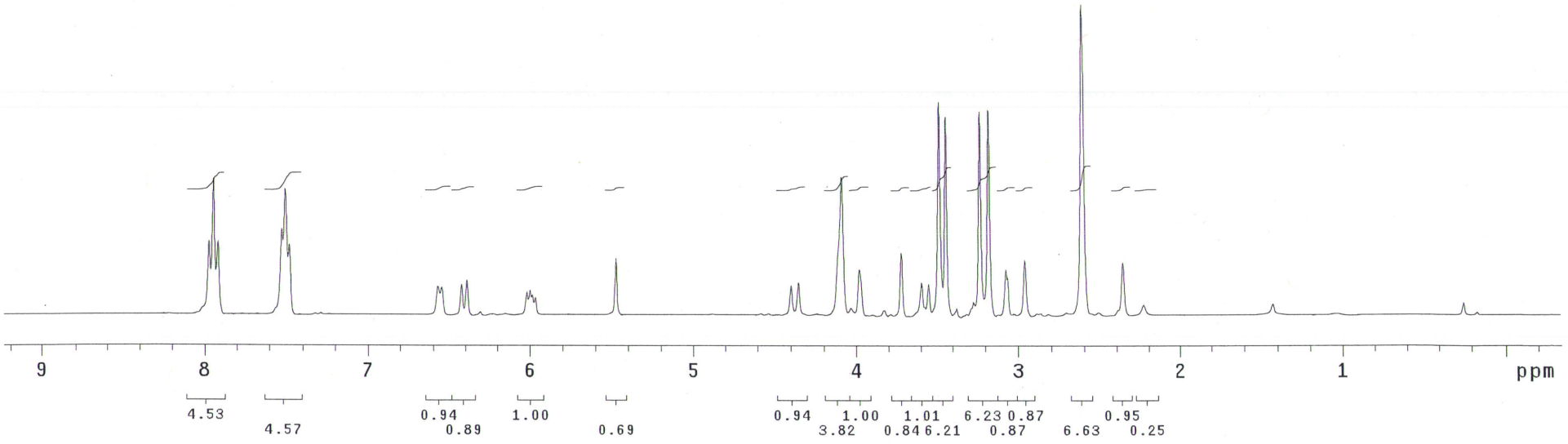

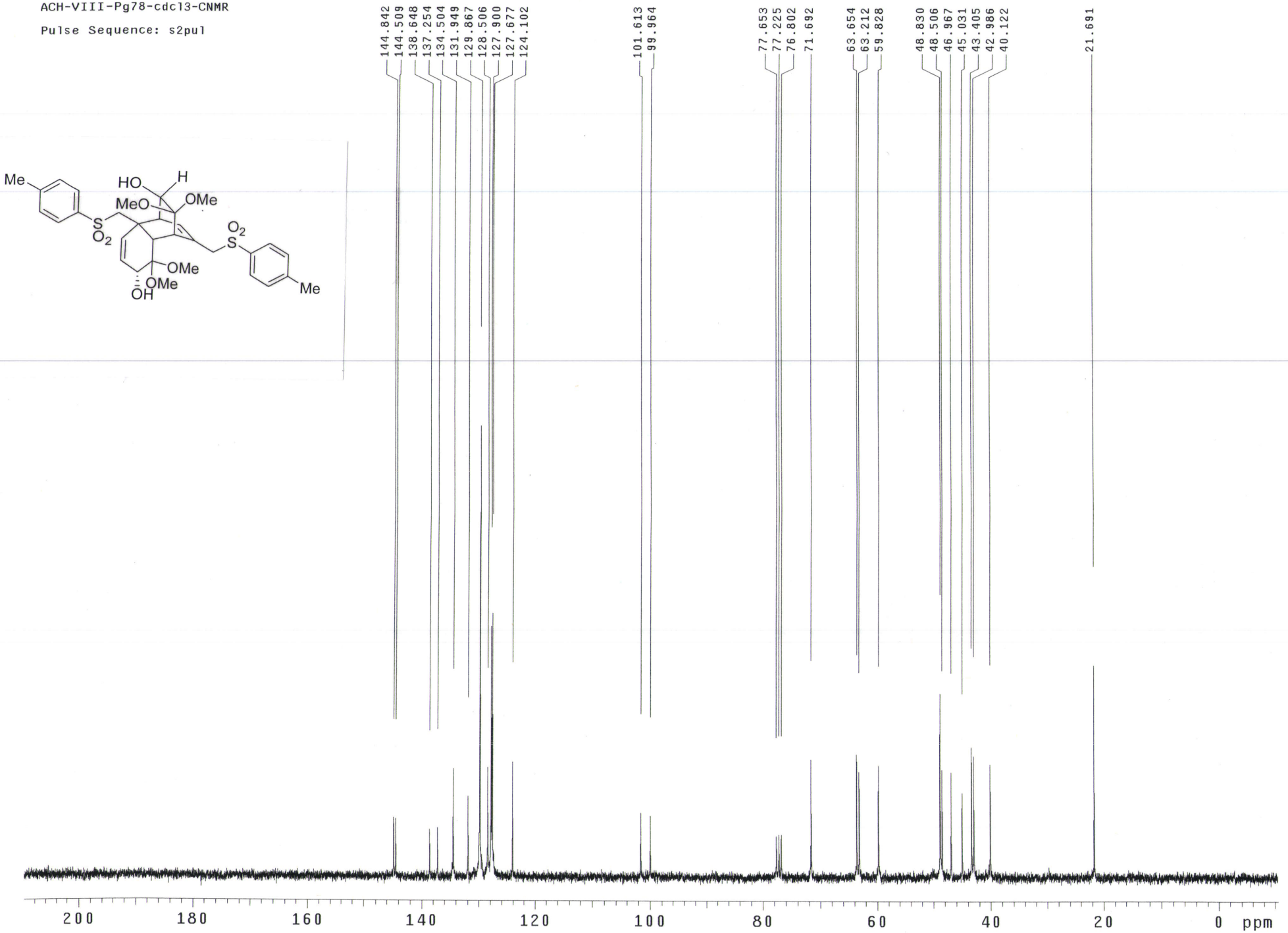
ACH-VIII-Pg78-cdcl3-CNMR
Pulse Sequence: s2pul
144.842
144.509
138.648
137.254
134.504
131.949
129.867
128.506
127.900
127.677
124.102
101.613
99.964
77.653
77.225
76.802
71.692
63.654
63.212
59.828
48.830
48.506
46.967
45.031
43.405
42.986
40.122
21.691
Me
HO
H
MeO
OMe
S
O2
O2
S
OMe
OMe
OH
Me
200
180
160
140
120
100
80
60
40
20
0
ppm

thesis-53-cdcl3-HNMR

Pulse Sequence: s2pul
 Solvent: CDCl3
 Ambient temperature
Operator: vnmr_vb
File: thesis-53-cdcl3-HNMR
INOVA-500 "fao"

 Relax. delay 1.000 sec
 Pulse 18.4 degrees
 Acq. time 1.995 sec
 Width 4506.5 Hz
 16 repetitions
OBSERVE H1, 300.1176154 MHz
DATA PROCESSING
FT size 32768
Total time 0 min, 54 sec

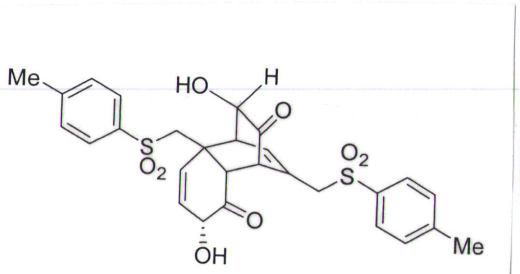

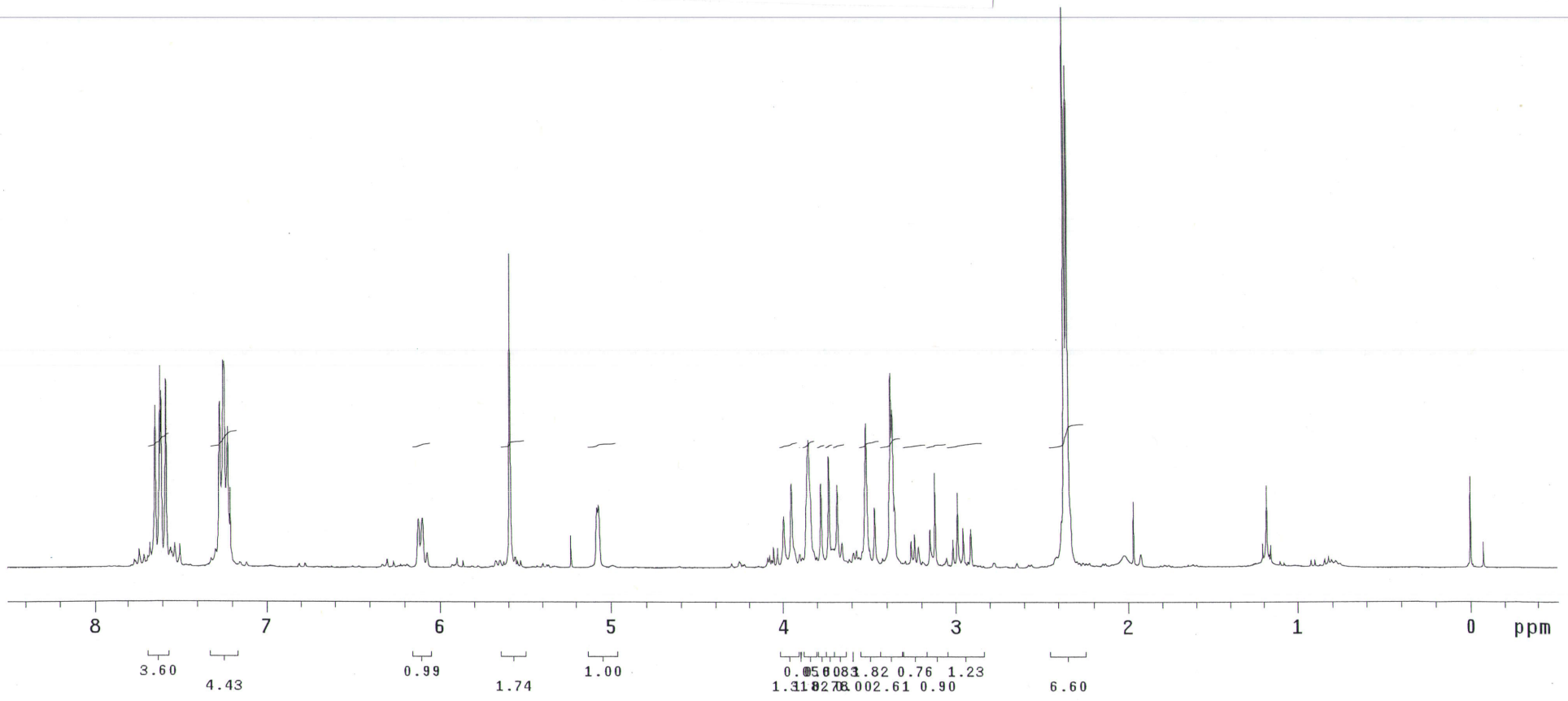

thesis-53-cdcl3-CNMR

Pulse Sequence: s2pul
Solvent: CDCl3
Ambient temperature
Operator: vnmr_vb
File: thesis-53-cdcl3-CNMR
INOVA-500 "fao"

Relax. delay 1.000 sec
Pulse 105.4 degrees
Acq. time 1.815 sec
Width 21917.8 Hz
384 repetitions
OBSERVE C13, 75.3761481 MHz
DECOUPLE H1, 299.7672516 MHz
Low power 5 dB atten.
continuously on
WALTZ-16 modulated
DATA PROCESSING
Line broadening 1.0 Hz
FT size 131072
Total time 48 min, 11 sec

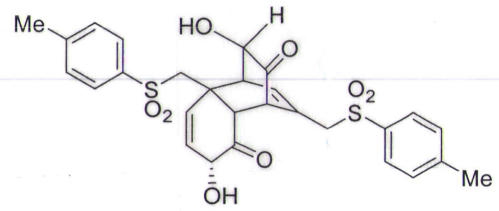

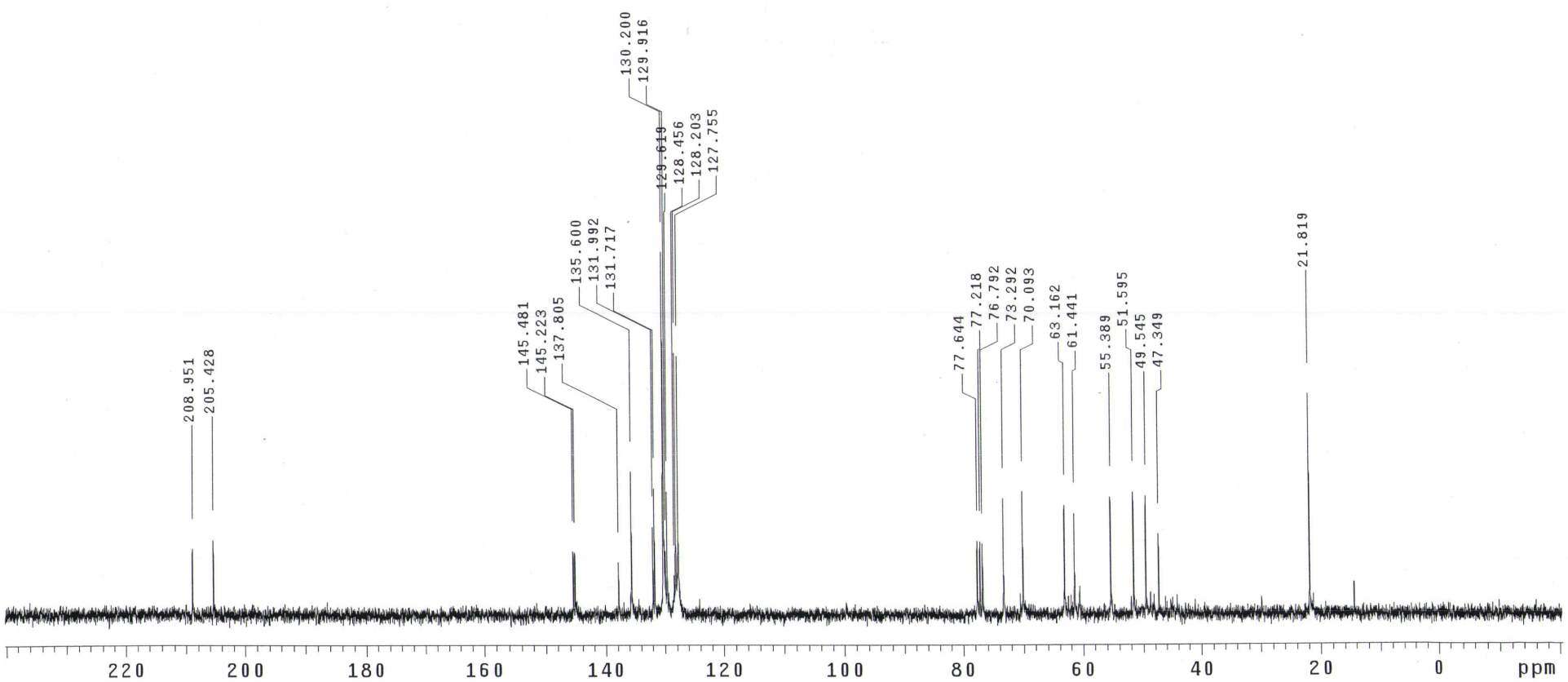

thesis-50-cdcl3-HNMR

Pulse Sequence: s2pul

Solvent: cdcl3
Temp. 25.0 C / 298.1 K
Operator: vnmr_jk
File: thesis-50-cdcl3-HNMR
INOVA-500 "fao"

Relax. delay 1.000 sec
Pulse 78.0 degrees
Acq. time 1.450 sec
Width 5517.2 Hz
4 repetitions
OBSERVE H1, 599.7430118 MHz
DATA PROCESSING
Resol. enhancement 4.0 Hz
Gauss apodization 0.200 sec
FT size 16384
Total time 0 min, 9 sec

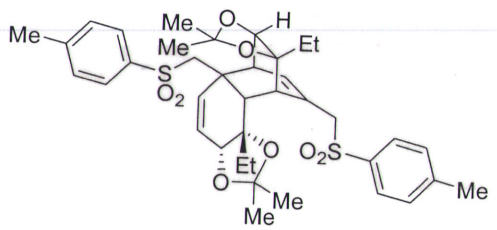

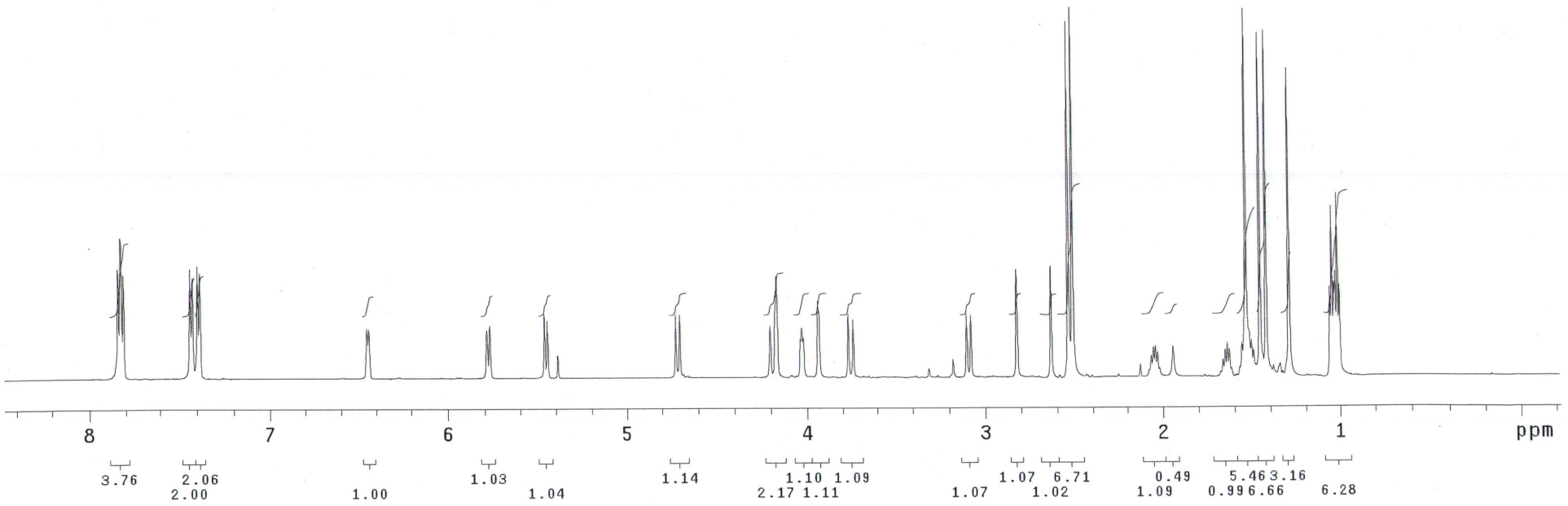

thesis-50-cdcl3-CNMR

Pulse Sequence: s2pul

Solvent: cdcl3
Temp. 25.0 C / 298.1 K
Operator: vnmr_jk
File: thesis-50-cdcl3-CNMR
INOVA-500 "fao"

Relax. delay 1.000 sec
Pulse 86.5 degrees
Acq. time 0.484 sec
Width 33071.5 Hz
28640 repetitions
OBSERVE C13, 150.8055011 MHz
DECOUPLE H1, 599.7456303 MHz
Low power 10 dB atten.
continuously on
WALTZ-16 modulated
DATA PROCESSING
Line broadening 1.0 Hz
FT size 32768
Total time 4146 hr, 25 min, 10 sec

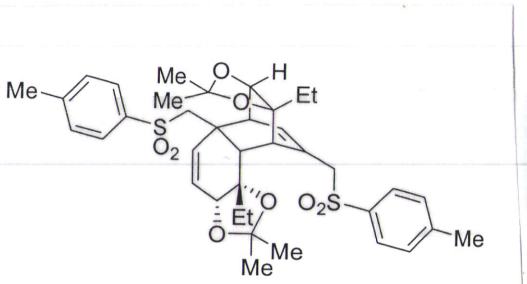

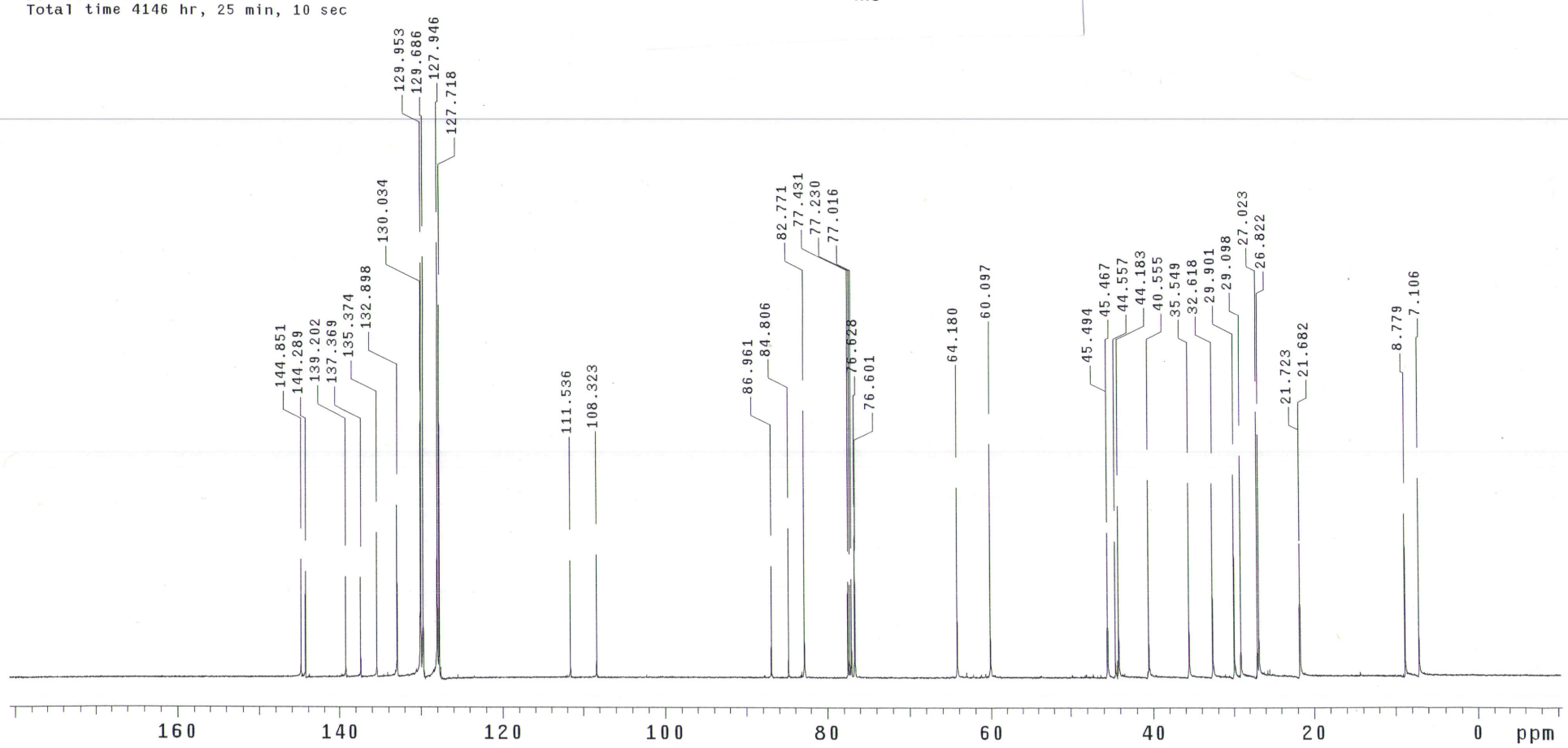

STANDARD PROTON PARAMETERS

Pulse Sequence: s2pul

Solvent: cdcl3
Temp. 25.0 C / 298.1 K
Operator: vnmr_jk
File: thesis-51-cdcl3-HNMR-1
INOVA-500 "fao"

Relax. delay 1.000 sec
Pulse 78.0 degrees
Acq. time 0.870 sec
Width 9199.6 Hz
4 repetitions
OBSERVE H1, 599.7432511 MHz
DATA PROCESSING
Resol. enhancement -0.0 Hz
FT size 16384
Total time 0 min, 7 sec

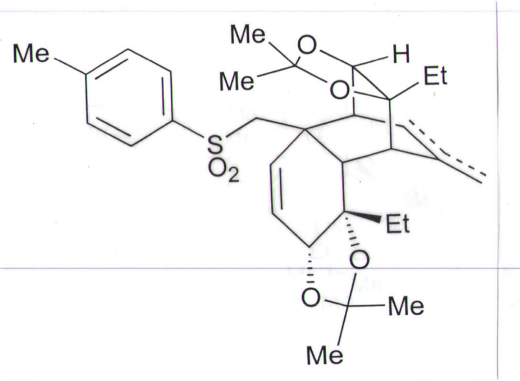

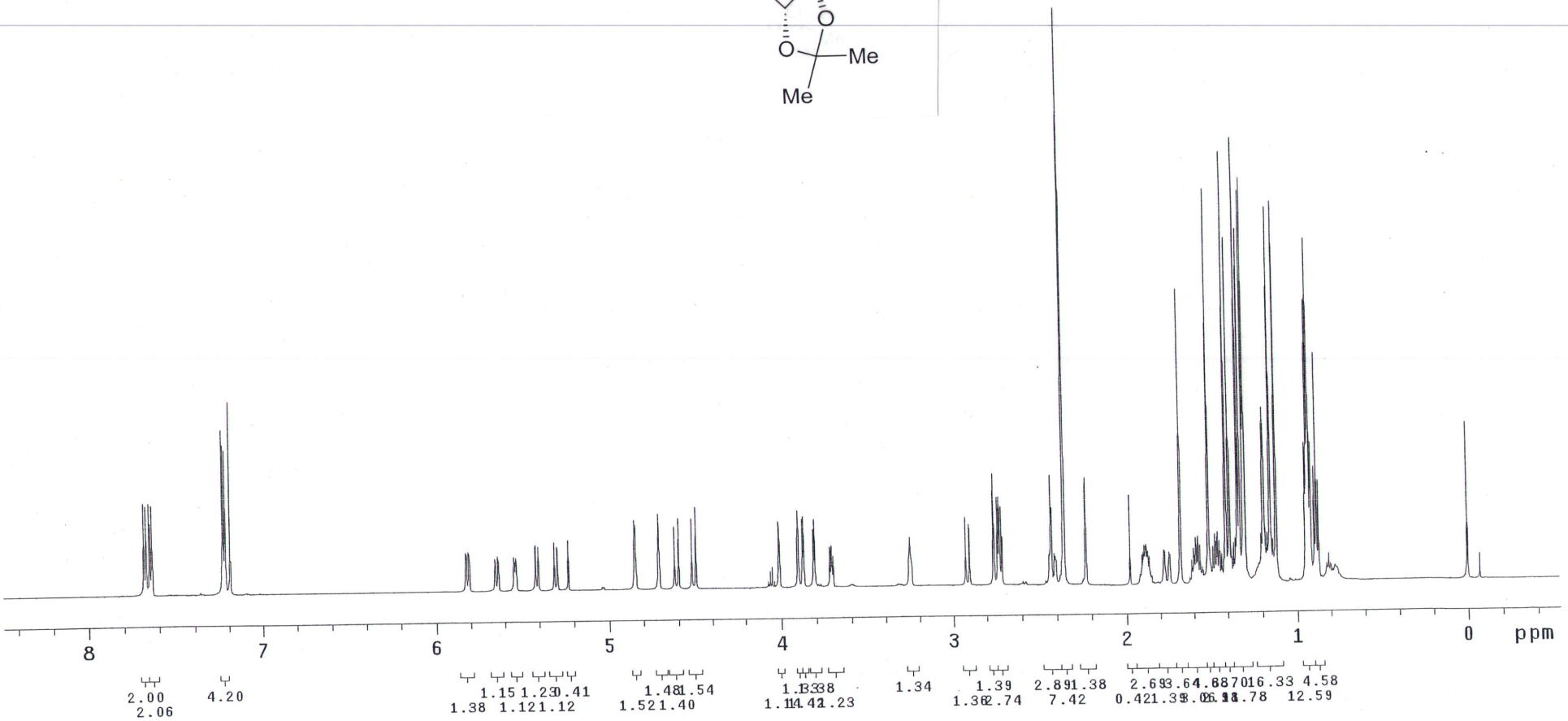

STANDARD CARBON PARAMETERS

Pulse Sequence: s2pul

Solvent: cdcl3
Temp. 25.0 C / 298.1 K
Operator: vnmr_jk
File: c13
INOVA-500 "fao"

Relax. delay 1.000 sec
Pulse 86.5 degrees
Acq. time 0.889 sec
Width 36003.6 Hz
33472 repetitions
OBSERVE C13, 150.8055643 MHz
DECOUPLE H1, 599.7459936 MHz
Low power 10 dB atten.
continuously on
WALTZ-16 modulated
DATA PROCESSING
Line broadening 1.0 Hz
FT size 65536
Total time 5271 hr, 25 min, 2 sec

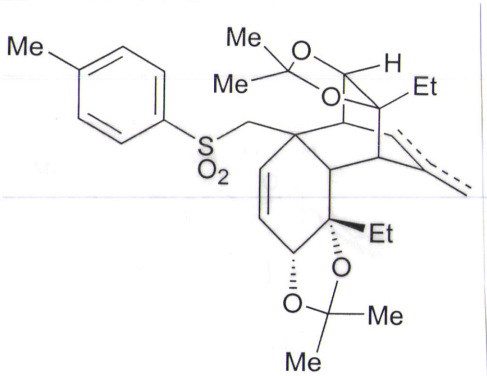

thesis-49-cd3od-HNMR

Pulse Sequence: s2pul

Solvent: CD3OD
Ambient temperature
Operator: vnmr_vb
File: thesis-49-cd3od-HNMR
INOVA-500 "fao"

Relax. delay 1.000 sec
Pulse 64.3 degrees
Acq. time 1.995 sec
Width 4506.5 Hz
16 repetitions
OBSERVE H1; 300.1187814 MHz
DATA PROCESSING
FT size 32768
Total time 0 min, 54 sec

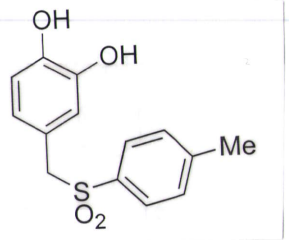

1.114

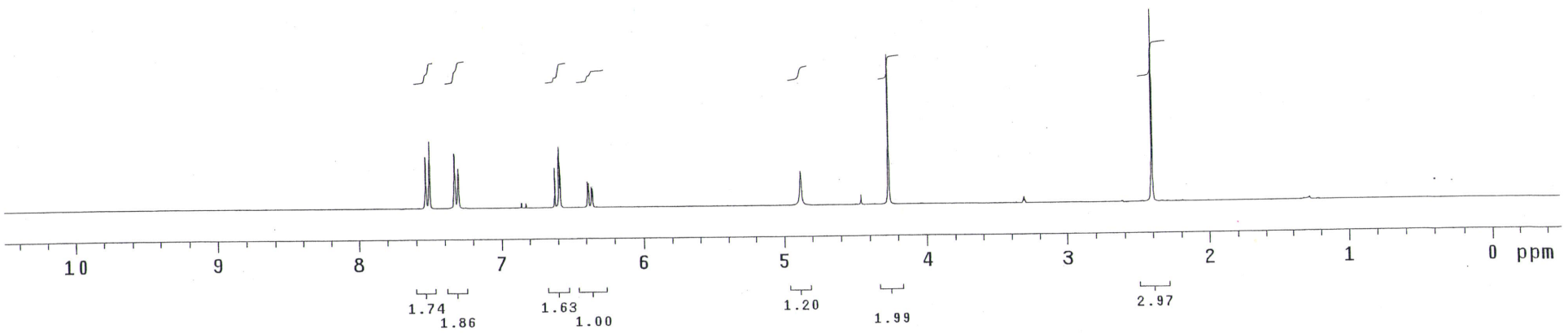

thesis-49-cd3od-CNMR

Pulse Sequence: s2pul

Solvent: CD3OD
Ambient temperature
Operator: vnmr_vb
File: thesis-49-cd3od-CNMR
INOVA-500 "fao"

Relax. delay 1.000 sec
Pulse 43.3 degrees
Acq. time 1.815 sec
Width 18761.7 Hz
272 repetitions
OBSERVE C13, 75.4648125 MHz
DECOUPLE H1, 300.1202380 MHz
Low power 1023 dB atten.
continuously on
WALTZ-16 modulated
DATA PROCESSING
Line broadening 1.0 Hz
FT size 131072
Total time 78 hr, 26 min, 0 sec

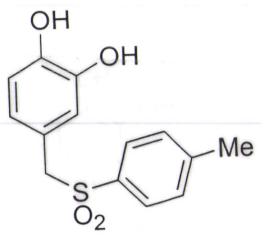

1.114

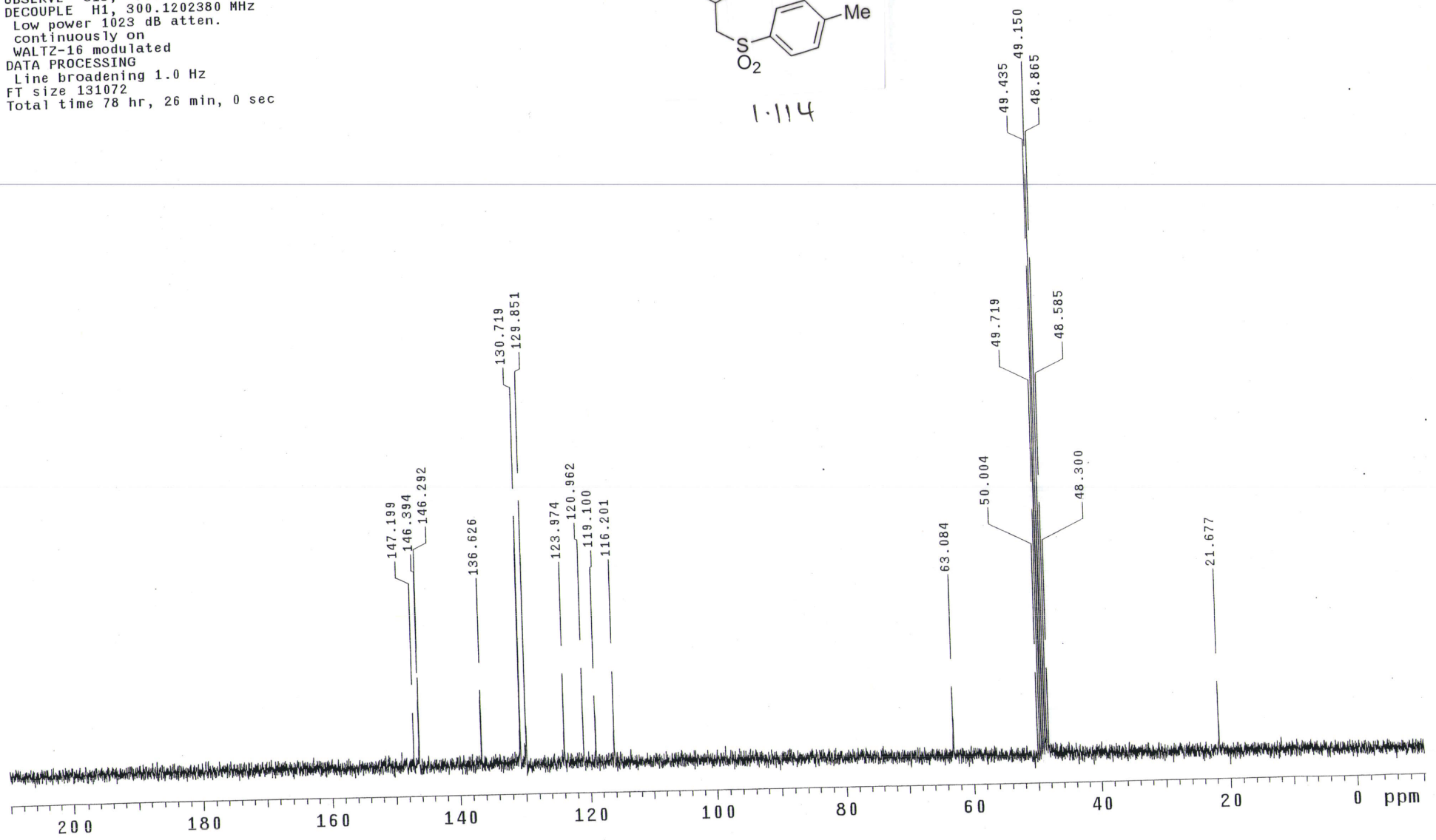

ACH-VIII-Pg5-cdcl3-HNMR

Pulse Sequence: s2pul
Solvent: CDCl3
Ambient temperature
Operator: vnmr_vb
File: thesis-1-cdcl3-HNMR
INOVA-500 "fao"

Relax. delay 1.000 sec
Pulse 58.9 degrees
Acq. time 3.744 sec
Width 4000.0 Hz
16 repetitions
OBSERVE H1, 299.7657527 MHz
DATA PROCESSING
FT size 32768
Total time 1 min, 25 sec

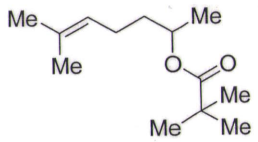

ACH-VIII-Pg5-cdcl3-CNMR

Pulse Sequence: s2pul
 Solvent: CDCl3
 Ambient temperature
Operator: vnmr_vb
File: thesis-1-cdcl3-CNMR
INOVA-500 "fao"

 Pulse 105.4 degrees
 Acq. time 1.815 sec
 Width 16501.7 Hz
 240 repetitions
OBSERVE C13, 75.3761470 MHz
DECOUPLE H1, 299.7672516 MHz
 Low power 5 dB atten.
 continuously on
 WALTZ-16 modulated
DATA PROCESSING
 Line broadening 1.0 Hz
FT size 65536
Total time 31 min, 7 sec

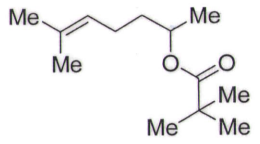

ACH-VIII-Pg5-cdcl3-HNMR

Pulse Sequence: s2pul

Solvent: CDCl3
Ambient temperature
Operator: vnmr_vb
File: thesis-1-cdcl3-HNMR
INOVA-500 "fao"

Relax. delay 1.000 sec
Pulse 58.9 degrees
Acq. time 3.744 sec
Width 4000.0 Hz
16 repetitions
OBSERVE H1, 299.7657527 MHz
DATA PROCESSING
FT size 32768
Total time 1 min, 25 sec

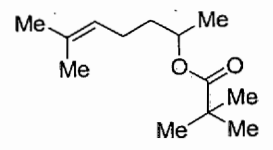

2.141

ACH-VIII-Pg5-cdcl3-CNMR

Pulse Sequence: s2pul

Solvent: CDCl3
Ambient temperature
Operator: vnmr_vb
File: thesis-1-cdcl3-CNMR
INOVA-500 "fao"

Pulse 105.4 degrees
Acq. time 1.815 sec
Width 16501.7 Hz
240 repetitions
OBSERVE C13, 75.3761470 MHz
DECOUPLE H1, 299.7672516 MHz
Low power 5 dB atten.
continuously on
WALTZ-16 modulated
DATA PROCESSING
Line broadening 1.0 Hz
FT size 65536
Total time 31 min, 7 sec

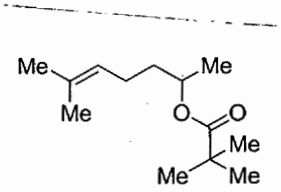

2.141

ACH-VIII-Pg33-cdcl3-HNMR

Pulse Sequence: s2pul

Solvent: CDCl3
Ambient temperature
Operator: vnmr_vb
File: thesis-2-cdcl3-HNMR
INOVA-500 "fao"

Relax. delay 1.000 sec
Pulse 18.4 degrees
Acq. time 1.995 sec
Width 4506.5 Hz
16 repetitions
OBSERVE H1, 300.1176007 MHz
DATA PROCESSING
FT size 32768
Total time 0 min, 54 sec

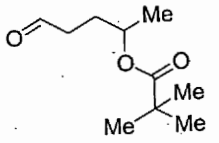

2.142

ACH-VIII-Pg33-cdcl3-CNMR

Pulse Sequence: s2pul
Solvent: CDCl3
Ambient temperature
Operator: vnmr_vb
File: thesis-2-cdcl3-CNMR
INOVA-500 "fao"

Pulse 43.3 degrees
Acq. time 1.815 sec
Width 18761.7 Hz
336 repetitions
OBSERVE C13, 75.4646149 MHz
DECOUPLE H1, 300.1190556 MHz
Low power 1023 dB atten.
continuously on
WALTZ-16 modulated
DATA PROCESSING
Line broadening 2.0 Hz
FT size 131072
Total time 50 hr, 39 min, 20 sec

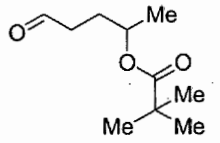

2.142

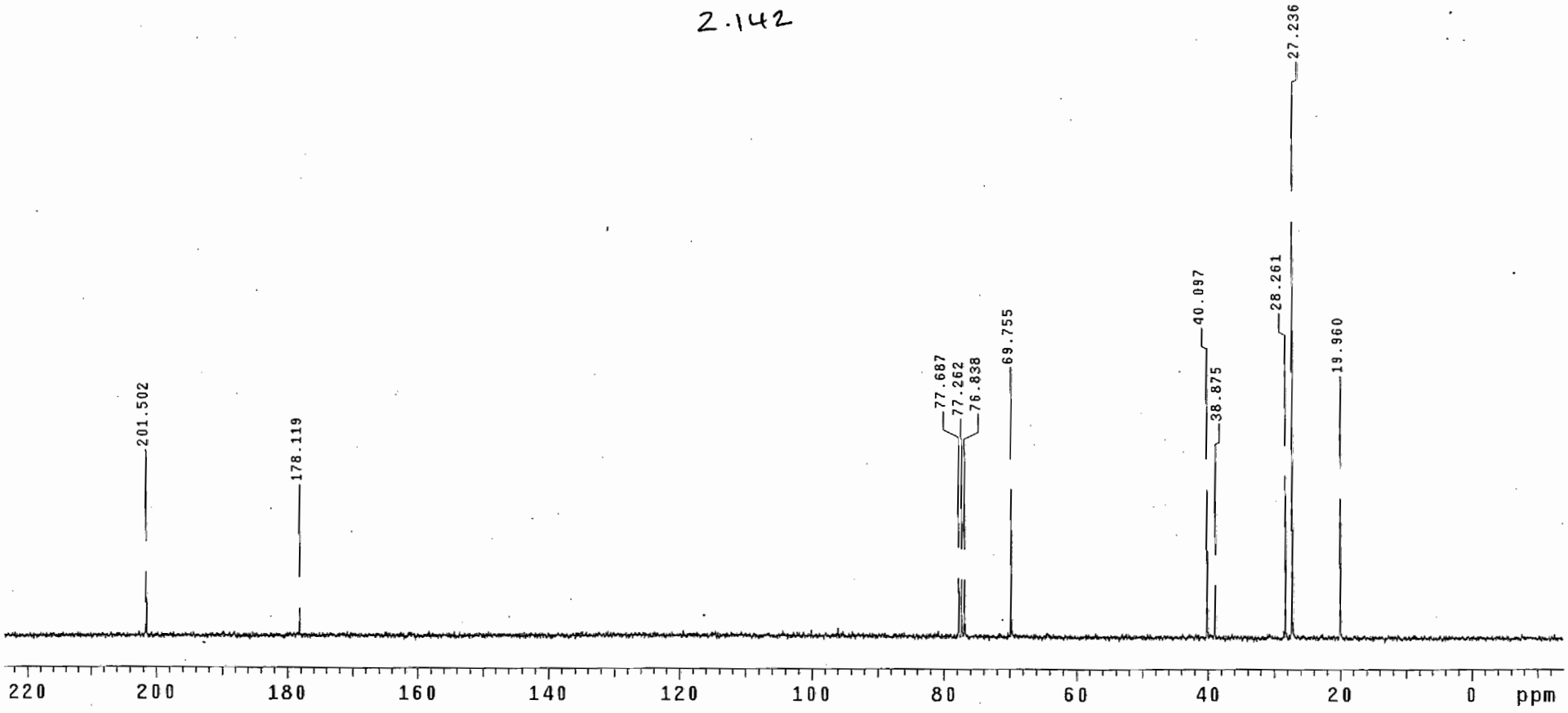

ACH-VIII-Pg9-cdcl3-HNMR

Pulse Sequence: s2pul
Solvent: CDCl3
Ambient temperature
Operator: vnmr_vb
File: thesis-2-cdcl3-HNMR
INOVA-500 "fao"

Pulse 58.9 degrees
Acq. time 3.744 sec
Width 4000.0 Hz
16 repetitions
OBSERVE H1, 299.7657527 MHz
DATA PROCESSING
FT size 32768
Total time 1 min, 7 sec

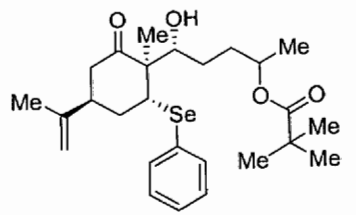

2.146

ACH-VIII-Pg9-cdcl3-CNMR

Pulse Sequence: s2pul

Solvent: CDCl3
Ambient temperature
Operator: vnmr_vb
File: thesis-9-cdcl3-CNMR
INOVA-500 "fao"

Pulse 105.4 degrees
Acq. time 1.815 sec
Width 27045.3 Hz
320 repetitions
OBSERVE C13, 75.3761506 MHz
DECOUPLE H1, 299.7672516 MHz
Low power 5 dB atten.
continuously on
WALTZ-16 modulated
DATA PROCESSING
Line broadening 1.0 Hz
FT size 131072
Total time 31 min, 7 sec

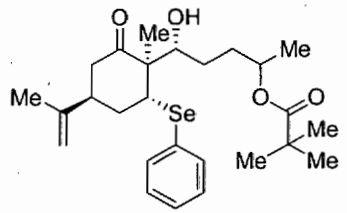

2.146

ACH-VIII-Pg14-cdcl3-HNMR

Pulse Sequence: s2pul

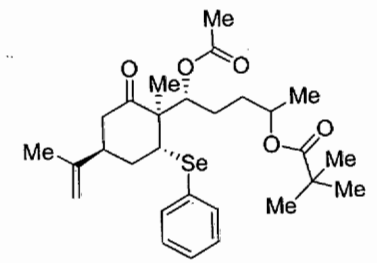

2.147

ACH-VIII-Pg14-cdcl3-CNMR

Pulse Sequence: s2pul

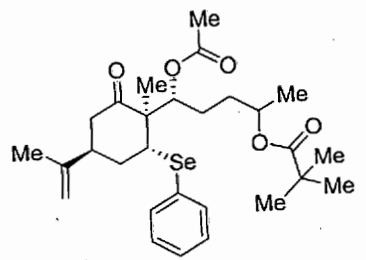

2.147

STANDARD 1H OBSERVE

Pulse Sequence: s2pul
Solvent: CDCl3
Ambient temperature
Operator: vnmr_vb
File: thesis-5-cdcl3-HNMR
INOVA-500 "fao"

Relax. delay 1.000 sec
Pulse 64.3 degrees
Acq. time 1.995 sec
Width 4506.5 Hz
16 repetitions
OBSERVE H1, 300.1176007 MHz
DATA PROCESSING
FT size 32768
Total time 0 min, 54 sec

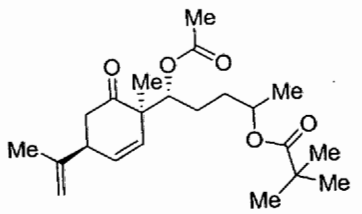

2.148

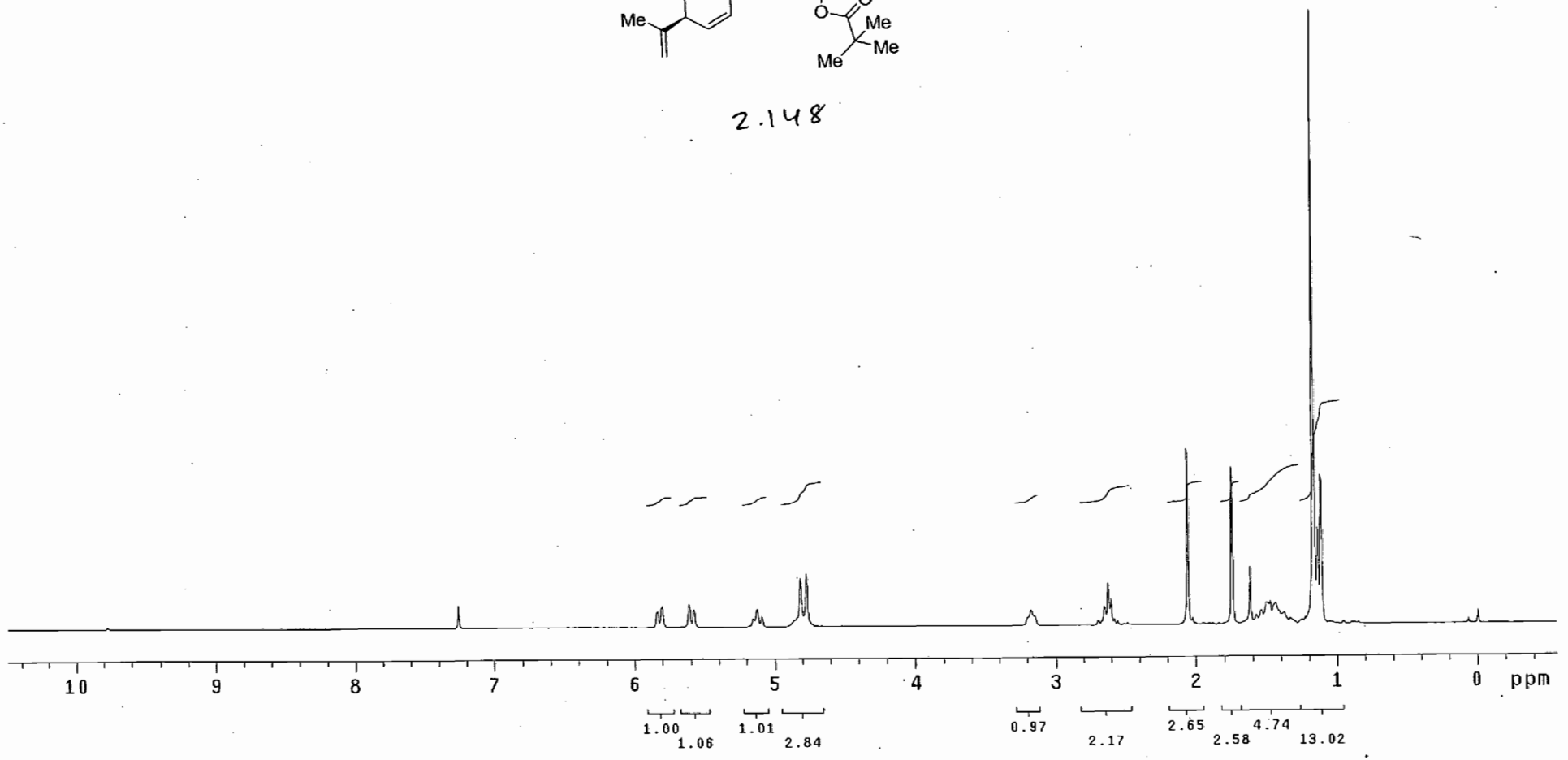

ACH-VIII-Pg15-cdcl3-CNMR

Pulse Sequence: s2pul
Solvent: CDCl3
Ambient temperature
Operator: vnmr_vb
File: thesis-5-cdcl3-CNMR
INOVA-500 "fao"

Relax. delay 1.000 sec
Pulse 105.4 degrees
Acq. time 1.815 sec
Width 27294.4 Hz
4480 repetitions
OBSERVE C13, 75.3761449 MHz
DECOUPLE H1, 299.7672516 MHz
Low power 5 dB atten.
continuously on
WALTZ-16 modulated
DATA PROCESSING
Line broadening 1.0 Hz
FT size 131072
Total time 78 hr, 26 min, 34 sec

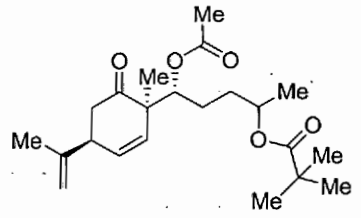

2.148

ACH-VIII-Pg16-cd3od-HNMR

Pulse Sequence: s2pul
Solvent: CD3OD
Ambient temperature
Operator: vnmr_vb
File: thesis-6-cd3od-HNMR
INOVA-500 "fao"

Pulse 58.9 degrees
Acq. time 3.744 sec
Width 4000.0 Hz
16 repetitions
OBSERVE H1, 299.7669175 MHz
DATA PROCESSING
FT size 32768
Total time 1 min, 7 sec

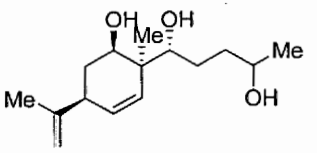

2.149

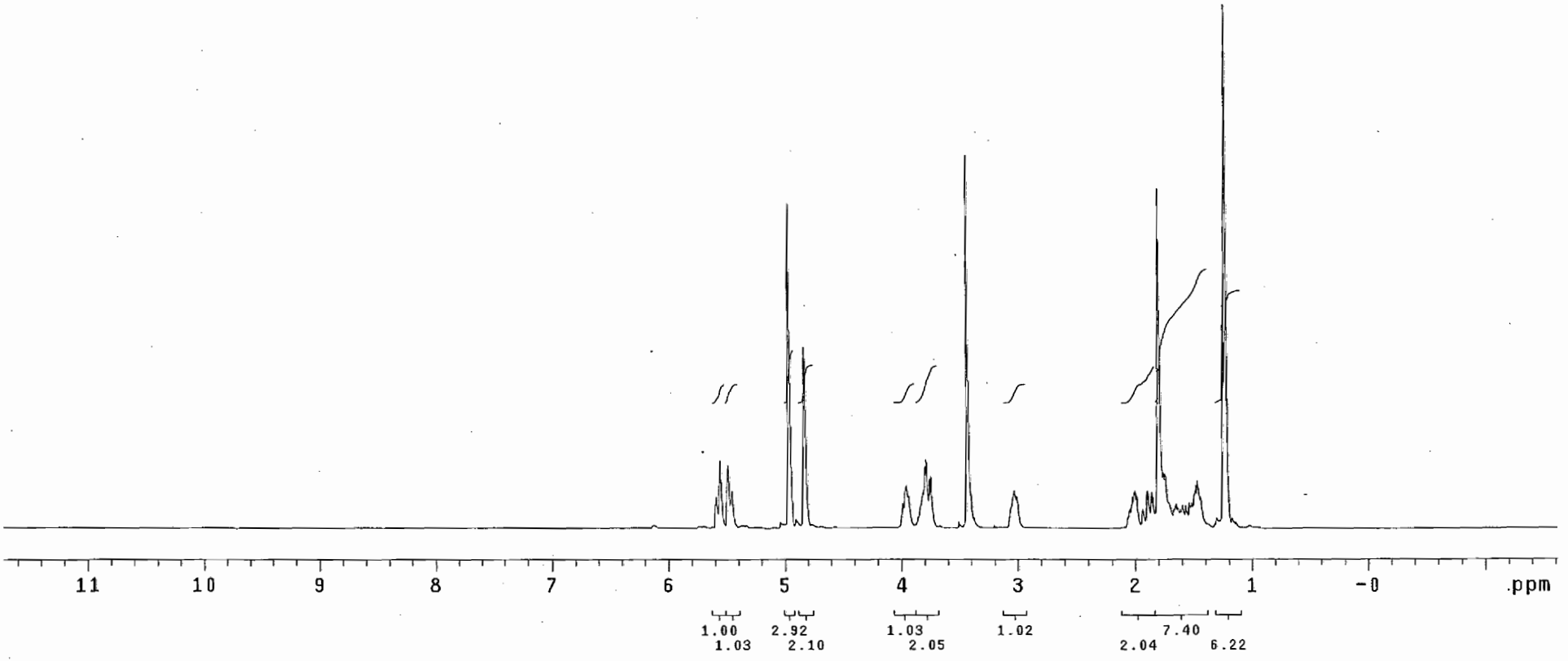

13C OBSERVE

Pulse Sequence: s2pul
Solvent: CD3OD
Ambient temperature
Operator: vnmr_vb
File: thesis-6-cd3od-CNMR
INOVA-500 "fao"

Pulse 105.4 degrees
Acq. time 1.815 sec
Width 16501.7 Hz
176 repetitions
OBSERVE C13, 75.3763437 MHz
DECOUPLE H1, 299.7684327 MHz
Low power 5 dB atten.
continuously on
WALTZ-16 modulated
DATA PROCESSING
Line broadening 1.0 Hz
FT size 65536
Total time 31 min, 7 sec

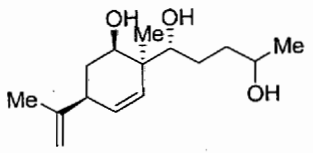

2.149

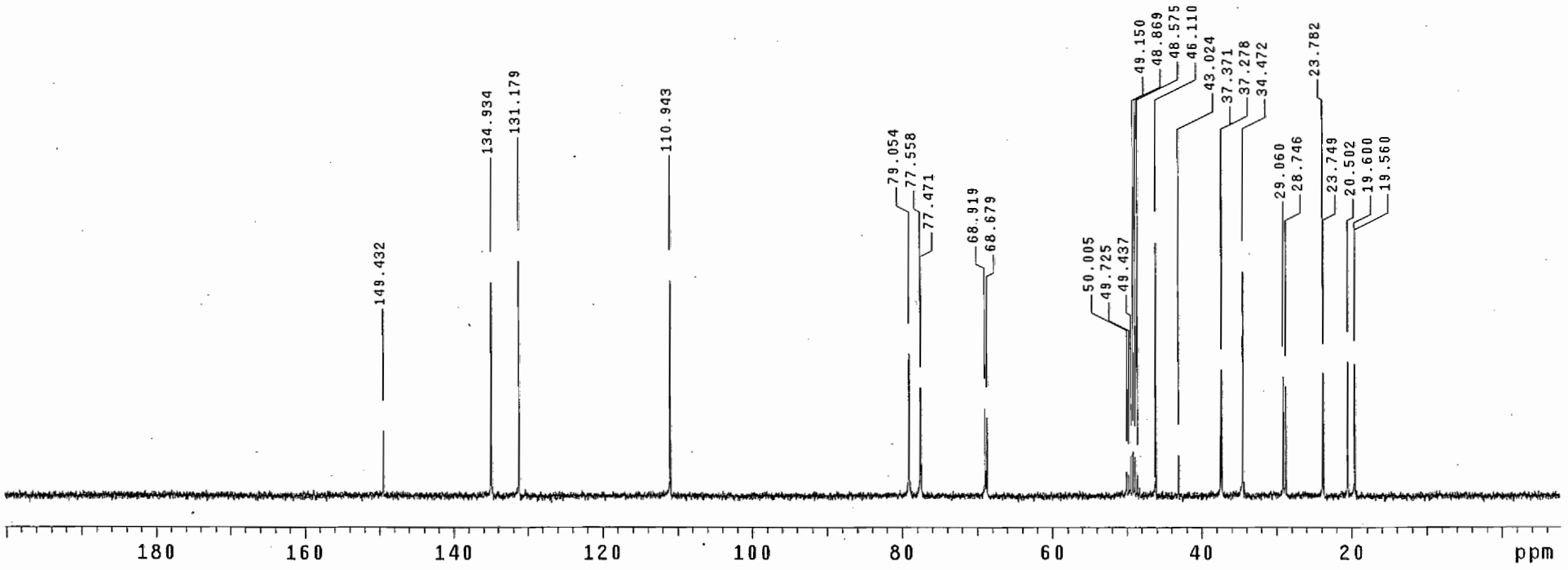

thesis-7-cd3od-HNMR

Pulse Sequence: s2pul

Solvent: Cd3OD
Ambient temperature
Operator: vnmr_vb
File: thesis-7-cd3od-HNMR
INOVA-500 . "fao"

Relax. delay 1.000 sec
Pulse 64.3 degrees
Acq. time 1.995 sec
Width 4506.5 Hz
16 repetitions
OBSERVE H1, 300.1187832 MHz
DATA PROCESSING
FT size 32768
Total time 0 min, 54 sec

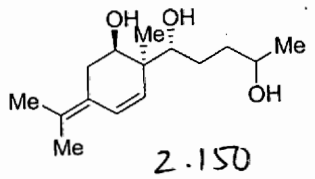

2.150

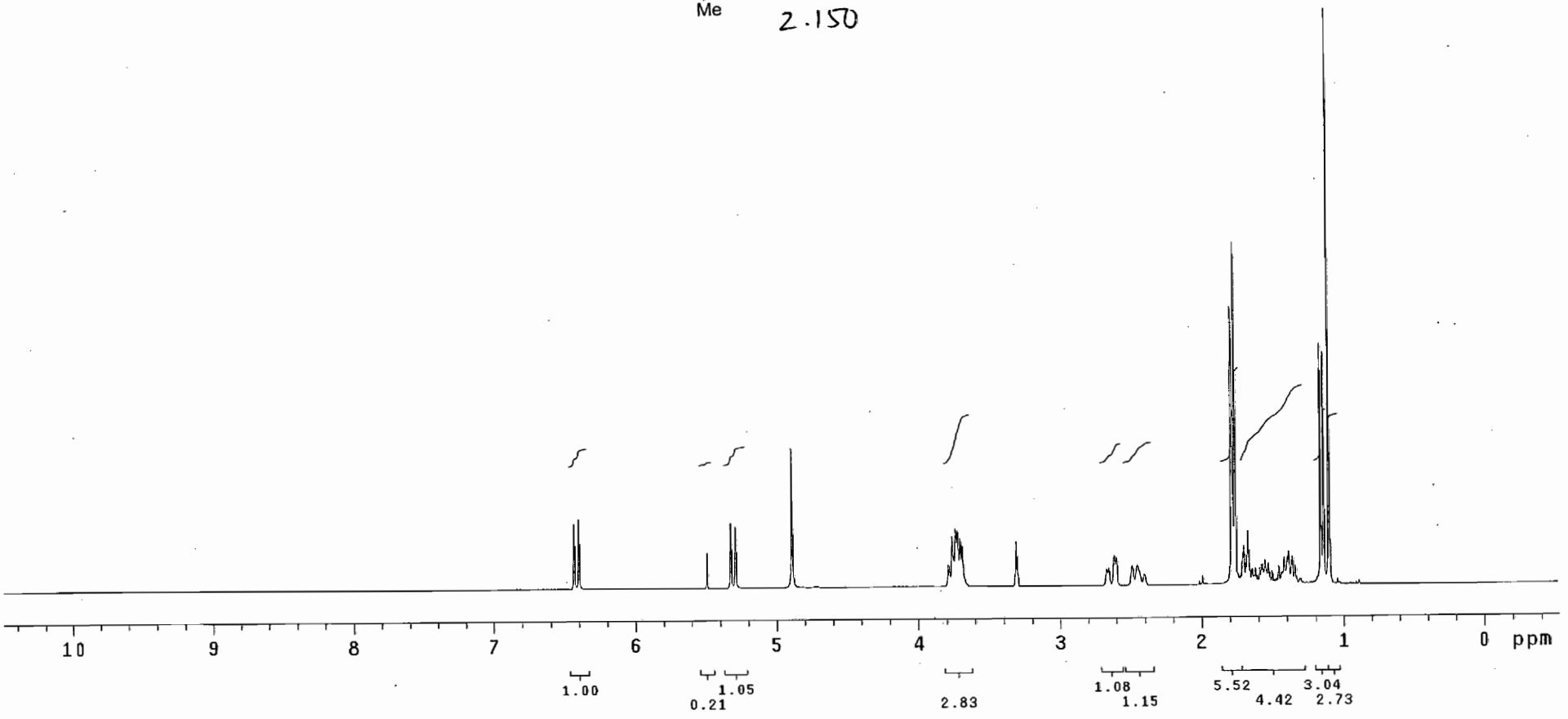

ACH-VIII-Pg17-cd3od-CNMR

Pulse Sequence: s2pul

Solvent: CD3OD
Ambient temperature
Operator: vnmr_vb
File: thesis-7-cd3od-CNMR
INOVA-500 "fao"

Pulse 105.4 degrees
Acq. time 1.815 sec
Width 16501.7 Hz
160 repetitions
OBSERVE C13, 75.3763463 MHz
DECOUPLE H1, 299.7684327 MHz
Low power 5 dB atten.
continuously on
WALTZ-16 modulated
DATA PROCESSING
Line broadening 1.0 Hz
FT size 65536
Total time 31 min, 7 sec

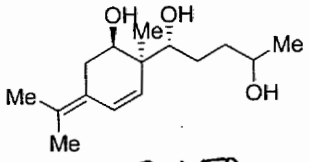

2.150

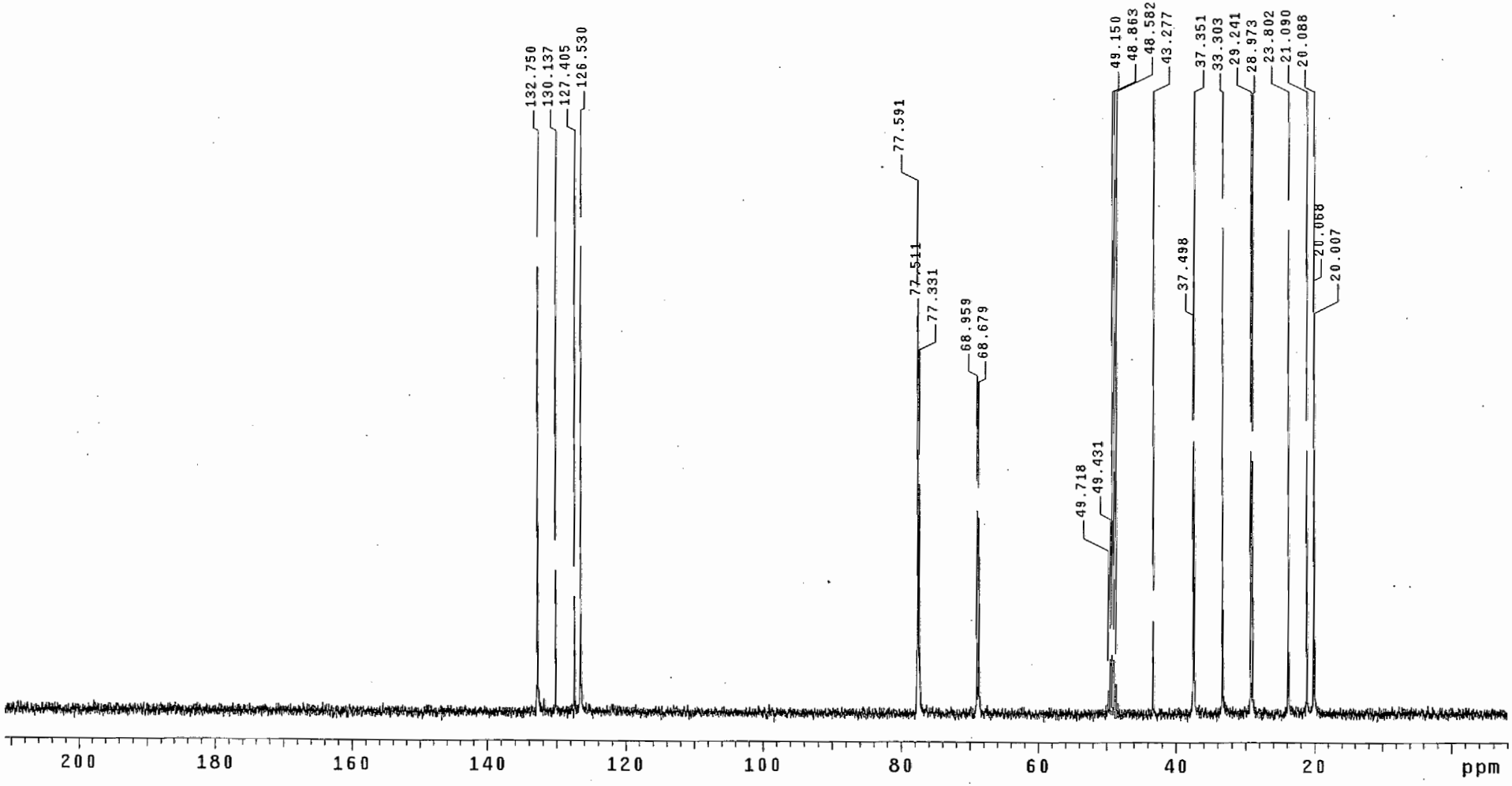

thesis-8-cdcl3-HNMR

Pulse Sequence: s2pul
Solvent: CDCl3
Ambient temperature
Operator: vnmr_vb
File: thesis-8-cdcl3-HNMR
INOVA-500 "fao"

Relax. delay 1.000 sec
Pulse 18.4 degrees
Acq. time 1.995 sec
Width 4506.5 Hz
16 repetitions
OBSERVE H1, 300.1176007 MHz
DATA PROCESSING
FT size 32768
Total time 0 min, 54 sec

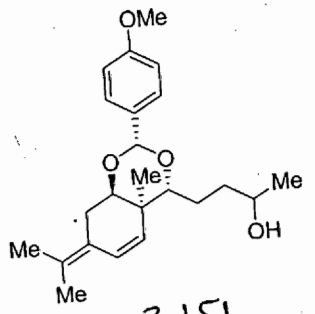

2.151

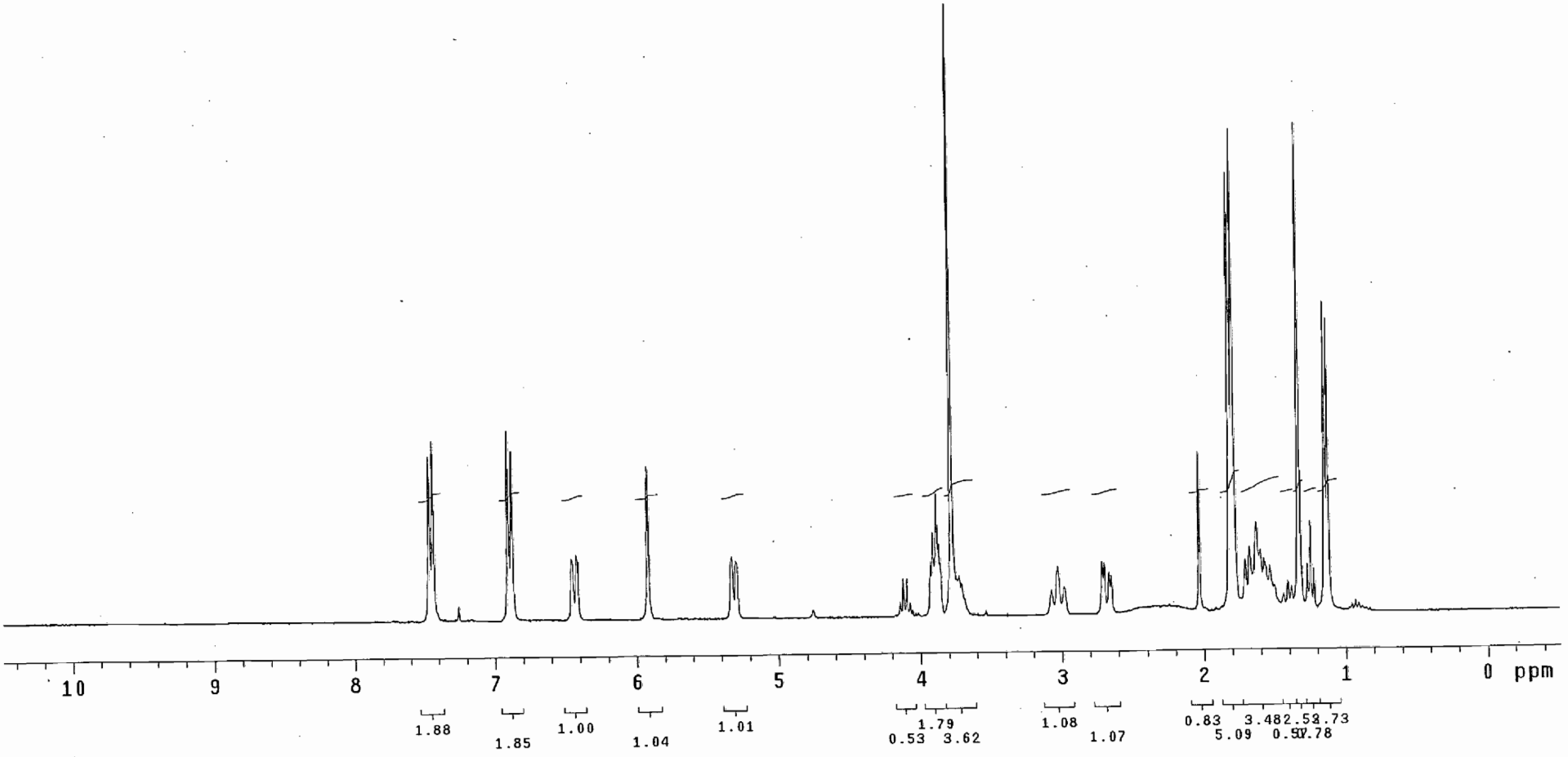

ACH-VI-Pg112-13CNMR-cdcl3-pure

Pulse Sequence: s2pul

Solvent: CDCl3
Ambient temperature
Operator: vnmr_vb
File: thesis-8-cd3od-CNMR
INOVA-500 "fao"

Relax. delay 1.000 sec
Pulse 43.3 degrees
Acq. time 1.815 sec
Width 18761.7 Hz
160 repetitions
OBSERVE C13, 75.4646236 MHz
DECOUPLE H1, 300.1190556 MHz
Low power 1023 dB atten.
continuously on
WALTZ-16 modulated
DATA PROCESSING
Line broadening 1.0 Hz
FT size 131072
Total time 48 min, 11 sec

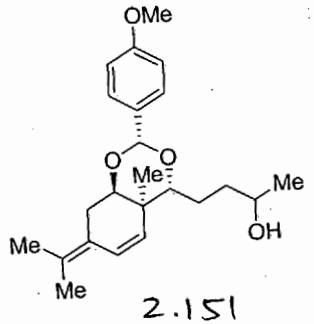

2.151

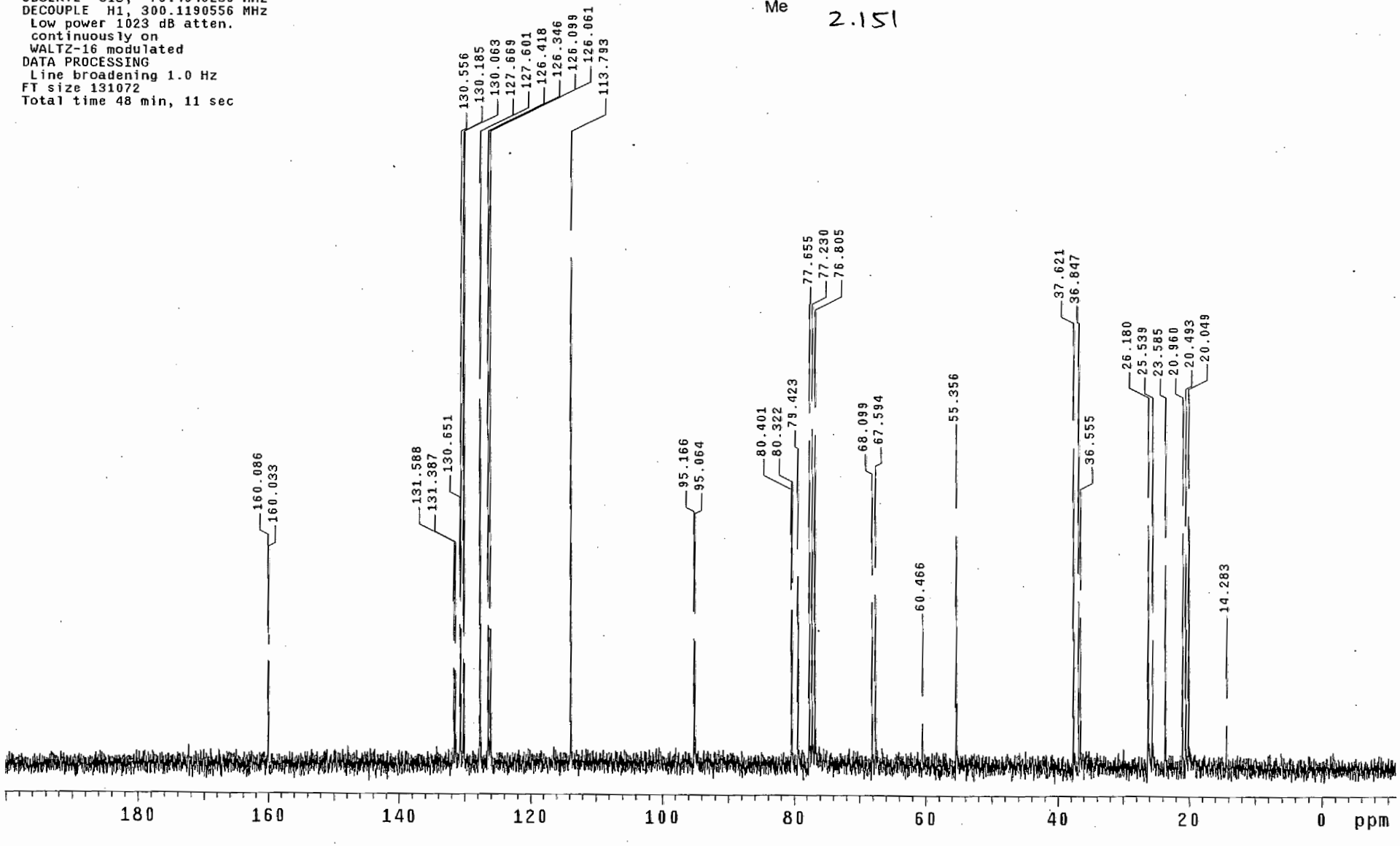

thesis-9-cdcl3-HNMR

Pulse Sequence: s2pul

Solvent: CDCl3
Temp. 25.0 C / 298.1 K
File: thesis-9-cdcl3-HNMR
INOVA-500 "fao"

Relax. delay 1.000 sec
Pulse 4.0 usec
Acq. time 1.685 sec
Width 4748.9 Hz
4 repetitions
OBSERVE H1, 499.8888064 MHz
DATA PROCESSING
FT size 16384
Total time 0 min, 16 sec

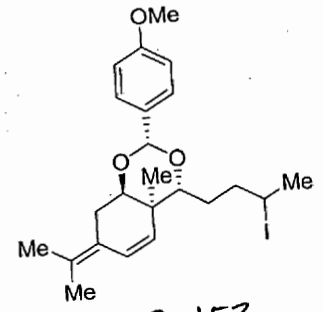

2.153

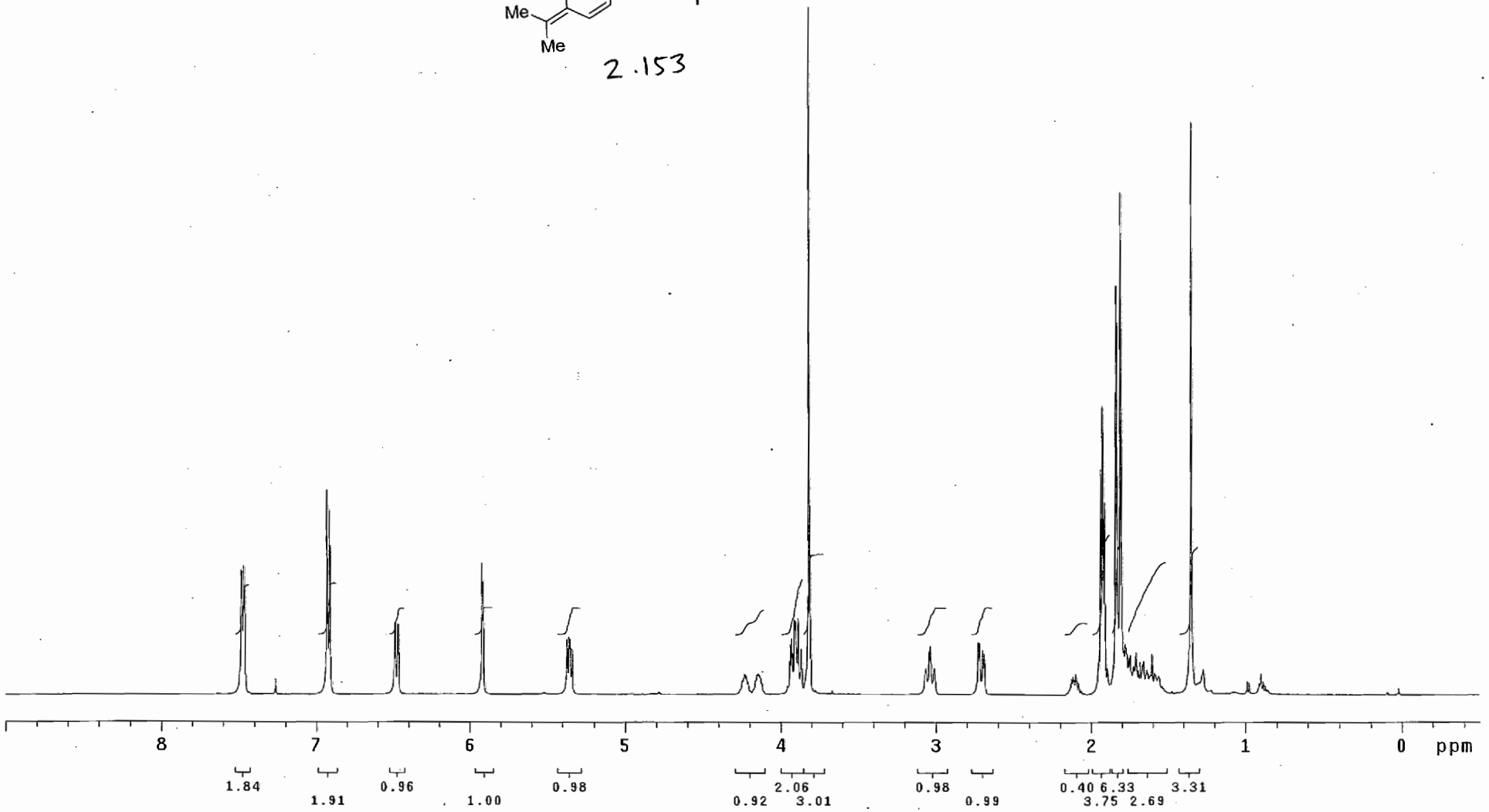

thesis-9-cdcl3-CNMR

Pulse Sequence: s2pul

Solvent: CDCl3
Temp. 25.0 C / 298.1 K
User: 1-14-87
File: thesis-9-cdcl3-CNMR
INOVA-500 "fao"

Relax. delay 0.800 sec
Pulse 51.9 degrees
Acq. time 0.593 sec
Width 26999.7 Hz
2000 repetitions
OBSERVE C13, 125.6971229 MHz
DECOUPLE H1, 499.8909306 MHz
Low power 10 dB atten.
continuously on
WALTZ-16 modulated
DATA PROCESSING
Line broadening 1.0 Hz
FT size 65536
Total time 38 hr, 55 min, 52 sec

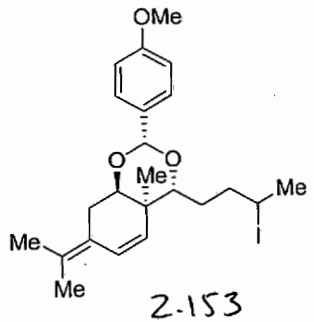

2-153

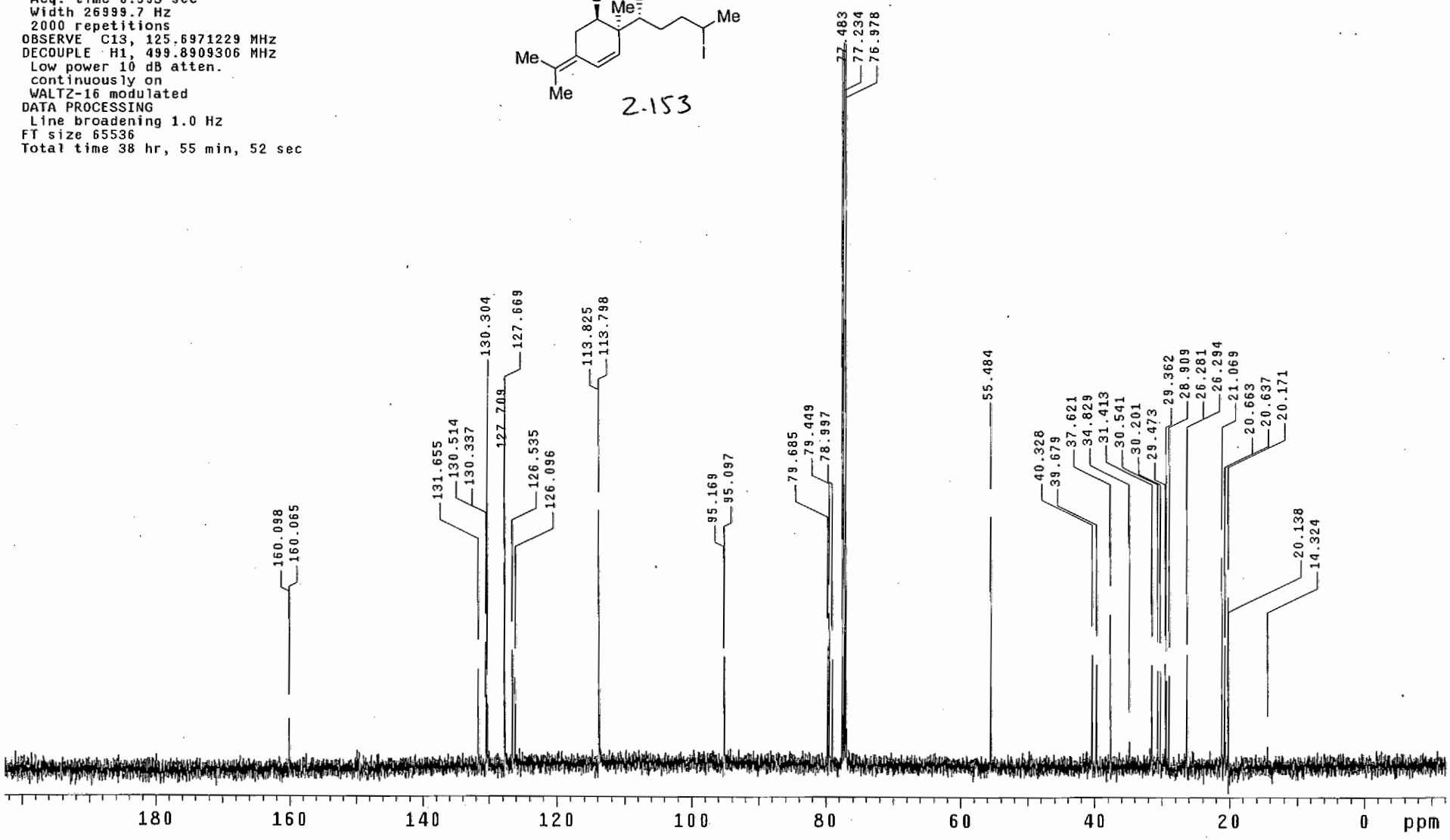

thesis-13-cdcl3-HNMR

Pulse Sequence: s2pul

Solvent: CDCl3
Ambient temperature
Operator: vnmr_vb
File: thesis-13-cdcl3-HNMR
INOVA-500 "fao"

Relax. delay 1.000 sec
Pulse 18.4 degrees
Acq. time 1.995 sec
Width 4506.5 Hz
16 repetitions
OBSERVE H1, 300.1176007 MHz
DATA PROCESSING
FT size 32768
Total time 0 min, 54 sec

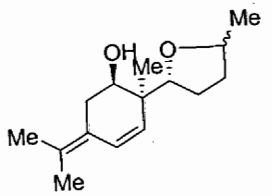

2.154

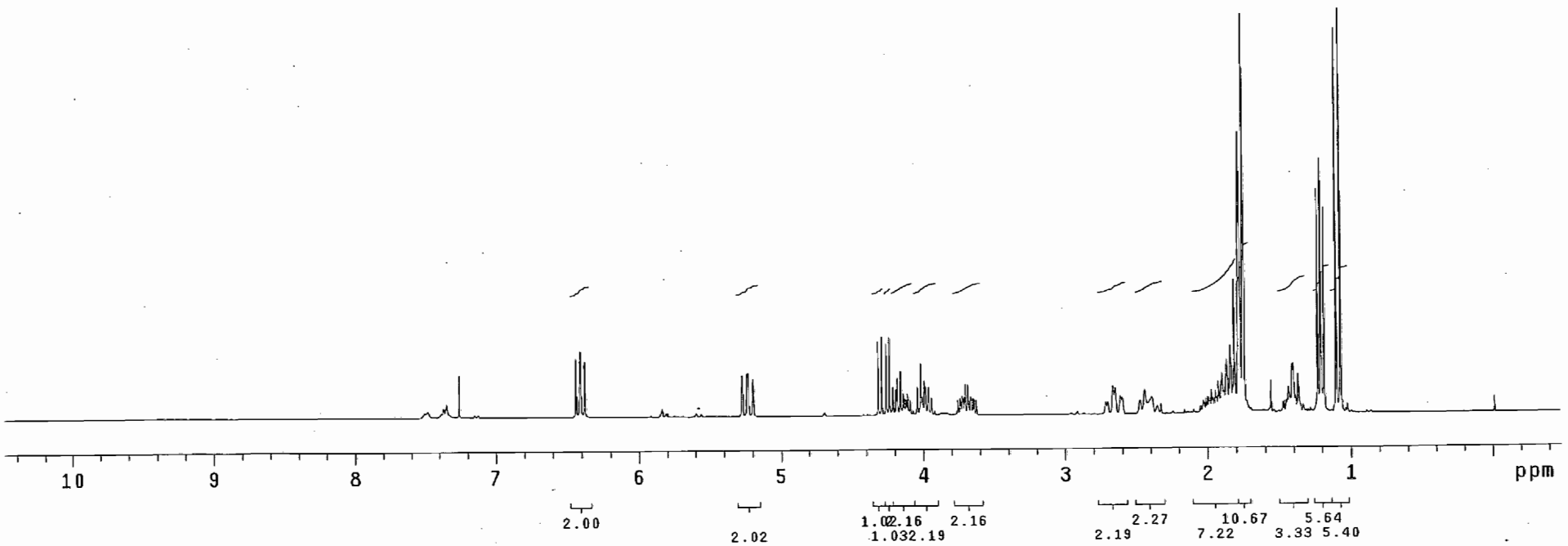

thesis-13-cdcl3-CNMR

Pulse Sequence: s2pul

Solvent: CDCl3
Ambient temperature
Operator: vnmr_vb
File: thesis-13-cdcl3-CNMR
INOVA-500 "fao"

Pulse 105.4 degrees
Acq. time 1.815 sec
Width 16501.7 Hz
1024 repetitions
OBSERVE C13, 75.3761405 MHz
DECOUPLE H1, 299.7672516 MHz
Low power 5 dB atten.
continuously on
WALTZ-16 modulated
DATA PROCESSING
Line broadening 1.0 Hz
FT size 65536
Total time 31 min, 7 sec

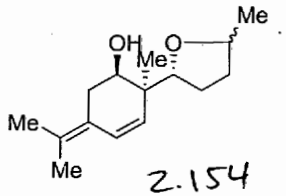

2.154

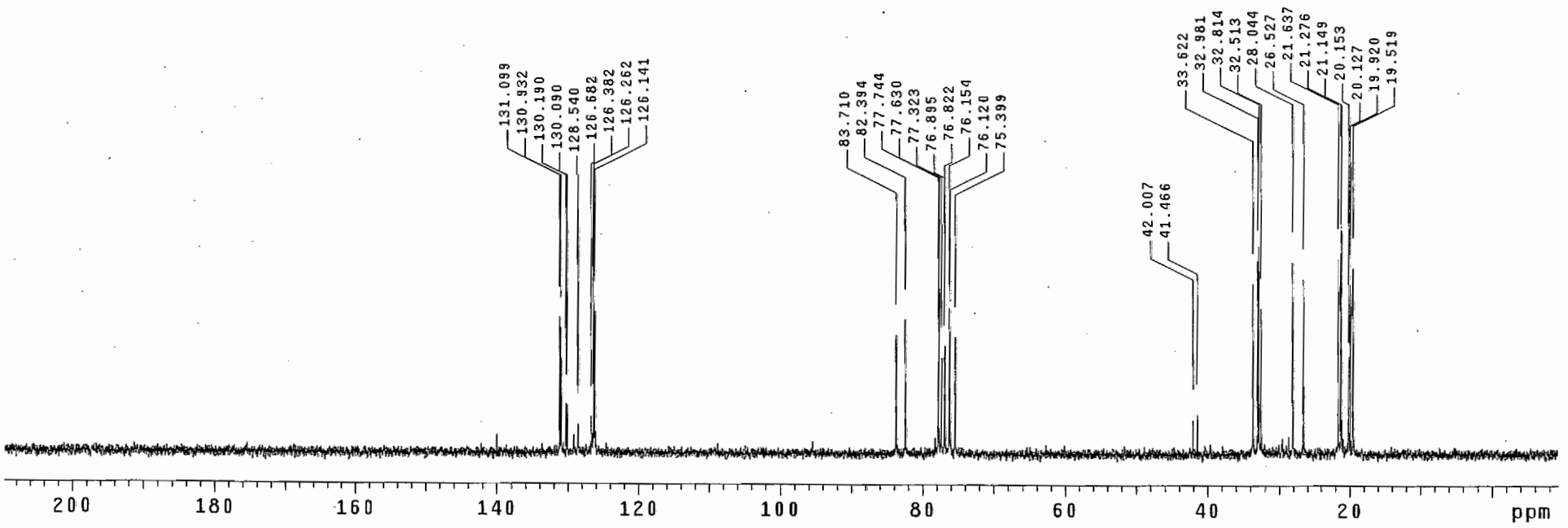

thesis-10-cdcl3-HNMR

Pulse Sequence: s2pul

Solvent: CDCl3
Ambient temperature
Operator: vnmr_vb
File: thesis-10-cdcl3-HNMR
INOVA-500 "fao"

Pulse 58.9 degrees
Acq. time 3.744 sec
Width 4000.0 Hz
16 repetitions
OBSERVE H1, 299.7657527 MHz
DATA PROCESSING
FT size 32768
Total time 1 min, 7 sec

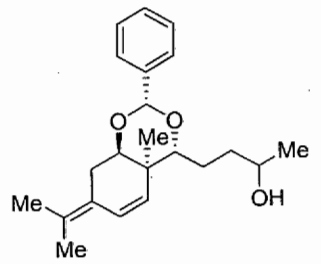

2.155

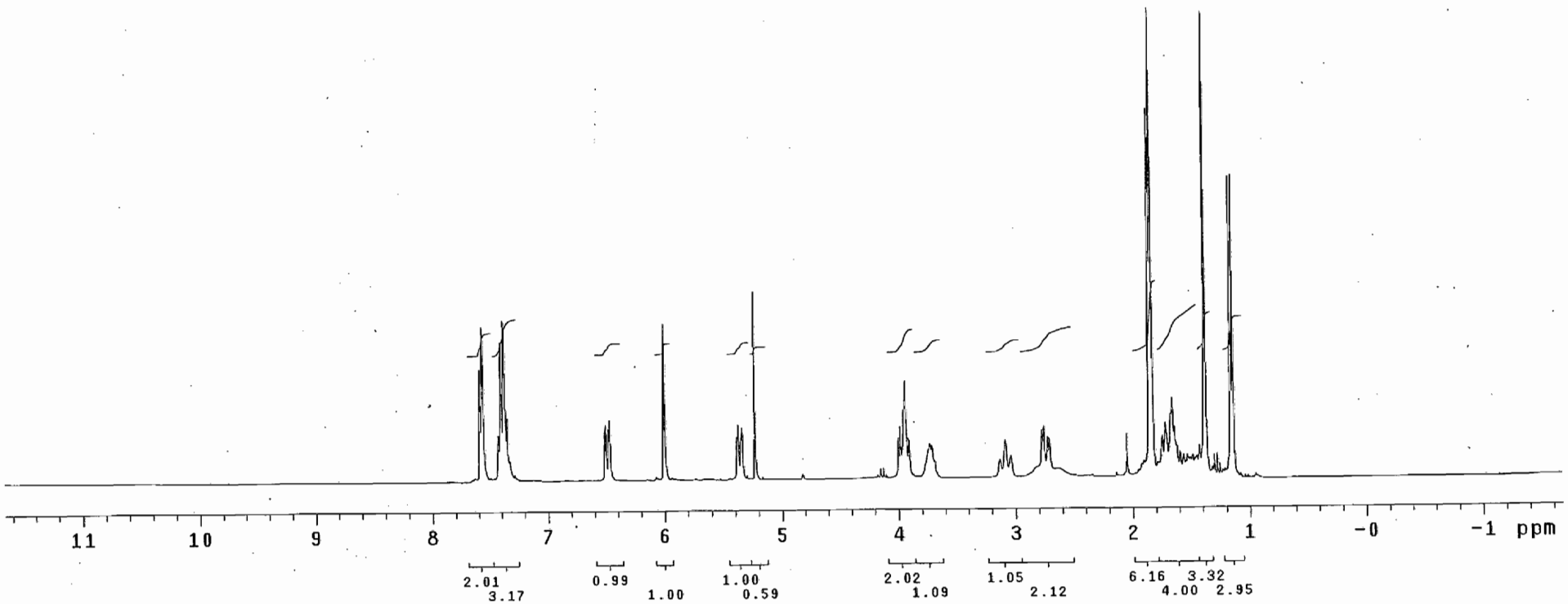

thesis-10-cdcl3-CNMR

Pulse Sequence: s2pul

Solvent: CDCl3
Ambient temperature
Operator: vnmr_vb
File: thesis-10-cdcl3-CNMR
INOVA-500 "fao"

Pulse 105.4 degrees
Acq. time 1.815 sec
Width 24235.1 Hz
240 repetitions
OBSERVE C13, 75.3761703 MHz
DECOUPLE H1, 299.7672516 MHz
Low power 5 dB atten.
continuously on
WALTZ-16 modulated
DATA PROCESSING
Line broadening 1.0 Hz
FT size 131072
Total time 31 min, 7 sec

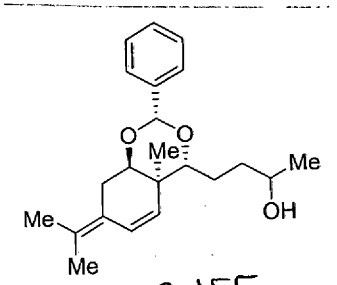

2.155

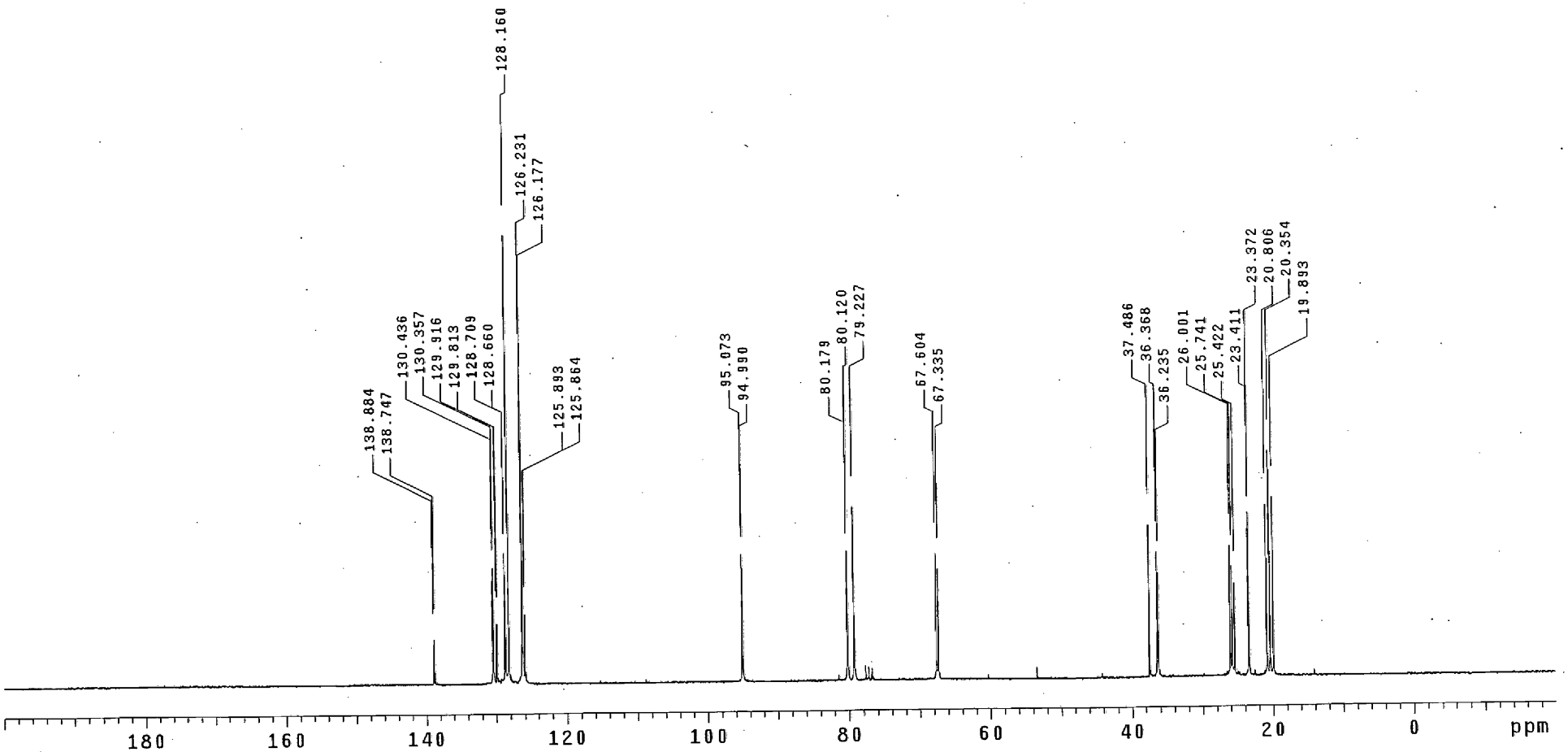

thesis-11-cdcl3-HNMR

Pulse Sequence: s2pul
Solvent: CDCl3
Ambient temperature
Operator: vnmr_vb
File: thesis-11-cdcl3-HNMR
INOVA-500 "fao"

Pulse 58.9 degrees
Acq. time 3.744 sec
Width 4000.0 Hz
16 repetitions
OBSERVE H1, 299.7657527 MHz
DATA PROCESSING
FT size 32768
Total time 1 min, 7 sec

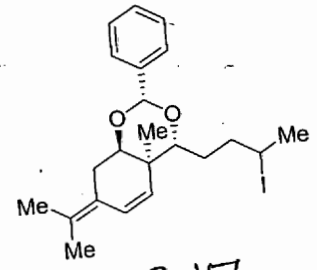

2.156

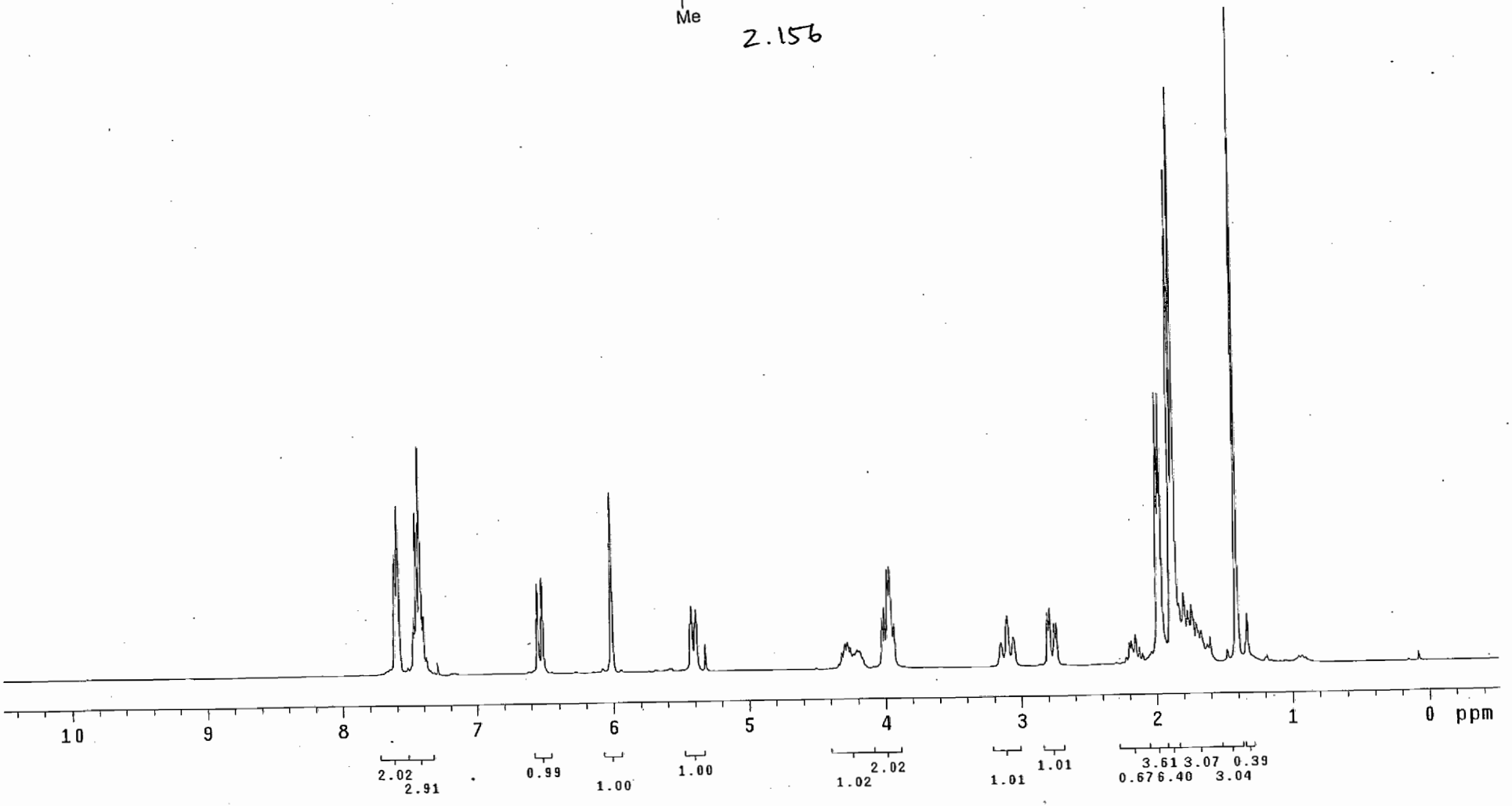

thesis-11-cdcl3-CNMR

Pulse Sequence: s2pul
Solvent: CDCl3
Ambient temperature
Operator: vnmr_vb
File: thesis-11-cdcl3-CNMR
INOVA-500 "fao"

Pulse 105.4 degrees
Acq. time 1.815 sec
Width 16501.7 Hz
320 repetitions
OBSERVE C13, 75.3761540 MHz
DECOUPLE H1, 299.7672516 MHz
Low power 5 dB atten.
continuously on
WALTZ-16 modulated
DATA PROCESSING
Line broadening 1.0 Hz
FT size 65536
Total time 31 min, 7 sec

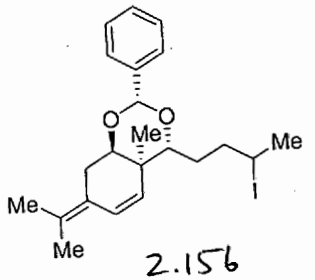

2.156

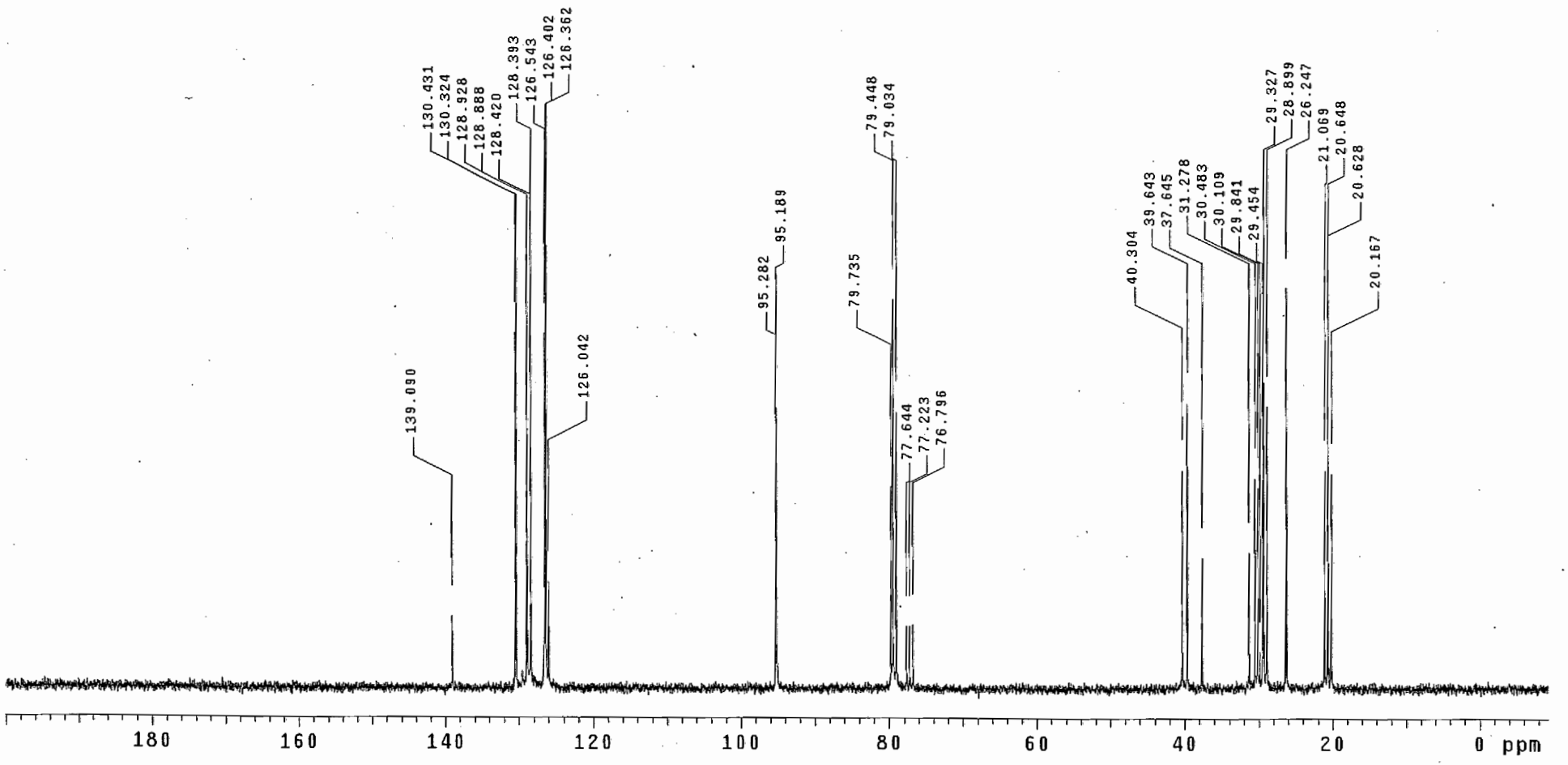

thesis-15-cd3od-HNMR

Pulse Sequence: s2pul

Solvent: CD3OD
Ambient temperature
Operator: vnmr_vb
File: thesis-15-cd3od-HNMR
INOVA-500 "fao"

Relax. delay 1.000 sec
Pulse 18.4 degrees
Acq. time 1.995 sec
Width 4506.5 Hz
16 repetitions
OBSERVE H1, 300.1188186 MHz
DATA PROCESSING
FT size 32768
Total time 0 min, 54 sec

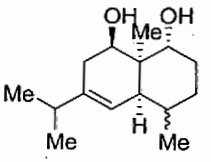

2.166 a/b

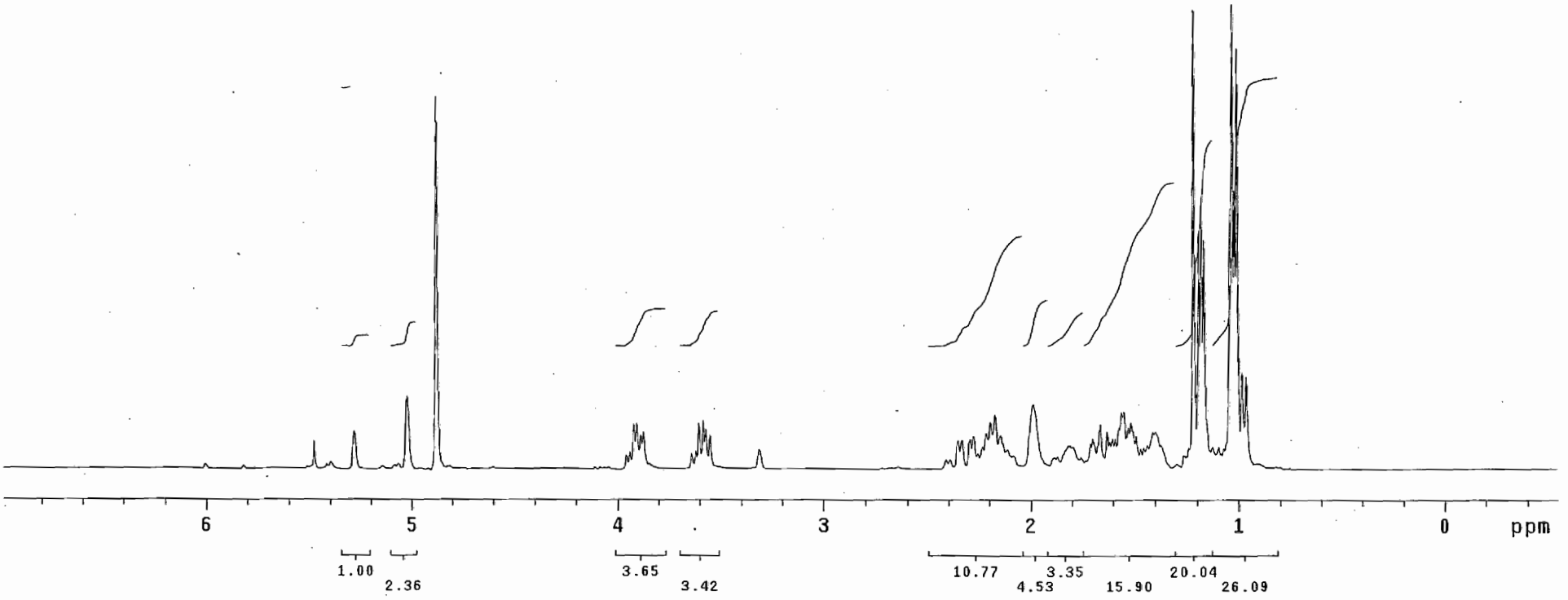

thesis-15-cdcl3-CNMR

Pulse Sequence: s2pul

Solvent: CDCl3
Ambient temperature
Operator: vnmr_vb
File: thesis-15-cdcl3-CNMR
INOVA-500 "fao"

Pulse 105.4 degrees
Acq. time 1.815 sec
Width 16501.7 Hz
400 repetitions
OBSERVE C13, 75.3761621 MHz
DECOUPLE H1, 299.7672516 MHz
Low power 5 dB atten.
continuously on
WALTZ-16 modulated
DATA PROCESSING
Line broadening 1.0 Hz
FT size 65536
Total time 50 hr, 39 min, 53 sec

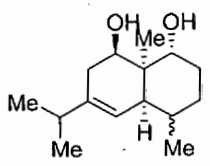

2.166 a/b

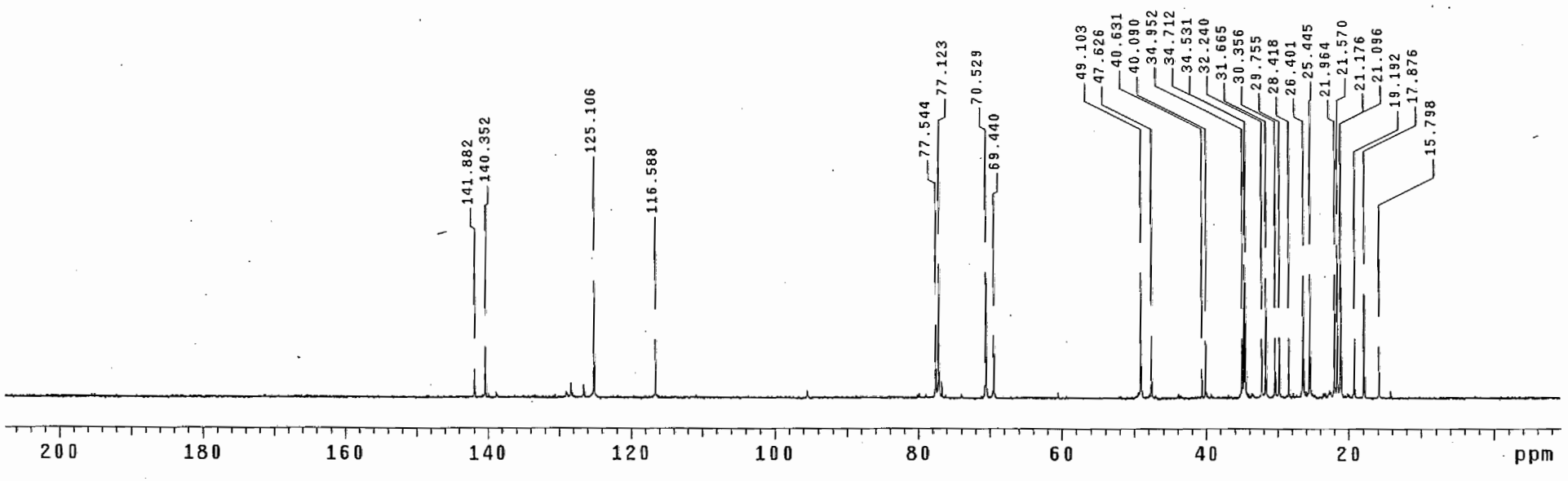

thesis-17-cdcl3-HNMR

Pulse Sequence: s2pul

Solvent: CDCl3
Ambient temperature
Operator: vnmr_vb
File: thesis-17-cdcl3-HNMR
INOVA-500 "fao"

Relax. delay 1.000 sec
Pulse 18.4 degrees
Acq. time 1.995 sec
Width 4506.5 Hz
16 repetitions
OBSERVE H1, 300.1176007 MHz
DATA PROCESSING
FT size 32768
Total time 0 min, 54 sec

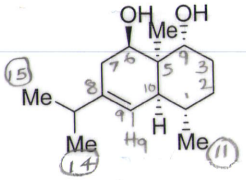

2·166a

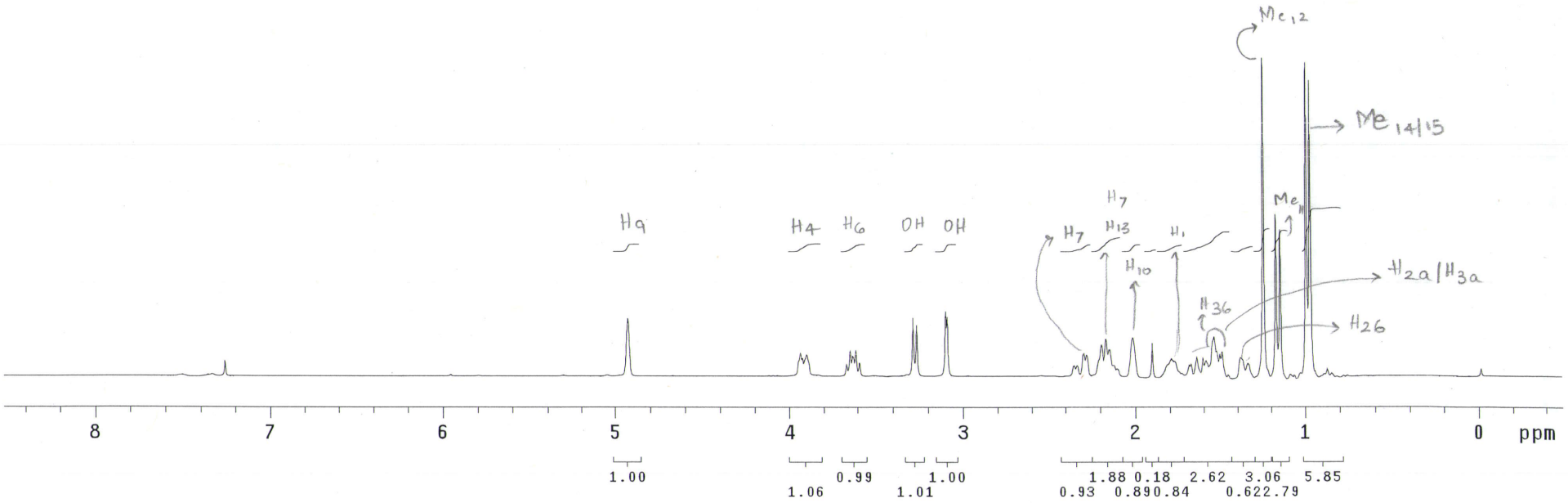

thesis-17-cdcl3-CNMR

Pulse Sequence: s2pul
 Solvent: CDCl3
 Ambient temperature
Operator: vnmr_vb
File: thesis-17-cdcl3-CNMR
INOVA-500 "fao"

 Pulse 105.4 degrees
 Acq. time 1.815 sec
 Width 16501.7 Hz
 208 repetitions
OBSERVE C13, 75.3761530 MHz
DECOUPLE H1, 299.7672516 MHz
 Low power 5 dB atten.
 continuously on
 WALTZ-16 modulated
DATA PROCESSING
 Line broadening 1.0 Hz
FT size 65536
Total time 50 hr, 39 min, 53 sec

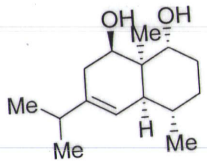

2-166a

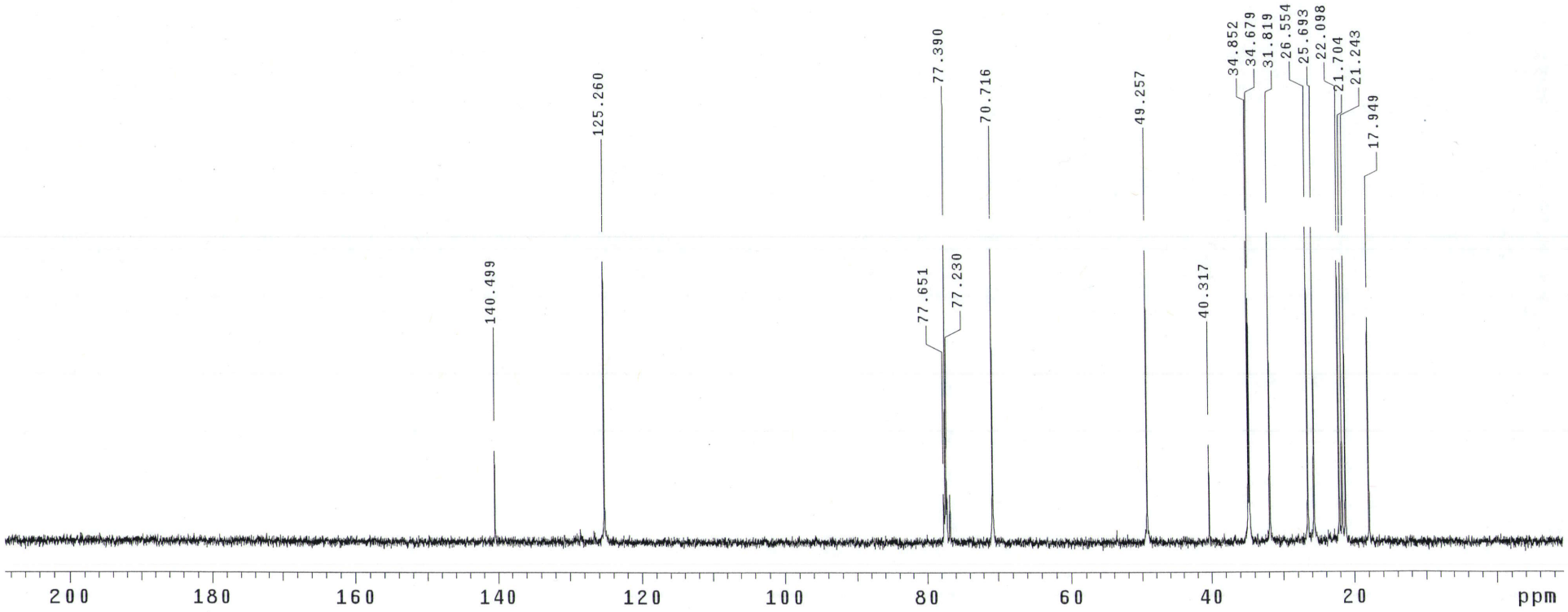

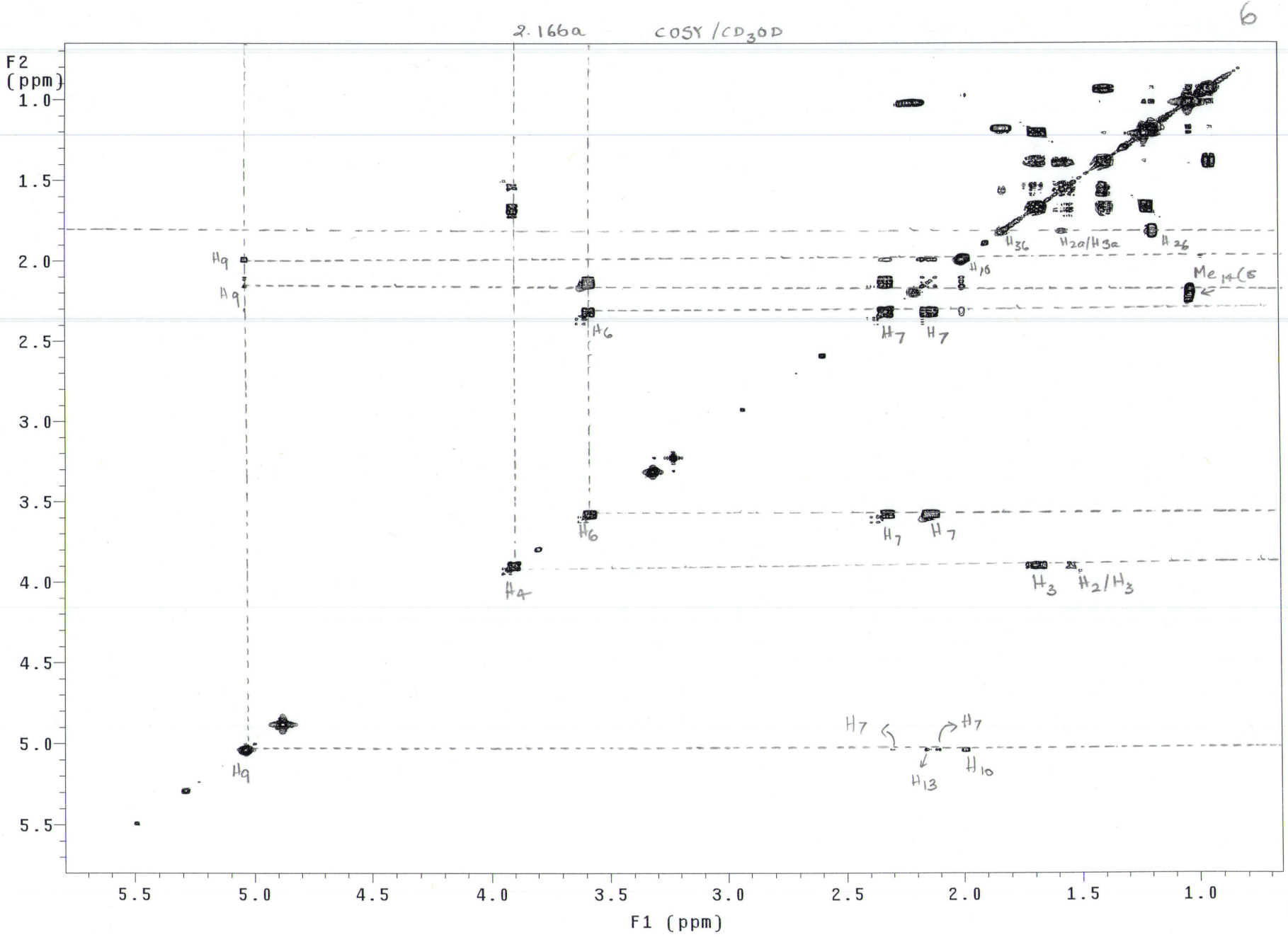
2.166a
COSY / CD3OD
6
F2 (ppm)
F1 (ppm)
1.0
1.5
2.0
2.5
3.0
3.5
4.0
4.5
5.0
5.5
H9
H9
H6
H6
H4
H7
H7
H7
H7
H3
H2/H3
H9
H7
H7
H13
H10
H36
H2a/H3a
H26
H16
Me 14(15)

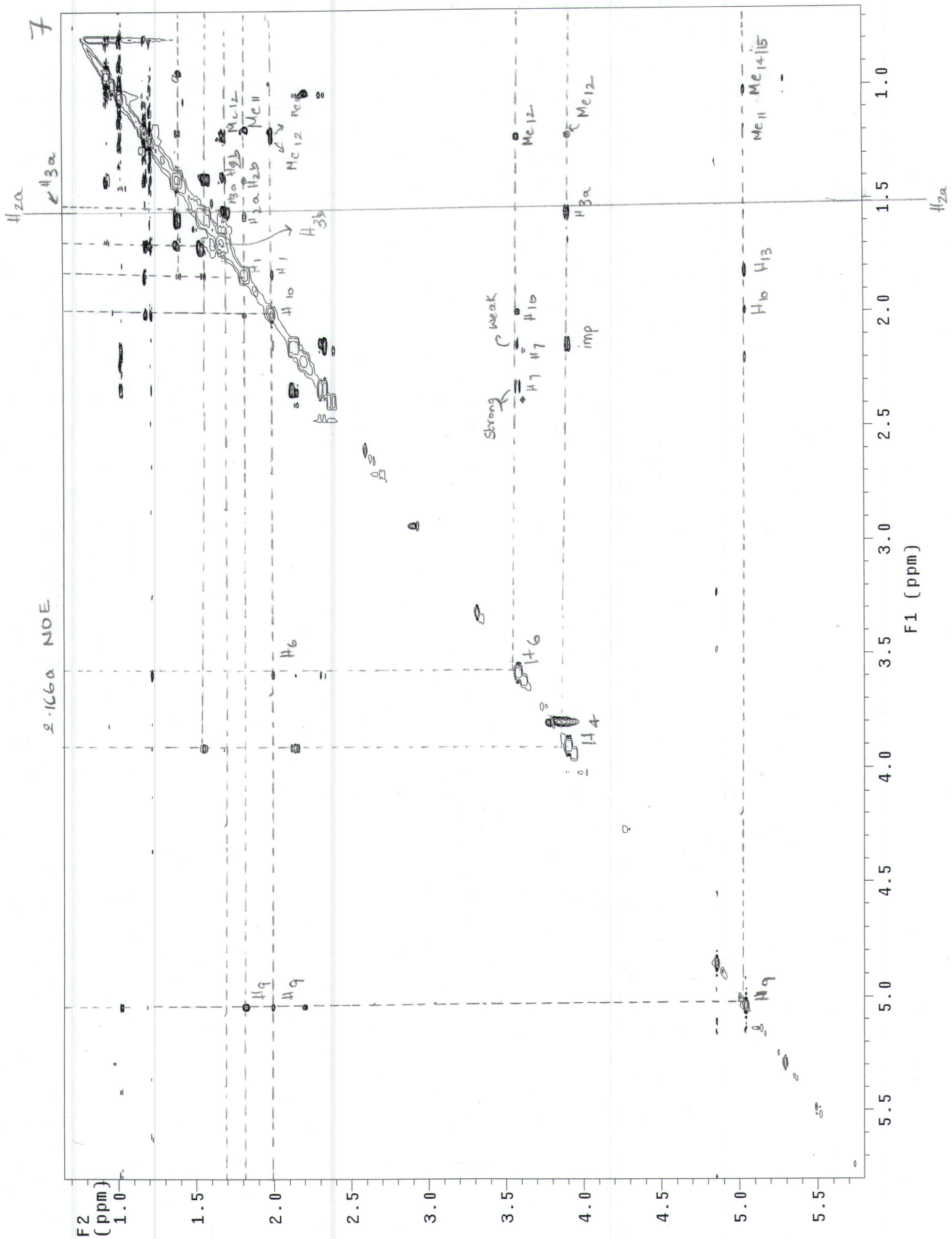
F2 (ppm)
F1 (ppm)
NOE
2.166a
H2a
H3a
H3b
H6
H9
H10
H7
H4
H13
Me12
Me11
Me14&15
Strong
weak
imp

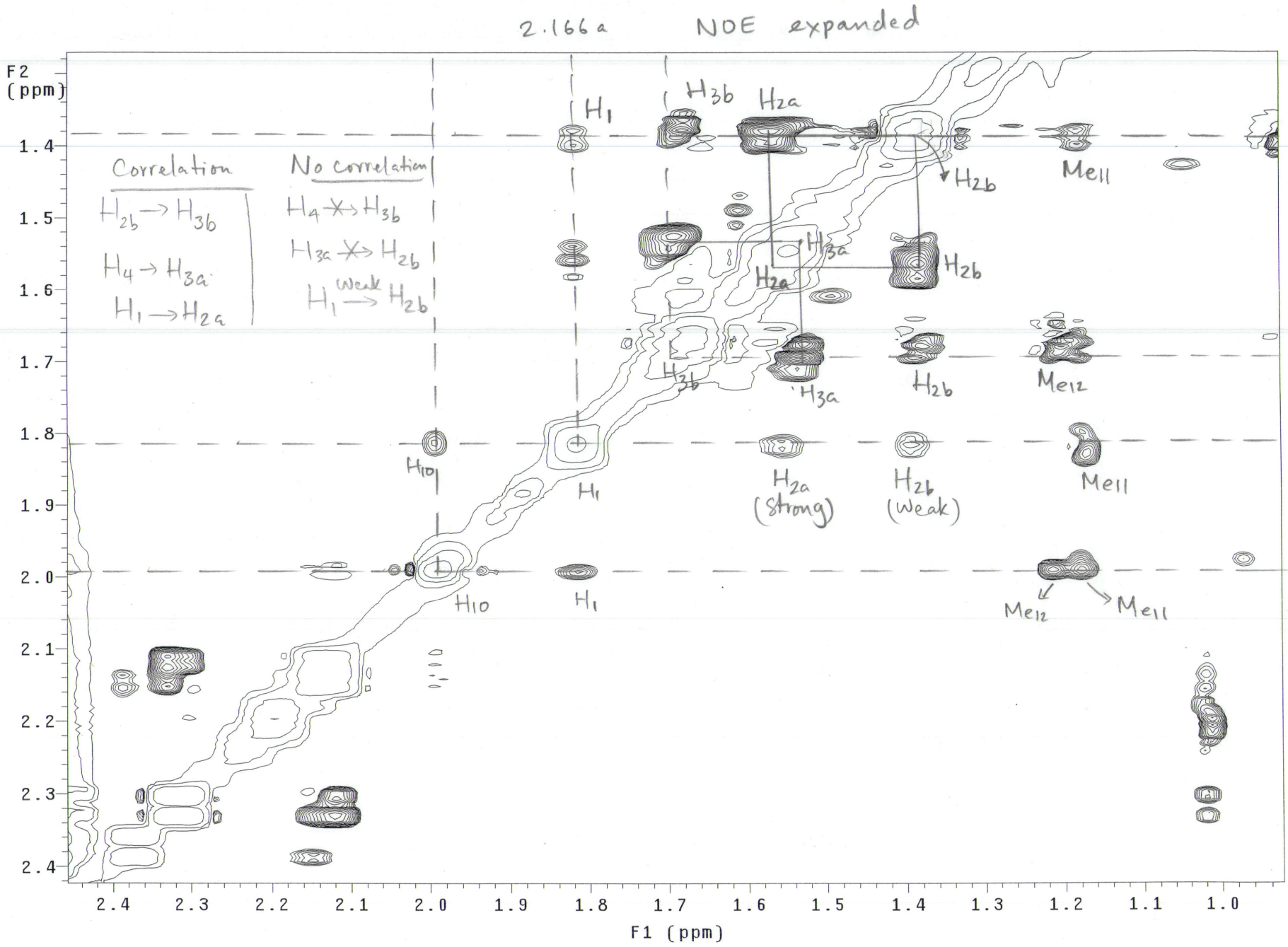
2.166a NOE expanded
F2 (ppm)
F1 (ppm)
Correlation
$H_{2b} \rightarrow H_{3b}$
$H_4 \rightarrow H_{3a}$
$H_1 \rightarrow H_{2a}$
No correlation
$H_4 \not\rightarrow H_{3b}$
$H_{3a} \not\rightarrow H_{2b}$
$H_1 \xrightarrow{weak} H_{2b}$
H_1
H_{3b}
H_{2a}
H_{2b}
Me11
H_{3a}
Me12
H_{10}
H_{2a} (strong)
H_{2b} (weak)

thesis-16-HNMR-cdcl3

Pulse Sequence: s2pul

Solvent: CDCl3
Ambient temperature
Mercury-300 "tigger"

PULSE SEQUENCE
Relax. delay 1.000 sec
Pulse 64.3 degrees
Acq. time 1.995 sec
Width 4506.5 Hz
16 repetitions
OBSERVE H1, 300.1176007 MHz
DATA PROCESSING
FT size 32768
Total time 0 min, 58 sec

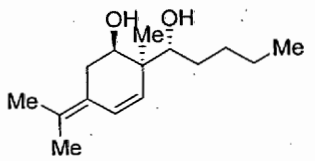

2.167

thesis-16-cdcl3-CNMR

Pulse Sequence: s2pul

Solvent: cdcl3
Temp. 25.0 C / 298.1 K
Operator: vnmr_jk
File: thesis-16-cdcl3-CNMR
INOVA-500 "fao"

Relax. delay 1.000 sec
Pulse 108.2 degrees
Acq. time 0.941 sec
Width 34013.6 Hz
23488 repetitions
OBSERVE C13, 150.8055139 MHz
DECOUPLE H1, 599.7459956 MHz
Low power 10 dB atten.
continuously on
WALTZ-16 modulated
DATA PROCESSING
Line broadening 1.0 Hz
FT size 131072
Total time 54 hr, 9 min, 33 sec

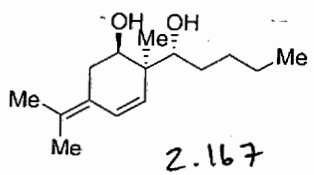

2.167

thesis-19-cdcl3-HNMR

Pulse Sequence: s2pul

Solvent: CDCl3
Ambient temperature
Operator: vnmr_vb
File: thesis-19-cdcl3-HNMR
INOVA-500 "fao"

Pulse 58.9 degrees
Acq. time 3.744 sec
Width 4000.0 Hz
16 repetitions
OBSERVE H1, 299.7657527 MHz
DATA PROCESSING
FT size 32768
Total time 1 min, 7 sec

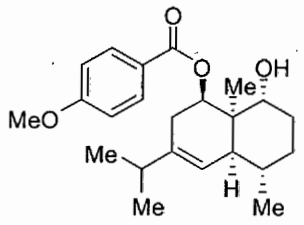

2.171

thesis-19-cdcl3-CNMR

Pulse Sequence: s2pul

Solvent: CDCl3
Ambient temperature
Operator: vnmr_vb
File: thesis-19-cdcl3-CNMR
INOVA-500 "fao"

Pulse 105.4 degrees
Acq. time 1.815 sec
Width 16501.7 Hz
320 repetitions
OBSERVE C13, 75.3761505 MHz
DECOUPLE H1, 299.7672516 MHz
Low power 5 dB atten.
continuously on
WALTZ-16 modulated
DATA PROCESSING
Line broadening 1.0 Hz
FT size 65536
Total time 31 min, 7 sec

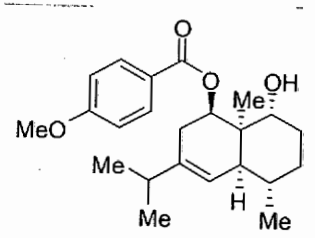

2.171

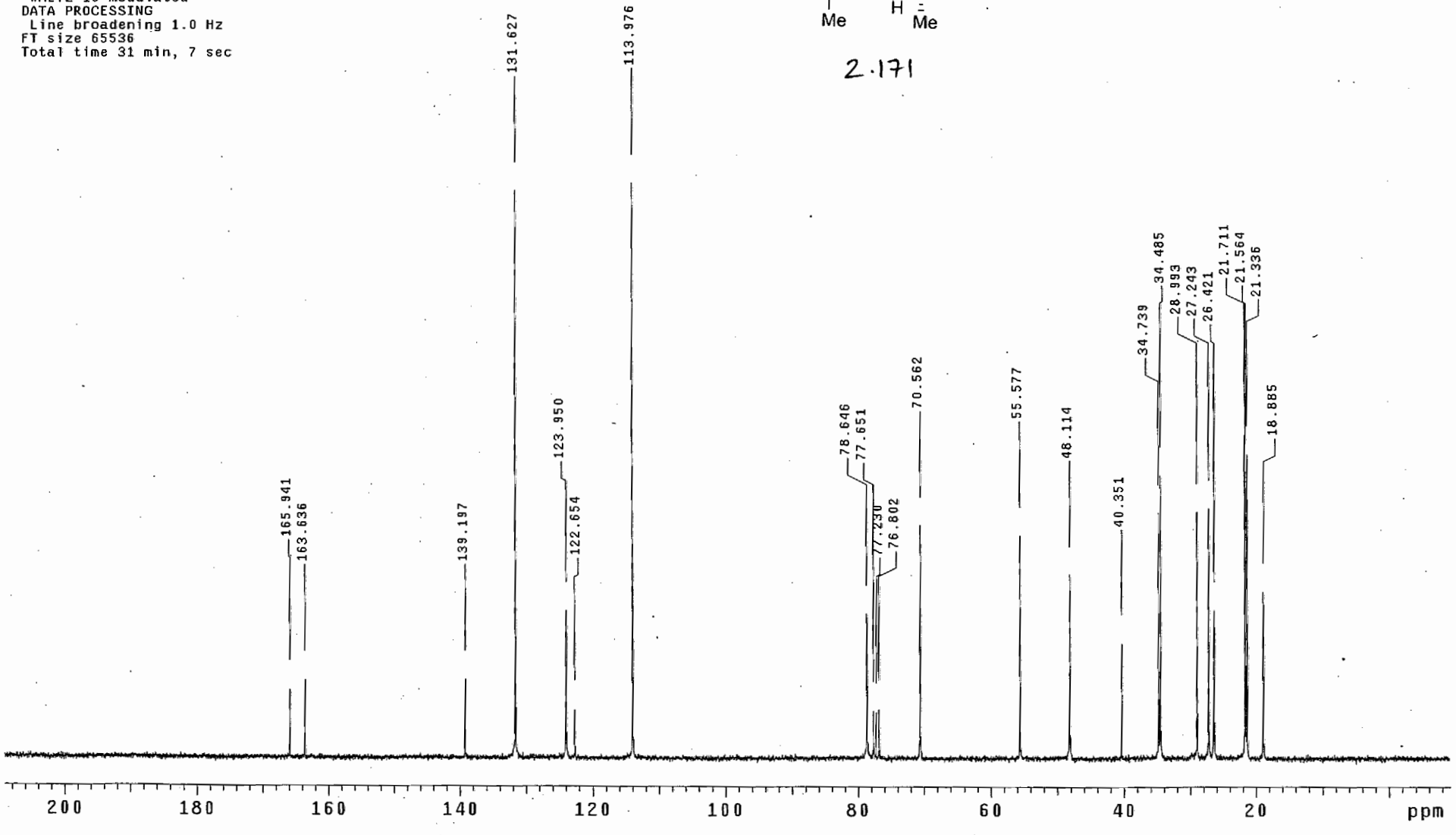

thesis-18-cdcl3-HNMR

Pulse Sequence: s2pul

Solvent: CDCl3
Ambient temperature
Operator: vnmr_vb
File: thesis-18-cdcl3-HNMR
INOVA-500 "fao"

Relax. delay 1.000 sec
Pulse 64.3 degrees
Acq. time 1.995 sec
Width 4506.5 Hz
16 repetitions
OBSERVE H1, 300.1176007 MHz
DATA PROCESSING
FT size 32768
Total time 0 min, 54 sec

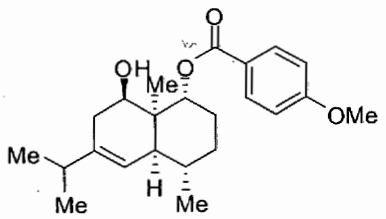

2.172

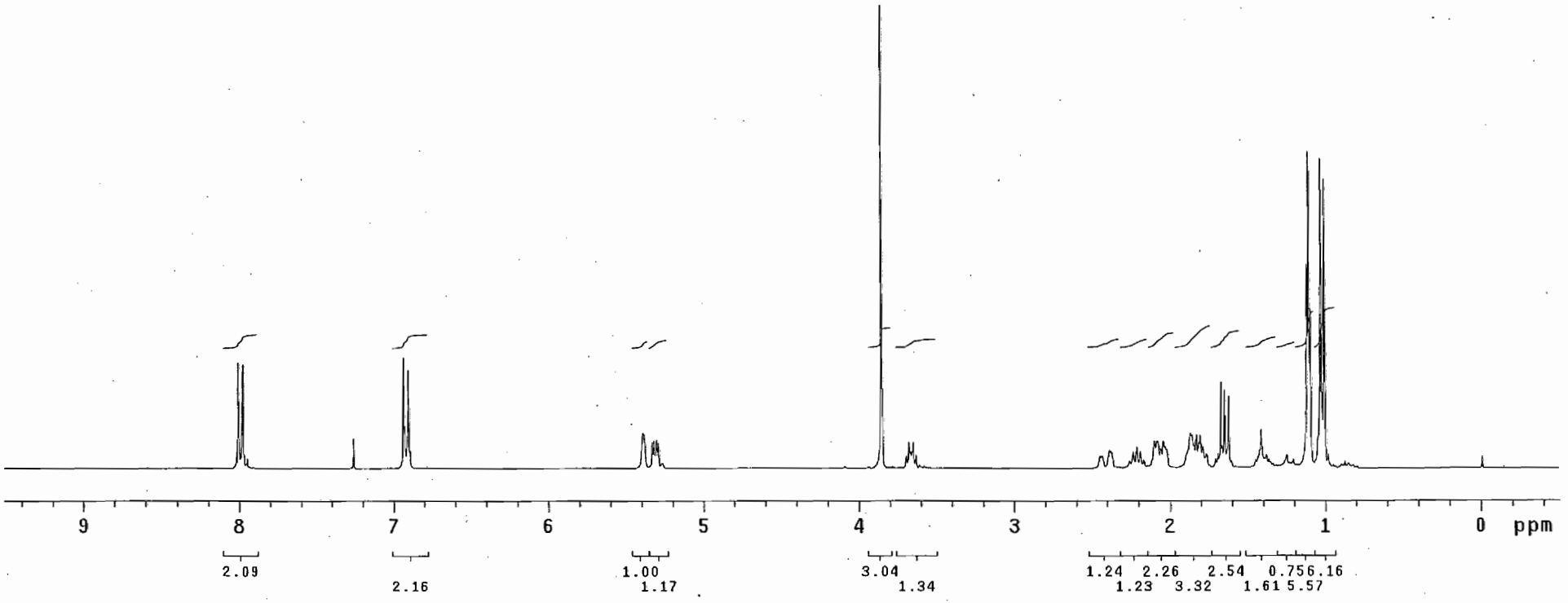

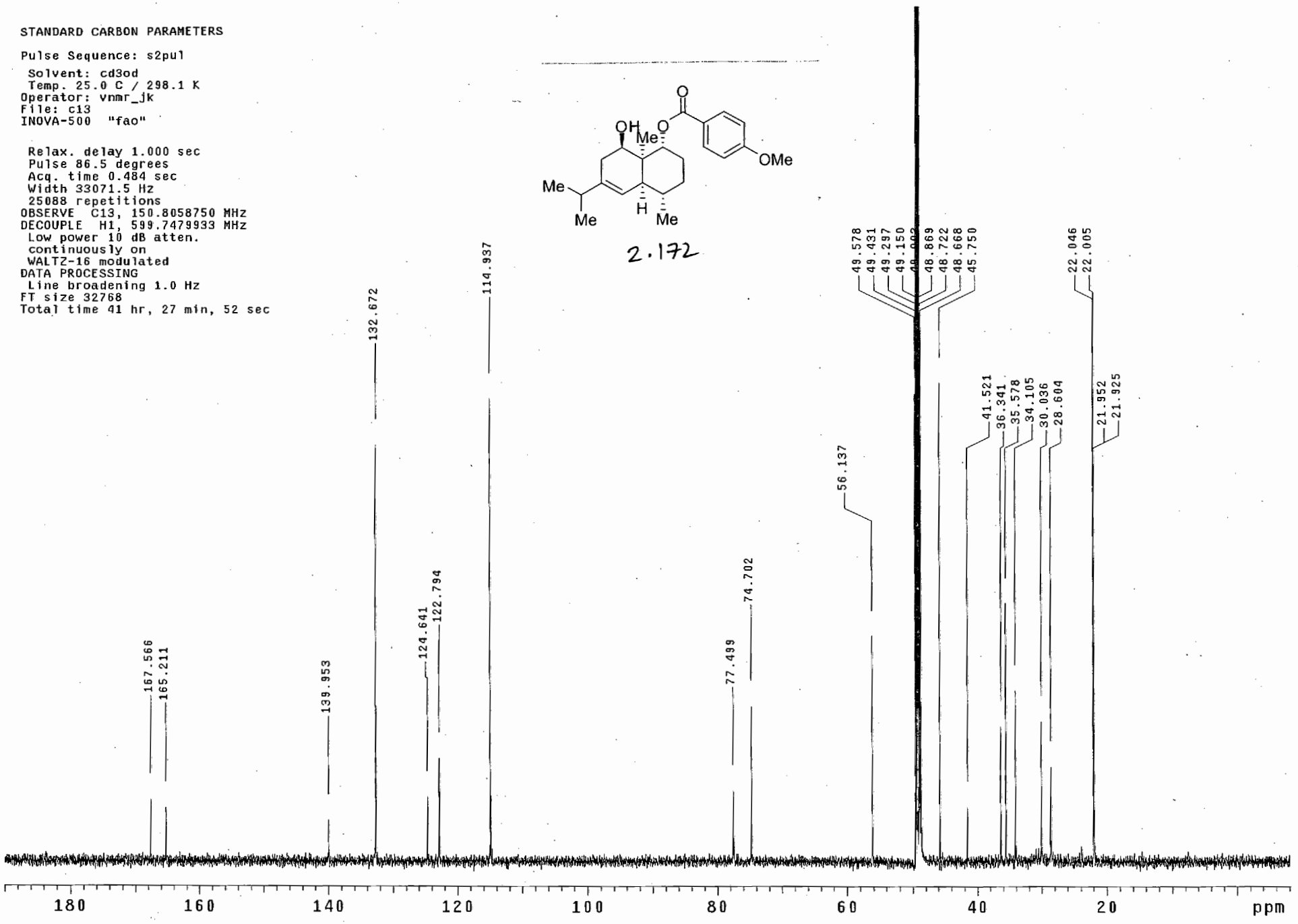
STANDARD CARBON PARAMETERS
Pulse Sequence: s2pul
Solvent: cd3od
Temp. 25.0 C / 298.1 K
Operator: vnmr_jk
File: c13
INOVA-500 "fao"
Relax. delay 1.000 sec
Pulse 86.5 degrees
Acq. time 0.484 sec
Width 33071.5 Hz
25088 repetitions
OBSERVE C13, 150.8058750 MHz
DECOUPLE H1, 599.7479933 MHz
Low power 10 dB atten.
continuously on
WALTZ-16 modulated
DATA PROCESSING
Line broadening 1.0 Hz
FT size 32768
Total time 41 hr, 27 min, 52 sec
OH
Me
O
O
OMe
Me
H
Me
Me
2.172
167.566
165.211
139.953
132.672
124.641
122.794
114.937
77.499
74.702
56.137
49.578
49.431
49.297
49.150
48.869
48.722
48.668
45.750
41.521
36.341
35.578
34.105
30.036
28.604
22.046
22.005
21.952
21.925
180
160
140
120
100
80
60
40
20
ppm

thesis-20-cdcl3-HNMR

Pulse Sequence: s2pul
 Solvent: CDCl3
 Ambient temperature
Operator: vnmr_vb
File: thesis-20-cdcl3-HNMR
INOVA-500 "fao"

 Relax. delay 1.000 sec
 Pulse 18.4 degrees
 Acq. time 1.995 sec
 Width 4506.5 Hz
 16 repetitions
OBSERVE   H1, 300.1176007 MHz
DATA PROCESSING
FT size 32768
Total time 0 min, 54 sec

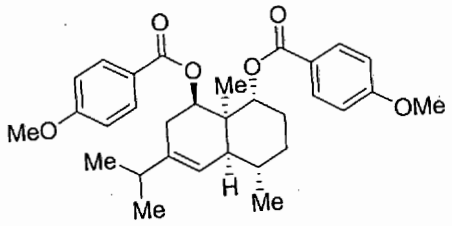

2-173

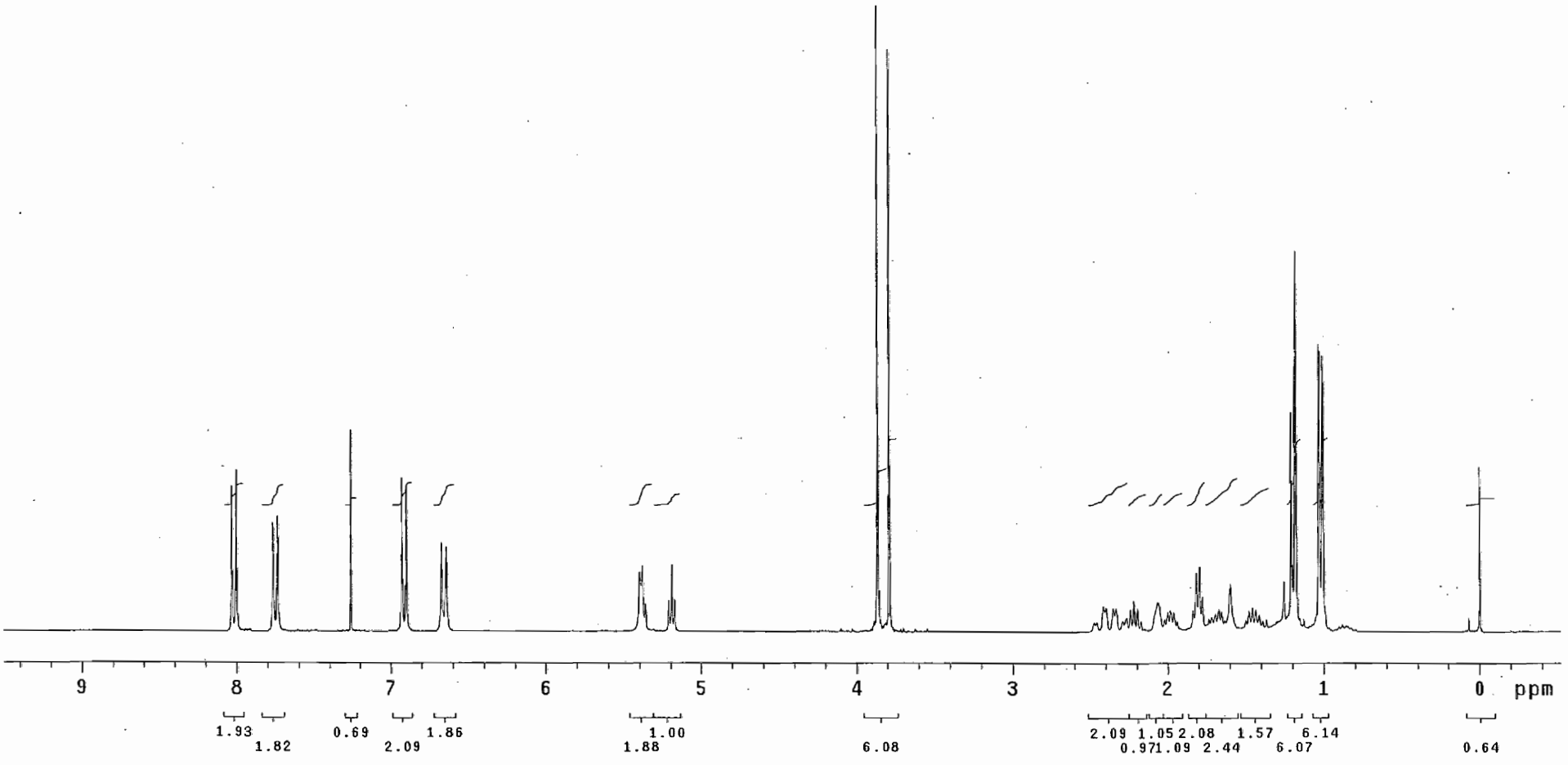

thesis-20-cdcl3-CNMR

Pulse Sequence: s2pul
Solvent: CDCl3
Ambient temperature
Operator: vnmr_vb
File: thesis-20-cdcl3-CNMR
INOVA-500 "fao"

Relax. delay 2.000 sec
Pulse 105.4 degrees
Acq. time 1.815 sec
Width 16501.7 Hz
17456 repetitions
OBSERVE C13, 75.3761490 MHz
DECOUPLE H1, 299.7672516 MHz
Low power 5 dB atten.
continuously on
WALTZ-16 modulated
DATA PROCESSING
Line broadening 1.0 Hz
FT size 65536
Total time 106 hr, 13 min, 14 sec

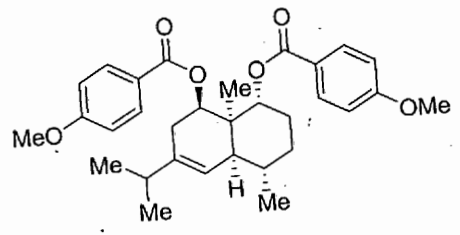

2-173

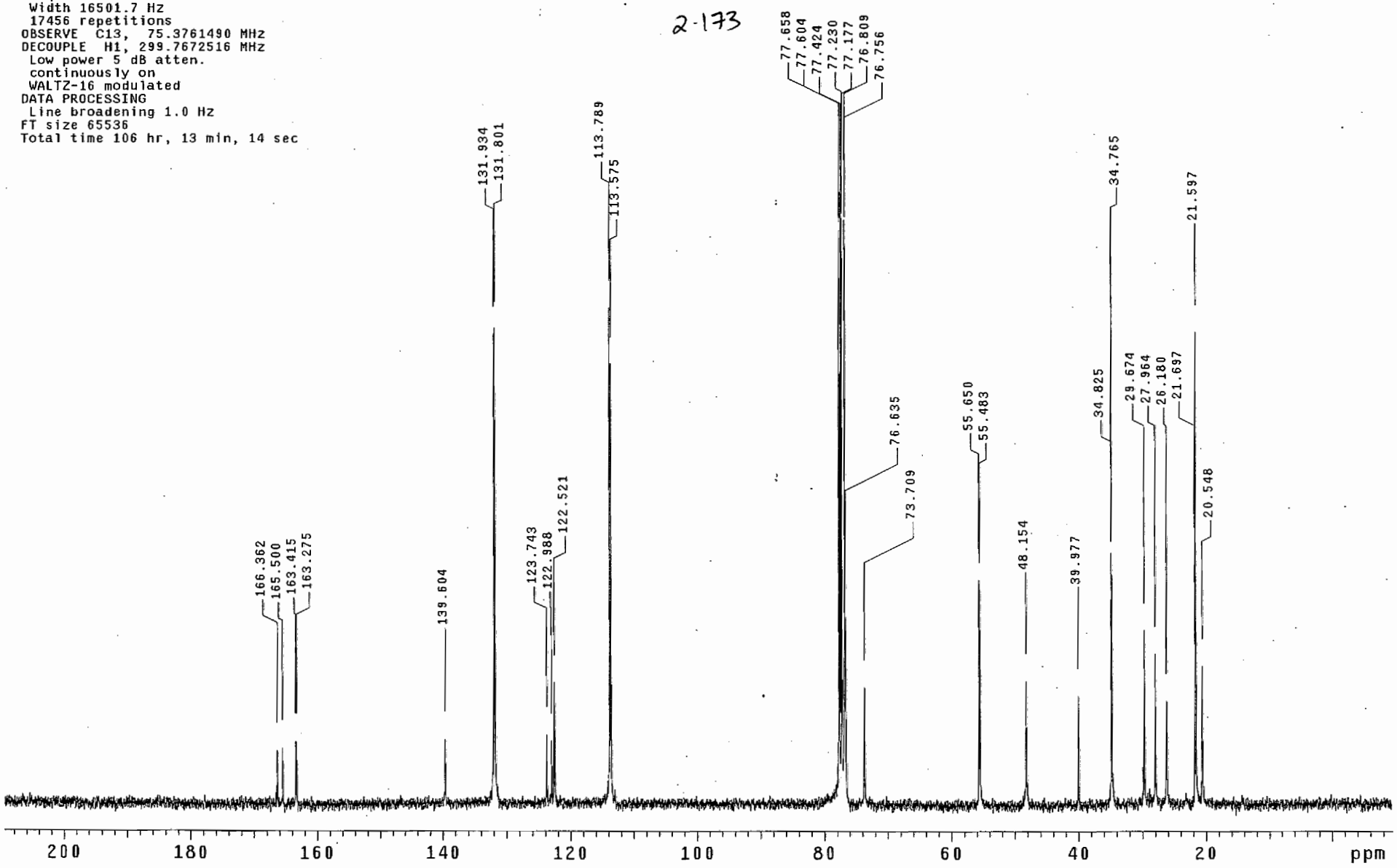

ACH-VIII-Pg29-cdcl3-HNMR

Pulse Sequence: s2pul

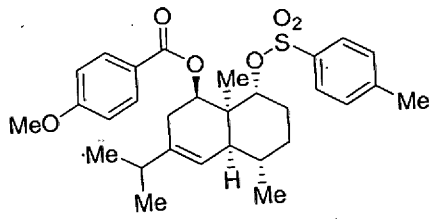

2.178

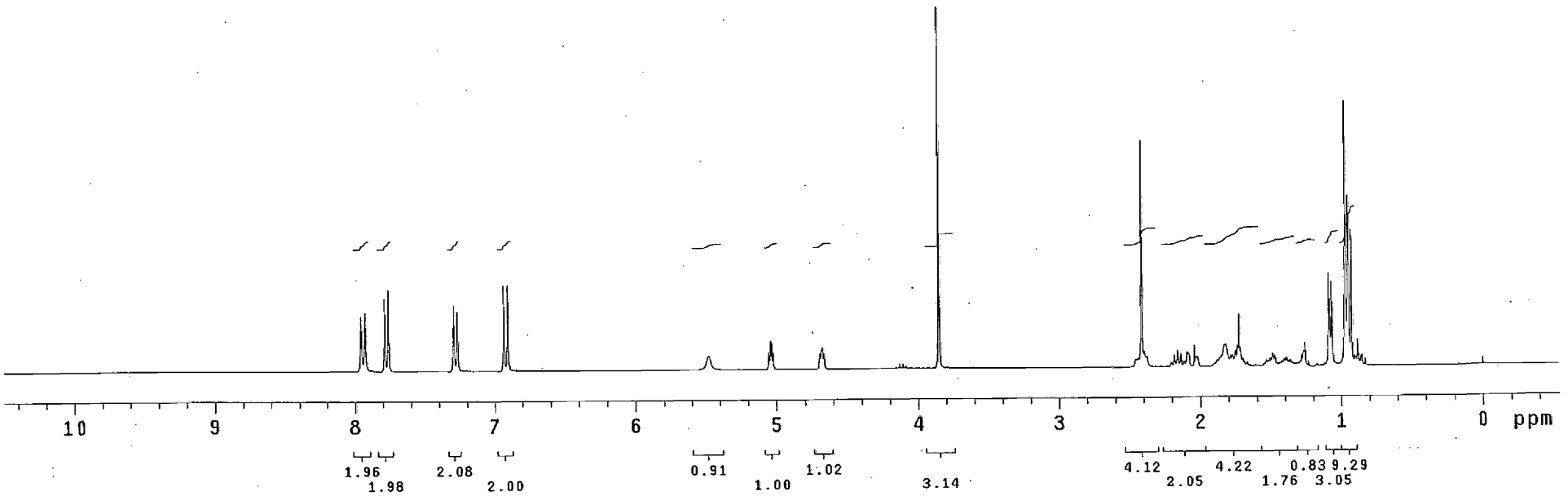

thesis-21-cdcl3-CNMR

Pulse Sequence: s2pul
Solvent: CDCl3
Ambient temperature
Operator: vnmr_vb
File: thesis-21-cdcl3-CNMR
INOVA-500 "fao"

Pulse 105.4 degrees
Acq. time 1.815 sec
Width 16501.7 Hz
3072 repetitions
OBSERVE C13, 75.3761525 MHz
DECOUPLE H1, 299.7672516 MHz
Low power 5 dB atten.
continuously on
WALTZ-16 modulated
DATA PROCESSING
Line broadening 1.0 Hz
FT size 65536
Total time 50 hr, 39 min, 53 sec

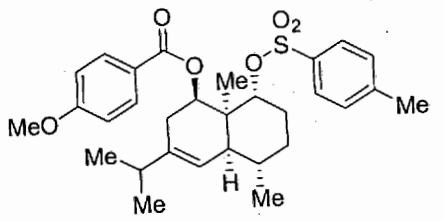

2.178

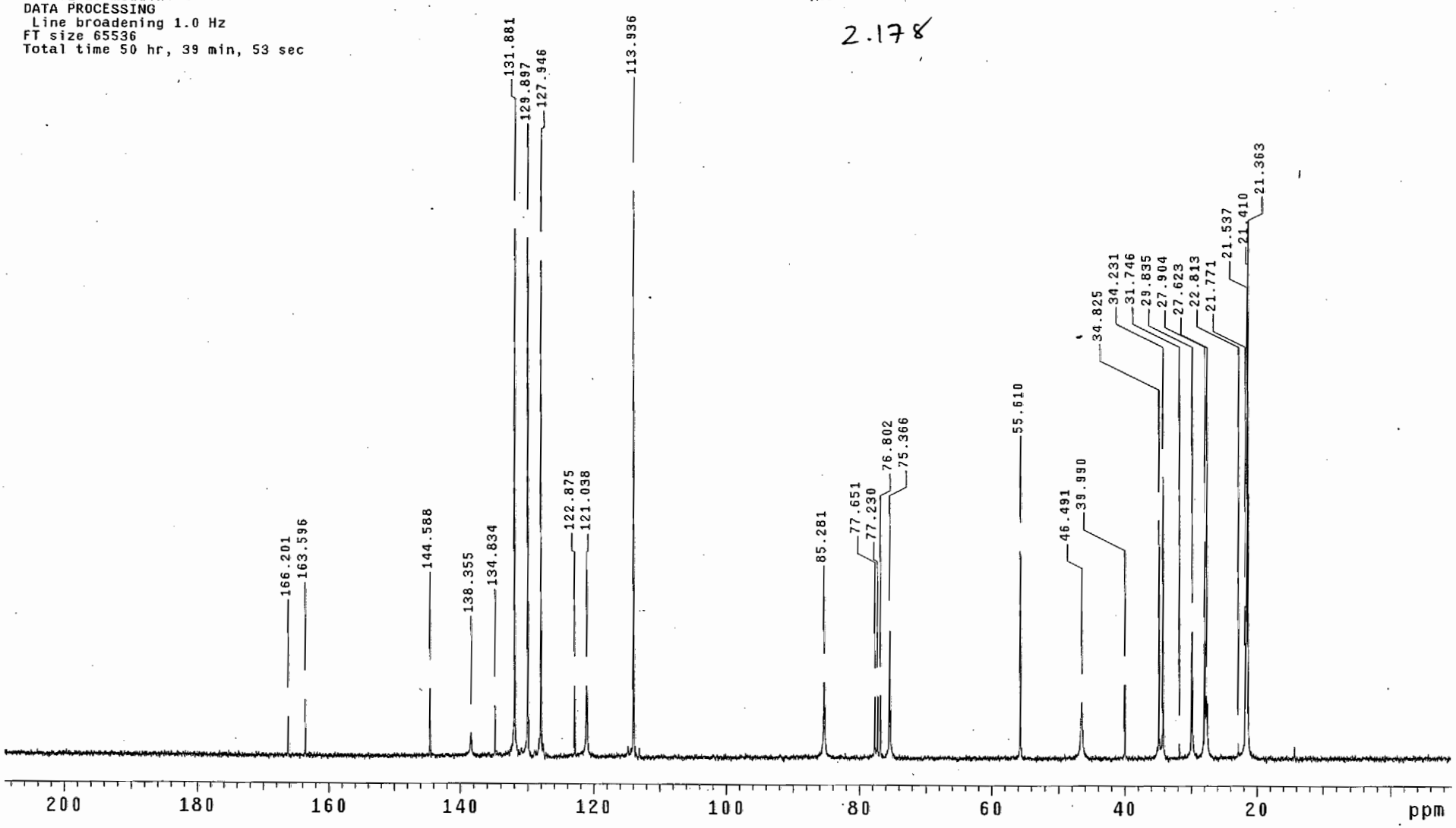

thesis-22-cdcl3-HNMR

Pulse Sequence: s2pul

Solvent: CDCl3
Ambient temperature
Operator: vnmr_vb
File: thesis-22-cdcl3-HNMR
INOVA-500 "fao"

Relax. delay 1.000 sec
Pulse 64.3 degrees
Acq. time 1.995 sec
Width 4506.5 Hz
16 repetitions
OBSERVE H1, 300.1176007 MHz
DATA PROCESSING
FT size 32768
Total time 0 min, 54 sec

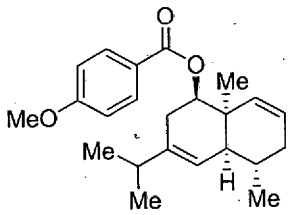

2-179

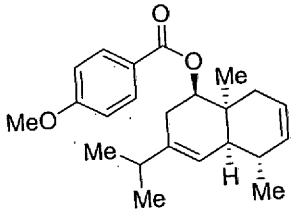

2-180

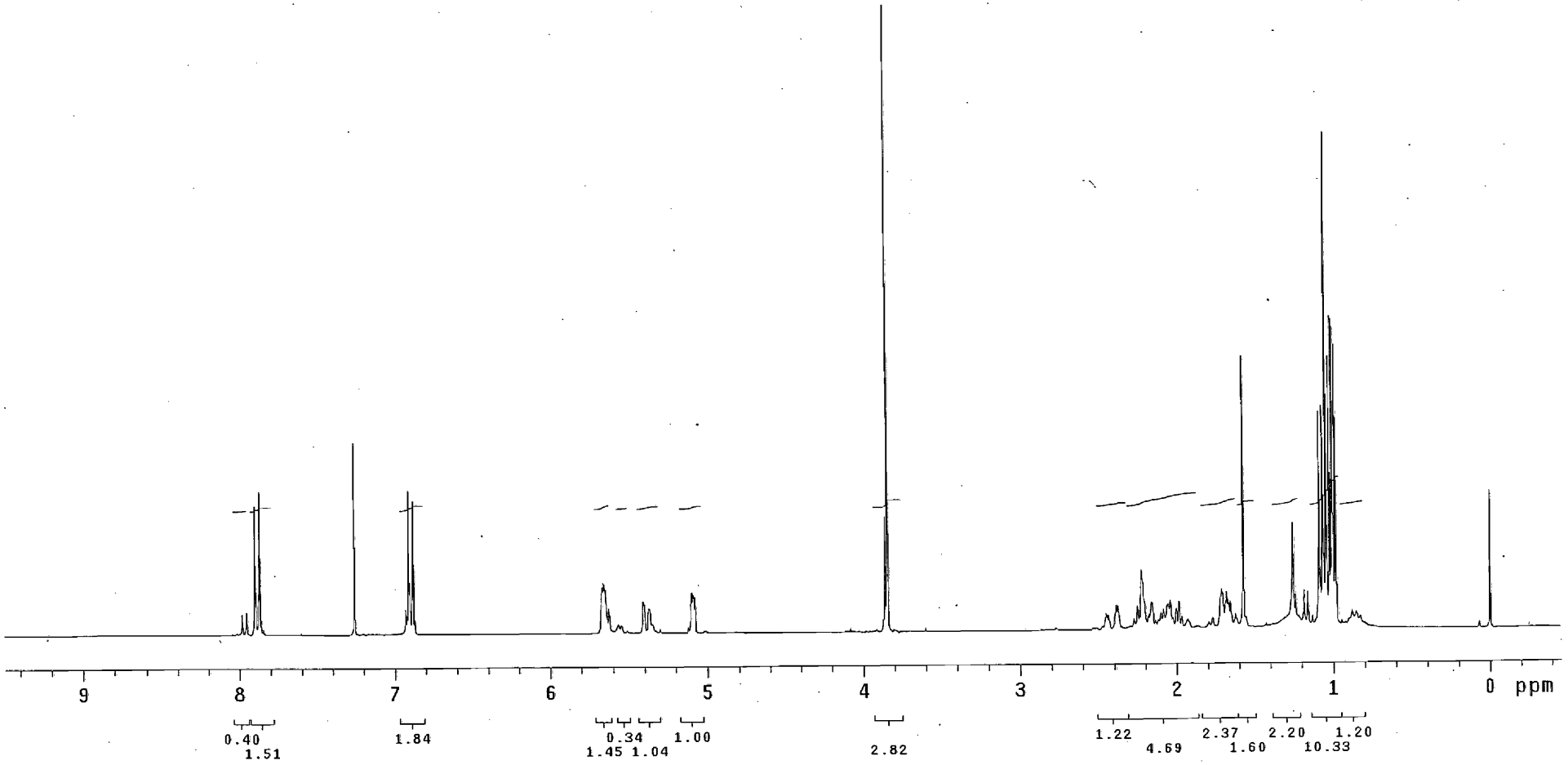

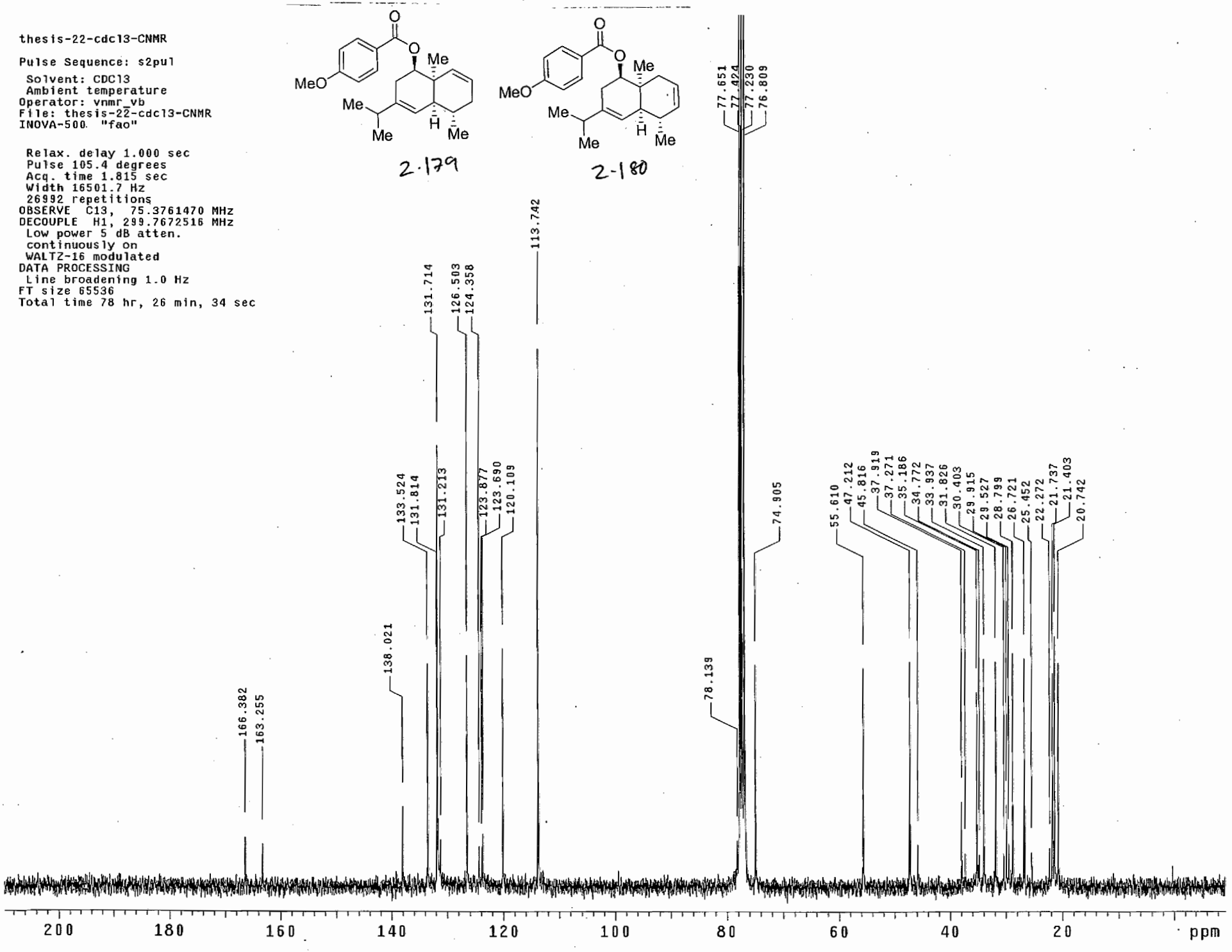
thesis-22-cdcl3-CNMR
Pulse Sequence: s2pul
Solvent: CDCl3
Ambient temperature
Operator: vnmr_vb
File: thesis-22-cdcl3-CNMR
INOVA-500 "fao"
Relax. delay 1.000 sec
Pulse 105.4 degrees
Acq. time 1.815 sec
Width 16501.7 Hz
26992 repetitions
OBSERVE C13, 75.3761470 MHz
DECOUPLE H1, 299.7672516 MHz
Low power 5 dB atten.
continuously on
WALTZ-16 modulated
DATA PROCESSING
Line broadening 1.0 Hz
FT size 65536
Total time 78 hr, 26 min, 34 sec
2-179
2-180
166.382
163.255
138.021
133.524
131.814
131.714
131.213
126.503
124.358
123.877
123.690
120.109
113.742
78.139
77.651
77.424
77.230
76.809
74.905
55.610
47.212
45.816
37.919
37.271
35.186
34.772
33.937
31.826
30.403
29.915
29.527
28.799
26.721
25.452
22.272
21.737
21.403
20.742
200
180
160
140
120
100
80
60
40
20
ppm

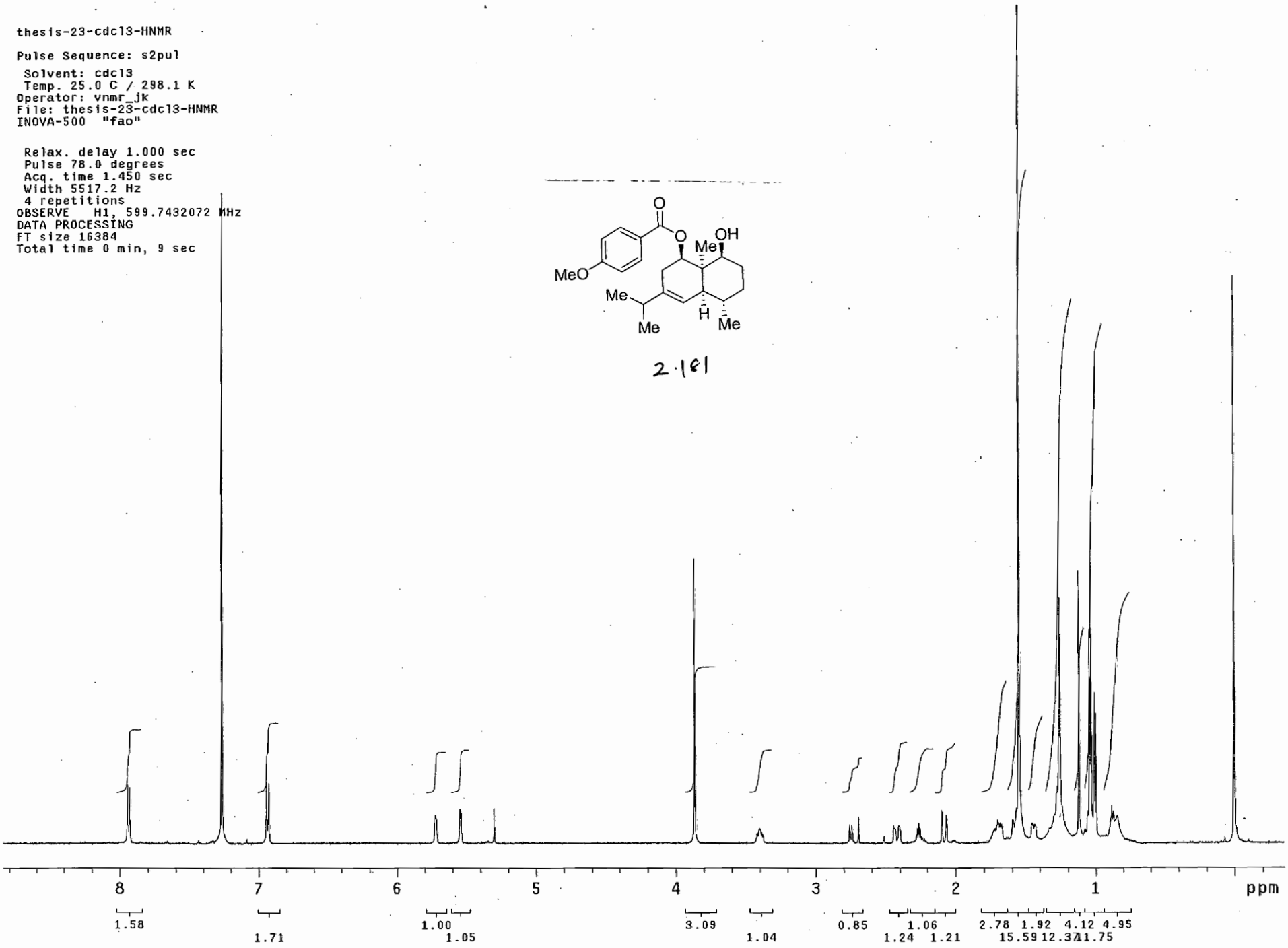
thesis-23-cdcl3-HNMR
Pulse Sequence: s2pul
Solvent: cdcl3
Temp. 25.0 C / 298.1 K
Operator: vnmr_jk
File: thesis-23-cdcl3-HNMR
INOVA-500 "fao"
Relax. delay 1.000 sec
Pulse 78.0 degrees
Acq. time 1.450 sec
Width 5517.2 Hz
4 repetitions
OBSERVE H1, 599.7432072 MHz
DATA PROCESSING
FT size 16384
Total time 0 min, 9 sec
MeO
O
O
OH
Me
Me
H
Me
Me
2·181
8
7
6
5
4
3
2
1
ppm
1.58
1.71
1.00
1.05
3.09
1.04
0.85
1.06
1.24
1.21
2.78
1.92
4.12
4.95
15.59
12.37
11.75

thesis-23-cdcl3-CNMR

Pulse Sequence: s2pul

Solvent: cdcl3
Temp. 25.0 C / 298.1 K
Operator: vnmr_jk
File: thesis-23-cdcl3-CNMR
INOVA-500 "fao"

Relax. delay 1.000 sec
Pulse 86.5 degrees
Acq. time 0.500 sec
Width 32000.0 Hz
67392 repetitions
OBSERVE C13, 150.8055149 MHz
DECOUPLE H1, 599.7457546 MHz
Low power 10 dB atten.
continuously on
WALTZ-16 modulated
DATA PROCESSING
Line broadening 1.0 Hz
FT size 32768
Total time 41 hr, 54 min, 52 sec

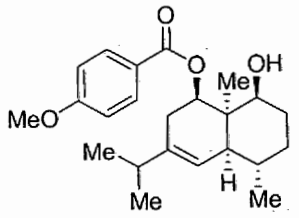

2-181

thesis-54-cdcl3-HNMR

Pulse Sequence: s2pul

Solvent: CDCl3
Ambient temperature
Operator: vnmr_vb
File: thesis-54-cdcl3-HNMR
INOVA-500 "fao"

Relax. delay 1.000 sec
Pulse 64.3 degrees
Acq. time 1.995 sec
Width 4506.5 Hz
16 repetitions
OBSERVE H1, 300.1176007 MHz
DATA PROCESSING
FT size 32768
Total time 0 min, 54 sec

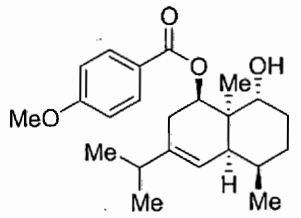

2.187

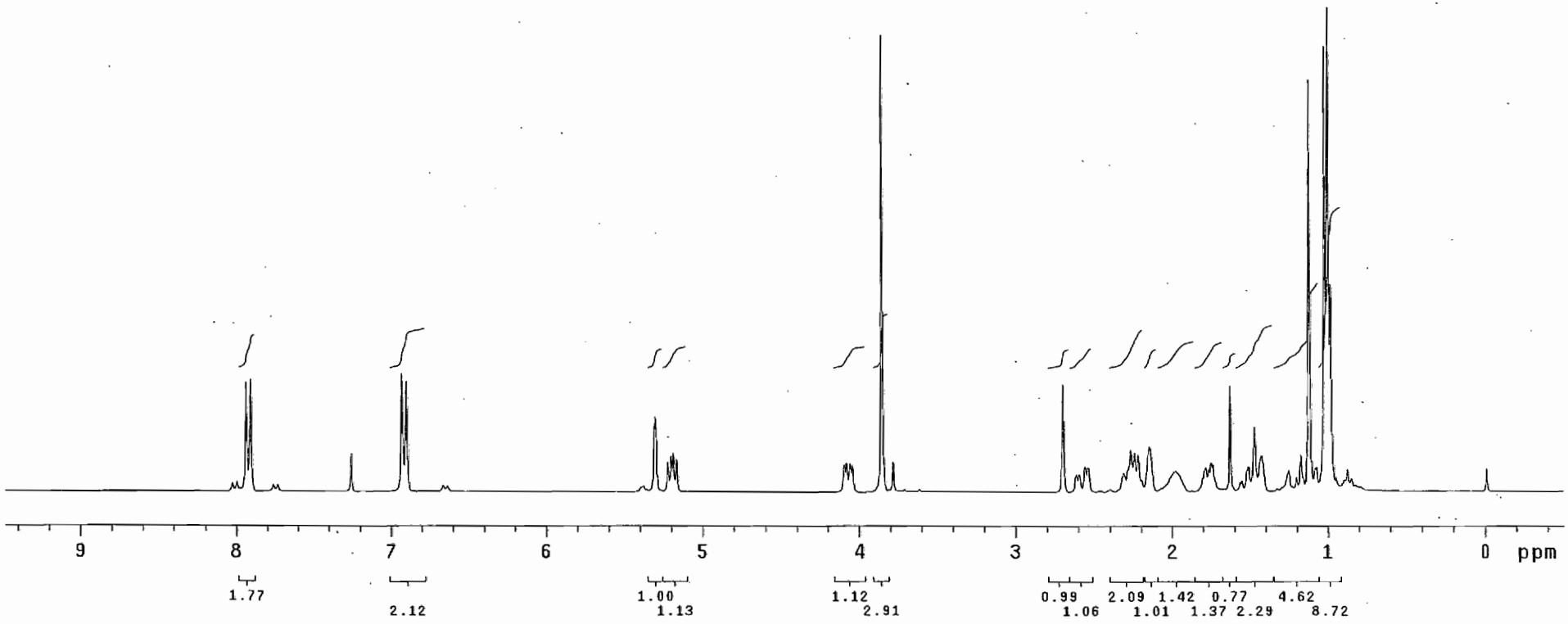

thesis-54-cddcl3-CNMR

Pulse Sequence: s2pul

Solvent: CDCl3
Ambient temperature
Operator: vnmr_vb
File: thesis-54-cdcl3-CNMR
INOVA-500 "fao"

Pulse 105.4 degrees
Acq. time 1.815 sec
Width 16501.7 Hz
416 repetitions
OBSERVE C13, 75.3761485 MHz
DECOUPLE H1, 299.7672516 MHz
Low power 5 dB atten.
continuously on
WALTZ-16 modulated
DATA PROCESSING
Line broadening 1.0 Hz
FT size 65536
Total time 31 min, 7 sec

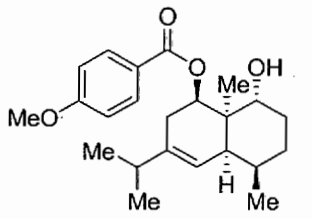

2.187

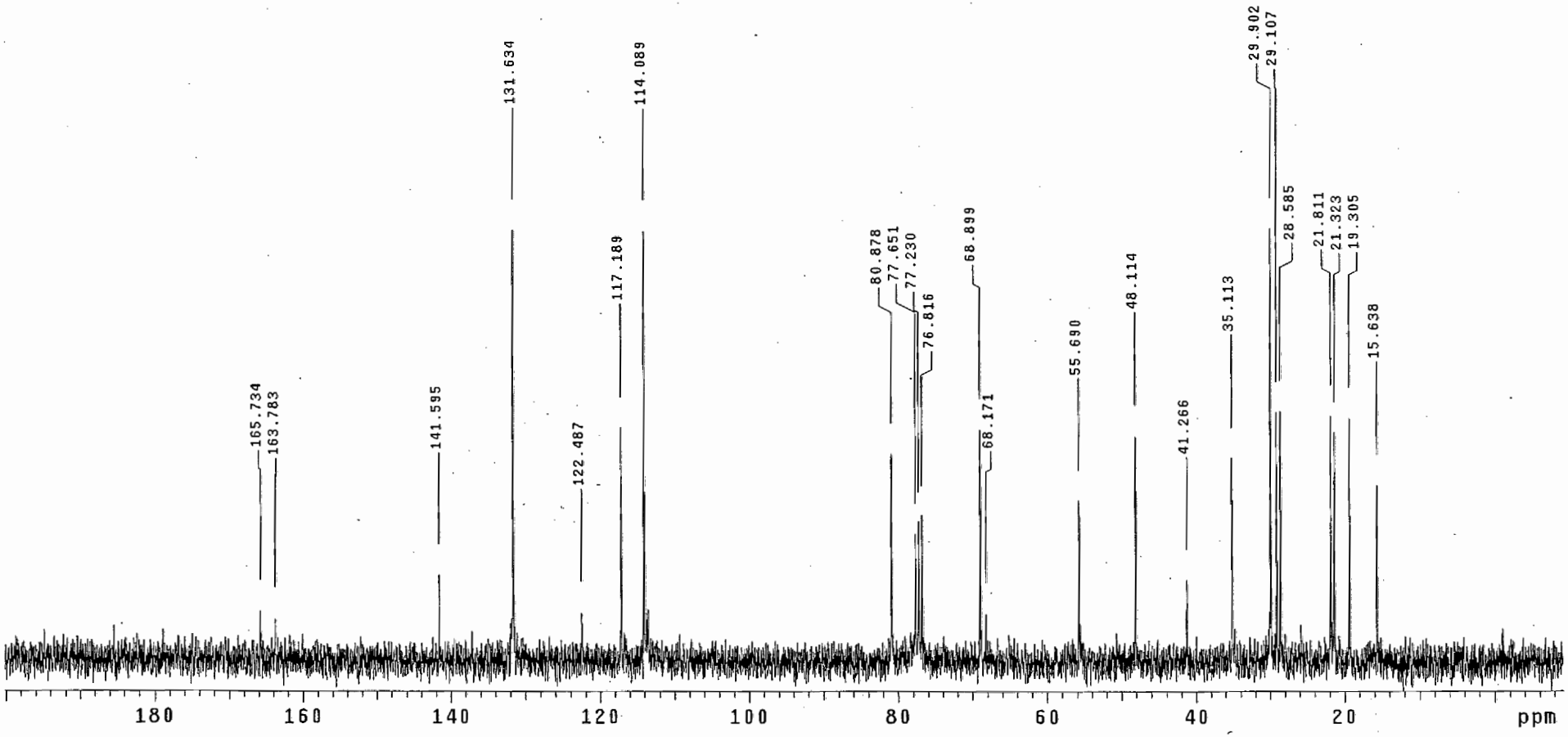

thesis-24-cdcl3-HNMR

Pulse Sequence: s2pul

Solvent: cdcl3
Temp. 25.0 C / 298.1 K
Operator: vnmr_jk
File: thesis-24-cdcl3-HNMR
INOVA-500 "fao"

Relax. delay 1.000 sec
Pulse 78.0 degrees
Acq. time 1.450 sec
Width 5517.2 Hz
4 repetitions
OBSERVE H1, 599.7432482 MHz
DATA PROCESSING
FT size 16384
Total time 0 min, 9 sec

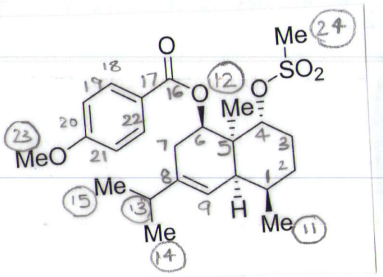

2.190

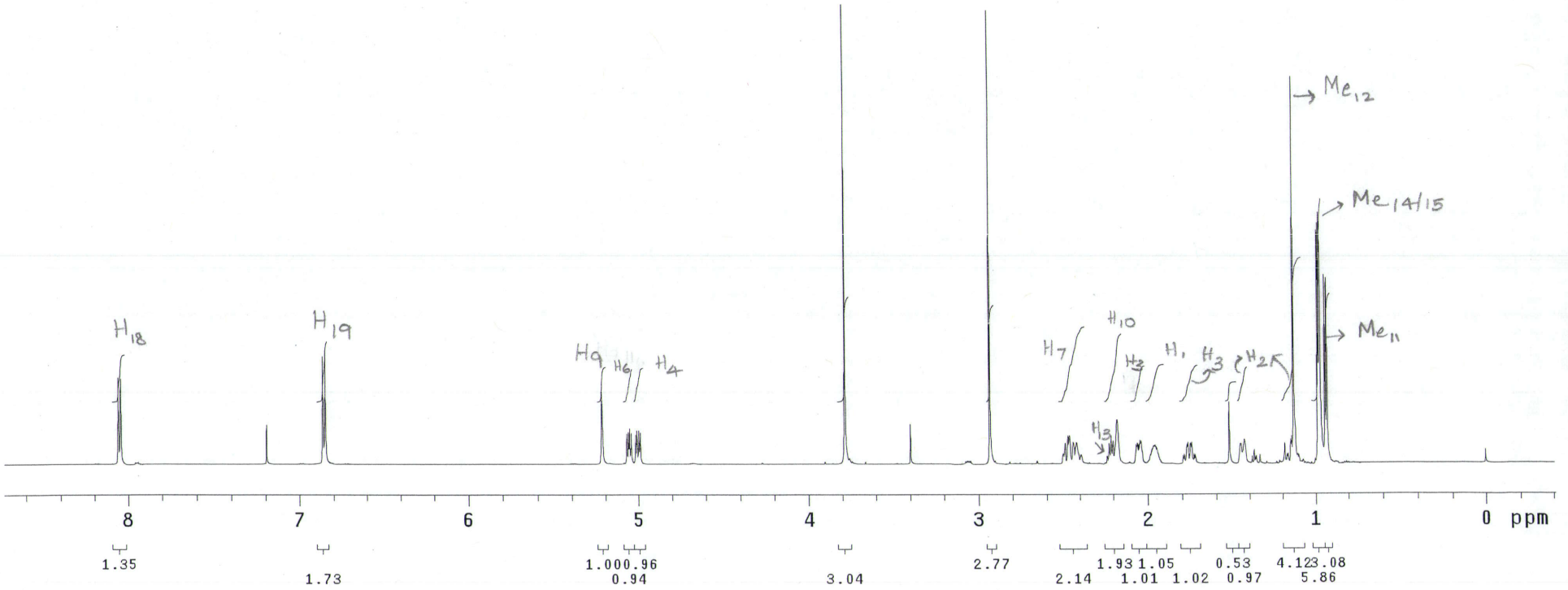

thesis-24-cdcl3-CNMR

Pulse Sequence: s2pul

Solvent: cdcl3
Temp. 25.0 C / 298.1 K
Operator: vnmr_jk
File: thesis-24-cdcl3-CNMR
INOVA-500 "fao"

Relax. delay 1.000 sec
Pulse 86.5 degrees
Acq. time 0.484 sec
Width 33071.5 Hz
28368 repetitions
OBSERVE C13, 150.8055475 MHz
DECOUPLE H1, 599.7457546 MHz
Low power 10 dB atten.
continuously on
WALTZ-16 modulated
DATA PROCESSING
Line broadening 2.0 Hz
FT size 32768
Total time 4146 hr, 25 min, 1 sec

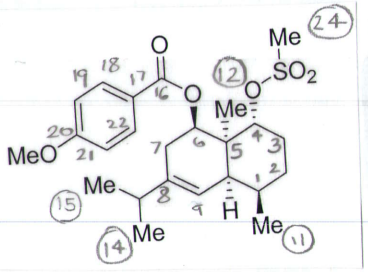

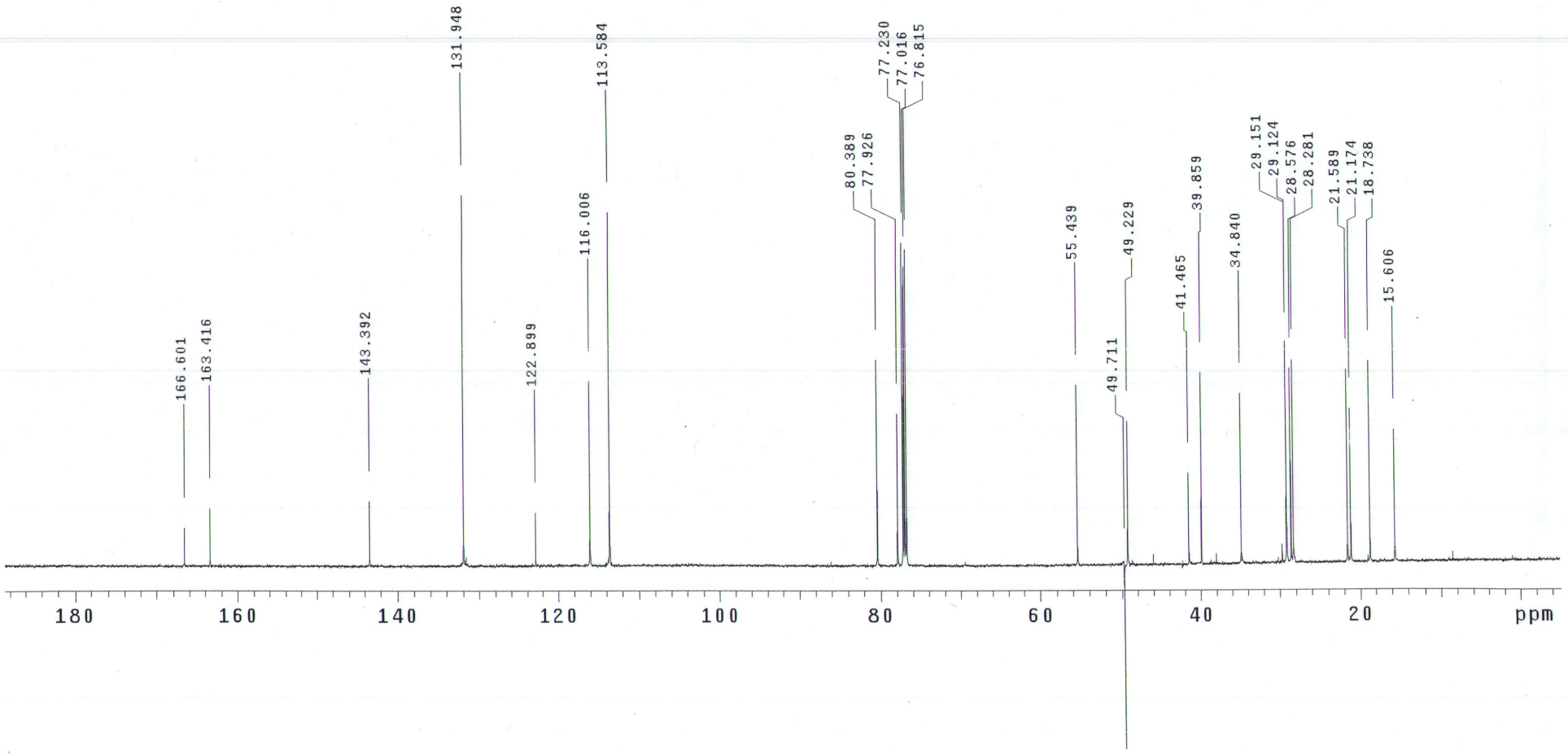

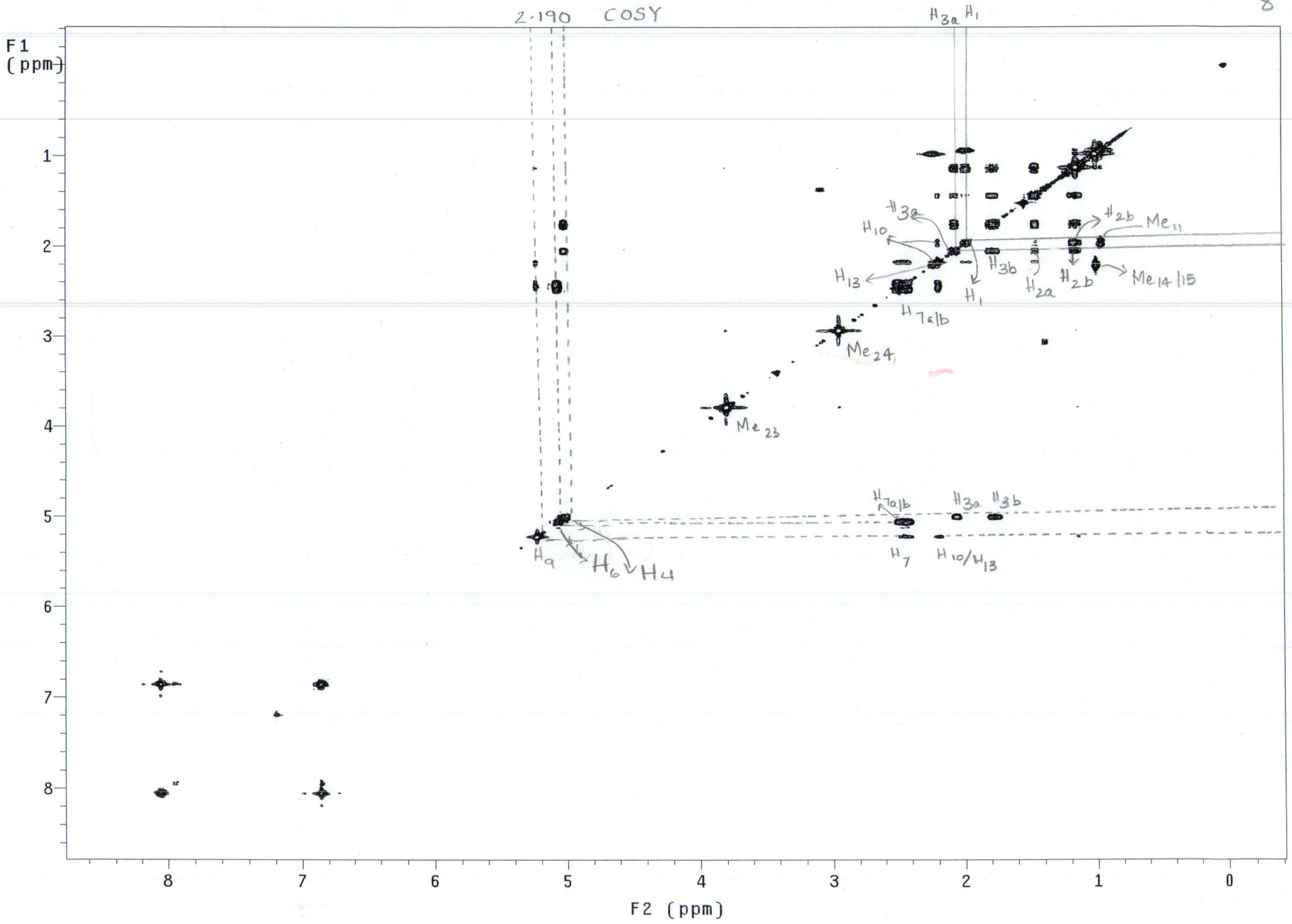
2-190 COSY
F1 (ppm)
F2 (ppm)
H3a H1
H3a
H10
H2b Me11
H13
H3b
H2a
H2b
Me14 15
H1
H7a1b
Me24
Me23
H7a1b
H3a H3b
H9
H6
H4
H7
H10/H13

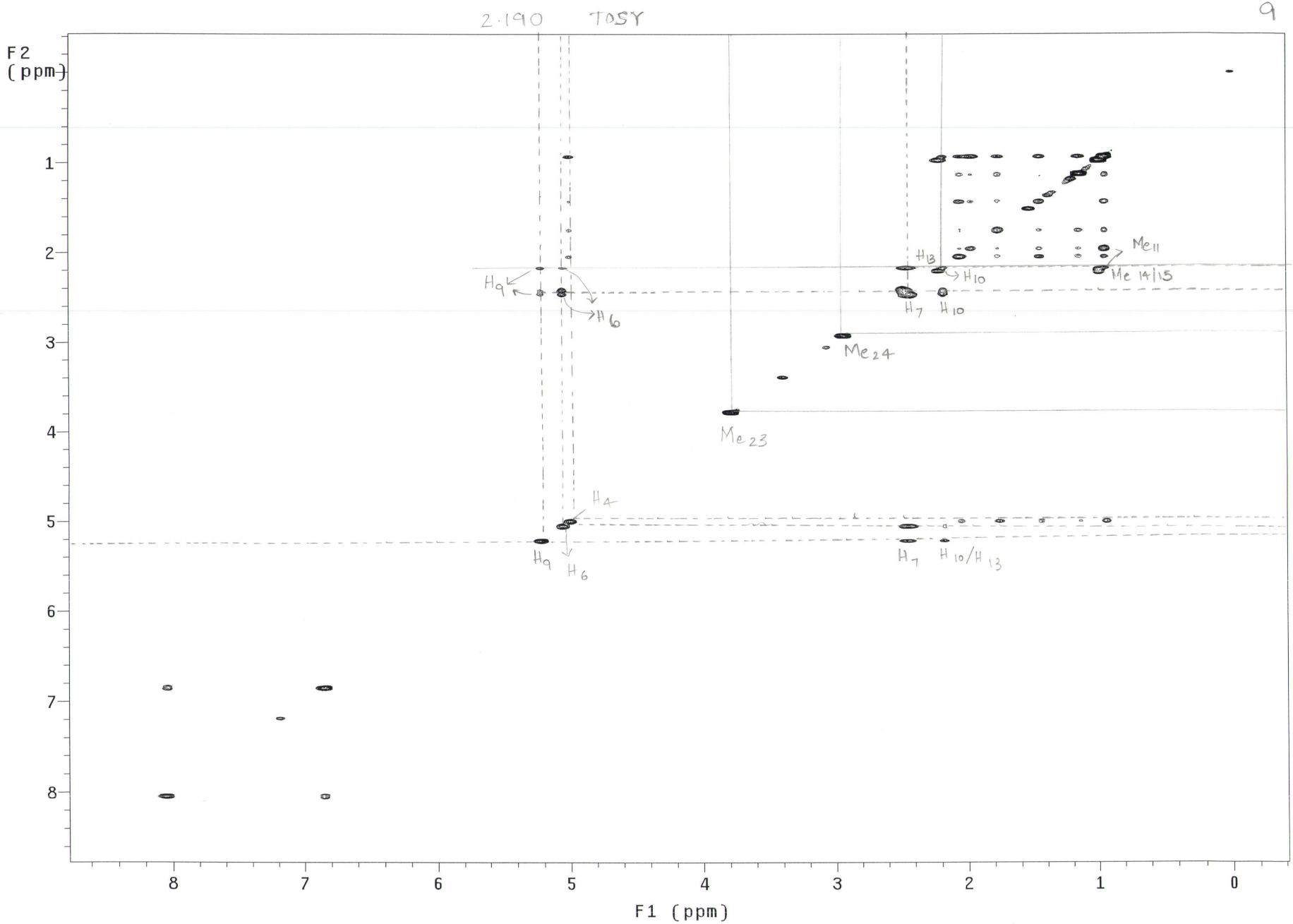
2·190 TOSY
F2 (ppm)
F1 (ppm)
1
2
3
4
5
6
7
8
0
H9
H6
H4
H13
H10
Me11
Me 14/15
H7
H10
Me24
Me23
H9
H6
H7
H10/H13

thesis-24-cdcl3-APT

Pulse Sequence: apt
Solvent: cdcl3
Temp. 25.0 C / 298.1 K
Operator: vnmr_jk
File: apt
INOVA-500 "fao"

Relax. delay 1.000 sec
1st pulse 24.0 usec
2nd pulse 10.0 usec
Acq. time 0.484 sec
Width 33071.5 Hz
4668 repetitions
OBSERVE C13, 150.8055162 MHz
DECOUPLE H1, 599.7457546 MHz
Low power 10 dB atten.
on during acquisition
WALTZ-16 modulated
DATA PROCESSING
Line broadening 4.0 Hz
FT size 32768
Total time 1 hr, 57 min, 33 sec

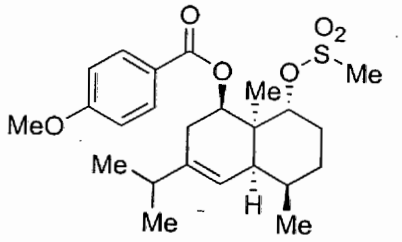

2.190

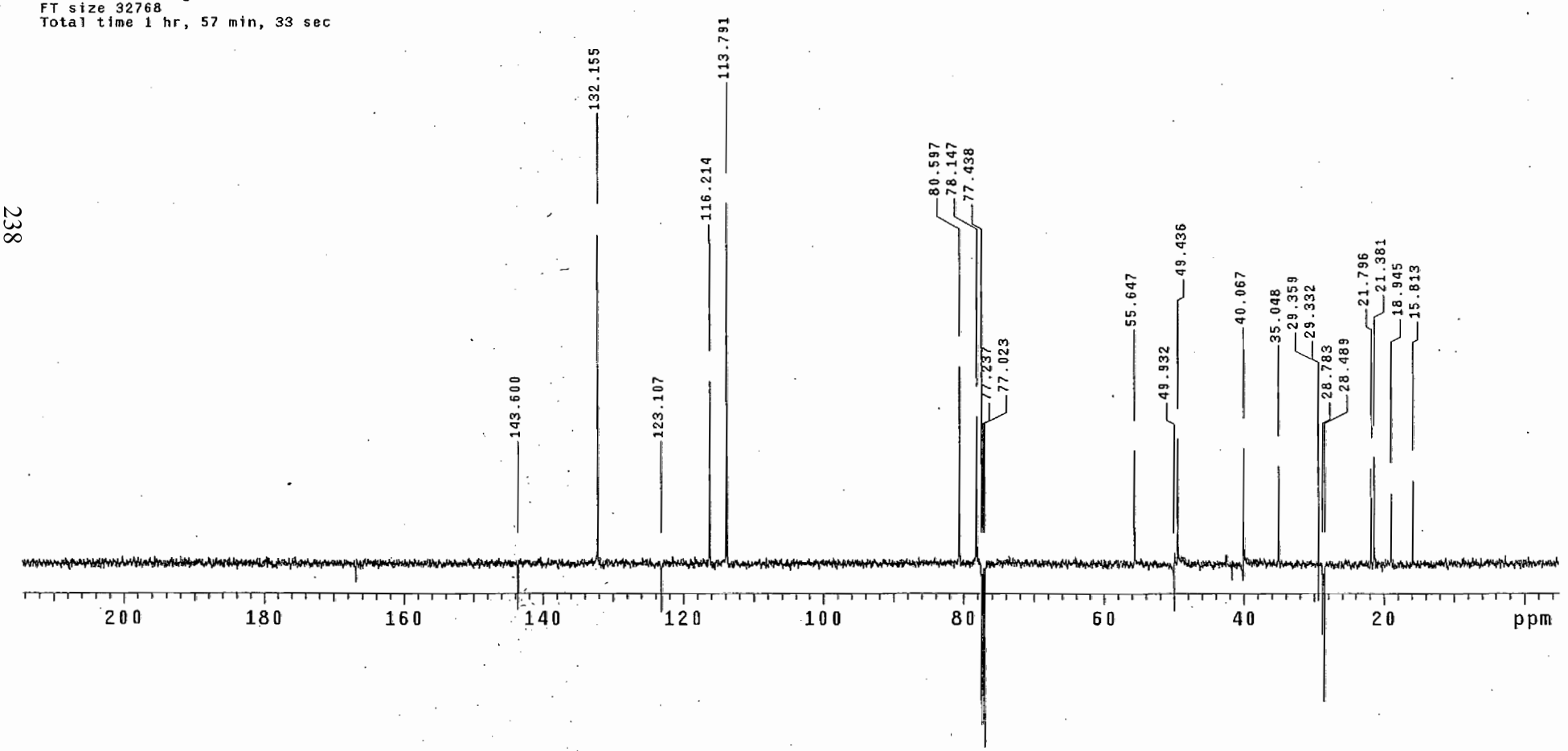

2-190 HMQC

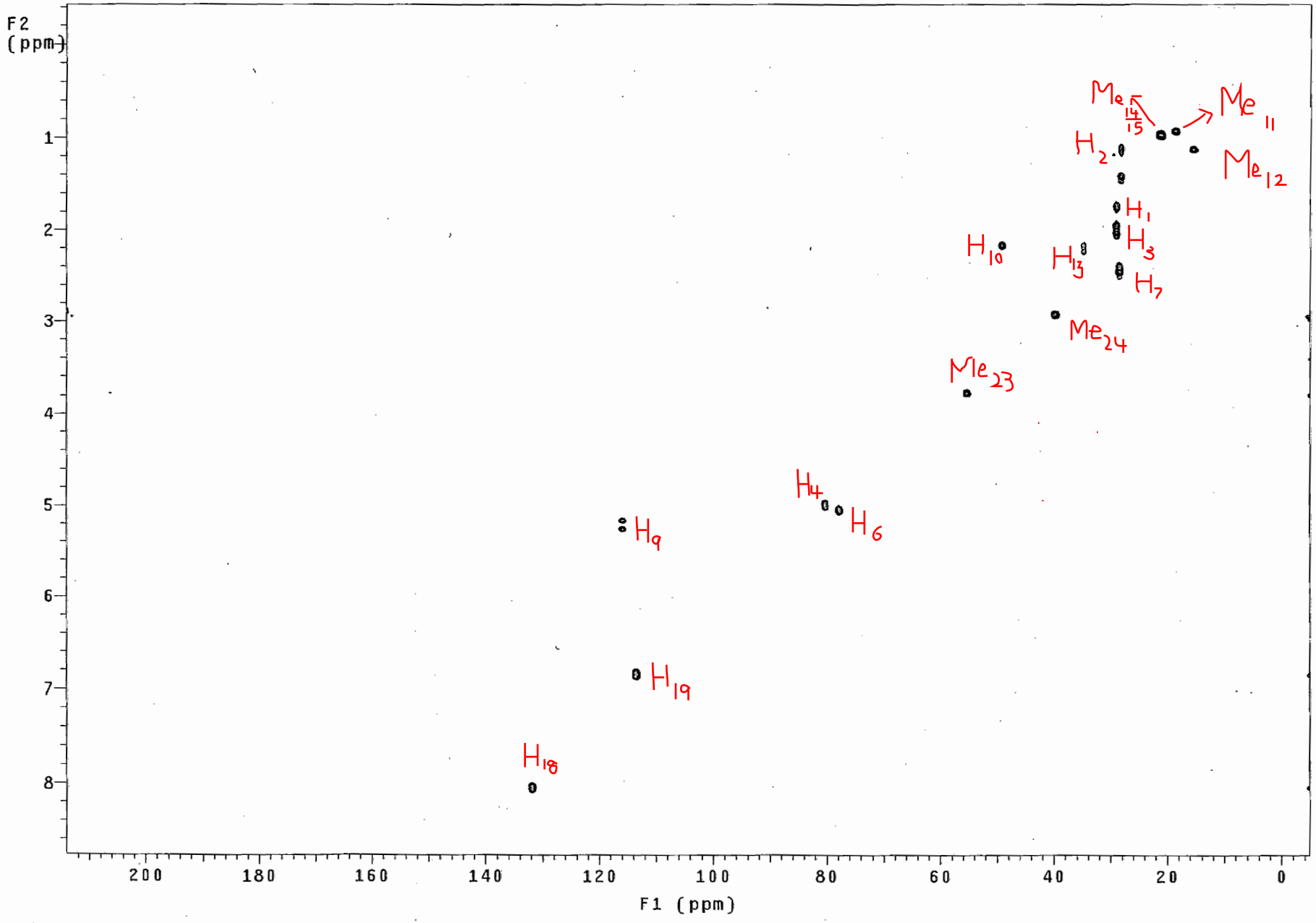
F2 (ppm)
1
2
3
4
5
6
7
8
200
180
160
140
120
100
80
60
40
20
0
F1 (ppm)
Me15
14
15
Me11
H2
Me12
H1
H10
H3
H13
H7
Me24
Me23
H4
H6
H9
H19
H18

2.190 NOE

12

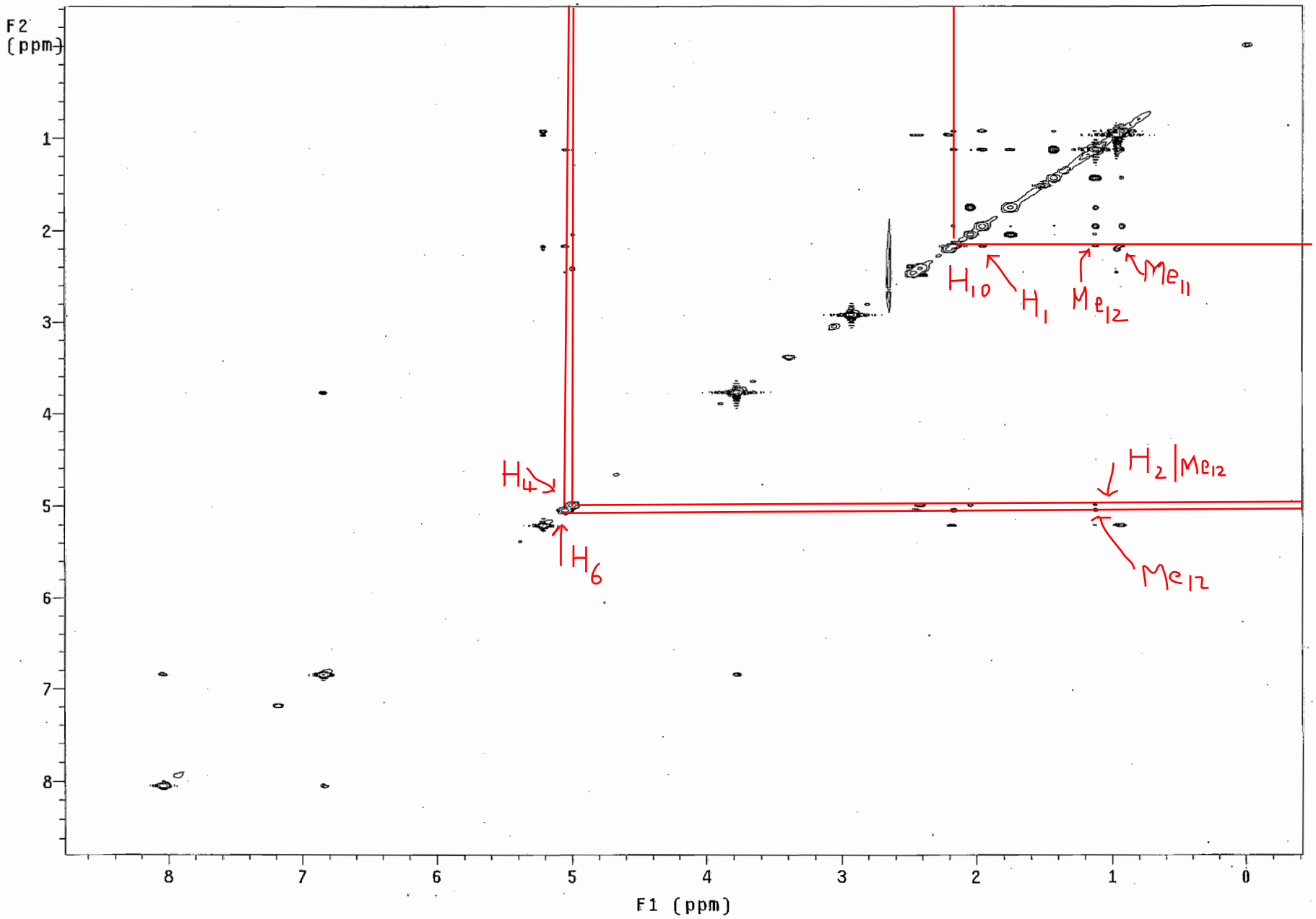

thesis-25-cdcl3-HNMR

Pulse Sequence: s2pul

Solvent: cdcl3
Temp. 25.0 C / 298.1 K
Operator: vnmr_jk
File: h1
INOVA-500 "fao"

Relax. delay 1.000 sec
Pulse 78.0 degrees
Acq. time 1.450 sec
Width 5517.2 Hz
4 repetitions
OBSERVE H1, 599.7432085 MHz
DATA PROCESSING
Resol. enhancement -0.0 Hz
FT size 16384
Total time 0 min, 9 sec

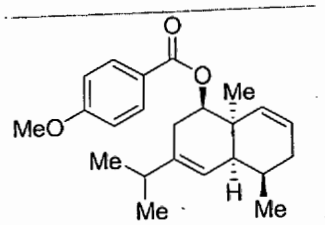

2.194

thesis-25-cdcl3-CNMR

Pulse Sequence: s2pul

Solvent: cdcl3
Temp. 25.0 C / 298.1 K
Operator: vnmr_jk
File: thesis-25-cdcl3-CNMR
INOVA-500 "fao"

Relax. delay 1.000 sec
Pulse 86.5 degrees
Acq. time 0.500 sec
Width 32000.0 Hz
51856 repetitions
OBSERVE C13, 150.8055149 MHz
DECOUPLE H1, 599.7457546 MHz
Low power 10 dB atten.
continuously on
WALTZ-16 modulated
DATA PROCESSING
Line broadening 1.0 Hz
FT size 32768
Total time 41 hr, 54 min, 52 sec

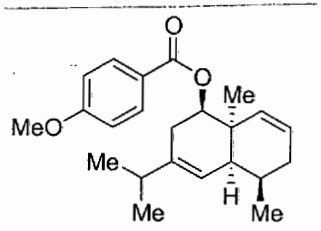

2.194